Separation of Carbon Dioxide from Nitrogen Using Poly(vinyl alcohol)-Amine Blend Membranes

by

Gil J. Francisco

A thesis

presented to the University of Waterloo

in fulfillment of the

thesis requirement for the degree of

Doctor of Philosophy

in

Chemical Engineering

Waterloo, Ontario, Canada, 2006

Author's Declaration

I hereby declare that I am the sole author of this thesis. This is the true copy of the thesis, including any required final revisions, as accepted by my examiners.

I understand that my thesis may be made electronically available to the public.

Abstract

In this research, a facilitated transport membrane was developed. The reactive membrane consisted of a carrier entrapped in poly(vinyl alcohol) “PVA”matrix cast on a polysulfone support. PVA was selected to hold the reactive carrier because of its hydrophilicity and compatibility with the carrier. Several reactive amines were examined for their suitability as carrier. Among the amines tested as a carrier for CO_2, diethanolamine “DEA” demonstrates a greater improvement in the permeation of CO_2 as well as selectivity over N_2. DEA is a secondary amine and one of the most commonly used amines for gas treating due to its favourable reaction kinetics with acid gases and because of its stability when regenerated.

Initially, pure gas permeation was employed for materials selection and membrane preparation procedures. The effects of process conditions on the membrane performance, which involve carrier concentrations, feed pressures and operating temperatures were examined. Then the effects of membrane thickness and long-term stability tests were conducted.

Once the appropriate membrane materials and preparation procedures were established, the next phase of the study involved the determination of the actual separation of CO_2/N_2 mixtures. These experiments were carried out by adjusting the feed gas composition, feed pressures and operating temperature. In general, the results obtained with CO_2/N_2 mixtures were in agreement with those obtained with pure gas permeation experiments. It

was found that facilitation is more significant at lower CO_2 partial pressure differential across the membrane. At higher partial pressure differentials, the reactive membrane may no longer serve as a facilitating medium due to the saturation of the reactive part of the membrane. Under such conditions the permeance values and selectivity obtained were simply due to the solubility and diffusivity of the CO_2 and N_2 in the membrane matrix.

Since it was not possible to analyze concentration profiles inside the thin membrane experimentally, it was decided to analyze the effects of various parameters through the analytical transport equations. The zwitterion mechanism was used to illustrate the kinetics of the CO_2-DEA systems. The mass transport equations were solved numerically. All relevant physicochemical properties needed to implement the mass transport equations were taken from the literatures. The calculated results support the experimental trends that were observed for the CO_2 permeance as a function of partial pressure differentials and carrier concentrations.

Acknowledgements

In presenting this work, I am happy to acknowledge my indebtedness to the membrane group in our laboratory especially to Professors X. Feng and A. Chakma, the writer's advisers, who patiently provide their thorough guidance and valuable comments and expert suggestions.

Natural Sciences and Engineering Research Council (NSERC) of Canada for the financial support for this study.

G.J.F.

Table of Contents

Chapter 5

Chapter 6

List of Tables

List of Figures

Chapter 1

Introduction

The separation of CO_2 from different emission sources, particularly flue gas from power stations, steel works and chemical industries, has attracted a worldwide interest as a result of the enhanced greenhouse effect. The actual warming of the earth due to the atmospheric blanket is strongly influenced by small amounts of gases in the earth's atmosphere, particularly CO_2 and water vapour. These gases trap the heat due to their molecular structures, which absorb mainly reflected solar radiation from the earth's surface. H_2O vapour absorbs solar radiation in the range 4 to 7 microns while CO_2 absorbs radiation in the range of 13 to 19 microns (Halmann *et al*, 1999). Hence, they are called greenhouse gases. Some of the conventional methods of gas purification include scrubbing with physical and chemical solvents (Kohl and Nielsen, 1997), cryogenic distillation (Astarita, *et.al*., 1983) and membranes.

Furthermore, a large amount of CO_2 must be removed from gases at high pressure in the manufacture of hydrogen, ammonia and natural gas. The partial pressure of CO_2 in the feed gas for treating is usually in the range of 207 to 2760 kPa. The concentration of CO_2 in the treated gas must be 1 to 2% in the case of pipeline natural gas, below 0.10% in the case of H_2 and NH_3 synthesis gas (to avoid poisoning the catalyst) and below 150 ppm for liquefied natural gas (Astarita, *et.al*., 1983). The separation methods for removing CO_2 can either be bulk or trace removal depending on the application. The principal factors that are usually considered when choosing a suitable separation schemes are

product purity, feed and product gas partial pressure requirements, operating temperatures, energy requirements, and the presence of impurities in the gas. Fig. 1.1 shows the approximate ranges of application of different types of gas treating processes for CO_2 removal in the feed gas. Amine-containing chemical solvents are generally preferred when the partial pressure of CO_2 in the feed gas is relatively low or when CO_2 reduced to a very low concentration in the treated gas. Physical solvents are used at high CO_2 pressures in the feed gas and when deep CO_2 removal is not required.

A membrane can be defined as a semi-permeable barrier that allows the preferential transport of certain components. Traditionally, thin non-porous polymeric films and microporous materials have been used as membranes. A membrane should exhibit high permeability and selectivity for the component to be separated. In general, permeability and selectivity of common polymeric membranes are inversely related (Kulkarni, *et.al*., 1983) . Thus, the conventional membranes are good for bulk acid gas removal; they are inferior to or they should be combined with other processes when the acid gases are present in low concentrations. That is because at low partial pressures of acid gases, the driving force for separation is reduced.

Carbon dioxide can be separated from flue gas using polymeric gas separation membranes. However, typical nonporous polymeric membranes exhibit CO_2/CH_4 and CO_2/N_2 selectivities around 15-35 (Stern , 1994; Koros, 1993). As the flue gas is at atmospheric pressure, compression is necessary in order to obtain sufficient driving force for the separation to take place. The energy consumption of the compression is

presumably the reason for the limitation of the process. Even if the CO_2/N_2 selectivities of these polymeric membranes can be increased to a higher level through further development, for example through the synthesis of a thin film composite membrane (asymmetric membrane) that exhibits a high flux for gas and vapour permeation and operates at higher driving force; it is still unlikely whether they can offer an economically feasible option because of the low CO_2 partial pressure in the flue gas.

In addition, the discovery and development of new polymers has made separation of gases by membranes competitive in relation to the conventional methods of scrubbing using physical or chemical solvents. As in the gas scrubbing processes, the absorption of the reactive gas (*e.g.* CO_2) can be improved by the addition of reactive carrier to the matrix. As a result, further increase in the mass transport can be achieved when the carrier reacts preferentially with a component of the diffusing gases. This phenomenon is referred to as facilitated transport.

In this research, poly(vinyl alcohol) (PVA) in the presence of an amine carrier is considered for separating CO_2 in CO_2/N_2 mixtures. The alkanolamine/PVA mixture was selected on the basis of the following criteria. a.) PVA needs to be compatible or miscible with the amine and must be one in which CO_2 is also soluble, and preferably one in which the N_2 is less soluble. In this thesis, the term alkanolamine is referred to as amine. CO_2 reaction with alkanolamines is thought to be identical to the reaction of amines; they're being virtually no reaction between CO_2 and the alcohol (-OH) groups of

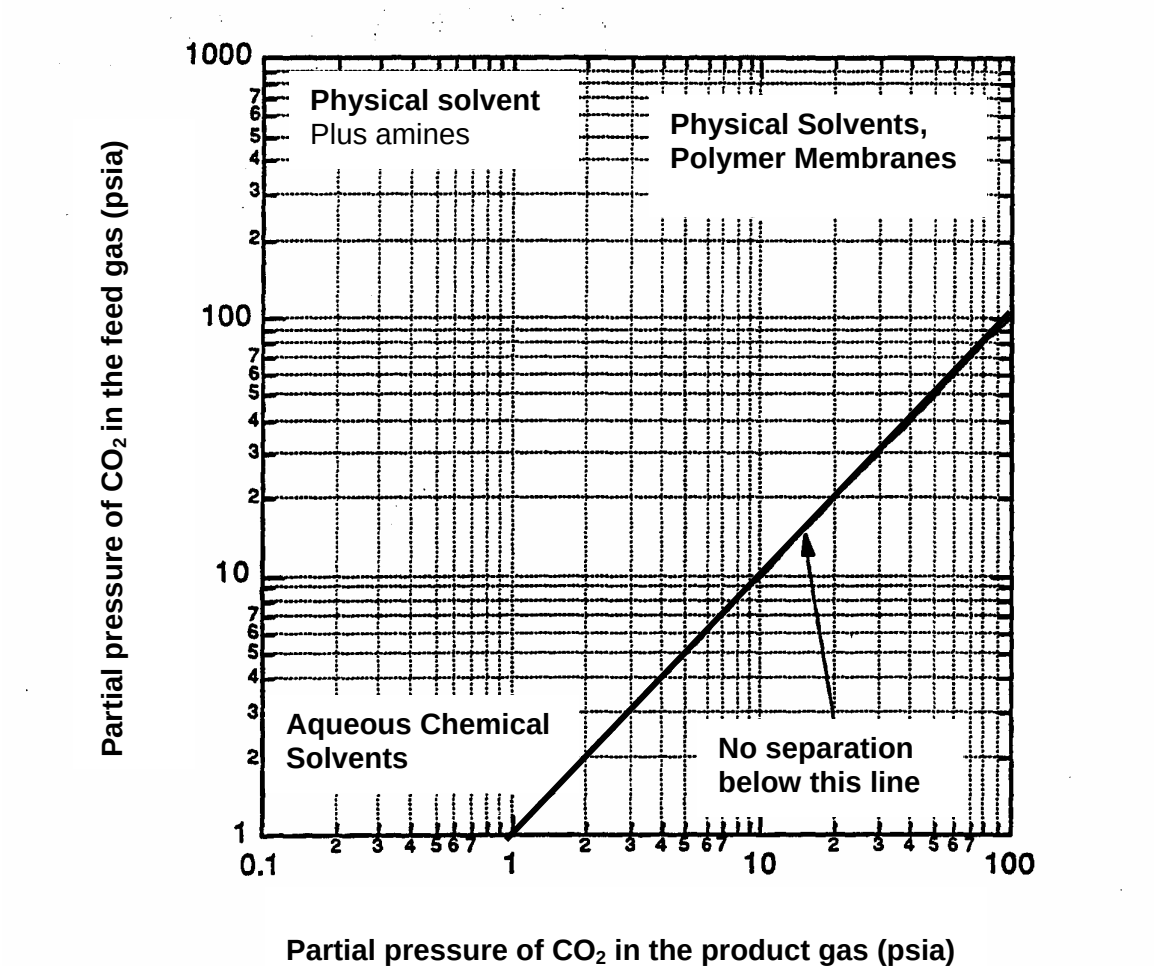

Fig. 1.1. Separation methods as function of feed and product CO_2 partial pressure specifications (Astarita, 1983).

alkanolamines. PVA and amines are both polar compounds. The electrostatic interaction of the hydroxyl groups of PVA with the amino group of amine is the reason for their solubility, *i.e*. amines is capable of forming hydrogen bonds with the PVA; and b) the amine must be non-volatile and reacts reversibly with CO_2. The properties of several alkanolamines are listed in Table 1.1.

Table 1.1. Physical Properties of Common Reagents used as Chemical Solvents for CO_2 (Kohl *et al.,* 1997)

Property	Monoethanolamine (MEA)	Diethanolamine (DEA)	Methyldiethanolamine (MDEA)	2-amino-2-methyl-1-propanol (AMP)
Mol. weight	61.09	105.14	119.17	89
Boiling point, ^{o}C				
101 kPa	171	decompose	247.2	165
6.7 kPa	100	187	164	–
1.3 kPa	69	150	128	–
Vapour pressure, kPa, 20 ^{o}C	0.05	0.001	0.001	0.13
Solubility in water, % wt at 20^{o}C	complete	96.4	complete	complete
Absolute viscosity, cps at 20^{o}C	24.1	380 (30 ^{o}C)	101	102(30^{o}C)
Heat of vaporization, Btu/lb at 101 kPa	355	288 (at 23mm Hg) (168.5^{o}C)	223	52.4 (110^{o}C)

A facilitated transport phenomenon is illustrated in Fig. 1.2. For the case of facilitated CO_2 transport, the carrier is dissolved into the membrane that separates the feed stream from the product /permeate stream. The feed stream is maintained at a certain pressure to maintain the carrier in its CO_2-carrier form while the permeate is at lower pressure to maintain the carrier in its uncomplex form. The carrier thus acts as a shuttle, picking CO_2 at the feed stream, diffusing across the membrane as CO_2-carrier complex, releasing CO_2 to the permeate stream, and then diffusing back to the feed side to repeat the process.

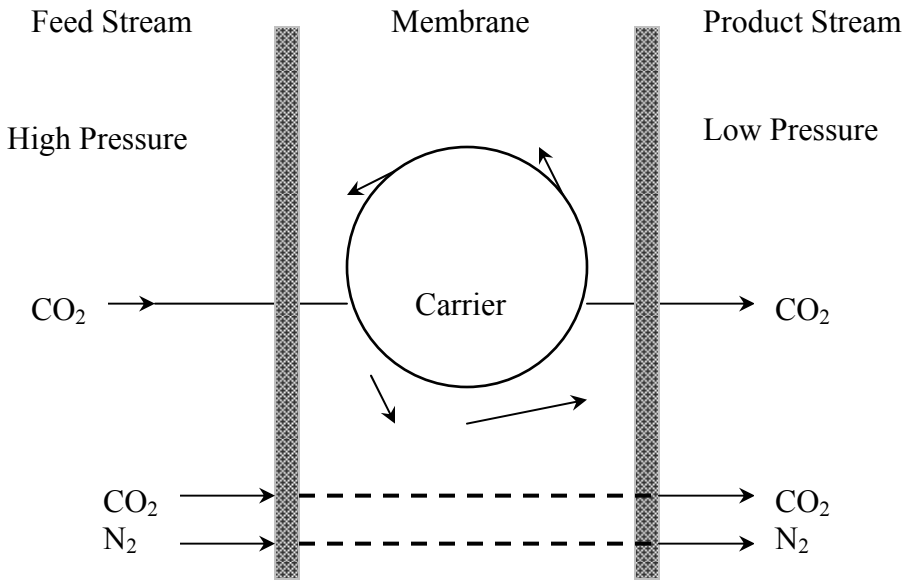

Fig. 1.2 Facilitated transport of CO_2 in the presence of a carrier in the membrane, along with transport of CO_2 and N_2 by ordinary solution-diffusion mechanism.

Because the carrier is specific to CO_2, the flux of CO_2 transport is enhanced with no or little effect on the flux of N_2, resulting in a higher CO_2 concentration on the permeate that

would not be possible in the absence of the carrier. Hence, the transport of CO_2 through facilitated membranes can be described as a four-step process:

a) CO_2 forms a complex at the feed side by reacting with a carrier present in the membrane,
b) the CO_2-carrier complex diffuses across the membrane,
c) CO_2 is released to the product stream,
d) the carrier is restored to its original forms or regenerated.

A detailed discussion of facilitated transport mechanism is provided in Chapter 2.3-2.4.

1.1 Objective of the Study

Facilitated transport membranes, in particular immobilized liquid membrane (ILM) for gas separation has attracted much attention as they have high selectivity compared to conventional polymeric membranes (Way, *et. al*. 1992). The common method of preparing an ILM is incorporating the carrier liquid in the membrane matrix by saturating a microporous polymeric membrane. The carrier liquid is held inside the pores of the polymeric support by surface tensions. These types of liquid membranes are usually operated by the sweep-gas to remove the permeate. The permeate side has nearly the same pressure as the feed side and a sweep gas usually helium carries the permeate. With this configuration, the ILM's need a small trans-membrane pressure differential due to its instability under a pressurized condition. In order for facilitated transport membranes to be economically viable, they need to be stable under a trans-membrane pressure conditions.

The main objective of this research is to develop a reactive membrane system to separate CO_2 from N_2. Such system should have a large CO_2 permeability in conjunction with high CO_2/N_2 selectivity, can withstand high trans-membrane pressure differentials and have long-term stability. The overall objective of this research is to develop a reactive membrane system for the separation of CO_2 from gas mixtures.

Specific objectives are:

1. Select a suitable reactive membrane system.
2. Optimize membrane preparation techniques.
3. Conduct permeation experiments with pure gases to characterize the membrane.
4. Determine its suitability and mass transfer characteristics by conducting permeation experiments with gas mixtures.
5. Analyze permeation results with the help of mass transport equations.

1.2 Organization of the Thesis

Chapter 1 presents an introduction to this study. The advantages of using facilitated transport membranes for gas separation are briefly discussed followed by the objective for this research. Short historical developments of facilitated transport membrane are discussed in Chapter 2. Theoretical discussions for the transport mechanism for both facilitated and un-facilitated transport and a review of recent development on these topics are also included in this chapter.

Detailed mechanisms and kinetics of the CO_2-DEA systems are presented in Chapter 3. The governing mass transport equations are analyzed in Chapter 4. Chapter 5 and 6 provide the experimental works carried out for this thesis. The numerical solutions to the transport equations are presented in Chapter 7. Finally, the overall conclusions along with contributions to research and recommendations for future works are summarized in Chapter 8. Derivations, sample calculations and other plots are presented in the appendices.

Chapter 2

Literature Review and Background

The historical development of facilitated transport/coupled transport is shown schematically in Fig. 2.1. This process originated in early experiments by biologists using natural carriers contained in the cell walls. As early as 1890, Pfeffer postulated transport properties in membranes using carriers. Perhaps the first facilitated transport experiment was performed by Osterhout, who studied the transport of ammonia across algae cell walls (Osterhout, 1935). By 1950's, the carrier concept was well developed, and investigators began to developed synthetic bio-membranes, analogues of the natural systems. For example, in the mid-1960's, Sollner and Shean (Bloch *et al.,* 1963) studied a number of coupled transport system using inverted U-tubes. At the same time, Bloch and Vofsi published the first of several papers in which coupled transport was applied to hydrometallurgical separations, namely, the separation of uranium using phosphate esters (Bloch *et al*., 1967). Because phosphate esters were also plasticizers for poly(vinyl chloride) (PVC), Bloch and Vofsi prepared immobilized liquid film by dissolving the esters in a PVC matrix. The PVC/ester film was cast on a paper support. Researchers actively pursued this work until in the late 1960's. At that time, interest in this approach slowed apparently because the fluxes obtained did not make the process competitive with the conventional separation processes. The interest at that time with the PVC matrix membranes was its utilization in ion selective membrane electrodes (Moody *et al*., 1979).

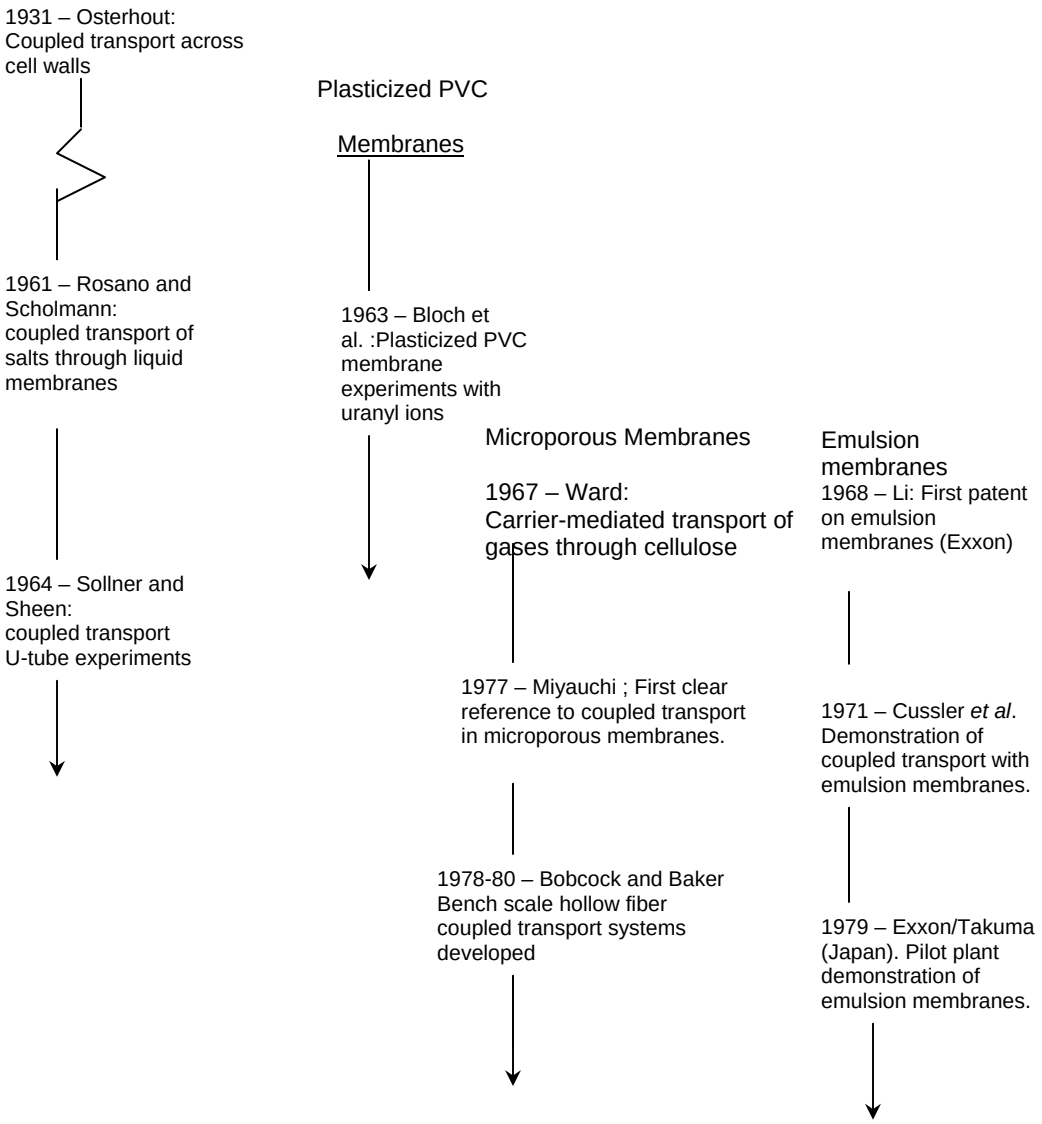

Fig. 2.1. Historical Development of Coupled/Facilitated Transport Membranes (Porter, 1990).

Table 2.1. First studies on facilitated transport systems for various gases.

Year	Gas	Carrier	Applications	References
1960	O_2	Hemoglobin, Fe, Co, Ru, Porphyrins, Ir, Mn complexes	O_2 enrichment for medical use, combustion, sewage treatment, welding and glass production	Basset and Shultz, 1960
1970	NO	Fe^{2+}		Ward, 1970
1967	CO_2	CO_3^{2-}, ethanolamines	Biogas purification, enhanced oil recovery, life support systems	Enns, 1967
1973	CO	Cu^{+}	Synthesis gas, purifications	Steighelman and Hughes, 1973
1977	H_2S	CO_3^{2-}	Gasification of coal, desulphurisation	Matson *et al*., 1977
1981	Olefins	Ag^{+}, Cu^{+}	C_2H_4 recovery	Hughes *et al*., 1981

In 1967, Ward and Robb reported the first study on the application of membranes with facilitated transport properties for gas separation. At that time, there were few gases for which suitable carriers were available and most effort has been dedicated to the clean up of acid gases. Table 2.1 shows some of the first investigations on facilitated transport system involving different gaseous permeates.

2.1 Recent Literature on the Separation of CO_2 from N_2 using Facilitated Transport Membranes.

Teramoto *et. al*. (2003) used polyethersulfone capillary ultrafiltration membrane substrate in which the carrier solution (MEA, DEA, or AMP) is forced to permeate through the membrane. In their experimental set-up (Fig.2.2), both the feed gas and the carrier solution are supplied to the lumen side (high pressure side, absorption side) of the capillary membrane module and the carrier solution is forced to permeate through membrane to the shell side (low pressure side, stripping side) which is maintained at low

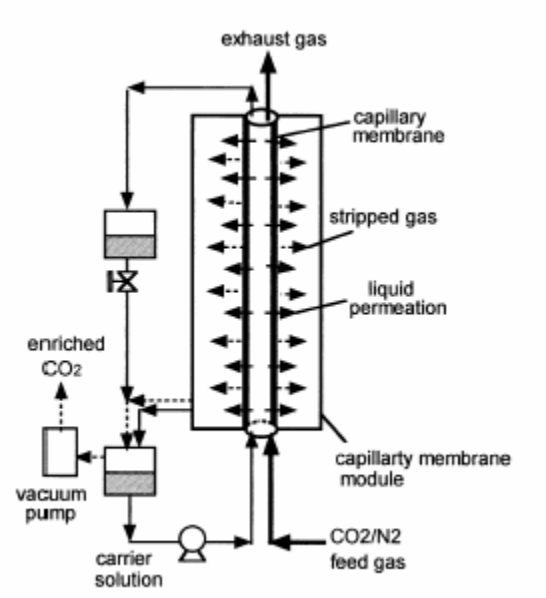

Fig.2.2Teramoto's set-up for the facilitated transport of CO_2 using capillary membrane module for simultaneous removal and enrichment of CO_2 (Teramoto, 2003).

pressure to strip and enrich the solute gas. The membrane system was tested for the separation of CO_2 and N_2. The feed side pressure was atmospheric and the permeate side was evacuated at about 10 kPa. They reported a selectivity of CO_2 over N_2 in the range of 430 to 1790 and claimed membrane stability over a period of one month. They proposed that the system is intermediate between a conventional gas absorption process and a facilitated transport membrane process.

In another paper, Kovvali and his coworkers (2002) used glycerol carbonate as a physical solvent for CO_2 separation from CO_2/N_2 mixtures. The CO_2-selective behavior of this solvent was investigated in an immobilized liquid membrane configuration. Hydrophilized poly(vinylidene fluoride) was employed as the substrate. They reported CO_2/N_2 selectivity in the range of 80-130 over large range of CO_2 partial pressures. Like any other set-up they also employed helium as the sweep gas in the permeate side. Addition of a small amount of facilitating carriers in the form of poly(amidoamine) dendrimer (generation 0) and sodium glycinate in the solvent significantly increased CO_2 facilitation at low CO_2 partial pressures (0.52 cm Hg). Likewise at high CO_2 feed partial pressures (30.27 cm Hg), they observed a loss of selectivity in the presence of the carriers. In that paper, they did not provide the kinetic and physical parameters of glycerol carbonate in the presence and absence of the carriers used in their study.

Poly(acrylic acid) / poly(vinyl alcohol) membrane was synthesized by Matsuyama *et al*. (2001) for the facilitated transport of CO_2.They used monoprotonated ethylenenediamine as the carrier of CO_2 which was incorporated into the membrane by ion exchange. The

membrane was reportedly highly swollen by the aqueous solution. The highest selectivity obtained was more than 1900 at CO_2 feed partial pressure of 6 kPa. The advantage of using ion exchange membranes as the support for the facilitated transport membrane is its ability to prevent membrane degradation. The reason is that immobilization of the ionic carrier in the ion-exchange membrane by an electrostatic force will prevent the washout and reduce the evaporative loss of the carrier. The important parameters that affect membrane performance are the ion-exchange capacity and water content

Based on the research work that are reported in the literature on facilitated transport membranes, it is clear that the permeate side of the membrane unit is under vacuum or swept with a helium stream to ensure that trans-membrane pressure is small. In this research, the permeate side is simply vented to the atmosphere.

Park *et al*. (2001) prepared a water-swollen hydrogel membranes for the separation of CO_2 from N_2. The membranes were prepared by dip-coating asymmetric porous polyetherimide membrane supports with poly(vinyl alcohol) – glutaraldehyde, where glutaraldehyde is acting as the cross linking agent. The permeate side of the membrane unit is under vacuum. They reported a CO_2/N_2 separation factor of 80 at room temperature. They also investigated the effect of additive, potassium bicarbonate and catalyst, sodium arsenite, on the permeation performance of the swollen membranes.

2.2 Gas Separation through Nonporous Membrane

Gas separation through nonporous membranes depend on the differences in the

permeabilities of various gases through a given membrane. The Fick's law is the simplest description of gas diffusion through a nonporous structure (Mulder, 1996),

$$N = -D\frac{dc}{dz} \tag{2.1}$$

where N is the flux through the membrane, D is the diffusion coefficient and the driving force dc/dz is the concentration gradient across the membrane. Assuming concentration independence of diffusion coefficient, under steady-state conditions this equation can be integrated to give:

$$N = \frac{D\left(C^0 - C^L\right)}{L} \tag{2.2}$$

where C^0 and C^L are the concentration of the gas in the membrane on the feed side and permeate side, respectively and L, is the thickness of the membrane.

The concentration of a gas dissolved in membrane is related to the partial pressure of the gas. When the gas pressure is not too high, there is a linear relationship between the gas concentration inside the membrane and the partial pressure of the gas outside the membrane,

$$C = H.p \tag{2.3}$$

where H is the solubility coefficient and p is the pressure of gas. Combining eq. (2.2) with eq. (2.3) gives:

$$N = \frac{DH\left(p^0 - p^L\right)}{L} \tag{2.4}$$

an equation which is generally used for the description of gas permeation through membranes. The product of the diffusion coefficient D that provides a measure of effective mobility of the penetrant in the polymer matrix and the solubility coefficient H which gives a measure of the amount of penetrant sorbed by the membrane under equilibrium conditions is called the permeability coefficient,

$$P = D.H \tag{2.5}$$

so that eq. (2.4) can be written as:

$$N = \frac{P\left(p^0 - p^L\right)}{L} \tag{2.6}$$

The permeation flux across a membrane as described by eq.(2.6) is proportional to the difference in partial pressure and inversely proportional to the membrane thickness.

Permeability is an important factor in determining the effectiveness of the membrane. The second important index of the performance of the membrane material is the separation factor of the membrane for component A relative to B and defined as:

$$\alpha_{A/B} = \frac{y_A / y_B}{x_A / x_B} \tag{2.7}$$

where y_A and x_A refer to the mole fractions of component A in the permeate and feed side, respectively. When the permeate pressure is negligible, $\alpha_{A/B}$ is equal to the ideal separation factor, $\alpha^*_{A/B}$:

$$\alpha^*_{A/B} = \left[\frac{D_A}{D_B}\right]\left[\frac{H_A}{H_B}\right] \tag{2.8}$$

where D_A/D_B is the diffusivity selectivity, and H_A/H_B is the solubility selectivity. The solubility selectivity is determined by the differences in the condensability of the two penetrants and by their interaction with membrane materials. The diffusivity selectivity is based on the inherent ability of the polymer matrices to function as size and shape selective media through segmental mobility. The permeability coefficient is often given in Barrer units. 1 Barrer = 10^{-10} cm^3(STP).cm/cm^2.s.cmHg = 0.76 x 10^{-7} m^3(STP).m/m^2.s.Pa.

Generally, the diffusion coefficient decreases with increasing molecular size because large molecules interact with more segments of the polymer chains than do small molecules, favouring the transport of small molecules such as nitrogen over the large one such as propane. However, solubility increases with increasing condensability and therefore increases with increasing molecular size. The effect of increasing permeant size on permeability is balanced between the opposing effects of the diffusion coefficient,

which decreases with increasing size, and the solubility, which increases with increasing size. This balance determines the selectivity of a membrane for any pair of gases.

The solution–diffusion mechanism is generally accepted to describe the transport of gases through all commercially important nonporous membranes. The mechanism involves the following steps (Wijmans *et al.,*1995): (a) sorption of the gas at one surface of the membrane, (b) dissolving of the gas into the membrane material, (c) diffusion of the gas through the membrane, (d) release of the gas from solution at the opposite surface of the membrane, and (e) desorption of the gas from the surface.

2.2.1 Effect of Temperature on Gas Permeation in Membranes

The temperature dependence of diffusion coefficient can be represented in an Arrhenius form (Barrer, R.M. and Chio, H.T., 1965):

$$D = D_o \, exp\left(-E_d / RT\right) \tag{2.9}$$

where E_d is the activation energy of diffusion and D_o is a constant. The activation energy is the average energy that must be localized next to the penetrant to generate a sufficiently large opening to permit the molecule to execute a jump. A similar relationship exists for the solubility coefficient:

$$H = H_O \, exp\left(-\Delta S_S / RT\right) \tag{2.10}$$

where ΔS_S is the heat of solution. Since the permeability is the product of solubility and diffusivity (eq.2.5), combining eqs. 2.9 and 2.10 gives the temperature dependence of the permeability coefficient (Barrer, R.M., 1965):

$$P = P_O \, exp\left(-E_p / RT\right) \tag{2.11}$$

where $$P_O = H_O D_O \tag{2.12}$$

$$E_p = \Delta S_S + E_d \tag{2.13}$$

E_p is the apparent activation energy for the permeation process.

2.2.2 Effect of Plasticization

According to the solution-diffusion mechanism, the diffusion and solubility coefficient are independent of the concentration of penetrant dissolved in the membrane. So that the permeability coefficient would not change with feed pressure. However, this happens only for non-condensable light gases such as N_2 and He. For larger and condensable gases such as CO_2, the permeability coefficient was found to be pressure or concentration dependent. It could be an exponential or linear function of pressure (Merkel, *et.al.*, 2000). Accordingly, the presence of the penetrant molecules in the membrane would increase the local segmental mobility of the polymer chain causing an increase in the penetrant diffusivity.

2.3 Description of Facilitated Transport Membrane

As discussed before, the commonly accepted mechanism for the transport of a penetrant in nonporous polymer membranes is solution-diffusion. Facilitated transport membranes also involve penetrant solubility and diffusion and in addition a reversible complexation reaction. The addition of complexation reaction makes facilitated transport similar to a chemical absorption process on the feed (high partial pressure) side of the membrane and a stripping (desorption) process on the product (permeates) side of the membrane. Facilitated transport has several general characteristics (Cussler, 1997):

a) high fluxes and selectivity because the mobile carrier selectively reacts with the diffusing solute,
b) the fluxes reaches a constant value at high solute concentrations due to insufficient carrier molecules available to react with all the available solutes,
c) fluxes are strongly coupled when two diffusing solutes react competitively with the mobile carrier and can be easily poisoned by irreversible reaction with the carrier.

The total mass transfer rate of the gas that reacts with the carrier is the sum of the flux of the carrier-gas complex and the flux of the free gas. In the limit of fast reactions, the rate of mass transfer is controlled by diffusion, while the reaction rate controls the mass transfer rate when the complexation reaction is slow. In between these two limiting regimes, the contribution of both reaction and diffusion are important. The reactive carrier mechanism is the reason that the flux of facilitated transport membranes is not always proportional to the driving force across the membrane. At very high driving

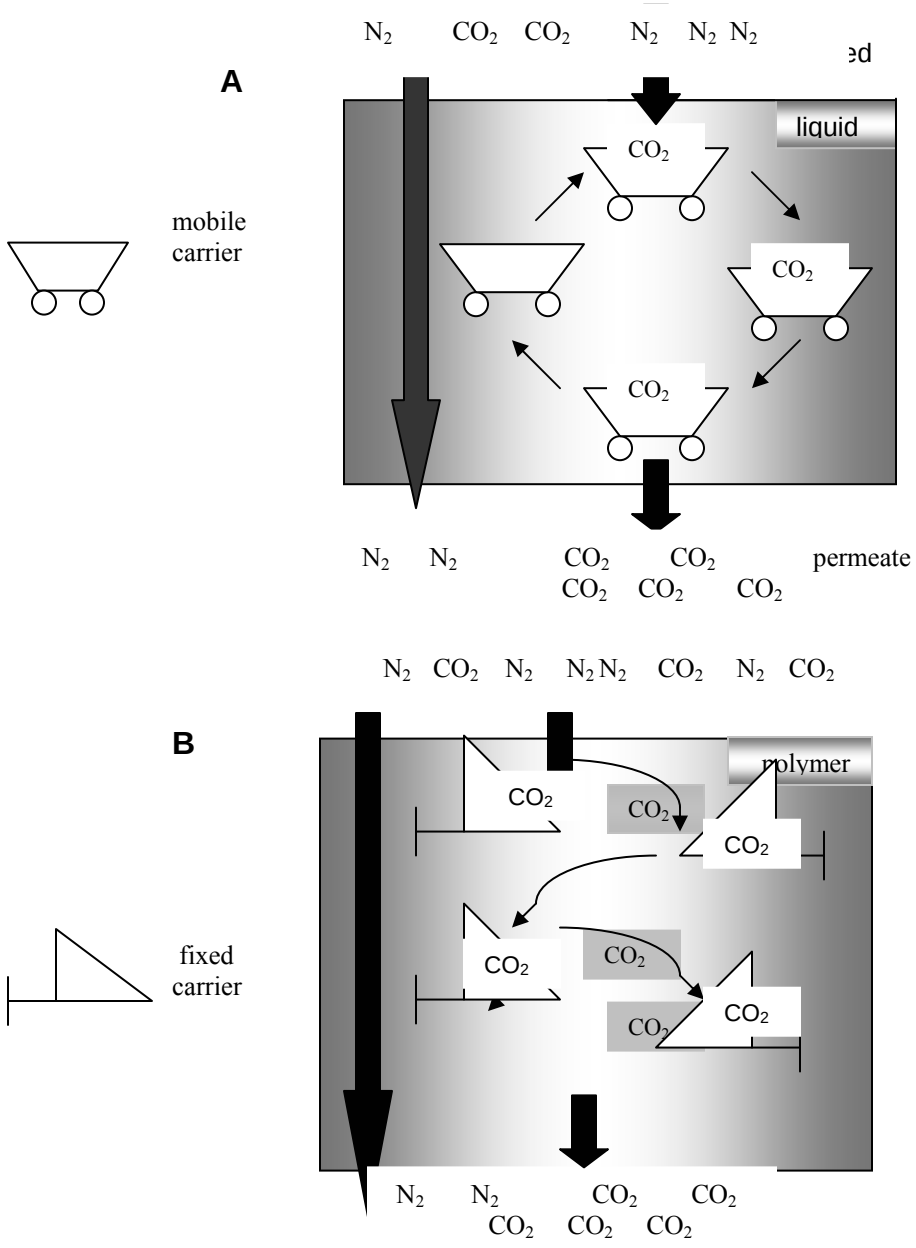

Fig. 2.3. Scheme for facilitated transport of gaseous molecules by a carrier through a membrane: (A) liquid membrane with a mobile carrier, (B) solid membrane with fixed carrier (Figoli *et al.*, 2001).

forces, all the carrier species are bound to solute molecules and an increase in driving force does not result in an increased flux from the reactive pathway. This condition is known as carrier saturation, which means that all available carrier has tied-up with the solute. At very low driving force conditions, the flux due to the solution-diffusion mechanism is very small, and the mass transport is mainly due to the diffusion of the carrier-gas complex. As the driving force decreases further, the flux of the uncomplexed gas molecules decreases much faster than the carrier transport. Therefore, the flux is also not directly proportional to the driving force when it is small.

In the case of polymeric membranes, the carrier can be chemically or physically bound to the solid matrix (fixed carrier system), whereby the solute hops from one site to the other. Mobile carrier molecules have been incorporated in liquid membranes, which consists of a solid polymer matrix (support) and a liquid phase containing the carrier molecules as shown in Fig 2.3 (Figoli *et al.*, 2001).

2.4 Properties of Carriers for Facilitated Transport Membranes

The selection of an appropriate carrier for a given separation depends on a variety of factors that are specific to the separation process. The following sections discuss some of the general characteristics of carriers most suited for chemical complexation in separation process.

2.4.1 Reactivity and Bonding

The carrier must undergo a reversible chemical reaction with the permeate, and this reaction must be selective with respect to other components of the mixture:

$$A + B \underset{k_r}{\overset{k_f}{\rightleftharpoons}} C \tag{2.14}$$

where $K_{eq} = \frac{k_f}{k_r}$ (2.15)

As shown in eq. (2.15), a parameter referred to as equilibrium factor, K_{eq}, provides a measure of the complexation reaction. Kemena *et. al*.(1983) reported an optimal value of this parameter close to 10 for a large number of conditions based on the results of their modeling studies. Their calculations suggested that the enthalpy of complexation reaction that will be useful for facilitated transport is between –17 and – 40 kJ/mol. These enthalpies corresponds to a relatively weak bond between the carrier and the permeate. Reactions are difficult to reverse without energy inputs for bond energies above 50 kJ/mol (King, 1987). Covalent bonds that holds organic molecules together range from 200-500 kJ/mol. So it can be inferred that types of bonding interactions that will be most useful for the facilitated transport include acid-base interactions (Brønsted-Lowry and Lewis), coordinate covalent bonds (bonds involving complex metal ions), and probably van der Waals interactions (see Fig.2.4).

The second important aspect for the complexation reaction is the degree of reversibility. A given value for $\boldsymbol{K_{eq}}$ is reflected in the magnitude of $\boldsymbol{k_r}$. Modeling studies indicate that

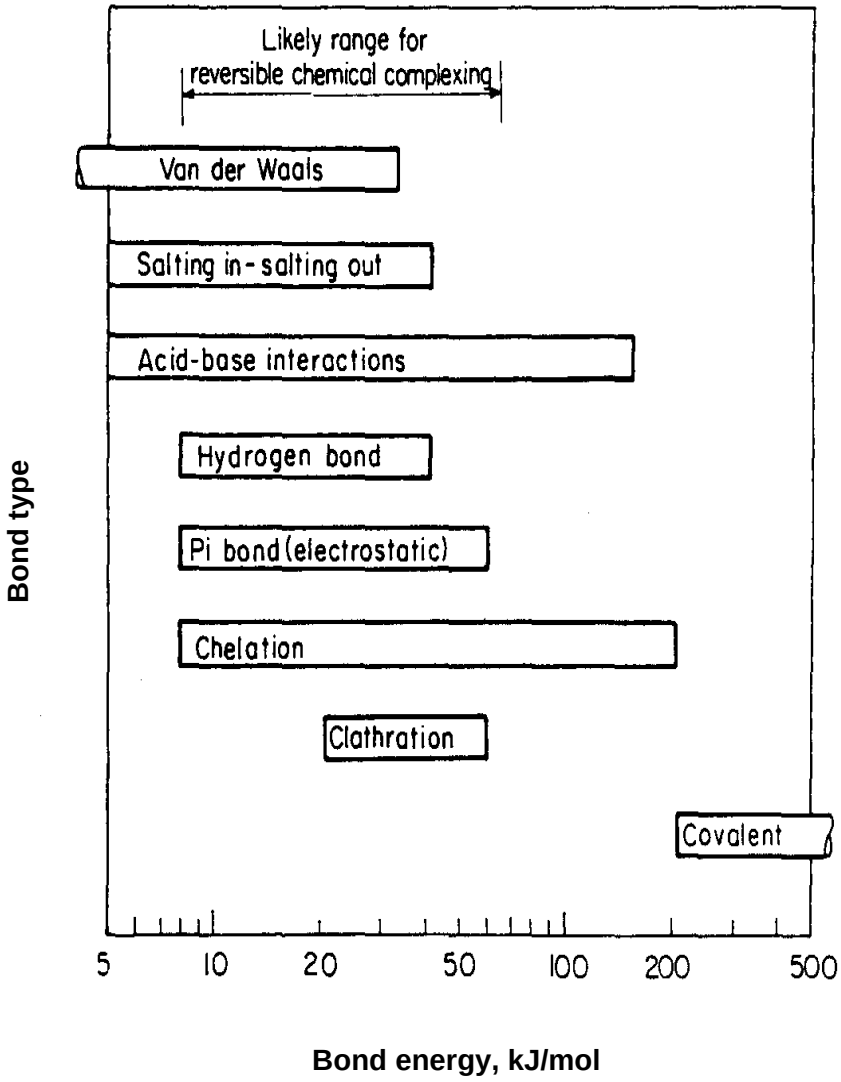

Fig.2.4 Types of bond and energies most suited for chemical complexation in separation process (King, C.J., 1987).

k_r should be large for good facilitation. If the bonding formed between the carrier and the permeate are not strong as mentioned above, satisfactorily large values of k_r should be

attainable in many cases. The k_r must be large enough to readily reverse the complexation process so that the carrier can be recycled without energy inputs.

In addition, a carrier should have: a) no side reactions, b) no irreversible or degradation reactions that may result to reduction of system capacity and long-term stability.

2.4.2 Solubility and Stability in the Membrane Phase

Basically, the more the carrier that is incorporated to the membrane, the greater the facilitative transport. However, too much presence of carrier molecules in the membrane may result to crowding that will depress the transport of the physically dissolve permeate. One way to attain high solubility is to use a carrier that is compatible with membrane matrix. In this research, poly(vinyl alcohol) and diethanolamine (DEA). The hydroxyl group of the PVA is capable of forming a hydrogen bond with the amino group of DEA. In other cases, structural modification of either the carrier or the membrane matrix can be performed to increase its solubility without altering the essential features of the complexation reaction (Matsuyama, *et.al*., 1996; Hess, *et.al*., 2006; Choi *et. al*., 2006).

Carriers for facilitated transport need to be stable with respect to the following principal factors: a) physical removal of the carrier from the membrane matrix when high trans-membrane pressure differential is applied, b) evaporation of the carrier with time and c) undesirable chemical reactions or irreversible products of reaction. Entrapment of the carrier to the membrane matrix is one way to avoid the carrier to be pushed out of the

matrix when high trans-membrane pressure differential is applied. Using carriers with high heat of vaporizations is a good approach to prevent loss due to evaporation.

Chapter 3

CO_2 –Amine Chemistry

Before the analysis diffusion-reaction transport equations, it is necessary at this stage to discuss the mechanisms and kinetics of the reaction of CO_2 with DEA.

Several authors have investigated the chemistry of CO_2-amine solutions over the years due to its important industrial application for the removal of CO_2 from gas streams. The overall reaction between CO_2 and primary or secondary amines is

$$CO_2 + 2R_1R_2NH \rightleftharpoons R_1R_2NH_2^+ + R_1R_2NCO_2^- \qquad (3.1)$$

where $\boldsymbol{R}$ represents the functional groups (for MEA, $\boldsymbol{R_1}$ = -H, $\boldsymbol{R_2}$ = $-CH_2CH_2OH$; for DEA, $\boldsymbol{R_1} = \boldsymbol{R_2} = -CH_2CH_2OH$). The Dankwerts' zwitterion mechanism has recently become one of the most widely accepted mechanism for primary and secondary amine reaction with CO_2 (Blauwhoff *et al*., 1984; Versteeg and Van Swaaij, 1988; Versteeg *et al*., 1990; Versteeg and Oyevaar, 1989; Glasscock *et al*., 1991; Little *et al*., 1992).

For the DEA, the diversity of results for the order of reaction with respect to the amine leads to reaction schemes that are quite different. When the reaction is first order, it results in the formation of carbamic acid that ionizes completely and immeadiately:

$$CO_2 + R_1R_2NH \longrightarrow R_1R_2NCOOH \quad (3.2)$$

$$R_1R_2NCOOH \longrightarrow R_1R_2NCOO^- + H^+ \quad (3.3)$$

$$R_1R_2NH + H^+ \longrightarrow R_1R_2NH_2^+ \quad (3.4)$$

In the above scheme, reactions (3.2) and (3.3) are instantaneous, and the rate determining step is reaction (3.4). Coldrey and Harris (1976) postulates diverse reactions which are competitive: reactions (3.2) to (3.4) lead to the formation of carbamate, and the reaction:

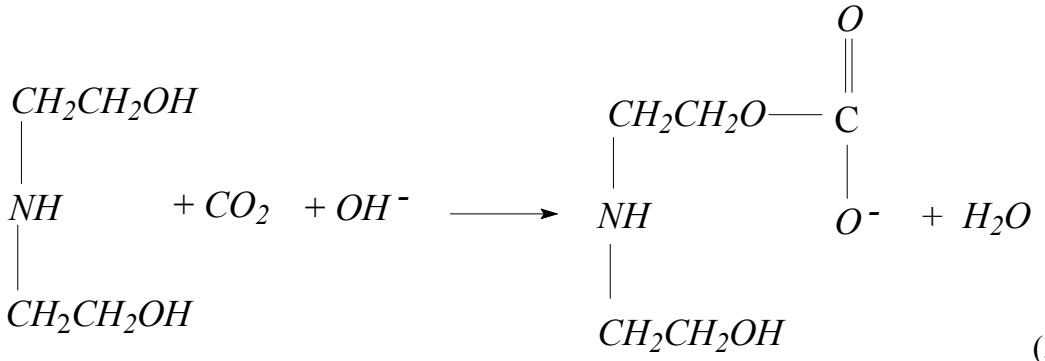

(3.5)

forms an alkyl carbonate, that will in turn decomposes into CO_2 and amine.

Hikita *et.al*. (1977) propose the formation of a dimer of the DEA, followed by the formation of a carbamate of this dimmer which ionizes. In this scheme,

$$2R_1R_2NH \longrightarrow (R_1R_2NH)_2 \quad (3.6)$$

$$CO_2 + (R_1R_2NH)_2 \longrightarrow R_1R_2NH_2\,NCOOR_1R_2 \quad (3.7)$$

$$R_1R_2NH_2NCOOR_1R_2 \longrightarrow R_1R_2NH_2^+ + R_1R_2NCOO^- \quad (3.8)$$

Reaction (3.7) would be the rate-limiting step.

Finally, Dankwerts (1979) suggested the zwitterion mechanism to describe the CO_2 amine reactions.

3.1 Dankwerts Mechanism for Primary and Secondary amines

Dankwerts (1979) reintroduced a mechanism proposed originally by Caplow (1968) that describes the reaction between CO_2 and alkanolamines. The reaction mechanisms involves two steps: a) the formation of a zwitterion intermediate and b) followed by the removal of a proton by a base.

$$CO_2 + R_1R_2NH \xrightarrow{k_1} R_1R_2NH^+CO_2^- \quad (3.9)$$

$$R_1R_2NH^+CO_2^- + B \xrightarrow{k_2} R_1R_2NCO_2^- + BH^+ \quad (3.10)$$

where B represents all the bases present. The extremes of the overall reaction order can be demonstrated in terms of the rate limiting step of the above reactions. When reaction (3.9), is considered the rate limiting step, reaction (3.10) does not affect the overall reaction kinetics and, if we assume elementary reaction kinetics, the reaction rate becomes:

$$r_{CO_2} = k_1[CO_2][R_1R_2NH] \tag{3.11}$$

where the pair of brackets represents concentration. The overall reaction rate is second order and first order with respect to the amine concentration. However, if reaction (3.10) becomes the rate limiting, the reverse reaction of reaction (3.9) becomes important. The reverse reaction of reaction (3.9) is much faster than the second step and equilibrium is established between $\boldsymbol{CO_2}$, $\boldsymbol{R_1R_2NH}$ and $\boldsymbol{R_1R_2NH^+CO_2^-}$ according to the following reaction mechanism

$$CO_2 + R_1R_2NH \underset{k_2}{\overset{k_1}{\rightleftharpoons}} R_1R_2NH^+CO_2^- \tag{3.12}$$

$$R_1R_2NH^+CO_2^- + B \xrightarrow{k_3} R_1R_2NCO_2^- + BH^+ \tag{3.13}$$

The equilibrium constant for reaction (3.12) can be defined as:

$$K_{eq} = \frac{k_1}{k_2} = \frac{[R_1R_2NH^+CO_2^-]}{[CO_2][R_1R_2NH]} \tag{3.14}$$

Eq. (3.14) can be rearranged for the zwitterions concentration to give:

$$[R_1R_2NH^+CO_2^-] = K_{eq}\,[CO_2]\,[R_1R_2NH] \tag{3.15}$$

Substitution of the zwitterions concentration of eq. (3.15) into the expression for the rate of formation of the carbamate ($R_1R_2NCO_2^-$) gives:

$$r_{carbamate} = -r_{CO_2} = K_{eq}\, k_3 [CO_2][B][R_1R_2NH] \qquad (3.16)$$

Eq. (3.16) indicates that the overall reaction is third order. The reaction rate becomes second-order with respect to the amine when the deprotonating base is considered to be the amine.

In order to explain the intermediate order, Dankwerts (1979) proposed the application of the quasi-steady state approximation for the intermediate zwitterion. This approximation assumes that the rate of zwitterion formation is equal to its depletion so that the net reaction rate of the zwitterion is zero:

$$r_{zwitterion} = k_1[CO_2][R_1R_2NH] - k_2\left[R_1R_2NH^+CO_2^-\right] - k_3\left[R_1R_2NH^+CO_2^-\right][B] = 0 \qquad (3.17)$$

Eq. (3.17) can be rearranged to determine the concentration for the zwitterions:

$$\left[R_1R_2NH^+CO_2^-\right] = \frac{k_1[CO_2][R_1R_2NH]}{k_2 + k_3[B]} \qquad (3.18)$$

Eq. (3.18) can be substituted for rate expression for the formation of carbamate to give:

$$r_{carbamate} = -r_{CO_2} = \frac{[CO_2][R_1R_2NH]}{\frac{1}{k_1} + \frac{k_2}{k_1 \sum k_3[B]}} \tag{3.19}$$

where $\sum k_3[B]$ is the contribution to the removal of the proton by all bases present in the solution. Eq. (3.19) can be simplified for two extreme cases:

a) the second term in the denominator is << $1/k_1$. This results in a simple second-order kinetics, which is the case, observed experimentally for aqueous MEA solutions:

$$r_{CO_2} = -k_1[CO_2][R_1R_2NH] \tag{3.20}$$

b) The second term in the denominator is >> $1/k_1$. This results in a more complex expression of kinetics:

$$r_{CO_2} = -\frac{k_1}{k_2}[CO_2][R_1R_2NH]\sum k_3[B] \tag{3.21}$$

Eq. (3.21) shows that it is possible that the overall reaction order is three. In the transition region between two asymptotic cases, the overall reaction order changes between two and three. Hence, the Dankwerts' reaction mechanism covers the shifting reaction orders for the reaction between CO_2 and various primary and secondary amines.

For a reversible reaction particularly for secondary amines, the Dankwerts mechanism is:

$$CO_2 + R_1R_2NH \underset{k_2}{\overset{k_1}{\rightleftharpoons}} R_1R_2NH^+CO_2^- \tag{3.22}$$

$$R_1R_2NH^+CO_2^- + R_1R_2NH \underset{k_4}{\overset{k_3}{\rightleftharpoons}} R_1R_2NCO_2^- + R_1R_2NH_2^+ \tag{3.23}$$

The expression for the rate of zwitterion formation with application of the quasi-steady gives:

$$r_{zwitterion} = k_1C_AC_B - k_2C_{Z^*} - k_3C_{Z^*}C_B + k_4C_CC_D = 0 \tag{3.24}$$

where the subscripts $\boldsymbol{A = CO_2}$, $\boldsymbol{B = R_1R_2NH}$, $\boldsymbol{C = R_1R_2NCO_2^-}$, $\boldsymbol{D = R_1R_2NH_2^+}$, $\boldsymbol{Z^* = R_1R_2NH^+CO_2^-}$ and $\boldsymbol{C_i}$ represents the concentration of each specie. So that the expression for the concentration of zwitterion:

$$C_{Z^*} = \frac{k_1C_AC_B + k_4C_CC_D}{k_2 + k_3C_B} \tag{3.25}$$

The rate expression for the formation of CO_2 is:

$$r_A = k_3C_{Z^*}C_B - k_4C_CC_D \tag{3.26}$$

Substituting Eq. (3.25) into Eq. (3.26) gives:

$$r_A = k_3 C_B \left[\frac{k_1 C_A C_B + k_4 C_C C_D}{k_2 + k_3 C_B} \right] - k_4 C_C C_D \tag{3.27}$$

$$r_A = \frac{k_1 k_3 C_A C_B{}^2 - k_4 k_2 C_C C_D}{k_2 + k_3 C_B} \tag{3.28}$$

The right hand side Eq. (3.28) can be simplified by multiplying both the numerator and denominator by $\left(\frac{1}{k_1 k_3 C_B} \right)$ to give:

$$-r_A = \frac{C_A C_B - \left(\frac{k_2 k_4 C_C C_D}{k_1 k_3 C_B} \right)}{\frac{k_2}{k_1 k_3 C_B} + \frac{1}{k_1}} \tag{3.29}$$

Eq. (3.29) is the rate expression for the formation of CO_2 that will be used in this study.

Chapter 4

Analysis of Diffusion-Reaction Transport Equations

In this chapter, a transport equation based on simultaneous process of diffusion and chemical reaction in the facilitated transport is analyzed. In the analysis, it was assumed that CO_2 is diffusing steadily across a thin membrane and react reversibly with the DEA present in the thin membrane. Also, the presence of PVA in the membrane was assumed to have a negligible effect on the transport of the species involved. The Dankwerts mechanism discussed in Chapter 3 was used to illustrate the reaction of CO_2 with DEA.

4.1 Analysis of the Transport Mechanism

A membrane with flat plate geometry is considered and one-dimensional transport perpendicular to the membrane surface was assumed as shown in Fig.(4.1). At steady state, conservation of each of the species is governed by an equation of the form:

$$\frac{dN_i}{dz} = -r_i \qquad (4.1)$$

where N_i is the flux of species i , r_i is the reaction rate and **z** is the coordinate in the direction of transport. The flux of species i can be described by Fick's law:

$$N_i = -D_i \frac{dC_i}{dz} \tag{4.2}$$

The reaction of CO_2 and secondary amines resulted in the formation of ions in the form of carbamates *($R_2NCO_2^-$)* and protonated amines *($R_2NH_2^+$)*. When ionic species are involved in the transport, a flux expression due to elelectric field should be added to the Fick's equation. The flux of these ionic species can be described by the Nernst-Plank equation expressed as follows (Newman, 1991):

$$N_j = N_J^{dif} + N_J^{mig} = -D_j \frac{dC_j}{dz} - \mu_j C_j Z_j \Pi \frac{d\phi}{dz} \tag{4.3}$$

where μ_j ($m^2.mol.J^{-1}.s^{-1}$) is the mobility of the ion *j* which denotes the average velocity of a species in the solutuion when acted upon by a force of 1 Newton.mol^{-1}, Π = 96,485 C.mol^{-1} is the Faraday's constant, *Zj* is the ionic valence of species *j* and ϕ (volts, V) is the electrical potential. The second term in the right-hand side of eq. (4.3) represents the motion of the ionic species under the influence of the electric field, $d\phi/dz$ .The electric field results from a departure from electrical neutrality because the more mobile ions diffuse ahead of the less mobile ions and the electric field produced acts as a restoring force to speed up the less mobile ions and to slow down the more mobile ions.

Going back to the CO_2-amine system, electroneutrality must therefore be satisfied, i.e.

$$\int_0^L \sum \left(Z_j C_j \right) dz = 0 \tag{4.4}$$

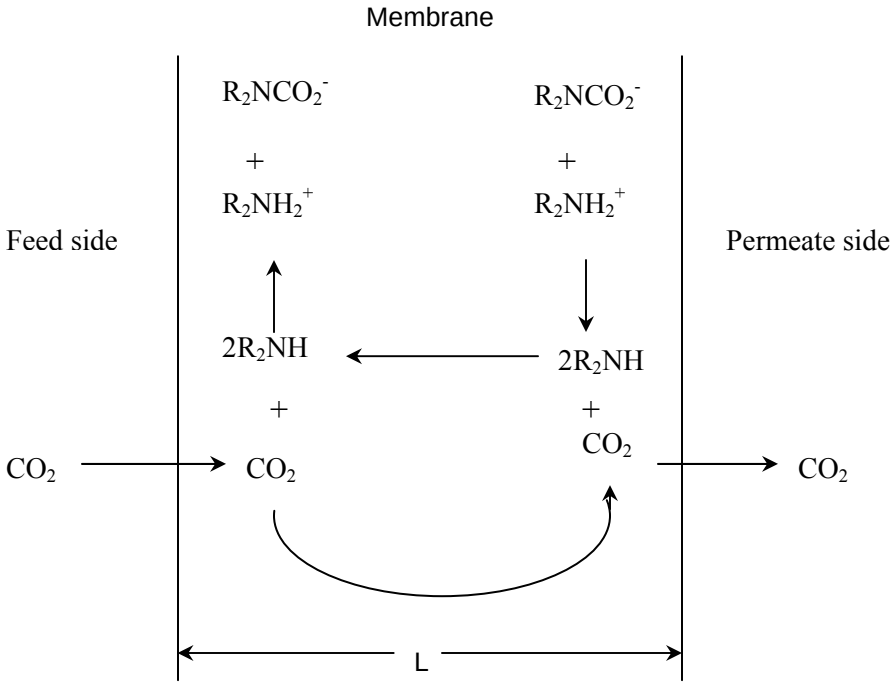

Figure 4.1. Schematic diagram of facilitated transport of CO_2 through a membrane containing amine.

Thus,

$$\int_0^L \left(C_D - C_C \right) dz = 0 \tag{4.5}$$

where C_C and C_D represent the $R_2NCO_2^-$,and $R_2NH_2^+$ respectively. Meldon *et. al*. (1982) suggested that the assumption of electroneutrality is satisfied if the membrane thickness is larger than the average separation distance between the the positive and negative ions. This distance is known as Debye length which is defined as:

$$\lambda = \sqrt{\frac{\delta RT}{\Pi^2 \left(C_C + C_D\right)}} \tag{4.6}$$

where δ = 695.4 x 10^{-12} $C^2.J^{-1}.m^{-1}$ is the permittivity for water, R = 8.314 $J.mol^{-1}.K^{-1}$ is the ideal gas constant. For the system under study, $C_C + C_D$ = 1.5 molar. So that the estimated Debye length is 3.5 x 10^{-4} μm. The average membrane thickness without the support is approximately 20 μm, far greater than the estimated Debye length.

With the condition of electroneutrality now satisfied within the membrane, the concentration of carbamates and the protonated amines are equal and Eq. (4.5) can be integrated to give:

$$C_D = C_C \tag{4.7}$$

Another assumption to be considered is that the diffussion coefficient of amine (B), carbamates (*C*) and the protonated amines (*D*) are equal,

$$D_B = D_C = D_D \tag{4.8}$$

A widely used correlation for diffusivity coefficient is Wilke-Chang equation (Poling *et al.,*2000):

$$D_{ab} = \frac{7.4 \times 10^{-8} (\omega M_b)^{0.5} T}{\eta_b V_a^{0.6}} \tag{4.9}$$

where D_{ab} ($cm^2.s^{-1}$) is diffusion coefficient of solute *a* in solvent *b*, M_b ($g.mol^{-1}$) is molecular weight of solvent *b*, η (centipoise, cP) is viscosity of solvent *b*, V_a ($cm^3.mol^{-1}$) is the molar volume of solute *a* at its *normal boiling temperature*, ω (dimensionless) is the association factor for solvent *b* to define the molecular weight of the solvent with respect to the diffusion process, Wilke and Chang recommended that ω be chosen as 2.6 if the solvent is water and 1.0 if it is unassociated, and *T*(K) is the temperature.

From Eq. (4.9), it is shown that the diffusion coefficient depends on the ratio of the square root of the molecular weight and the molar volume of the solute raised to the power of -0.6. Table 4.1 compares the molecular weight and estimated molar volumes for *DEA*, $R_2NCO_2^-$ and $R_2NH_2^+$.

As shown in Table 4.1, the relative differences in the properties of these species are small which is an indication that their diffusivity coefficients can be assumed to be equal. So that the electrical potential term Eq. (4.3) can be neglected and the flux can be assumed to be due to Fickian diffusion only. With the diffusivity coefficient constant, the continuity equation becomes:

$$D_i \frac{d^2 C_i}{dz^2} = r_i \qquad (i = CO_2,\ R_2NH,\ R_2NCO_2^-,\ R_2NH_2^+) \tag{4.10}$$

where r_i represent the reaction rate of species i.

Table 4.1. Comparison of the molecular weight and molar volume for amine and amine based species.

Species	Mol. Weight, M g/mol	Molar volume[a] $(Vb)^{-0.6}$ $(mol/cm^3)^{0.6}$
$(CH_2CH_2OH)_2NH$	105	0.0549
$(CH_2CH_2OH)_2\ NCO_2^-$	148	0.0516
$(CH_2CH_2OH)_2NH_2^+$	106	0.0547

a) Estimated by the additive volume method suggested by Schroeder (Poling *et.al*.,2000).

4.2 Boundary Conditions

The boundary conditions on CO_2 are:

$$\text{at } z = 0, \quad C_A = C_A^0 \qquad \text{at } z = L, \quad C_A = C_A^L \tag{4.11}$$

From Henry's law,

$$C_A = H_A p_A \tag{4.12}$$

where p_A and H_A are the partial pressure and the Henry's constant for CO_2 in amine solution, respectively. Therefore,

$$\text{at } z = 0,\ C_A^0 = H_A p_A^0, \qquad \text{at } z = L,\ C_A^L = H_A p_A^L \tag{4.13}$$

The amine and the amine complexes are not allowed to cross the boundaries of the membrane, hence their fluxes must be zero at $z = 0$ and $z = L$, or

$$\frac{dC_B}{dz} = \frac{dC_C}{dz} = \frac{dC_D}{dz} = 0 \tag{4.14}$$

The conservation of the amine in the membrane can be expressed as

$$\int_0^L (C_B + C_C + C_D)dz = C_T L \tag{4.15}$$

where C_T is the total concentration of amine B and the amine complexes (carbamates and protonated amines) and L is the membrane thickness. At this point it is necessary to write the mass balances for CO_2 A; the amine *B*, carbamates *C* and the protonated amine *D* according to the overall equation:

$$CO_2\,(A) + 2R_1R_2NH\,(B) \rightleftharpoons R_1R_2NCO_2^-\,(C) + R_1R_2NH_2^+\,(D) \quad (4.16)$$

The steady state differential mass balance equation for each species are:

$$0 = D_A \frac{d^2C_A}{dz^2} - r \quad (4.17)$$

$$0 = D_B \frac{d^2C_B}{dz^2} - 2r \quad (4.18)$$

$$0 = D_C \frac{d^2D_C}{dz^2} + r \quad (4.19)$$

$$0 = D_D \frac{d^2D_D}{dz^2} + r \quad (4.20)$$

Adding Eq. (4.18) - (4.20) and integrating across the membrane and applying the boundary conditions in Eq. (4.14) gives:

$$D_B \frac{dC_B}{dz} + D_C \frac{dC_C}{dz} + D_D \frac{dC_D}{dz} = 0 \quad (4.21)$$

Further integration gives,

$$D_BC_B + D_CC_C + D_DC_D = C^* \quad (4.22)$$

where C^* is an integration constant. Eq. (4.22) can be rearranged:

$$D_C(C_C + C_B + C_D) + C_B\,(D_B - D_C) + C_D\,(D_D - D_C) = C^* \quad (4.23)$$

Eq.(4.23) is the balance equation for the total amount of amines and all its complex forms for the general case of non-equal diffusivities. Plugging the value of $(C_B + C_C + C_D)$ from Eq.(4.23) to Eq.(4.15) gives:

$$\left(C_B + C_C + C_D\right) = \frac{C^* - C_B\left(D_B - D_C\right) - C_D\left(D_D - D_C\right)}{D_C} \tag{4.24}$$

$$\int_0^L \frac{C^* - C_B\left(D_B - D_C\right) - C_D\left(D_D - D_C\right)}{D_C} dz = C_T L \tag{4.25}$$

Multiplying both sides of Eq. (4.25) by $\left(\frac{D_C}{L}\right)$ gives:

$$\frac{C^*}{L}\int_0^L dz - \frac{\left(D_B - D_C\right)}{L}\int_0^L C_B dz - \frac{\left(D_D - D_C\right)}{L}\int_0^L C_D dz = C_T D_C \tag{4.26}$$

$$C^* - \frac{\left(D_B - D_C\right)}{L}\int_0^L C_B dz - \frac{\left(D_D - D_C\right)}{L}\int_0^L C_D dz = C_T D_C \tag{4.27}$$

$$C^* = C_T D_C + \frac{\left(D_B - D_C\right)}{L}\int_0^L C_B dz + \frac{\left(D_D - D_C\right)}{L}\int_0^L C_D dz \tag{4.28}$$

If we assumed equal diffusivity coefficient, *i.e.* $D_B = D_C = D_D$, Eq. (4.28) becomes,

$$C^* = C_T D_C \tag{4.29}$$

Application of Eq. (4.29) to Eq. (4.23) gives:

$$C_T = C_B + C_C + C_D \tag{4.30}$$

Previously, we have demonstrated that $C_D = C_C$ [Eq. (4.7)], the above expression become

$$C_C = \frac{C_T - C_B}{2} = C_D \tag{4.31}$$

Eliminating C_C and C_D term in Eq. (3.29) by the use of Eq. (4.31) gives,

$$-r_{CO_2} = \frac{C_A C_B - \frac{(C_T - C_B)^2}{4KC_B}}{\frac{k_2}{k_1 k_3 C_B} + \frac{1}{k_1}} = \frac{1}{2} r_{DEA} \tag{4.32}$$

where $K = \frac{k_1 k_3}{k_2 k_4}$ (4.33)

Eq. (4.32) is the rate expression for formation of CO_2 that will be used in the analysis of the mass transport equation.

4.3 Nondimensionalization of the Rate Expression

At this point in the analysis of the mass transport equations, it is usually suggested to nondimensionalize the working equations and boundary conditions. There are several

reasons for this. Through nondimensionalization we are able to reduce the number of parameters in the differential equations in order to effect an efficient numerical solution. Others utilized this method because the dimensionless form of the problem is very useful for seeking for example a limiting or asymptotic forms of the solution for some large or small parameter values.

The governing rate equations and boundary conditions are cast into dimensionless forms using the membrane thickness L as the characteristic length while the feed CO_2 concentration C_A^0 and total amine concentration C_T as the characteristic concentrations. The dimensionless concentrations and length are defined as follow:

$$\overline{C}_A = \frac{C_A}{C_A^0} \tag{4.34}$$

$$\overline{C}_B = \frac{C_B}{C_T} \tag{4.35}$$

$$\bar{z} = \frac{z}{L} \tag{4.36}$$

A dimensional analysis of the balance equations result in the following dimensionless parameters (derivations are provided in Appendix C):

a) $m_1 = \frac{k_2}{k_3 C_T}$, dimensionless reaction rate constant

b) $m_2 = KC_A^0$, dimensionless reaction equilibrium constant

c) $m_3 = \dfrac{k_1 C_T L^2}{D_A}$, resembles a Damkohler number that measures diffusion time to reaction time

d) $m_4 = \dfrac{D_B C_T}{D_A C_A^0}$, mobility ratio

Schultz *et al.* (1974) introduced the Damköhler number to classify the analytical approximations for solving facilitated diffusion in flat layers. For large Damköhler numbers, chemical reaction will be much faster than diffusion through the entire volume of the system, which means that most of the volume will show species concentration dependence determined by the chemical reaction. For a simple reversible reaction this implies chemical equilibrium and the membrane is operating in the diffusion-limited regime. For small Damköhler numbers, diffusion is much faster than the chemical reaction, and chemical reaction is not able to alter diffusion-predicted concentration profiles significantly.

The non-dimensional governing equations are now:

$$-\bar{r}_A = \frac{d^2 \overline{C}_A}{d\bar{z}^2} \tag{4.37}$$

$$-\frac{d^2 \overline{C}_B}{d\bar{z}^2} = \frac{2}{m_4} \bar{r}_A = \bar{r}_B \tag{4.38}$$

where $\bar{r}_A$ and $\bar{r}_B$ is the dimensionless reaction rate expression for CO_2 and amine, respectively and the expression for $\bar{r}_A$:

$$-\bar{r}_A = m_3\left\{\frac{4m_2\bar{C}_A\bar{C}_B^2-\left(1-\bar{C}_B\right)^2}{4m_2\left(\bar{C}_B+m_1\right)}\right\}=\frac{m_3}{m_2}\left\{\frac{m_2\bar{C}_A\bar{C}_B^2-\frac{1}{4}\left(1-\bar{C}_B\right)^2}{\bar{C}_B+m_1}\right\} \tag{4.39}$$

The choice of dimensionless groups derived here is not unique. The dimensionless boundary conditions are:

$$\bar{z}=0: \qquad \bar{C}_A=1, \qquad \frac{d\bar{C}_B}{d\bar{z}}=0 \tag{4.40}$$

$$\bar{z}=1: \qquad \bar{C}_A=\frac{C_A^L}{C_A^0} \qquad \frac{d\bar{C}_B}{d\bar{z}}=0 \tag{4.41}$$

4.4 Facilitation Factor

A useful quantity known as facilitation factor F can be defined as the ratio of the facilitated flux of A to the Fickian flux:

$$F=\frac{-D_A\frac{dC_A}{dz}}{-D_A\left(\frac{C_A^L-C_A^0}{L}\right)}=\frac{d\bar{C}_A}{d\bar{z}}\left(\frac{C_A^0}{C_A^L-C_A^0}\right) \tag{4.42}$$

Since the permeate side of the membrane are exposed to the atmosphere, *i.e*. there is no accumulation of CO_2, C_A^L can be assummed to be very small so that the facilitation factor will now be $\frac{d\overline{C_A}}{d\bar{z}}$.

The expressions for C_A and C_B of eq. (4.37) and (4.38) are non-linear differential equations and therefore no exact analytical methods can be used to solve such a system of equations. To simplify the mathematics, a special case of fast reactions or large Damköhler number can be applied to simplify the solutions to the governing equations or else the model must be solved by numerical techniques.

4.5 Solutions to the Transport Equation

The solution to the transport equation involves solving a non-linear system of second order differential equations. Approximate solutions have been developed for in the case where the reactions attained equilibrium or else numerical approach is necessary.

4.5.1 Development Related to the Solutions of the Transport Equations

The following discussion traces the attempts performed by various investigators to obtain analytical as well as numerical solution to the governing equations, describing the steady state transport of permeating species across the membrane or liquid film where simultaneous diffusion and chemical reaction are occurring. Approximate analytical

solutions are derived for the facilitation factor in the two extreme regimes, diffusion controlled and reaction controlled, which were experimentally confirmed. The intermediate regimes are subject to numerical solution. Most of these investigators followed the standard reaction mechanisms occurring in the facilitated transport membranes in the form:

$$A + B \underset{k_r}{\overset{k_f}{\rightleftharpoons}} C$$

where A is the permeating specie, B is the carrier, C is the complex and k_f and k_r are the forward and reverse reaction rate constants repectively.

Donaldson and Quinn (1975) studied the facilitated transport in liquid membranes of the carbon dioxide system. Their model was developed as a means of determining diffusion and kinetic parameters for the reactive systems. The system was a CO_2 hydration for the formation of carbonate/bicarbonate ions.

Smith *et.al.* (1979) developed a facilitative transport model using the standard reaction mechanism mentioned above in which they solved one-dimensional, steady state equations considering both physical diffusion and chemical reaction terms. They introduced the assumption of equal carrier and complex diffusivities in order to simplify the analysis. The equations were solved using analytical techniques. Initially, they solved the system of nitric oxide-ferrous ion facilitative transport, obtaining comparable results with other studies. They also studied the CO_2-monoethanolamine (MEA) system. In this case, they did not clearly explain how the governing equations were incorporated into

their model. Since the kinetics of CO_2-amine systems involves a plethora of possibilities, they should be clear in describing which reaction equations they are following and what assumptions they are employing when simplifying their equations. They calculated the facilitation factors but no figures were presented to show the facilitation factor trends and profiles. Data analysis whether mathematical or experimental, should include the presentation of charts that describes any trends in the data.

Jain and Schultz (1982) solved the system of differential equations using orthogonal collocation for both equal and unequal diffusivities. Folkner and Noble (1983) reported a model of facilitative transport membranes under transient conditions. Their equations are one dimensional for the standard transport reaction mechanism with flat, cylindrical and spherical geometries. The effects of inverse Damköhler number, equilibrium constant and geometry on the facilitation factor were determined. The assumption of equal diffusivities was used without justification. No actual discussion was presented concerning how the governing equations were solved except to say "a computer package was used".

Basaran *et al.* (1989) presented two models for the facilitated transport of unequal and equal carrier and permeate-carrier complex diffusivities that also permit arbitrary kinetic rates. The first method was derived for very low Damkohler numbers and solved analytically using rectangular perturbation analysis. The second model was solved numerically applying Galerkin/finite element method that was solved by an iteration technique using Newton's method.

Guha *et.al*. (1990) investigated the steady state facilitated transport of CO_2 through an immobilized liquid membrane containing DEA solution. The system was represented by a set of coupled diffusion reaction equations that were solved numerically by finite difference method using the IMSL (International Mathematical Statistical Libraries) routine BVPFD. There was little discussion for this procedure.

In 1993, Davis and Sandall studied the CO_2/CH_4 separation by facilitated transport using amine-polyethylene glycol membranes. They developed a model to describe the transport process. The governing differential equations were solved numerically using the method of quasilinearization in conjunction with finite-difference solution, which is similar to the solutions of Kutchai *et al*. (1970).

Teramoto *et. al*. (1995) reported an approximate solution for the facilitation factor for the CO_2-amine systems. They conducted experimental work and found out that DEA system performed better than the MEA. They presented a set of algebraic equations that can be solved simultaneously to calculate the facilitation factor. Using trial and error calculations, approximate facilitation factors were calculated and compared with several reported numerical solutions with good agreement. Their model is applicable for both equal and unequal diffusivities of the carrier and complex respectively.

Recently, Morales-Cabrera *et al*. (2002) and Al-Marzouqi *et al*. (2002) derived an analytical solutions on these equations. Morales-Cabrera *et al*. obtained an approximate analytical solution to the non-linear diffusion reaction transport that is based on the

Taylor series expansion of the reaction rate around the two limiting surfaces of the liquid membrane. They claimed that the method provides reasonable estimations of the facilitation factor over the entire range of Damköhler number values, from the physical diffusion regime to the equilibrium chemical reaction regime. The model is valid for equal and unequal carrier complex diffusivities and cases of zero and nonzero downstream solute concentrations. Al-Marzouqi *et al*. (2002) derived an analytical equation for the facilitation factor that allows for unequal diffusivity of the carrier and permeate-carrier complex for reactions instantaneous with respect to mass transfer. The method is based on the equations derived by Olander (1960). They reported that the analytical solution can be applied for any set of diffusivities of reactants and product and does not involve any approximation or simplification.

In general, it appears that very few authors seem to provide useful, easy-to-understand information in their papers about their specific modeling procedures. Researchers should be more willing to share logical information in the hopes of aiding future works and to add credibility to their findings.

4.5.2 Approximate Solution to the Mass Transport Equation.

Analytical solutions for the limit of fast reactions are obtained by making approximations that will linearize the transport equations. The upper bound for facilitaion factor is where the reaction approaches equilibrium. Large Damköhler number, $\boldsymbol{m_3}$ characterizes fast

reactions so that it approaches equilibrium everywhere in the film (Goddard *et. al*., 1970). The reaction being study is:

$$CO_2\,(A) + 2R_2NH(\mathrm{B}) \rightleftharpoons R_2NCO_2^-\,(C) + R_2NH_2^+(D) \tag{4.16}$$

$$K_{eq} = \frac{C_C C_D}{C_A C_B^{\,2}}, \tag{4.43}$$

but $C_C = C_D$ [from Eq. (4.7)] and $C_T = C_B + C_C + C_D$ [from Eq. (4.30)] so that eq. (4.43) can be written as:

$$K_{eq} = \frac{C_C^{\,2}}{C_A\left(C_T - 2C_C\right)^2} \tag{4.44}$$

solving for C_C gives,

$$C_C = \frac{C_T\sqrt{K_{eq}C_A}}{1 + 2\sqrt{K_{eq}C_A}} \tag{4.45}$$

The total flux of CO_2 is the sum of the fluxes of CO_2 and carbamates, $R_2NCO_2^-$:

$$N_A^T = -D_A\frac{dC_A}{dz} - D_C\frac{dC_C}{dz} = N_A + N_C \tag{4.46}$$

Eq. (4.46) is integrated and with the application of the boundary conditions gives:

$$N_A^T = \frac{D_A}{L}\left(C_A^0 - C_A^L\right) + \frac{D_C}{L}\left(C_C^0 - C_C^L\right) \tag{4.47}$$

Substituting the expression for C_C of Eq. (4.45) to Eq. (4.47) gives:

$$N_A^T = \underbrace{\frac{D_A}{L}\left(C_A^0 - C_A^L\right)}_{N_A} + \underbrace{\frac{D_C C_T \sqrt{K_{eq}}}{L}\left[\frac{1}{\left(1+2\sqrt{K_{eq}C_A^0}\right)\left(1+2\sqrt{K_{eq}C_A^L}\right)}\right]\left[\sqrt{C_A^0} - \sqrt{C_A^L}\right]}_{N_C} \tag{4.48}$$

The first term on the right-hand side of Eq. (4.48) represents the flux due to solution-diffusion mechanism, and the second is the flux caused by complexation reactions.

If the effect of CO_2-DEA reaction is to be considered, the second term on the right-hand side of Eq. (4.48) may be simplified to limiting case that may explain the experimental observations. First, when C_A^0 and C_A^L are small (corresponds to low CO_2 feed pressures), Eq. (4.48) becomes,

$$N_C = \left(\frac{D_C C_T \sqrt{K_{eq}}}{L}\right)\left(\sqrt{C_A^0} - \sqrt{C_A^L}\right) \tag{4.49}$$

The flux is larger because it is proportional to $\sqrt{K_{eq}}C_T$ and thus affected by chemical reaction. The equilibrium facilitation factor is:

$$F_{eq} = \frac{N_A + N_C}{N_A} \tag{4.50}$$

$$F_{eq} = \frac{D_B C_T \sqrt{K_{eq}}}{D_A\left(\sqrt{C_A^0} - \sqrt{C_A^L}\right)\left(1 + 2\sqrt{K_{eq} C_A^0}\right)\left(1 + 2\sqrt{K_{eq} C_A^L}\right)} \tag{4.51}$$

4.5.3 Numerical Solution to the Mass Transport Equation

No exact closed form of the analytical solution to the non-linear boundary value problem for Eq. 4.37 and 4.38 are available. As mentioned above, both the semi analytical and numerical approaches have been applied to solve such system of equations.

In this thesis, a simpler numerical approach was adopted. Complete numerical solution of Eq. 4.37 and 4.38 involved the following procedures. First, the two sets of second order differential equations were converted into four first order ordinary differential equations as follows:

From Eq. 4.37 and 4.38, the governing equations are:

$$\frac{d^2 C_A}{dz^2} = r_A \quad \text{and} \quad \frac{d^2 C_B}{dz^2} = r_B, \quad \text{but } \frac{2}{m_4} r_A = r_B$$

where $r_A = \frac{m_3}{m_2}\left\{\frac{m_2 C_A C_B^2 - \frac{1}{4}(1 - C_B)^2}{C_B + m_1}\right\}$

For convenience, the bars above the dimensionless concentration and thickness are removed. So that the four first order differential equations are:

$$Y_1 = C_A \tag{4.52}$$

$$\frac{dY_2}{dz} = \frac{m_3}{m_2}\left[\frac{m_2 Y_1 Y_3^2 - 1/4(1-Y_3)^2}{C_B + m_1}\right] \tag{4.53}$$

$$Y_3 = C_B \tag{4.54}$$

$$\frac{dY_4}{dz} = \frac{2m_3}{m_4 m_2}\left[\frac{m_2 Y_1 Y_3^2 - 1/4(1-Y_3)^2}{Y_3 + m_1}\right] \tag{4.55}$$

Then eqs. 4.52 to 4.55 were solved using the ***bvp4c*** function in MATLAB (Mathworks). The complete program was presented in Appendix F. A brief description of the MATLAB function ***bvp4c*** is next.

bvp4c is a finite difference code in MATLAB (Mathworks) that implements the 3-stage Lobatto IIIa formula. This is a collocation formula and the collocation polynomial provides a C1-continuous solution that is fourth-order accurate uniformly in the interval of integration. Mesh selection and error control are based on the residual of the continuous solution. The collocation technique uses a mesh of points to divide the interval of integration into subintervals. The solver determines a numerical solution by solving a global system of algebraic equations resulting from the boundary conditions,

and the collocation conditions imposed on all the subintervals. The solver then estimates the error of the numerical solution on each subinterval. If the solution does not satisfy the tolerance criteria, the solver adapts the mesh and repeats the process. The user must provide the points of the initial mesh as well as an initial approximation of the solution at the mesh points.

4.6 Physicochemical Constants of the Membrane System

Important physicochemical properties of the CO_2-DEA system that are necessary in order to implement the diffusion-reaction transport equations were directly taken from the open literature. These include solubility, diffusivity, equilibrium and kinetic rate constants. Note that interpolation where performed when appropriate. Also, necessary corrections were carried out in the calculations in order to be consistent with the units.

Various techniques, *e.g.*, rapid mixing method, wetted wall, stopped flow technique and continuously stirred reactors, have been applied for the determination of the reaction kinetics of CO_2-amine system. However, due to the reaction that occurs between CO_2 and amine, it is not possible to obtain information directly on these properties and therefore they were usually estimated from the corresponding data of similar non-reacting gases. N_2O molecule is similar to the CO_2 molecule in configuration, molecular weight, electronic structure and molar volume. Table 4.2 listed the properties of these two gases.

The similarities of these two molecules were often used to estimate the properties of CO_2. Laddha *et.al*. (1981) demonstrated that the N_2O analogy may be applied to estimate the solubility of CO_2 in aqueous amine solution. Good estimates of solubility have been produced by equating the ratio of the solubilities of N_2O and CO_2 in non-reacting solvents to their ratio in reacting solvents. The solubility ratio can be written as follows:

$$(\text{solubility of } CO_2) = C_1 \, (\text{solubility of } N_2O) \tag{4.56}$$

where C_1 = (solubility of CO_2 in H_2O) / (solubility of N_2O in H_2O)

In terms of Henry's constant, the solubility ratio can be written as follows:

$$\frac{H_{CO_2}}{H^a_{CO_2}} = \frac{H_{N_2O}}{H^a_{N_2O}} \tag{4.57}$$

where the superscripts ***a*** indicates water as the solvent.

Table 4.2 Molecular Properties of CO_2 and N_2O

Property	CO_2	N_2O
Molecular Weight	44.0098	44.0128
Molecular Structure	O = C = O	N = N = O
Electronic Structure	:Ö: :C: : Ö:	N::N: : Ö:
Molar volume, (cm^3/mol)	34.0	36.4

4.6.1 Solubility of CO_2 and N_2O in Water and Amine Systems

The data of the solubility of CO_2 and N_2O in water presented in the literature was complied and presented by Versteeg and van Swaaij (1988) and they formulated the following relations:

$$H_{CO_2} = 3.54 \times 10^{-7} \, exp(2044/T) \tag{4.58}$$

$$H_{N_2O} = 1.17 \times 10 - 7 \, exp(2284/T) \tag{4.59}$$

where the unit of Henry's constant is $mol.m^{-3}.Pa^{-1}$ and T in K.

Similarly, Sada *et. al*.(1978), measured the variation of the solubility of N_2O in aqueous solution of DEA as a function of the DEA concentration and was correlated as follows (Blanc and Demarais, 1984):

$$ln\frac{H}{H^a} = 1.0406 \times 10^{-4} + 6.8433 \times 10^{-3} C_T + 1.33633 \times 10^{-2} C_T^2 - 1.1549 \times 10^{-3} C_T^3$$

(4.60)

Here H and H^a (bar.m^3.kmol^{-1}) are the Henry's constant or the solubility of CO_2 in DEA and in pure water systems, respectively, while C_T (kmol.m^{-3}) is the DEA concentration.

Note that necessary corrections were carried out in the calculations in order to be consistent in the units. Next is the diffusivity of CO_2 and DEA.

4.6.2 Diffusivity of CO_2 and DEA in Various DEA Solutions

Sada *et, al*. (1978), suggested that the N_2O analogy can also be applied to determined the diffusivity of CO_2 in aqueous amine solutions:

$$\left(D_{CO_2}\right)_{Amine} = \left(D_{CO_2}/D_{N_2O}\right)_{Water}\left(D_{N_2O}\right)_{Amine} \tag{4.61}$$

The diffusivity of CO_2 and N_2O in water published in the literature was compiled by Versteeg and van Swaaij (1988) and they derived the following correlation:

$$D_{CO_2} = 2.35\times10^{-6}\ exp(-2119/T) \tag{4.62}$$

$$D_{N_2O} = 5.07\times10^{-6}\ exp(-2371/T) \tag{4.63}$$

where D ($m^2.s^{-1}$) is the diffusivity coefficient and T (K) is the temperature. The diffusivity of N_2O at various DEA concentrations were taken from the data published by Tamimi *et.al*. (1994). For the diffusivity of DEA at various DEA concentrations, the data published by Snijder *et.al*. (1993) were used in the calculations. These authors applied the

Taylor dispersion technique in determining the diffusion coefficients of various amines in their corresponding solutions.

4.6.3 Kinetic Parameters

Going back to the CO_2-DEA reactions:

$$CO_2 + R_1R_2NH \underset{k_2}{\overset{k_1}{\rightleftharpoons}} R_1R_2NH^+CO_2^- \tag{4.64}$$

$$R_1R_2NH^+CO_2^- + R_1R_2NH \underset{k_4}{\overset{k_3}{\rightleftharpoons}} R_1R_2NCO_2^- + R_1R_2NH_2^+ \tag{4.65}$$

The reaction equilibrium constant, K_{eq}, is as follows:

$$K_{eq} = \frac{\left[R_1R_2NCO_2\right]\ \left[R_1R_2NH_2^+\right]}{\left[CO\right]\ \left[R_1R_2NH\right]^2} = \frac{k_1k_3}{k_2k_4} \tag{4.66}$$

The corresponding values for K_{eq}, k_1 and k_2/k_3 for the CO_2-DEA sytems are directly taken from the open literature and presented in Table 4.3. Interpolations were performed when necessary.

Table 4.3 Physicochemical Properties of CO_2-DEA Systems

Parameter \ DEA	10wt%	20wt%	30wt%	50wt%
Diffusivity DEA, $cm^{-2}.s^{-1}$	6.60×10^{-6}	5.30×10^{-6}	4.40×10^{-6}	2.50×10^{-6}
Diffusivity CO_2, $cm^2.s^{-1}$	1.42×10^{-5}	1.06×10^{-5}	7.49×10^{-6}	1.20×10^{-6}
Solubility, $mol.cm^{-3}$-$cmHg^{-1}$	4.38×10^{-7}	4.22×10^{-7}	3.78×10^{-7}	3.56×10^{-7}
Equilibrium constant, $cm^3.mol^{-1}$ (a)	1.43×10^{6}	1.43×10^{6}	1.43×10^{6}	1.43×10^{6}
Reaction constant ratio, k_2/k_3, $mol.cm^{-3}$ (b)	4.58×10^{-3}	4.58×10^{-3}	4.58×10^{-3}	4.58×10^{-3}
Reaction constant, k_1, $cm^3.mol^{-1}.s^{-1}$ (b)	3.17×10^{6}	3.17×10^{6}	3.17×10^{6}	3.17×10^{6}
DEA concentration, $mol.\ cm^{-3}$	9.58×10^{-4}	1.94×10^{-3}	2.94×10^{-3}	5.02×10^{-3}

(a) Bosch et al., 1990 (b) Versteeg and Oyevaar, 1989

4.7 Results of the Numerical Solution

The foregoing results are intended to analyze concentration profile inside the thin membrane and the effects of various parameters using the analytical transport equations that were solved numerically using MATLAB 7.2 (Mathworks).

Experimental data that were observed from the gas-mixture experiments (Chapter 6) suggest that the transport of CO_2 across the DEA membrane is a complex function of the parameters studied. The calculated results support the experimental trends that were observed for the CO_2 permeances as a function of partial pressure differentials and carrier concentrations. Thus, the diffusion-reaction transport equations can be applied to explore the influences of these parameters on the mass transport process modified by reversible chemical reactions.

In this chapter, quantitative explanation is proposed with the aid of the numerical solution of the diffusion-reaction equation. The concentration and reaction rate profiles are plotted to provide a picture of the diffusion-reaction process occurring in the reactive membrane. A parametric study was performed to describe the influence of CO_2 partial pressure differential and DEA concentration. Lastly, the CO_2 permeance through the reactive membrane is discussed.

4.7.1 Reaction Rate and Concentration Profiles

Figures 4.2 to 4.10 show the plots obtained from the numerical solution of the diffusion-reaction equations. The dimensionless reaction rate is defined by eq. 4.37 and 4.38. The

dimensionless parameters and facilitation factors are given in Table 6.1 and 6.2 in Chapter 6.

One may notice from the figures that in both absorption and desorption processes, the effect of the chemical reaction is to make the concentration gradient at the boundaries steeper than it would be in the absence of chemical reaction. Hence, a larger facilitation factor is obtained. Indeed, the facilitation factor may be so large so as to actually reduce the mass transfer resistance in the membrane to the point at which it is negligible as compared to the resistance in the gas phase (Astarita, 1983).

In the absence of chemical reaction, it implies that the CO_2 concentration profiles has almost zero curvature (Fig.4.3 and 4.6) and shows that the curvature is non-zero when chemical reaction takes place (Fig.4.2, 4.4 and 4.9). In particular, the curvature is concave for absorption and convex for desorption. However, there are conditions, described below where the facilitation factor is almost negligible, namely when the curvature of the concentration profile is very small or almost linear (see Fig.4.3 and 4.6).

At low CO_2 feed pressure, the CO_2 – DEA reaction seems to approach chemical equilibrium within the core of the membrane, which shows that the reaction is limited to the region near to the membrane boundaries (about 15% from each boundary). Apparently, the reaction rates are highest at the membrane boundaries and almost zero in the core of the reactive membrane. Thus, the reaction quickly approaches the state of equilibrium in the centre of the membrane and the forward and backward reactions are

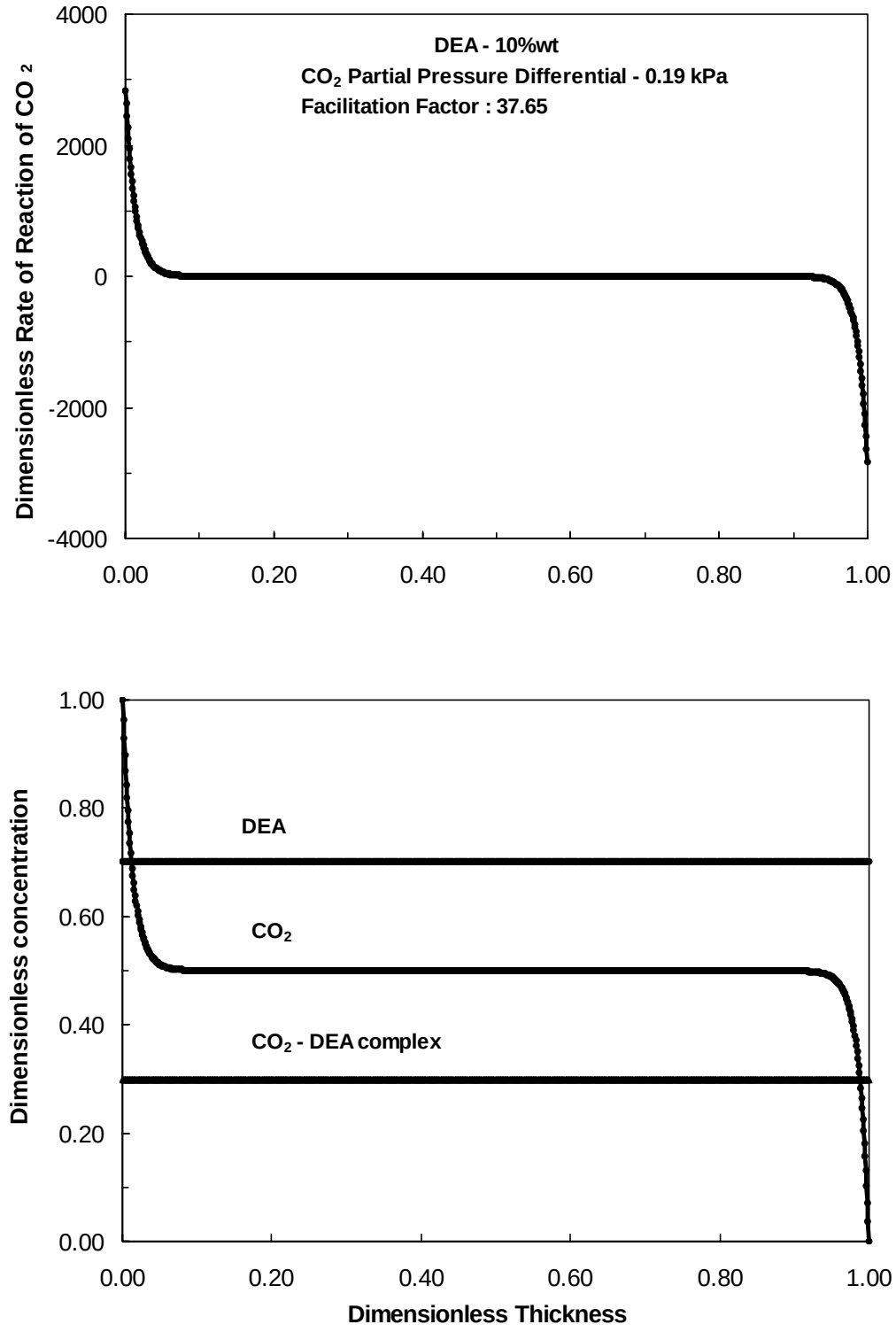

Figure 4.2 Dimensionless reaction and concentration profiles for the facilitated transport of CO_2 in 10wt% DEA and pressure differential of 0.19 kPa. T= 296K

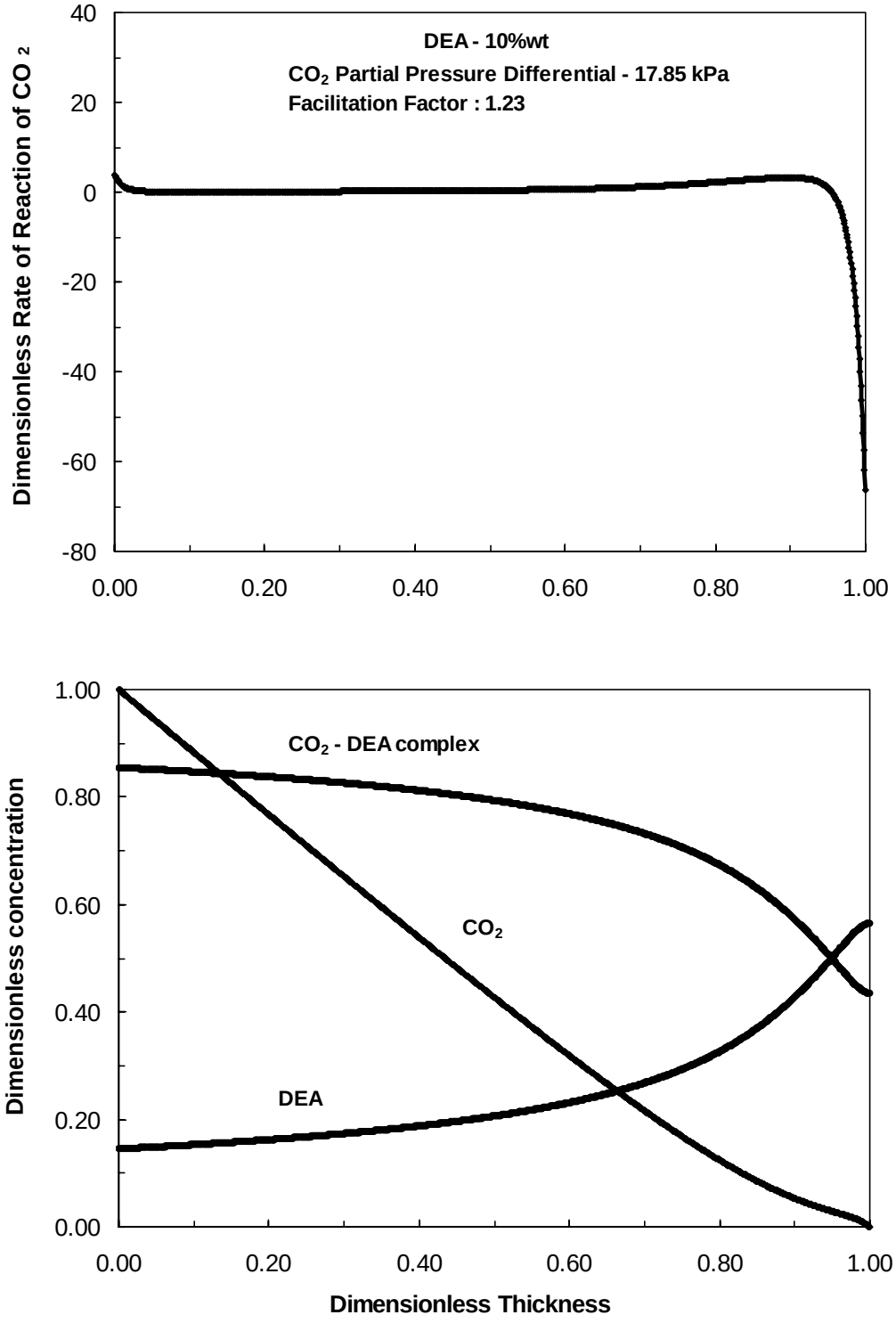

Figure 4.3 Dimensionless reaction and concentration profiles for the facilitated transport of CO_2 in 10wt% DEA and pressure differential of 17.85 kPa. T= 296K

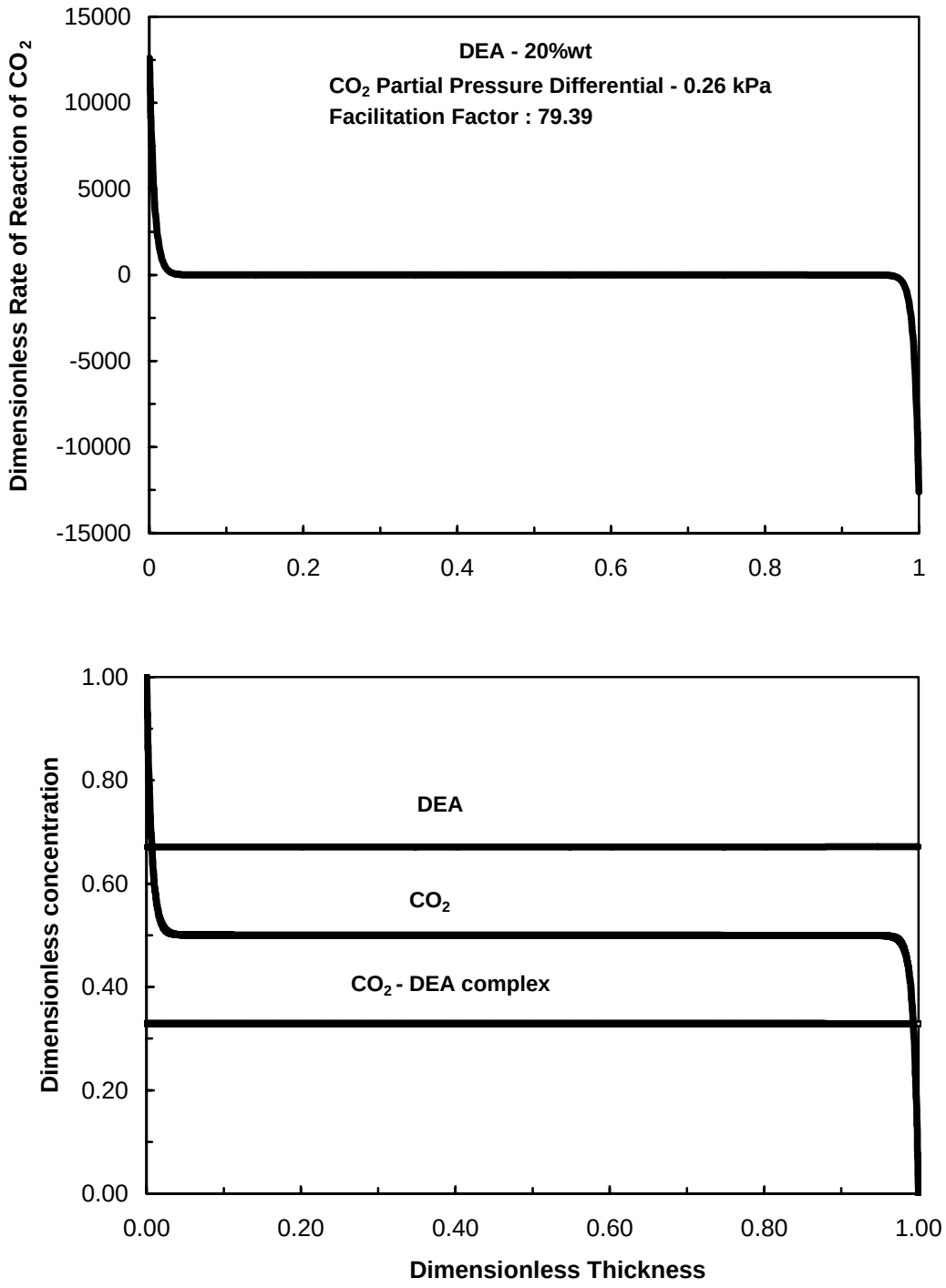

Figure 4.4 Dimensionless reaction and concentration profiles for the facilitated transport of CO_2 in 20wt% DEA and pressure differential of 0.26 kPa. T= 296K

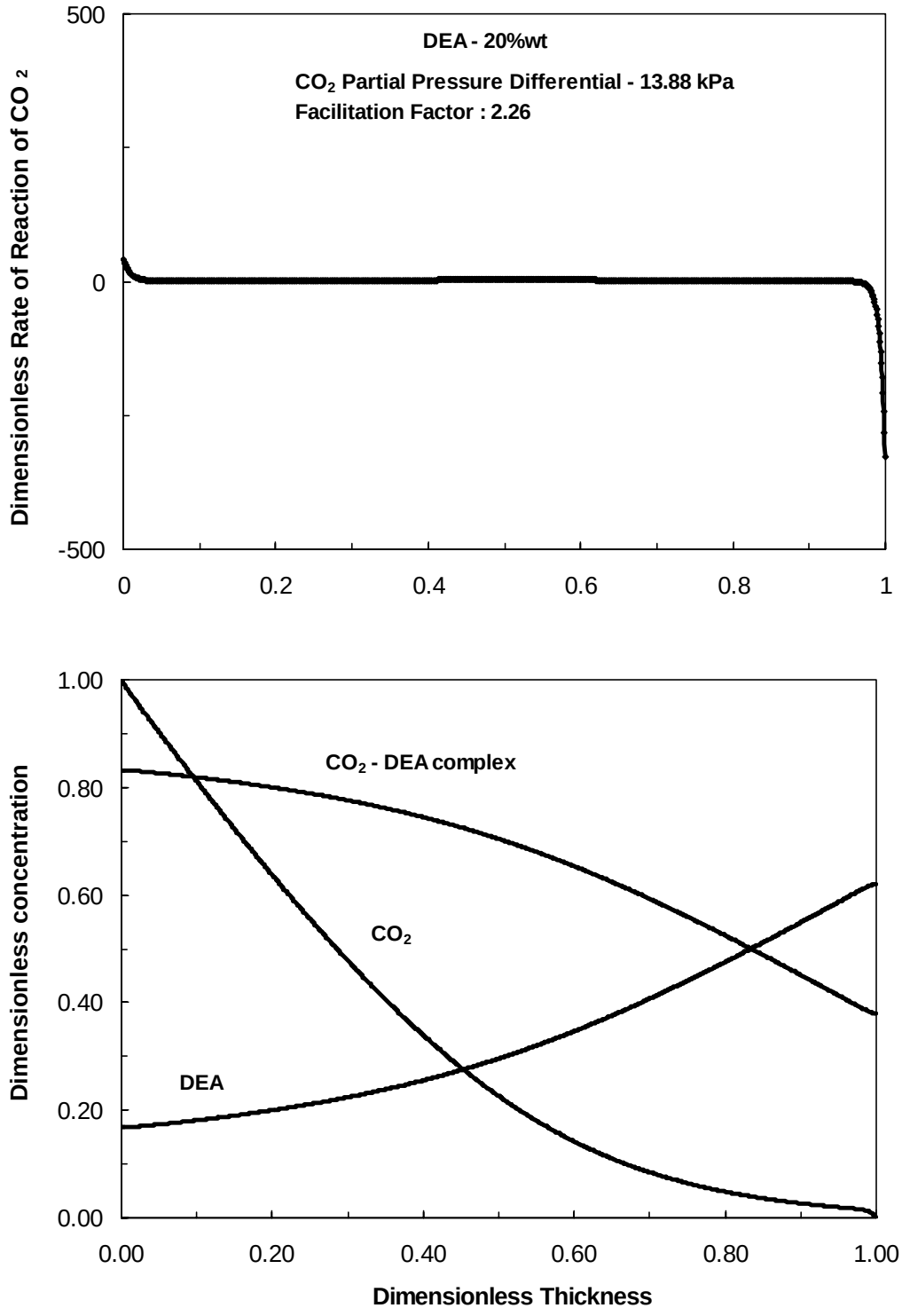

Figure 4.5 Dimensionless reaction and concentration profiles for the facilitated transport of CO_2 in 20wt% DEA and pressure differential of 13.88 kPa. T= 296K

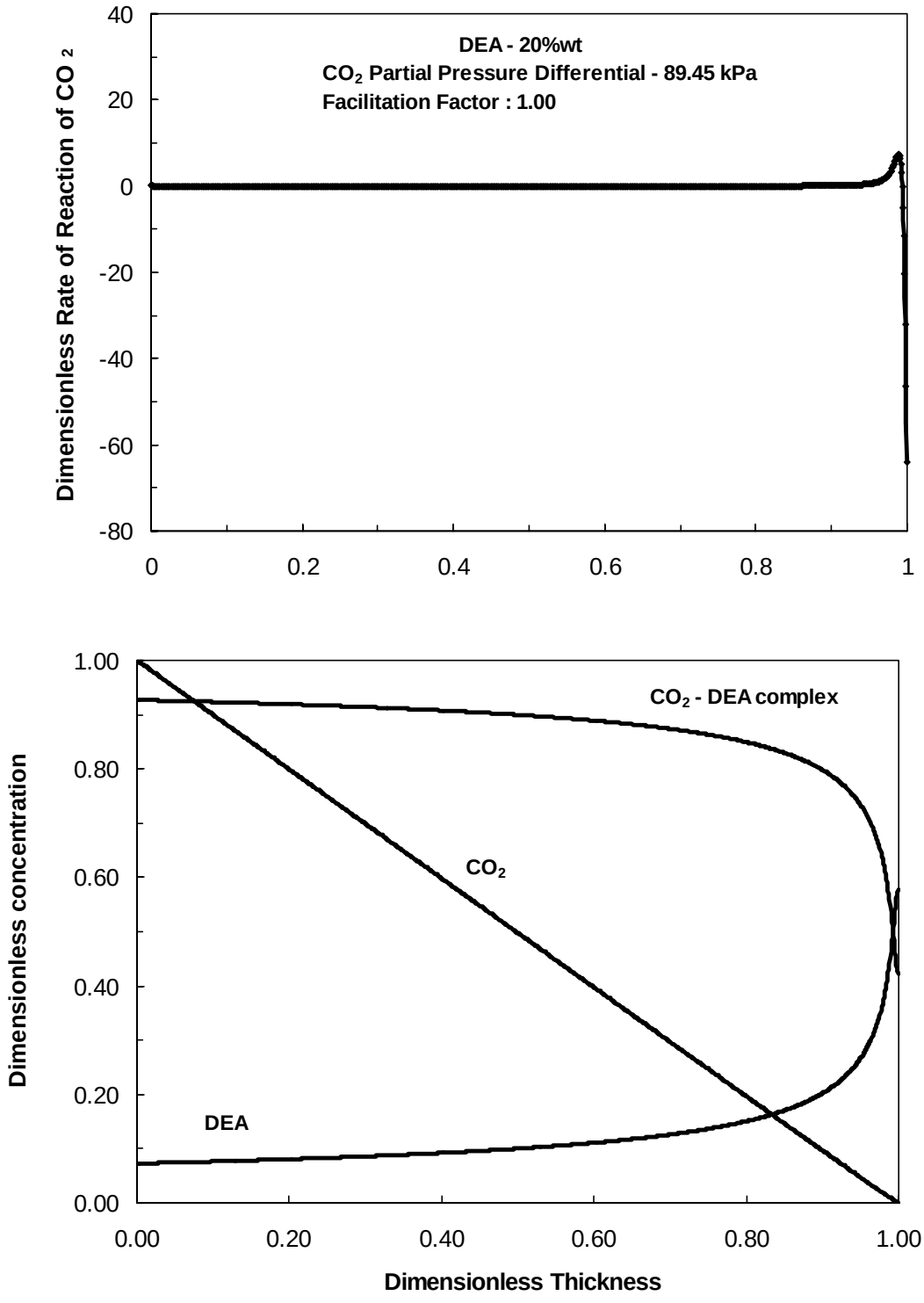

Figure 4.6 Dimensionless reaction and concentration profiles for the facilitated transport of CO_2 in 20wt% DEA and pressure differential of 89.45 kPa. T= 296K

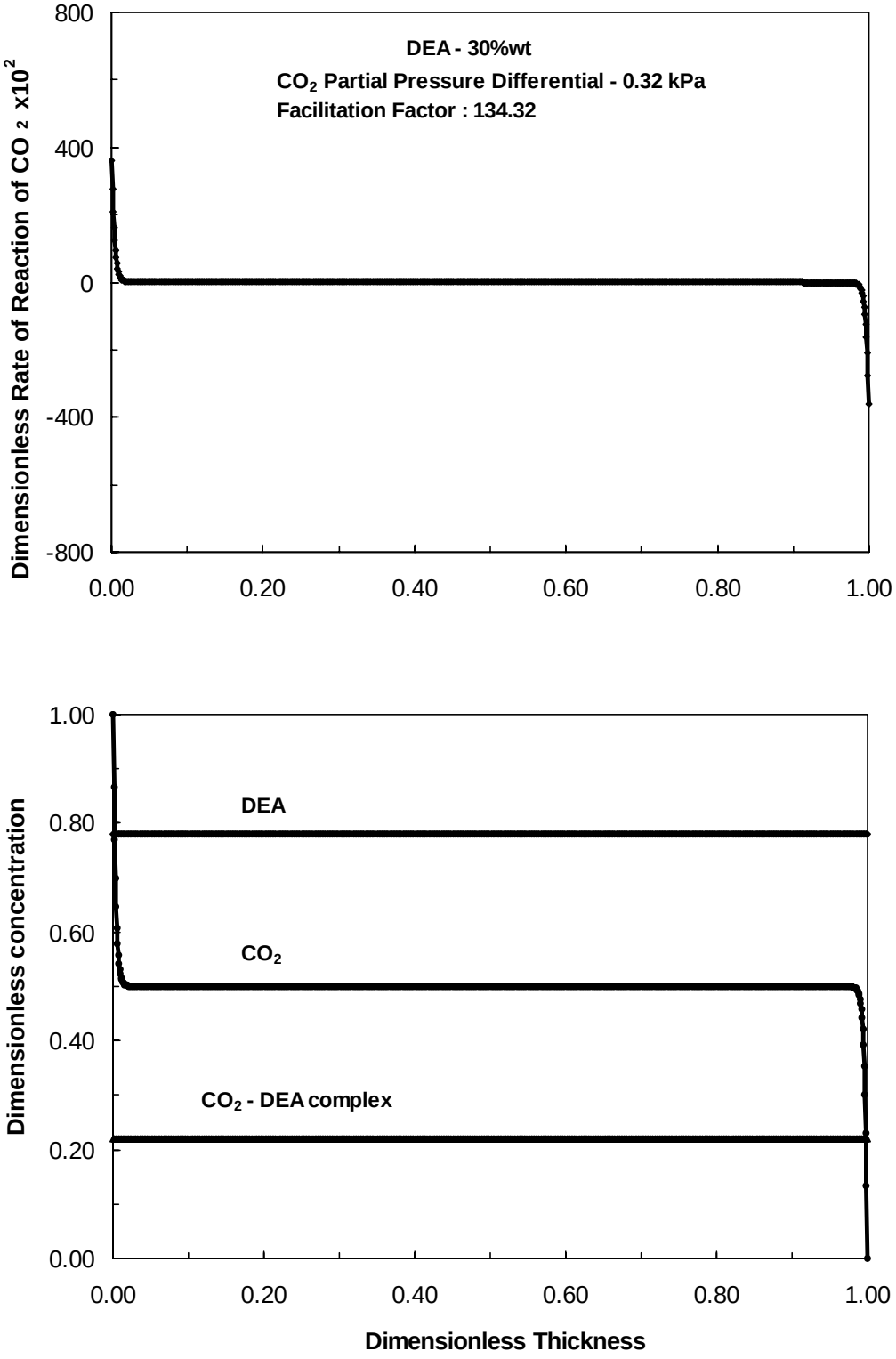

Figure 4.7 Dimensionless reaction and concentration profiles for the facilitated transport of CO_2 in 30wt% DEA and pressure differential of 0.32 kPa. T= 296K

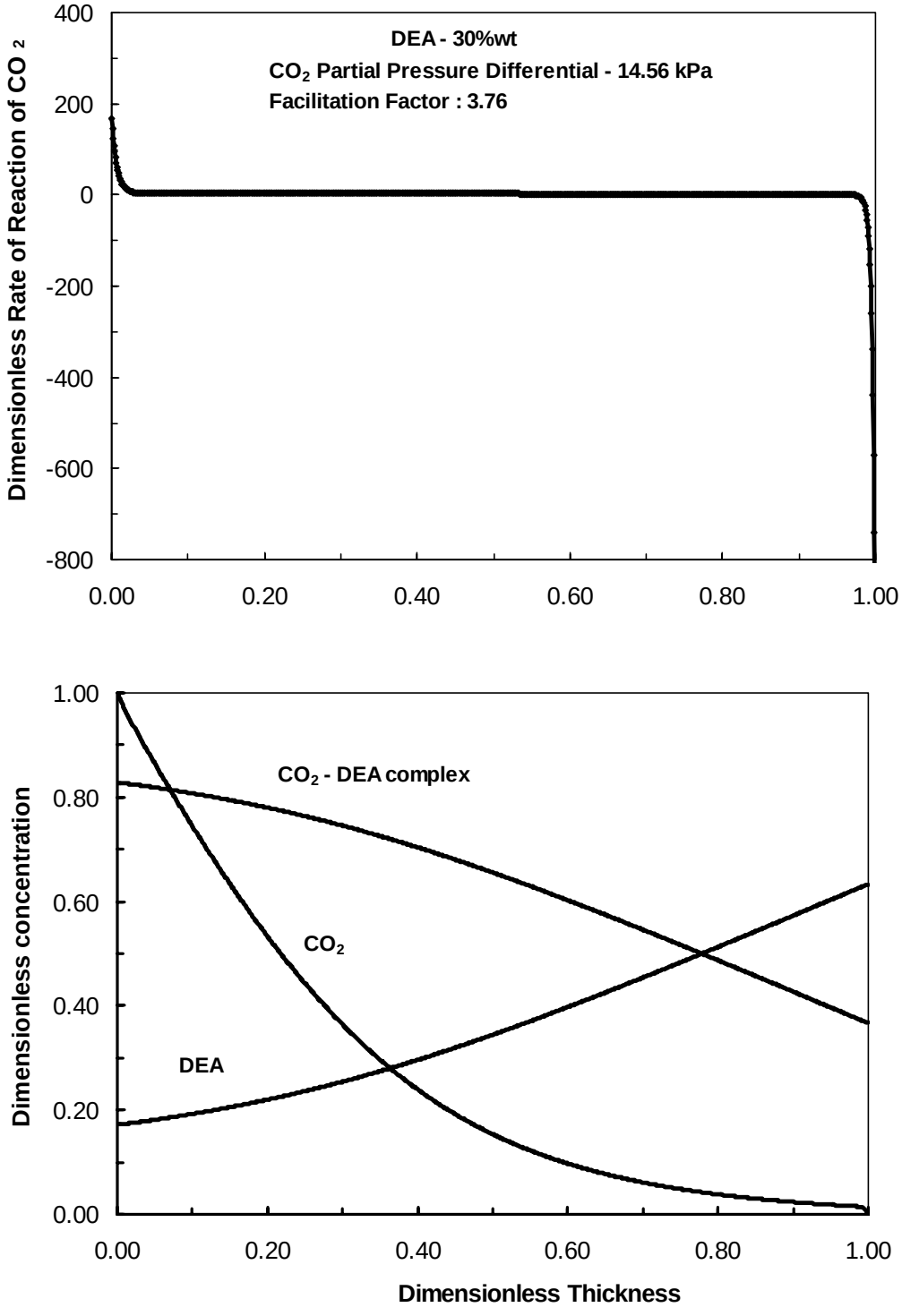

Figure 4.8 Dimensionless reaction and concentration profiles for the facilitated transport of CO_2 in 30wt% DEA and pressure differential of 14.56 kPa. T= 296K

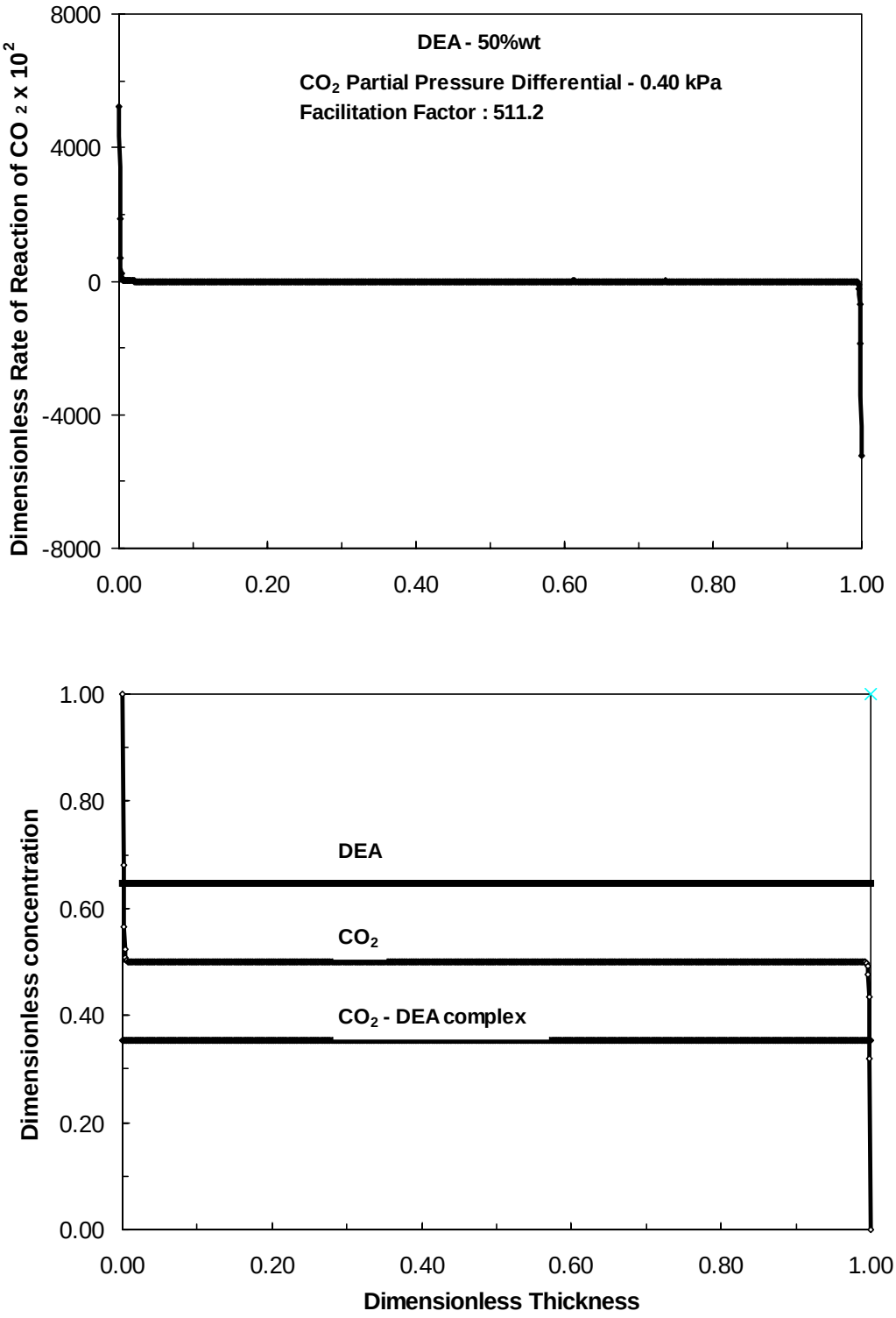

Figure 4.9 Dimensionless reaction and concentration profiles for the facilitated transport of CO_2 in 50wt% DEA and pressure differential of 0.40 kPa. T= 296K

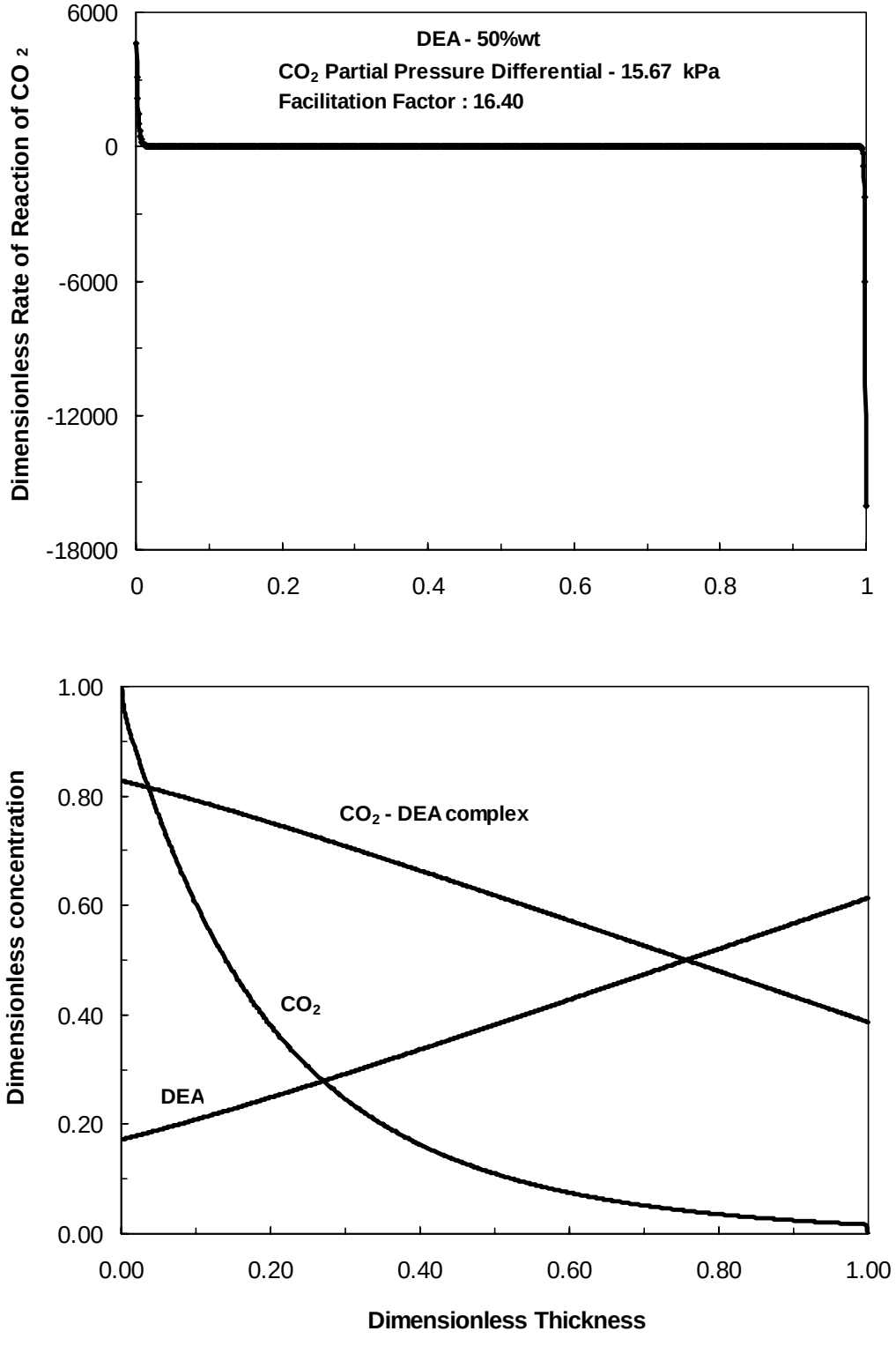

Figure 4.10 Dimensionless reaction and concentration profiles for the facilitated transport of CO_2 in 50wt% DEA and pressure differential of 15.67 kPa. T= 296K

limited to the regions near the membrane boundaries. This is manifested on the plots in which the concentration and reaction rate profiles are almost symmetrical. It implies that the process of absorption or the forward reaction and the desorption velocities are similar.

At higher CO_2 partial pressure differential , the profiles are somewhat asymmetric. It is evident that the desorption or stripping is substantially different from the absorption process. In this condition, the curvature of the concentration profile approched a smaller value or becoming linear.

Furthermore, a closer look at the reaction rate profile suggests that at $\boldsymbol{z = 0}$, the rate of the absortion process is smaller due to chemical saturation. This implies that the driving force for additional absorption remains lower. Conversely, at $\boldsymbol{z = 1}$, the reaction produces more of the CO_2-DEA complexes which are to be desorbed, thus providing a high concentration of these species in the matrix and a large driving force for the desorption, *i.e*. higher reaction rate at the desorption region of the membrane.

The facilitated transport of CO_2 is considered to be a globally non-reactive systems, i.e., systems which strictly acts as passive medium of transport and not as chemical reactors under steady state conditions (Schultz, 1974). At steady state the transport of CO_2 is mediated by the presence of DEA which shuttles back and forth across the thickness of the membrane. DEA at the feed side of the membrane react with CO_2 to produced carbamates and protonated amines species. These species then diffuses to the permeate side of the membrane where the desorption or reverse reaction is high thereby releasing

CO_2. The DEA is also produced and cycles back to the feed side where the process is repeated.

The affinity of CO_2 for the DEA plays an important influence on the behaviour of the mass transport. In the diffusion-reaction equation, this CO_2-DEA affinity is describe in terms of the dimensionless equilibrium constant $\boldsymbol{m_2}$ or maybe referred to as binding constant, which describes the behaviour of the forward and reverse reactions. In the extremes of very large or very small binding constant between the permeate and the carrier, the facilitation is decreased or entirely eliminated. When the binding constant is small, CO_2 is released quickly in the reverse reaction . Likewise, when $\boldsymbol{m_2}$ is large, the CO_2 molecules are bound strongly with the DEA or the amine. In such cases, the back and forth mechanism of the DEA is confined to the region near to the permeate side for a reason that much of the amine is tied-up with the CO_2 molecules for longer times and therefore not available for further CO_2 uptake. With smaller DEA concentration, $\boldsymbol{m_2}$ is obviously larger because the amount of unreacted amine is evidently reduced. Looking at the concentration profiles for the 20 wt% DEA between small (Fig.4.4) and large CO_2 partial pressure differential (Fig.4.6), illustrates a substantial reduction of DEA concentration in the case of a larger CO_2 partial pressure differential. A large $\boldsymbol{m_2}$ may also results in the asymmetrical CO_2 concentration profiles as shown in Fig.4.3, 4.5, and 4.8. Also, the concentration gradients of the CO_2-DEA complexes are steeper near the desorption or reverse region ($\boldsymbol{z = 1}$) of the membrane.

4.7.2 Effects of CO_2 Partial Pressure Differential and DEA Concentrations

The influences of CO_2 partial pressure differentials and DEA concentrations through the reactive membrane are studied with the help of the diffusion-reaction transport equation.

4.7.2.1 Effect of CO_2 Partial Pressure Differential

The results of the permeation experiments as well as the numerical solution demonstrate that the CO_2 permeance are largely facilitated when the CO_2 partial pressure differential are lower. This argument is clearly shown in Fig. 4.4 – 4.6 for 20wt% DEA. The facilitation factor as a function of CO_2 partial pressure differential is shown in Fig.4.11

The dimensionless parameters and facilitation factors are listed in Table 6.2. Fig. 4.11 suggests that the facilitation due to the presence of DEA increases dramatically when lower pressure differentials are applied, then increases abruptly for pressure differential lower than 6 kPa. It can be seen that a small range of pressure differential is required to attain a larger chemical facilitation. Kemena *et. al*.(1983) made a theoretical study on this subject and concluded that this facilitation, which occurs within a small range of pressure differentials, is related to a binding constant, $\boldsymbol{m_2}$. They reported an optimum range of $\boldsymbol{m_2}$ to be from 1 – 10 over a wide range of operating conditions. For example, Fig. 4.4, the calculated $\boldsymbol{m_2}$ is 0.12 at CO_2 partial pressure differential of 0.26 kPa. This results to a

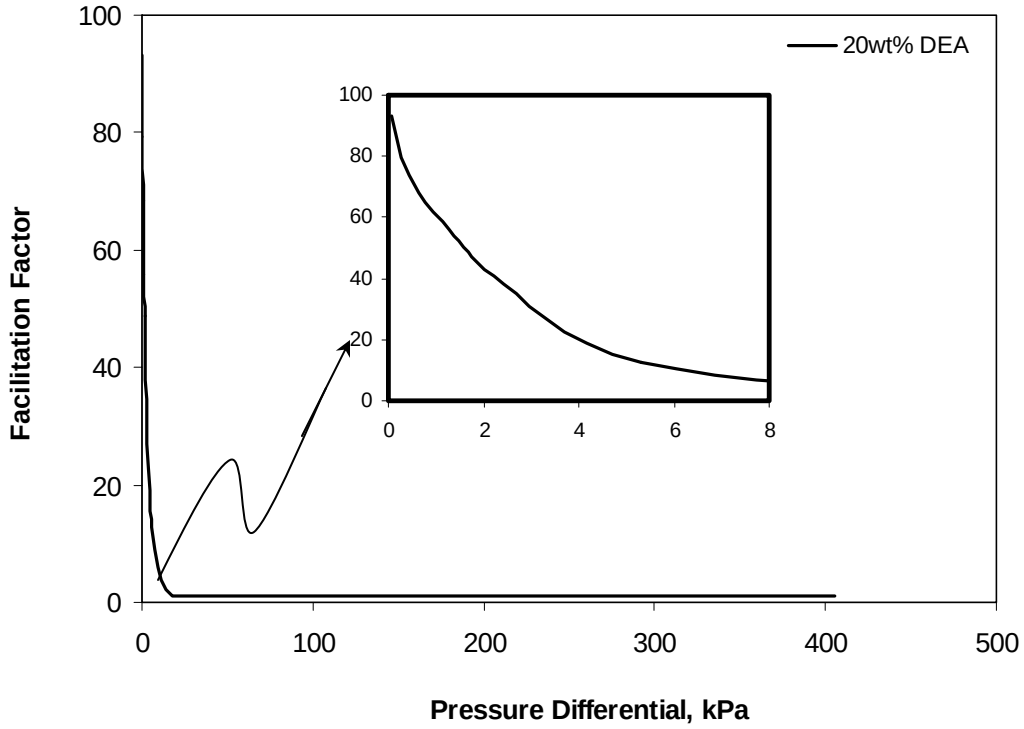

Figure 4.11 Facilitation factor for the 20% DEA membrane as a function of CO_2 pressure differentials. T= 296K

symmetric concentration and reaction rate profiles and a facilitation factor of 79.39 while in Fig. 4.5, m_2 is 6.28 (at CO_2 partial pressure differential of 13.88 kPa), resulting to an asymmetric profiles with facilitation factor of 2.26. According to our numerical solution, m_2 values below 7 could provide satisfactory facilitation factor.

Generally, the equilibrium of the CO_2-amine complexation reaction could provide a delicate balance. The dimensionless reaction equilibrium constant, m_2, must be sufficiently large to obtain large amount of complex and, hence, a high facilitation factor. On the other hand, the reverse rate must be large enough to readily reverse the

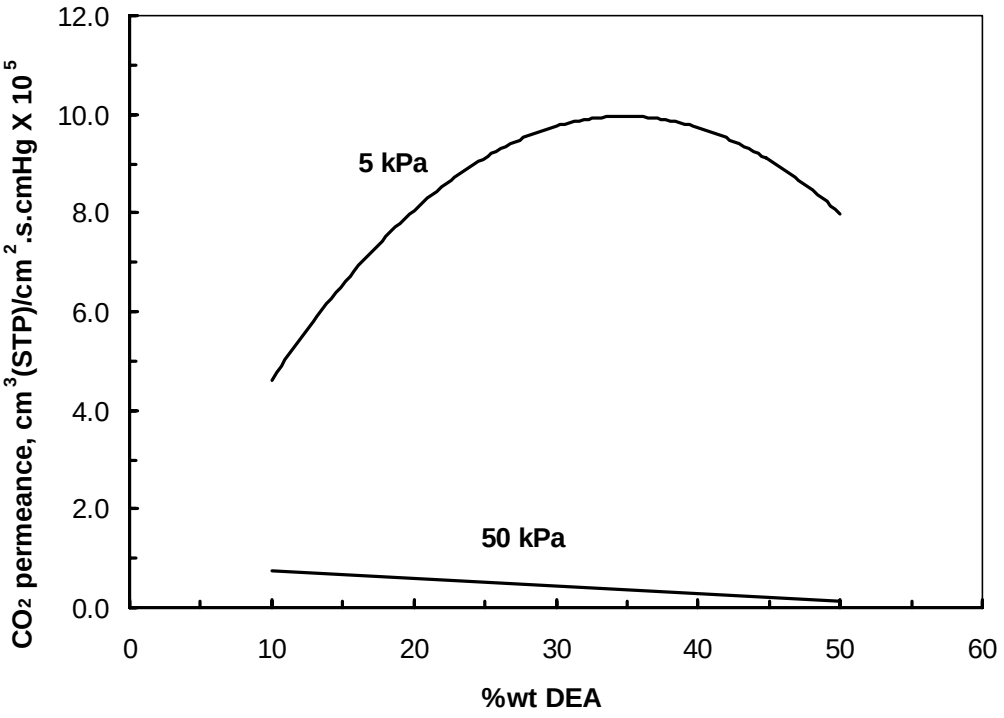

Figure 4.12 Calculated CO_2 permeance as a function of DEA concentration at CO_2 pressure differential of 5 and 50 kPa. T= 296K

complexation step so that the carrier can be regenerated and can be recycled to repeat the process. This important point is illustrated in Fig. 2.4. As shown in the figure, the likely range for bond energies is approximately 10-50 kJ/mol. This corresponds to a relatively weak bond between the solute and the carrier; covalent bonds that hold organic molecules together range from 200-500 kJ/mol. Bond energies less than 10 kJ/mol are similar to van der Waals interactions. Bond energies above 50 kJ/mol, reactions are difficult to reverse without energy inputs (King, C.J., 1987).

Therefore, the types of bonding interactions that will be most useful for facilitated

transport include acid-base interactions (e.g. Brønsted-Lowry and Lewis), coordinate-covalent bonds (*e.g*. those involving complex metal ions) and hydrogen bonds (see Fig. 2.4). Note that the CO_2-DEA reactions are considered to follow Lewis acid-base mechanism (Dankwerts, 1979).

4.7.2.2 Effect of DEA Concentration

Based on the numerical solution of the diffusion-reaction mass transport equations, the facilitation factor increases with increasing DEA concentration . For example, at CO_2 partial pressure differential of 0.19 kPa, a 10wt% DEA gives a facilitation factor of 37.65 (Fig.4.2) while 50wt% DEA gives a facilitation factor of 511.2 at a partial pressure differential of 0.4 kPa. However, the CO_2 permeance shows a different trend. As shown in Fig 4.12, at a partial pressure differential of 5.0 kPa, CO_2 permeance attained a maximum value at approximately 30 - 40wt% DEA. This is due to the reduction in the diffusivity and solubility of CO_2 with increasing DEA concentration. In the case of high CO_2 pressure differential (50 kPa) where the facilitation factor is one, the CO_2 permeance decreases with increasing DEA concentration and the it no longer function as a facilitating membrane.

4.7.3 Summary

An explanation for the experimental observations is proposed with the aid of the diffusion-reaction mass transport equations. It provides quantitative interpretation on the observed permeation behaviour of CO_2 through the reactive membrane. Also, the

numerical solution appears to be valid over wide range of partial pressure differentials. The numerical solutions of the governing differential equations were able to predict the same trends for the experimental permeance as a function of pressure differentials and concentrations. At low CO_2 pressure differential, the CO_2-DEA reaction attained equilibrium in the core of the membrane so that the forward and reverse reactions are confined regions near the physical boundaries of the membrane.

It can be concluded that the diffusion-reaction equations can be utilized to investigate the influences of these parameters on the transport of CO_2 through the reactive membrane provided that a reliable kinetic data is used.

Chapter 5

Material Selection and Membrane Preparation

In designing a membrane, the first considerations to be undertaken are the selection of the membrane materials and membrane preparation procedures. These are the main factors that will influence the mechanism of transport, membrane stability and membrane performance. The main objective of this chapter is to experimentally select the support layer for the PVA-amine blend solution that will provide mechanical strength as well as stability to the membrane. This was followed by the development of detailed membrane preparation procedures. Pure gas permeation was chosen for this chapter. Different amines were tested to select a carrier for CO_2 with appropriate properties to produce the highest gas permeation and selectivity. Then, optimum concentration of the carrier was determined and finally, membrane thickness, thermal and long- term stability tests were conducted.

5.1 Materials

Poly(vinyl alcohol) (PVA) (99%+ hydrolyzed; Mw = 133,000) was purchased from Polysciences Inc.; monoethanolamine (MEA), 2-amino-2methyl-1-propanol (AMP), diethanolamine (DEA) and N-methyldiethanolamine (MDEA) with purities of 99% were obtained from Aldrich Co. Deionized water was used to dissolve PVA. Research grade carbon dioxide and nitrogen (99+% pure) were purchased from Praxair. All materials were used without further purification. Hydrophilized microporous polysulfone (PSF)

membranes (Life Sciences, Pall Company, average thickness: 145μm, pore radius: 0.45 μm) were used as the support membranes.

5.2 Experimental Procedures

The set-up of the gas permeation experiments using the facilitated transport membranes is shown in Fig. 5.1 The apparatus consisted of a circular flat-type stainless steel membrane cell with permeation area of 13.85 cm^2, a gas flow system that delivered CO_2 and N_2, a water vapor saturator and pressure gauges. The membrane was moisturized by vapour deposition until its weight is increased by about 50% of its dry weight based on our preliminary results. This procedure is important because permeation rate of CO_2 is very small for dry membranes. The feed gas was saturated by water vapor after coming through the saturator. The feed pressure was maintained in the range of 170 to 273 kPa (25-75 psia) while the downstream/permeate was vented to the atmosphere. The permeate flow rates were measured by volume displacement using a soap bubble flow meter.

All experiments were performed at room temperature (296-298 K). Each experiment was repeated at least twice. The permeance reached steady state within 3-hours from the starting time. Steady-state permeation was determined by permeate flow rate measurements made at 30-minute intervals. Steady state was assumed to have reached when the flow rate no longer changed with time. The minimum test period for each membrane was 48 hours. During that time no significant changes in the membrane performance was observed. All data presented in the plots were the average of 5 steady state permeation rates with standard deviations of less than 1.0 $cm^3(STP)/cm^2.s.cmHg \times 10^5$

The experimental steady-state permeance through the membrane is calculated as follows.

$$J = \frac{273.15}{T} \cdot \frac{V}{t} \cdot \frac{1}{A} \cdot \frac{1}{p^0 - p^L} \tag{5.1}$$

where J (cm^3(STP). $cm^{-2}.s^{-1}.cmHg^{-1}$) is the permeance, T (K) is the room temperature, V (cm^3) is the volume of the permeate through the membrane over a period of time (t), A (cm^2) is the effective membrane area and p^0 and p^L are the upstream and downstream pressure respectively. The term $p^o - p^L$ is referred to as the pressure differential. To convert from cm^3(STP). $cm^{-2}.s^{-1}.cmHg^{-1}$, multiply J by 7.5 x 10^{-3} to give SI unit of m^3(STP). $m^{-2}.s^{-1}.kPa^{-1}$.

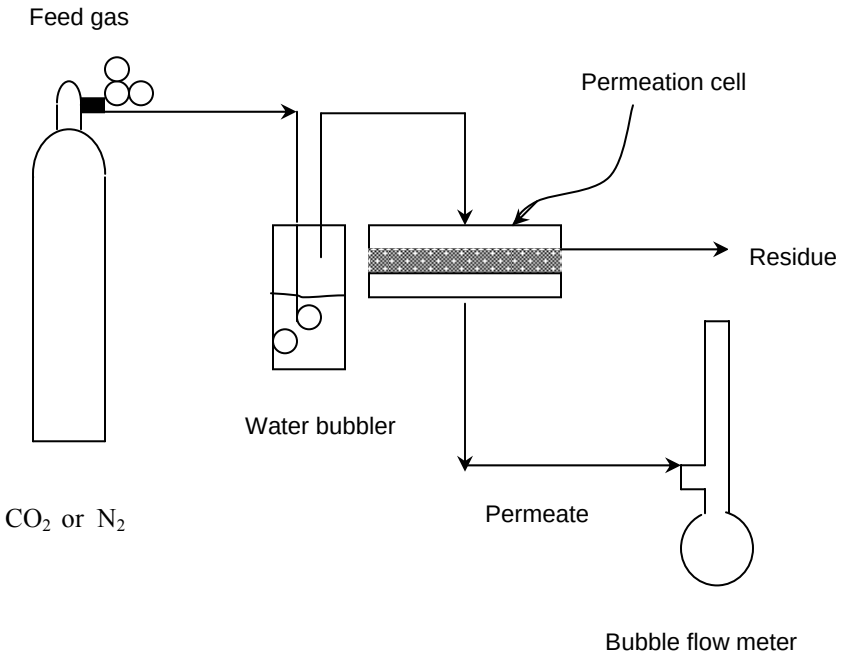

Figure 5.1 Schematic diagram of experimental set-up.

5.3 Membrane Preparation Procedures

1. PVA solution (10 wt.%) was prepared by dissolving pre-weighed dry PVA in water followed by heating at 90^{o}C for six hours with vigorous stirring on a tightly capped glass container.
2. Then the solution was allowed to cool down to 70^{o}C before adding the amine to prepare the desired composition. The PVA-amine mixture was then mixed continuously for 6 hours at 70^{0}C.
3. The solution was then cooled to room temperature for at least three hours, then degasified for one hour in a vacuum glass jar and allowed to stand for at least one day before casting.
4. Glass rod, equipped with a copper wire (diameter: 268 μm) on both side, was used to cast the PVA-amine mixture on the top of PSF substrate, which was in turn supported by glass plate.
5. The membrane was allowed to dry on top of the hot plate (low heat, 45^{0}C) for one hour so that the solution will spread evenly on the substrate. The membrane was further dried at room temperature for at least 24 hours before being used for permeation test or kept in a dessicator.

5.4 Results and Discussion

5.4.1 Choice of substrate

The criteria for the substrate membrane selection include support surface characteristics and the reactivity of the polymer substrate toward the fluids in contact with it. For this investigation, the substrate is in contact with three different materials namely, feed gas (CO_2 and N_2), PVA and the amines. Therefore, experiments were performed to choose a substrate that should be non-reactive and would not be degraded chemically or physically over an extended period of time and should be hydrophilic so that the casting solution would spread evenly throughout the surface.

Based on literature search, polysulfone (PSF) and poly(vinylidene fluoride) (PVDF) were the most commonly employed substrate materials due to their excellent chemical resistance. A strip of both membranes was immersed overnight to different MEA concentrations contained in Teflon sealed glass jars. The results of the experiments were presented in Fig 5.2. It is obvious that the aqueous amine solution attacked the PVDF membranes even in the lowest amine concentrations as can be seen from the change in colour. However, in the case of PSF there was no change in the colour even with pure amine. The chemical stability of PSF was also tested with all the remaining amines, *i.e.* AMP, DEA and MDEA and the results were the same as that of MEA. From these experimental observations it was decided to use PSF as substrate for the PVA-amine membranes.

Poly(vinyl alcohol) is utilized for numerous separation processes because of its low cost, chemical and mechanical stabilities against a wide range of reagents. Table 5.1 lists some of the important properties of PVA. PVA is produced commercially by the hydrolysis of poly(vinyl acetate), during which the acetate groups are progressively replaced by the hydroxyls (OH^-). The higher crystallinity of PVA can be attributed to the small size of the OH- groups, which allow the polymer chains to adopt a planar zig-zag conformation through hydrogen bonding (Hodge *et al.*, 1996). PVA is perhaps the simplest water-soluble hydrophilic polymer, with the highest glass transition temperature (Tg = 85 ^oC for 98-99% hydrolyzed PVA). It exhibits high packing efficiency due to the planar zig-zag conformation as crystalline aggregates caused by hydrogen bonding between the adjacent OH^- groups (Martien *et al.*, 1986). PVA could be cast from water as films, sheets and fibers with excellent mechanical properties. It can be used as a membrane in dehydration processes due to its high hydrophilicity, chemical stability and excellent film-forming capability. Because of its biocompatibility, PVA could also be used in a variety of biomedical applications (Carvalho *et. al*., 1996; Oda *et. al*., 1998).

5.4.2. Swelling Effect of Water in the PVA-DEA Membrane

As mentioned in the experimental procedures, the membrane should be moistened with de-ionized water before mounting into the permeation unit. In this section, experiments

Figure 5.2 Effect of exposing polysulfone(right) and polyvinylidene fluoride (left) on aqueous amine solution.

Table 5.1 Properties of poly(vinyl alcohol) (Finch, 1992).

Property	Data	Comments
Colour	White to ivory	
Storage stability	Indefinite in dry storage	
Light stability	Excellent	
Thermal stability	Depends on temperature	Gradual discoloration above 100 ^{o}C Darkens rapidly above 150 ^{o}C Decomposes rapidly above 200 ^{o}C
Effect of weak acids	Softens or dissolves	
Effect of strong acids	Dissolves or decomposes	
Effect of weak alkali	Softens or dissolves	
Effect of strong alkali	Softens or dissolves	
Effect of organic solvents	Generally resistant	
Specific gravity	1.23-1.31	Increases with degree of crystallinity
Specific volume	0.75-0.85 L/kg	
Specific heat	1.65-1.67 J/(g-K)	
Heat sealing temp (^{o}C)	160-210	Unplasticized polymer
Glass transition temp (^{o}C)	85 58	98-99% hydrolyzed 87-89% hydrolyzed
Melting point (^{o}C)	230 180	98-99% hydrolyzed 87-89% hydrolyzed
Degree of crystallinity	0-0.54	Increases with heat treatment and degree of hydrolysis

were conducted to demonstrate the effects of water in the membrane performance. PVA and PVA–DEA membranes were tested. Water vapour depositions were carried out at various times until the membrane samples with a variety of water content were available for testing. The feed pressure was maintained to approximately 204 kPa absolute. The water contents were determined from the difference in weight of the dry and wet membranes. Figure 5.3 to 5.5 show the CO_2 and N_2 permeance results for the PVA and PVA-DEA membranes swelled by water. The gas permeance were plotted versus the water content of the membranes. It is noted that the PVA-DEA membrane demonstrated high permeance compared to PVA membranes. Dry membranes show very small gas permeance. For CO_2, water content of 20 to 50wt% shows relatively stable permeance similar in behaviour to N_2 permeance, resulting in CO_2/N_2 selectivity in the range of 75-86. However, as the water content increased to about 70wt%, the permeance of both CO_2 and N_2 are almost similar to one another leading to selectivity of about 4. We observed that the surface of the membrane containing 70wt% water appears to be sticky. As the water was absorbed through the membrane, the water molecules diffuse and attach themselves into the hydroxyl groups of the PVA chains. This process likely disrupts the inter- and intra-molecular hydrogen bonding in the PVA structure leading to an increase in chain segmental mobility and creates free volume or empty space in the polymer, thereby swelling the membranes. This results in an increase in penetrant diffusivity and therefore permeances. For water content of about 70wt% or higher, the collapse of selectivity may be attributed to the attainment of large disruptions of the inter- and intra-chain hydrogen bonding apparently reaching maximum chain mobility and free volume, forming a gel-like polymer matrix.

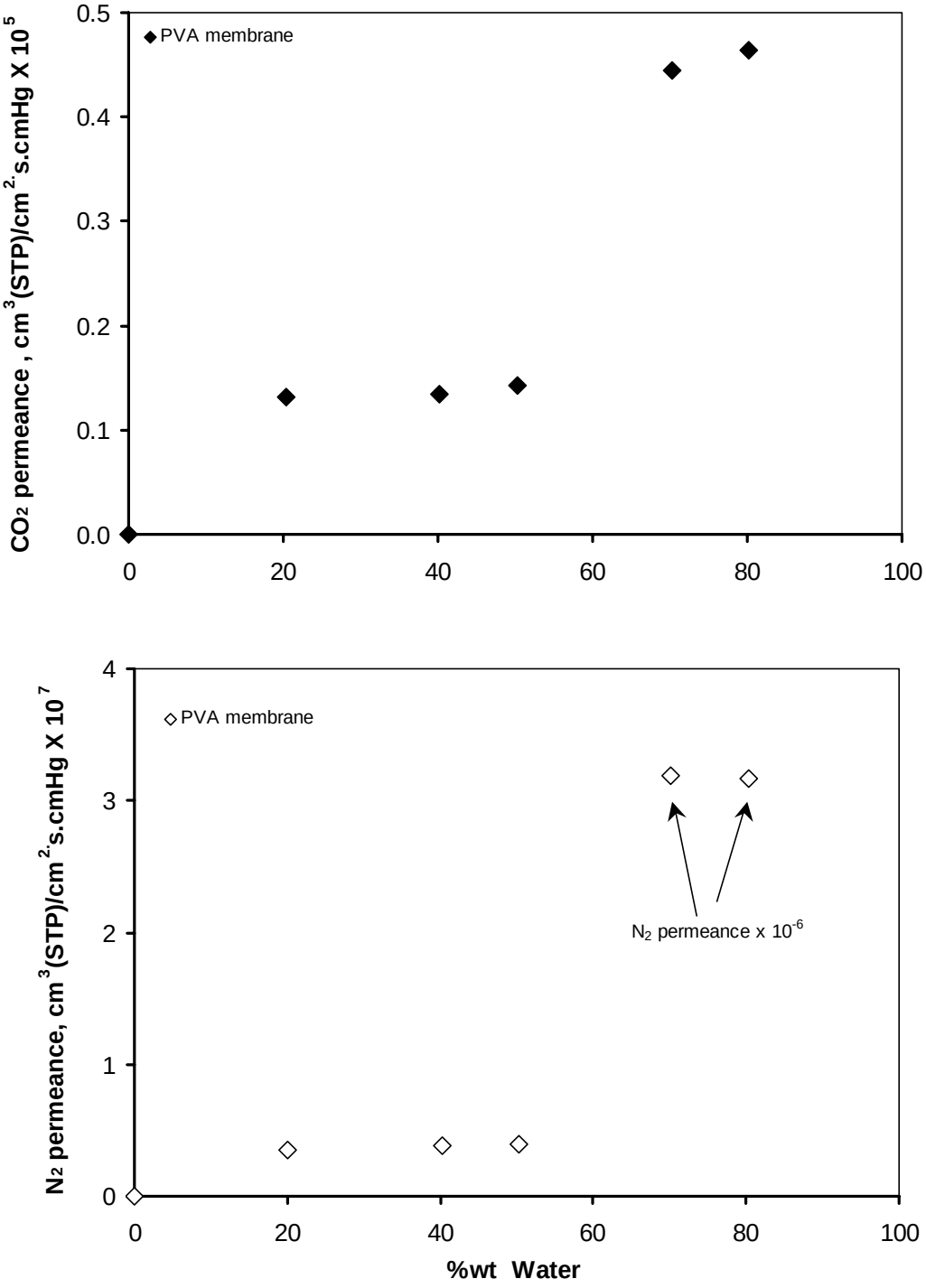

Figure 5.3 Permeances of CO_2 and N_2 for the PVA membrane as a function of membrane water contents at feed pressure of 204 kPa.

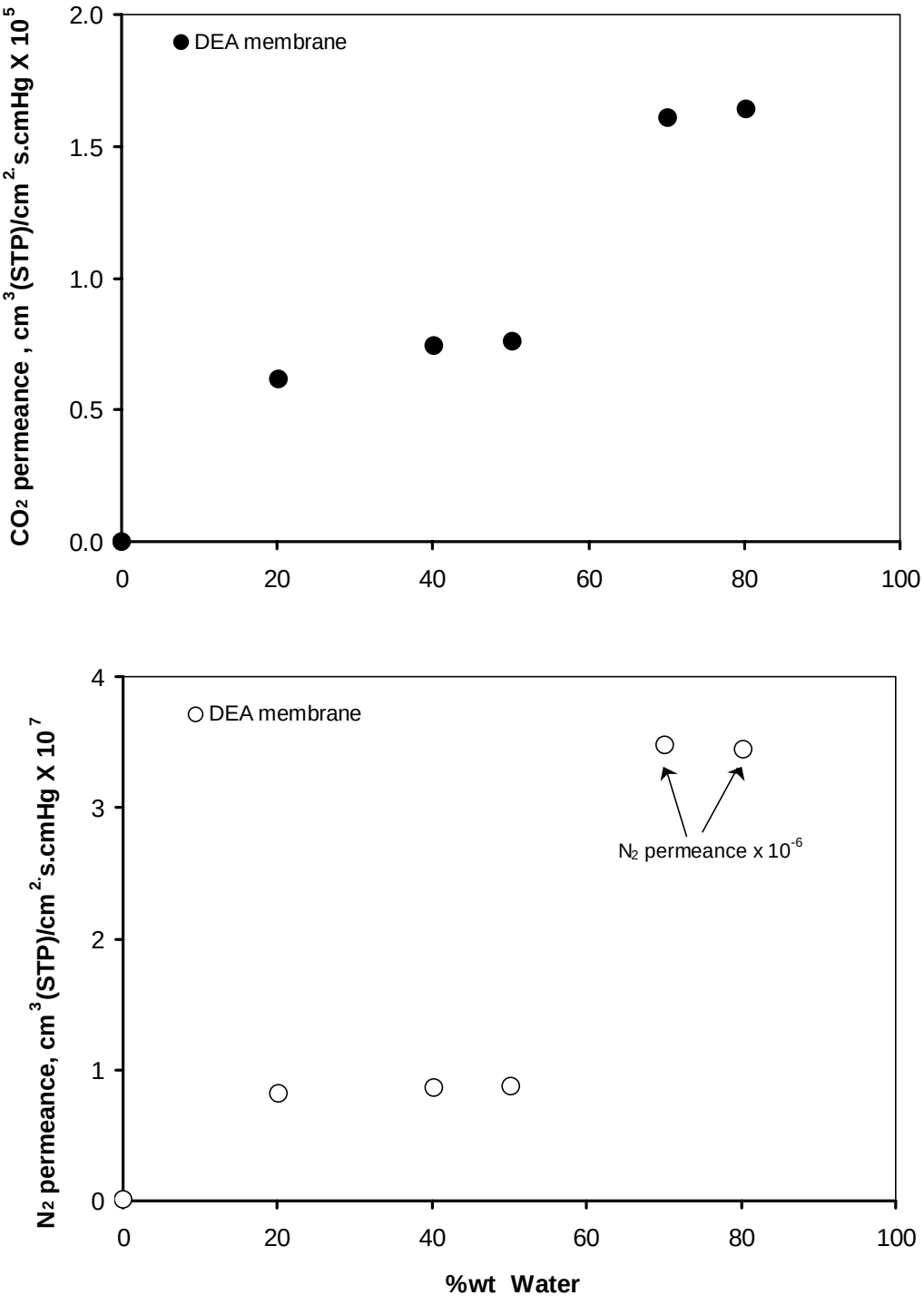

Figure 5.4 Permeances of CO_2 and N_2 for the PVA-DEA membrane as a function of membrane water contents at feed pressure of 204 kPa.

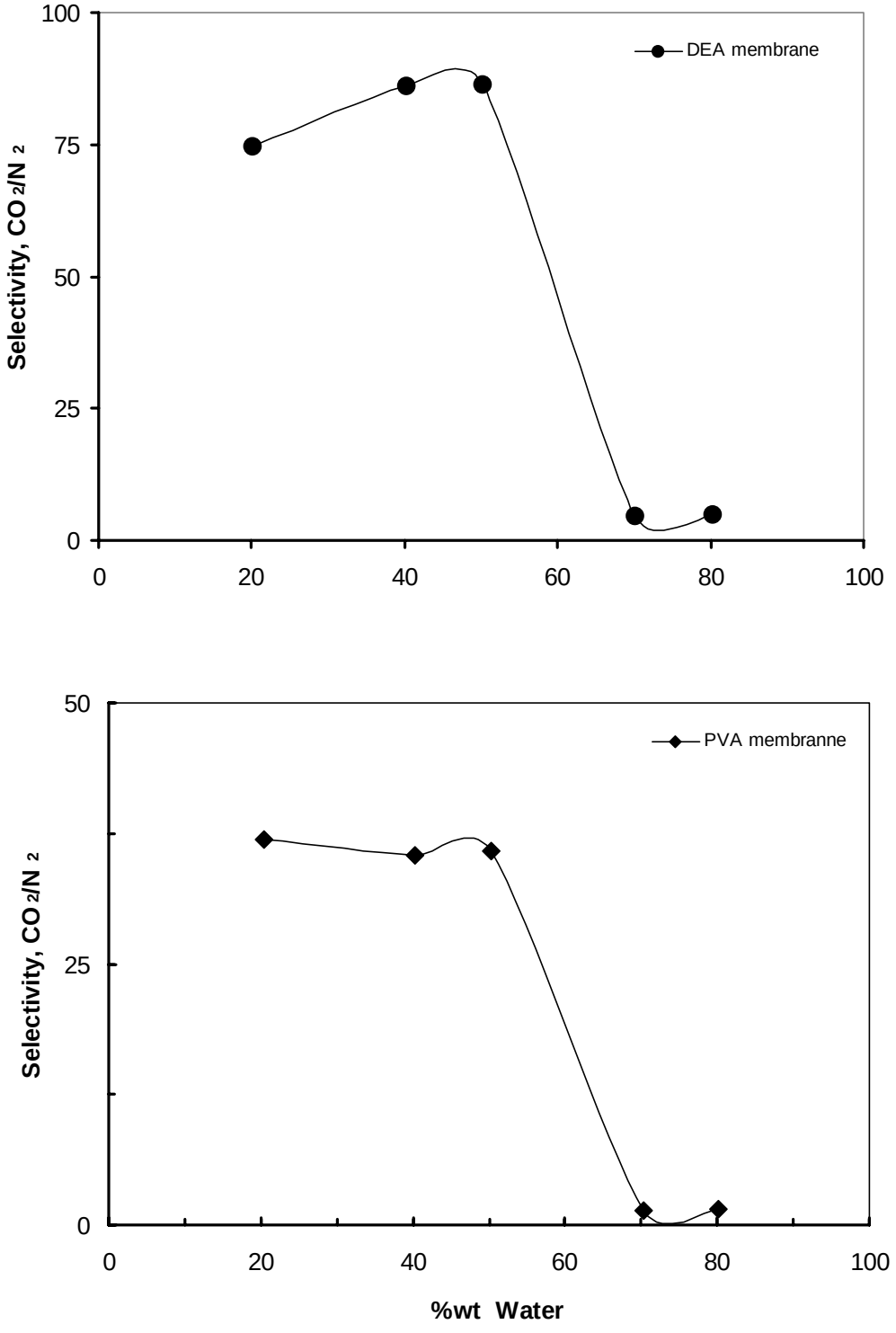

Figure 5.5 Selectivity of CO_2 over N_2 for the PVA-DEA and PVA membrane as a function of membrane water contents at feed pressure of 204 kPa.

5.4.3 Choice of Amines

A series of experiments were performed to determine which amine would demonstrate the highest permeances and facilitation for CO_2 permeation across the reactive membrane. AMP, DEA, MEA and MDEA were incorporated into the PVA membranes each at concentrations ranging from approximately 16 to 50wt %. Pure gas permeation was carried out at feed pressures of 170 to 273 kPa (25 to 40 psia) while the permeate was kept at atmospheric pressure.

The results for these experiments were presented in Figures 5.6 to 5.15. Among the amines tested, DEA gives the highest CO_2 permeance for the feed pressures tested. In general, the permeance of CO_2 for various amines are in the order of DEA > AMP > MEA > MDEA. For comparison purposes, the CO_2 permeance in the PVA membrane are also plotted. It is seen in Figures 5.7, 5.9, 5.11 and 5.13 that for each amine membrane, the permeance of N_2, which is transported by solution-diffusion mechanism was almost independent of the N_2 feed pressures while CO_2 permeances for the PVA membrane increased slightly with increasing feed pressures. This pressure dependence could be attributed to the interaction of CO_2 to the PVA matrix leading to an increase in local segmental motion of the polymer chain causing an increase in penetrant diffusivity. For larger and condensable gases such as CO_2, the permeability coefficient was found to be pressure dependent. It could either be an exponential or linear function of feed pressure (Merkel *et al*., 2000). These authors also reported that the permeability coefficients of more condensable gases have stronger dependence on pressure.

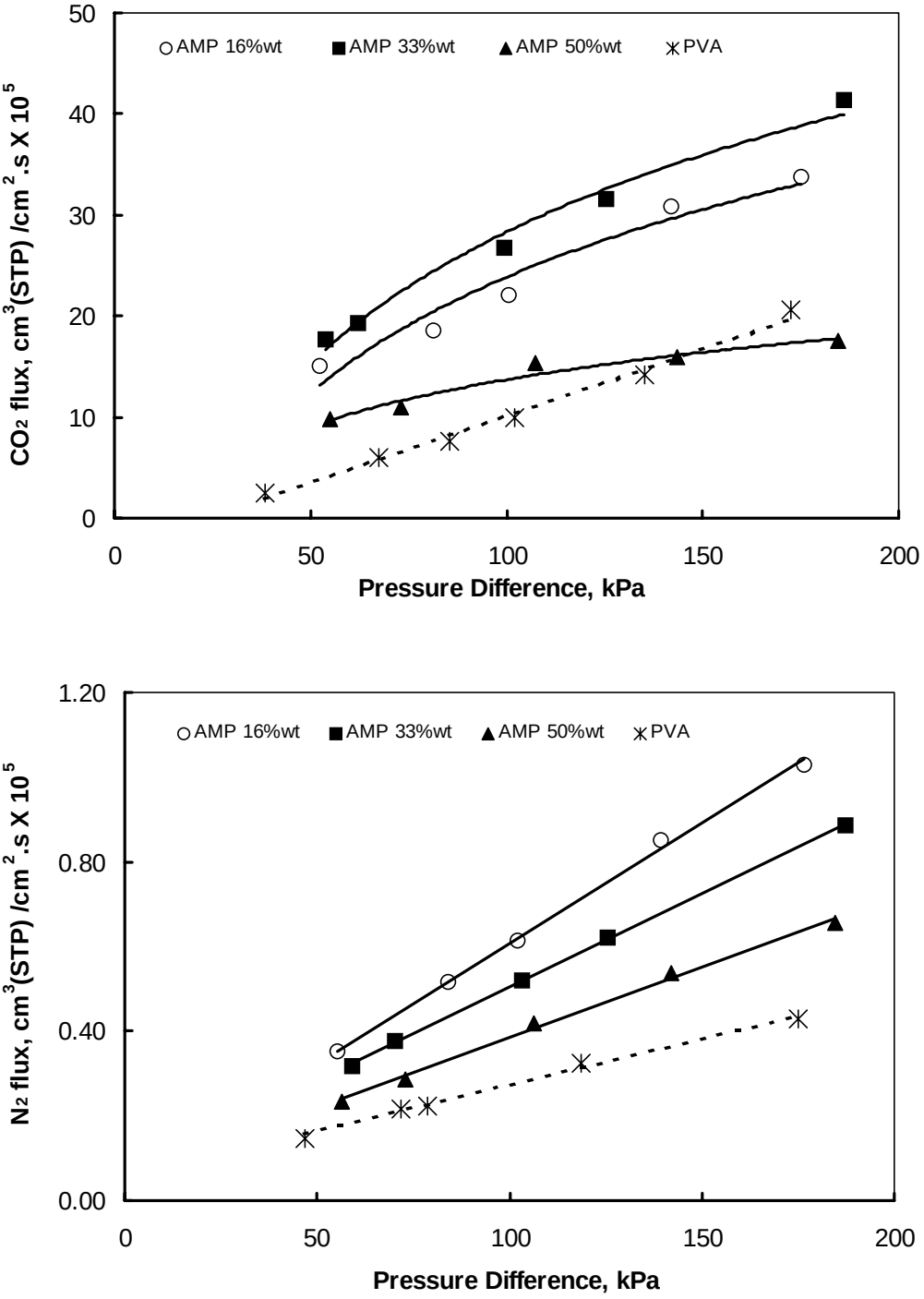

Figure 5.6 Fluxes of CO_2 and N_2 for PVA-AMP membrane as a function of feed pressure at different concentrations.

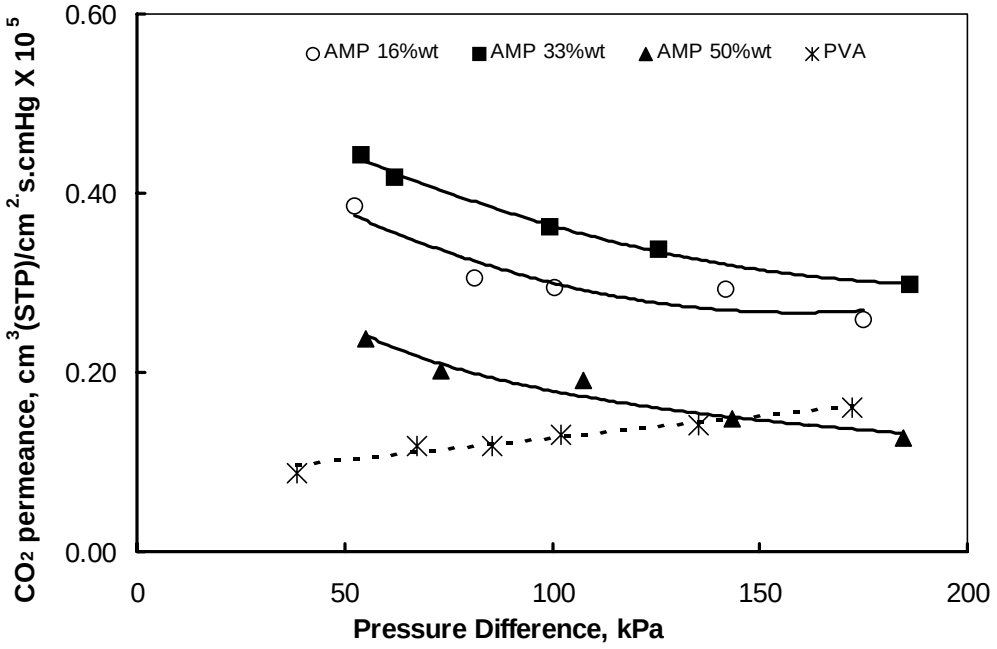

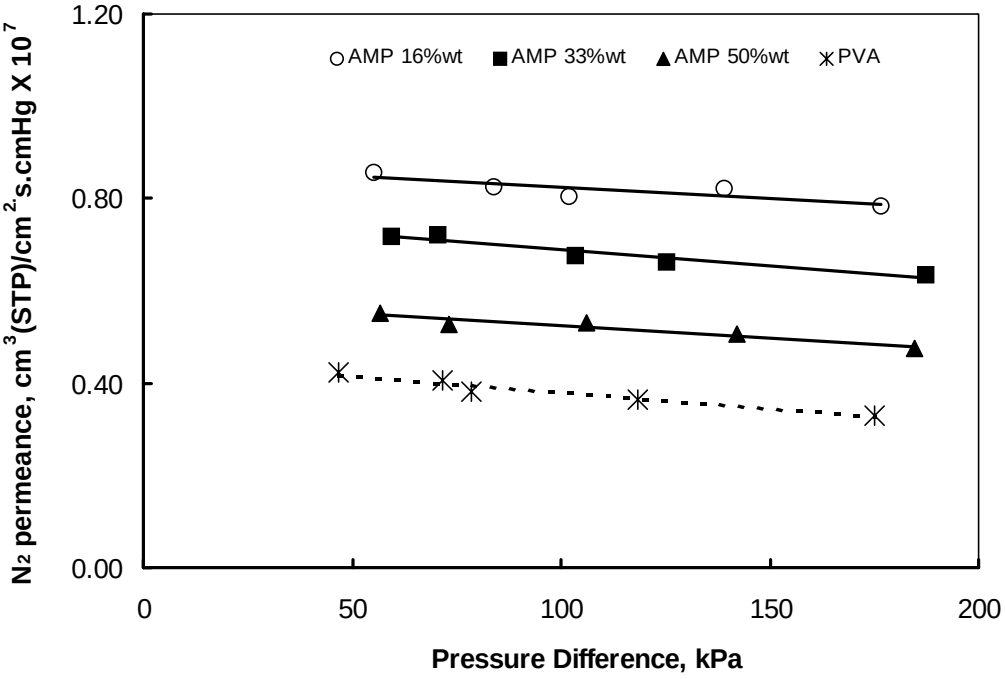

Figure 5.7 Permeances of CO_2 and N_2 for PVA-AMP membrane as a function of feed pressure at different concentrations.

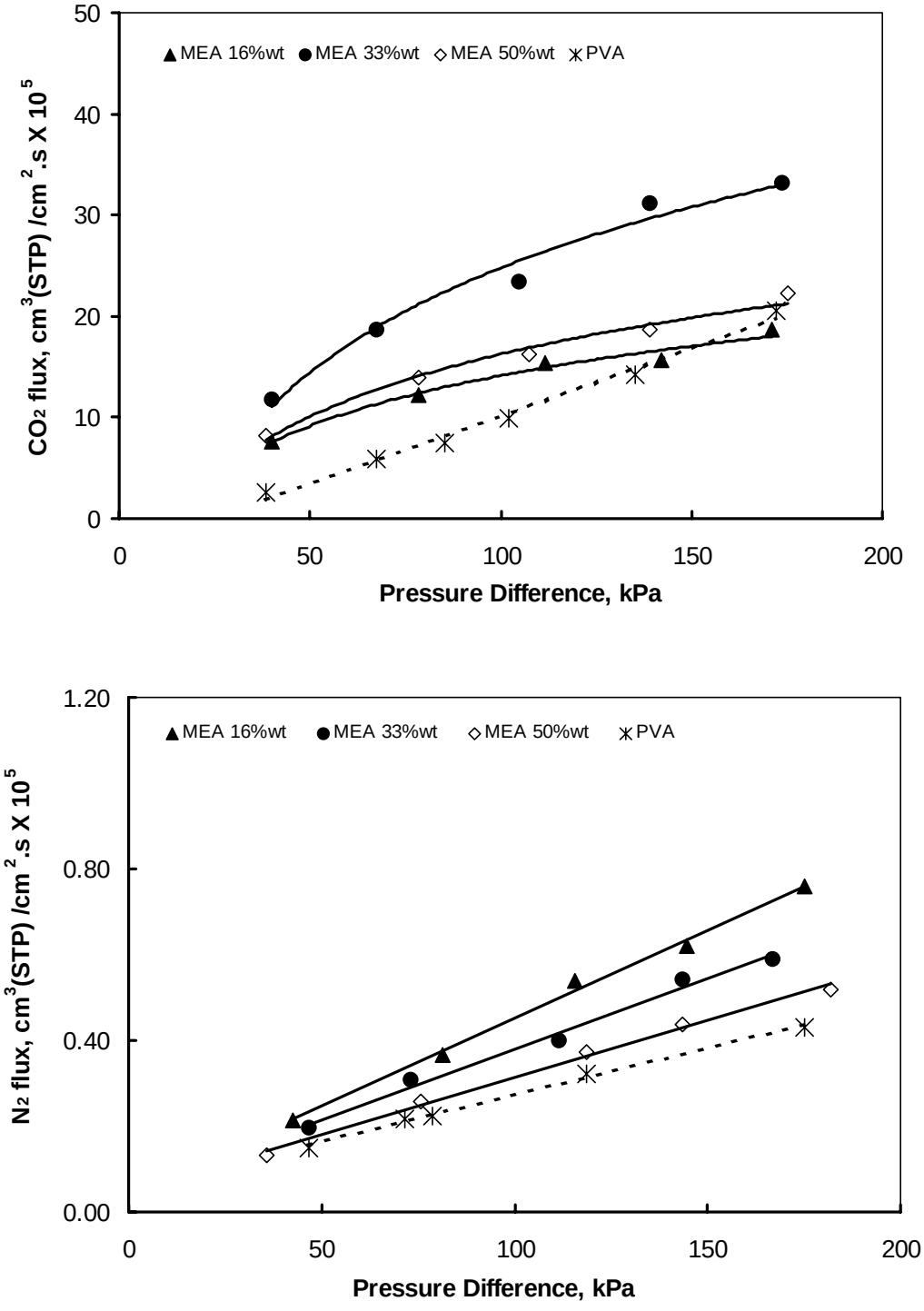

Figure 5.8 Fluxes of CO_2 and N_2 for the PVA-MEA membrane as a function of feed pressure at different concentrations.

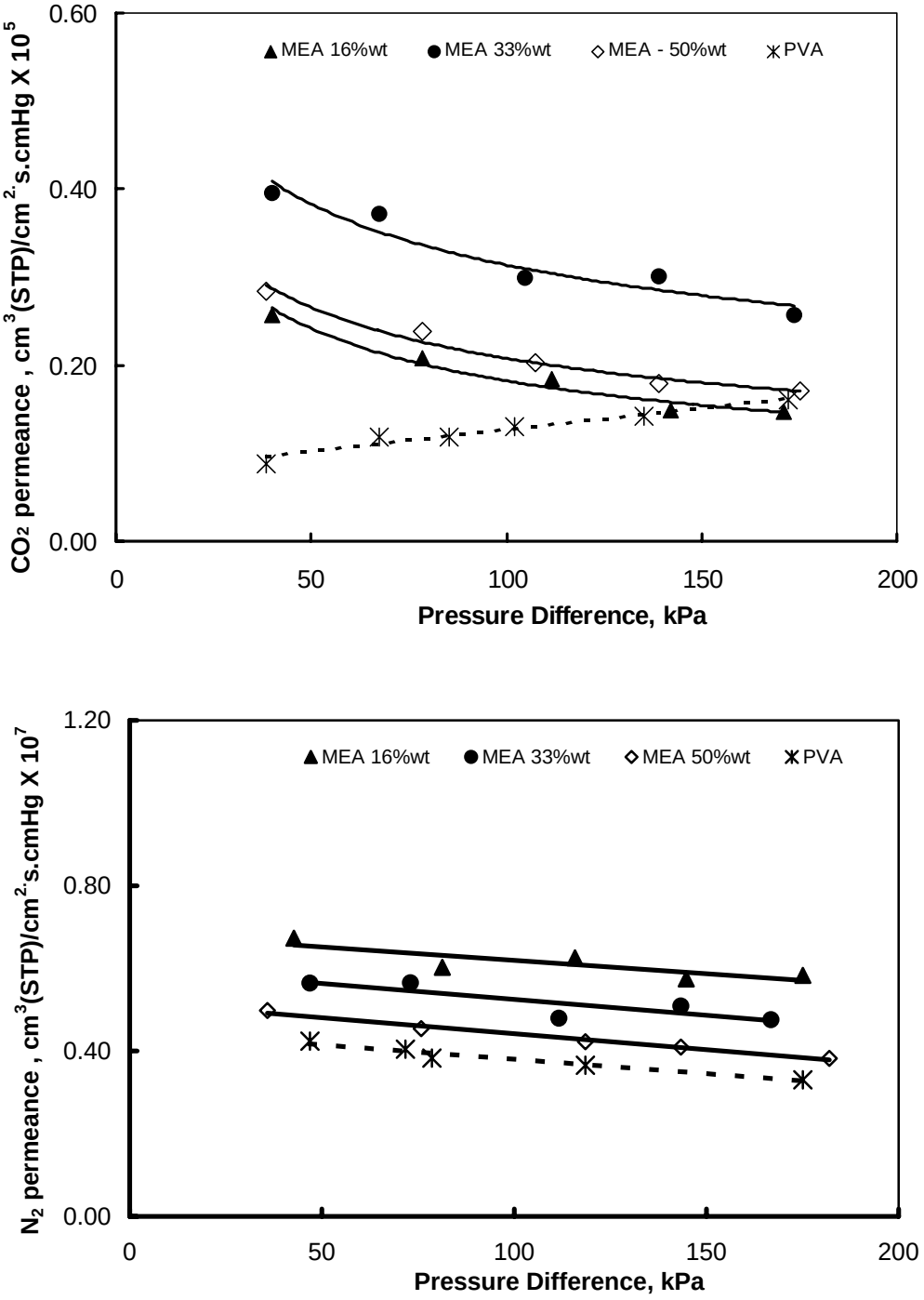

Figure 5.9 Permeances of CO_2 and N_2 for the PVA-MEA membrane as a function of feed pressure at different concentrations.

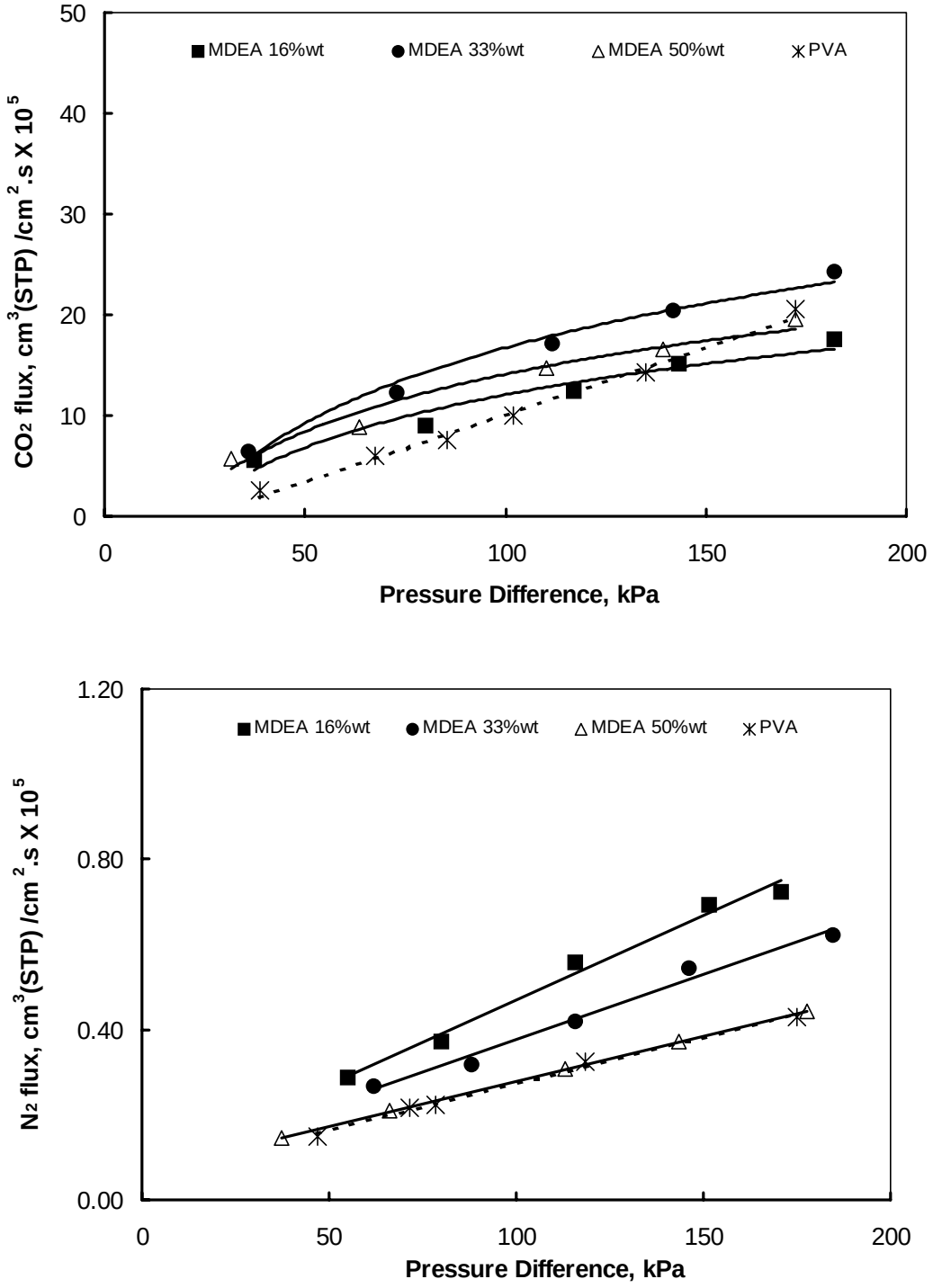

Figure 5.10 Fluxes of CO_2 and N_2 for the PVA-MDEA membrane as a function of feed pressure at different concentrations.

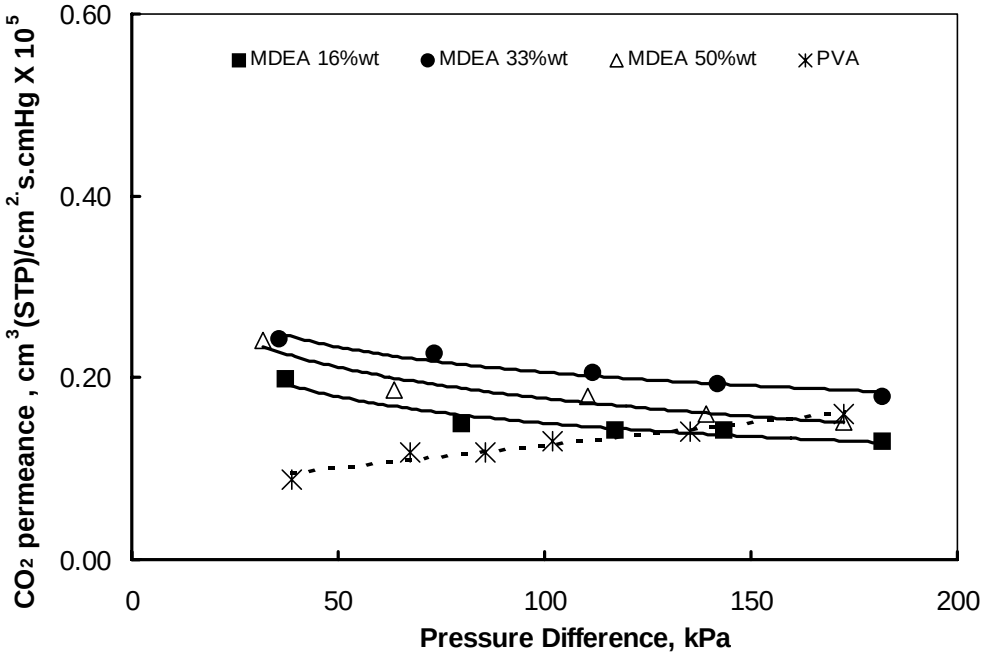

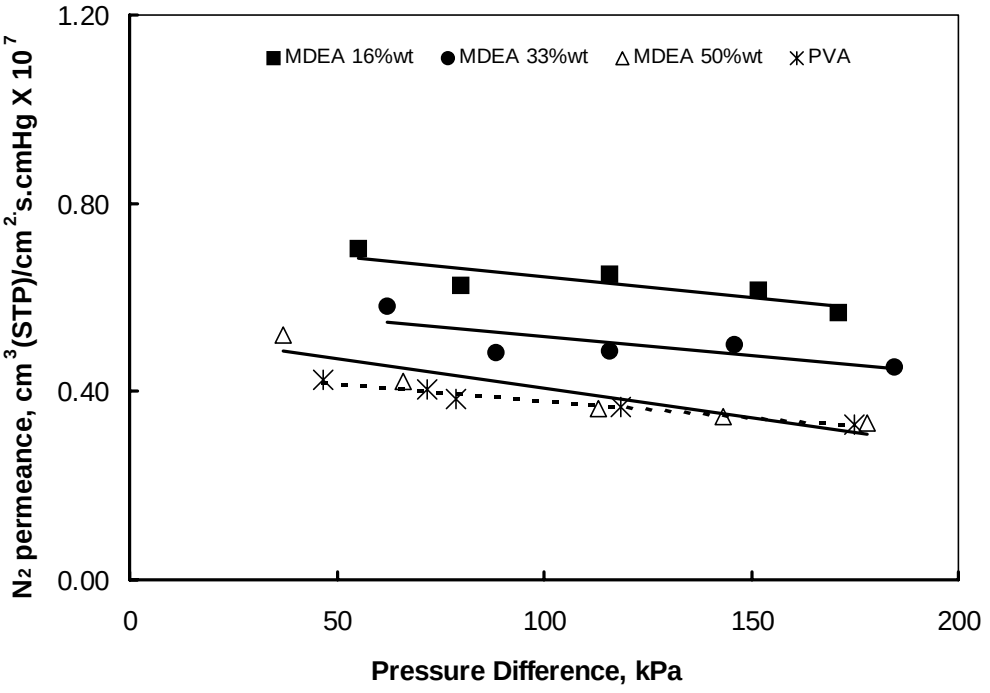

Figure 5.11 Permeances of CO_2 and N_2 for the PVA-MDEA membrane as a function of feed pressure at different concentrations.

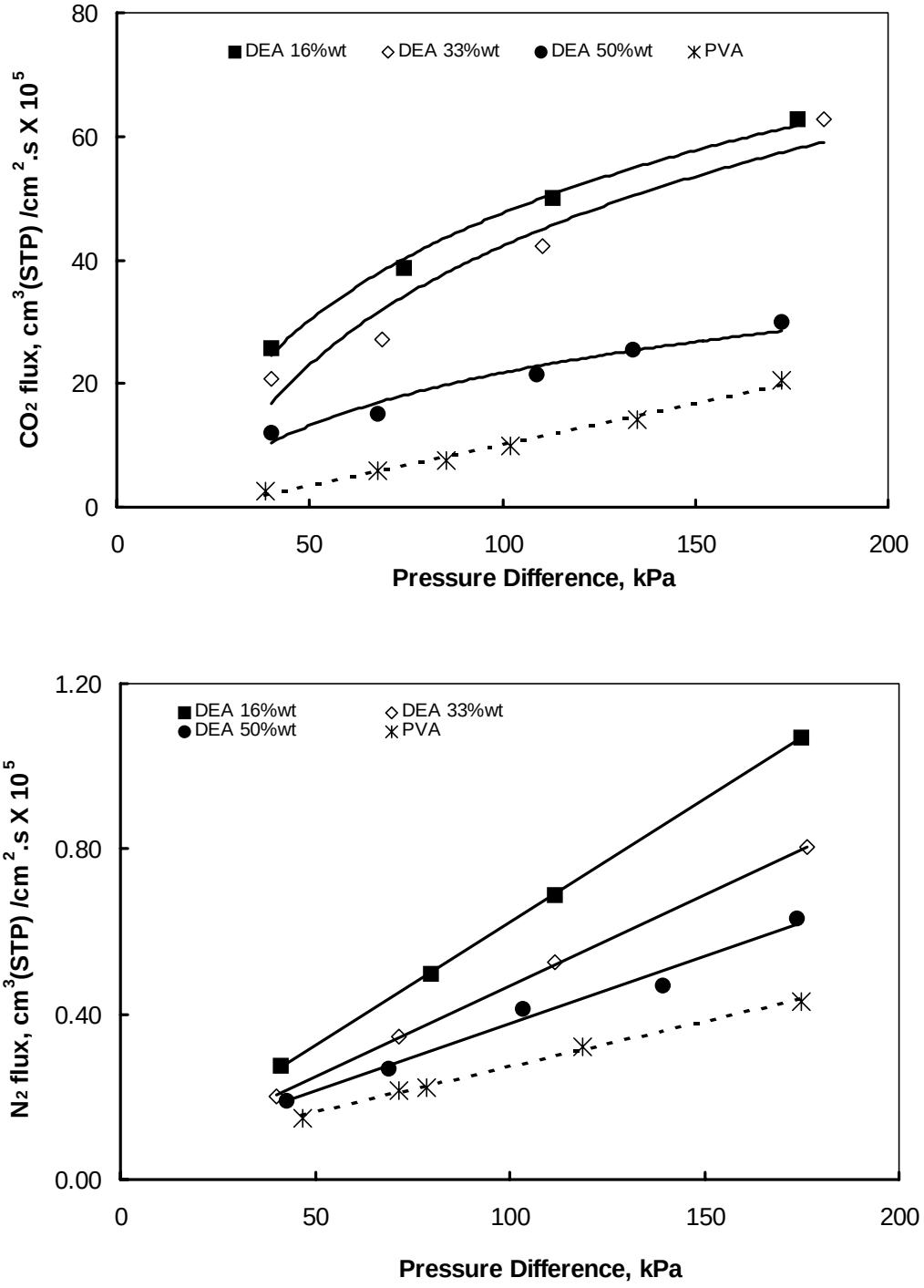

Figure 5.12 Fluxes of CO_2 and N_2 for the PVA-DEA membrane as a function of feed pressure at different concentrations.

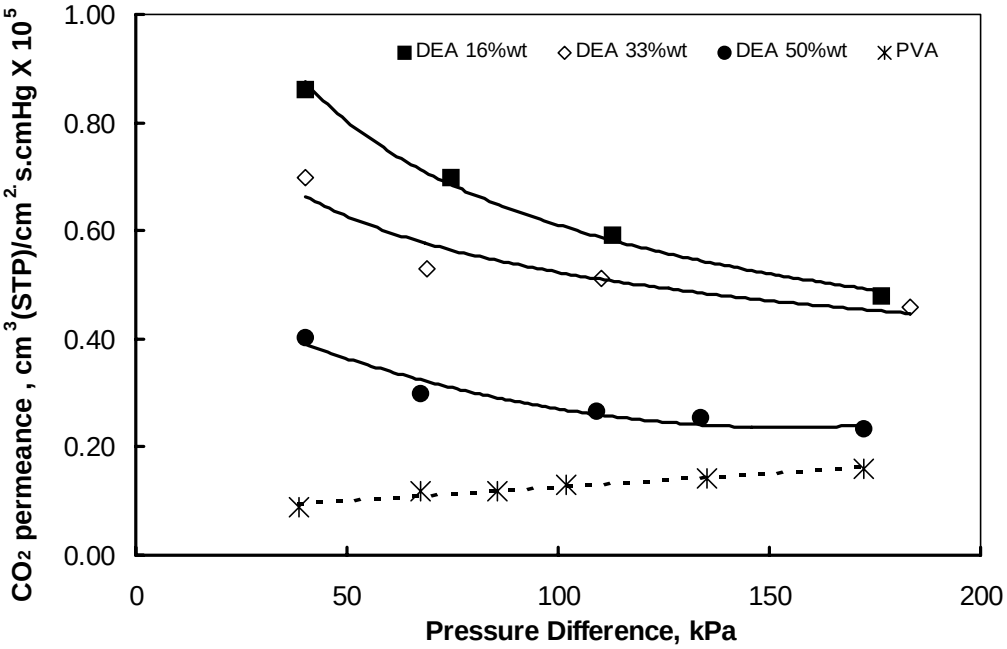

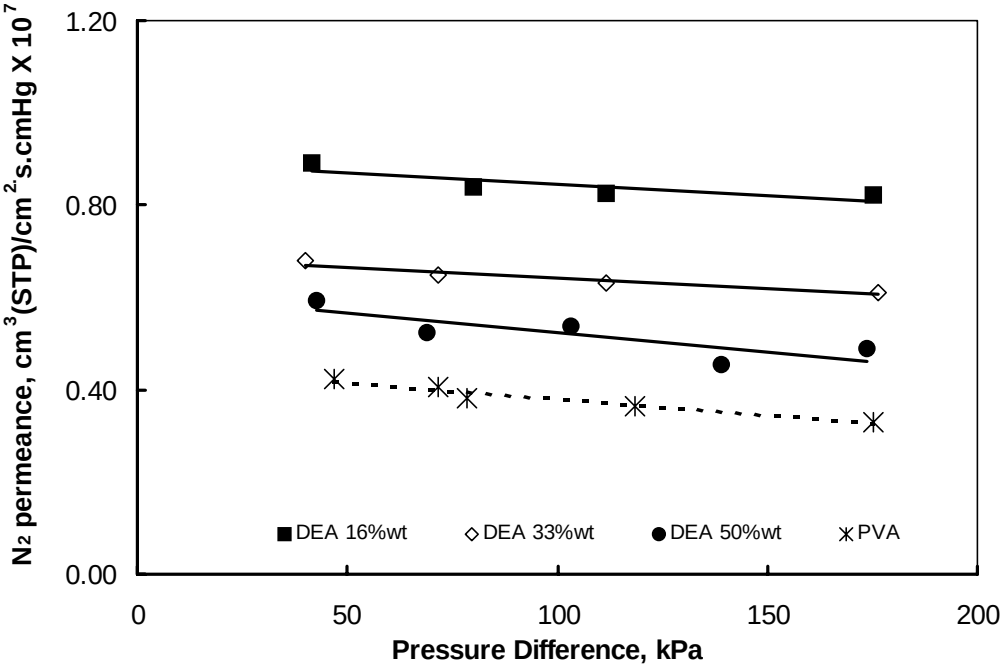

Figure 5.13 Permeances of CO_2 and N_2 for the PVA-DEA membrane as a function of feed pressure at different concentrations.

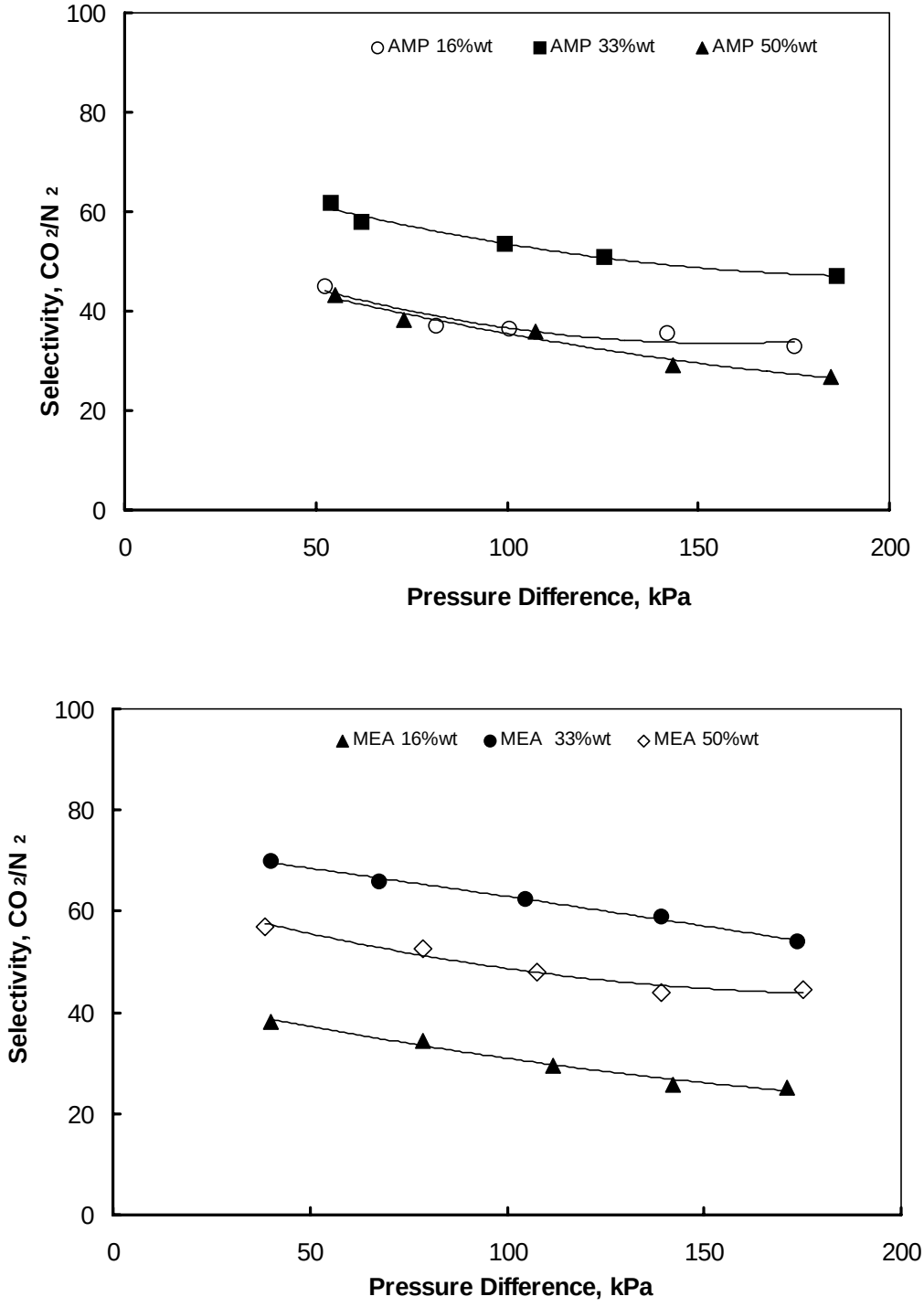

Figure 5.14 Selectivity of CO_2 over N_2 for the PVA-AMP and PVA-MEA membranes as a function of feed pressure at different concentrations.

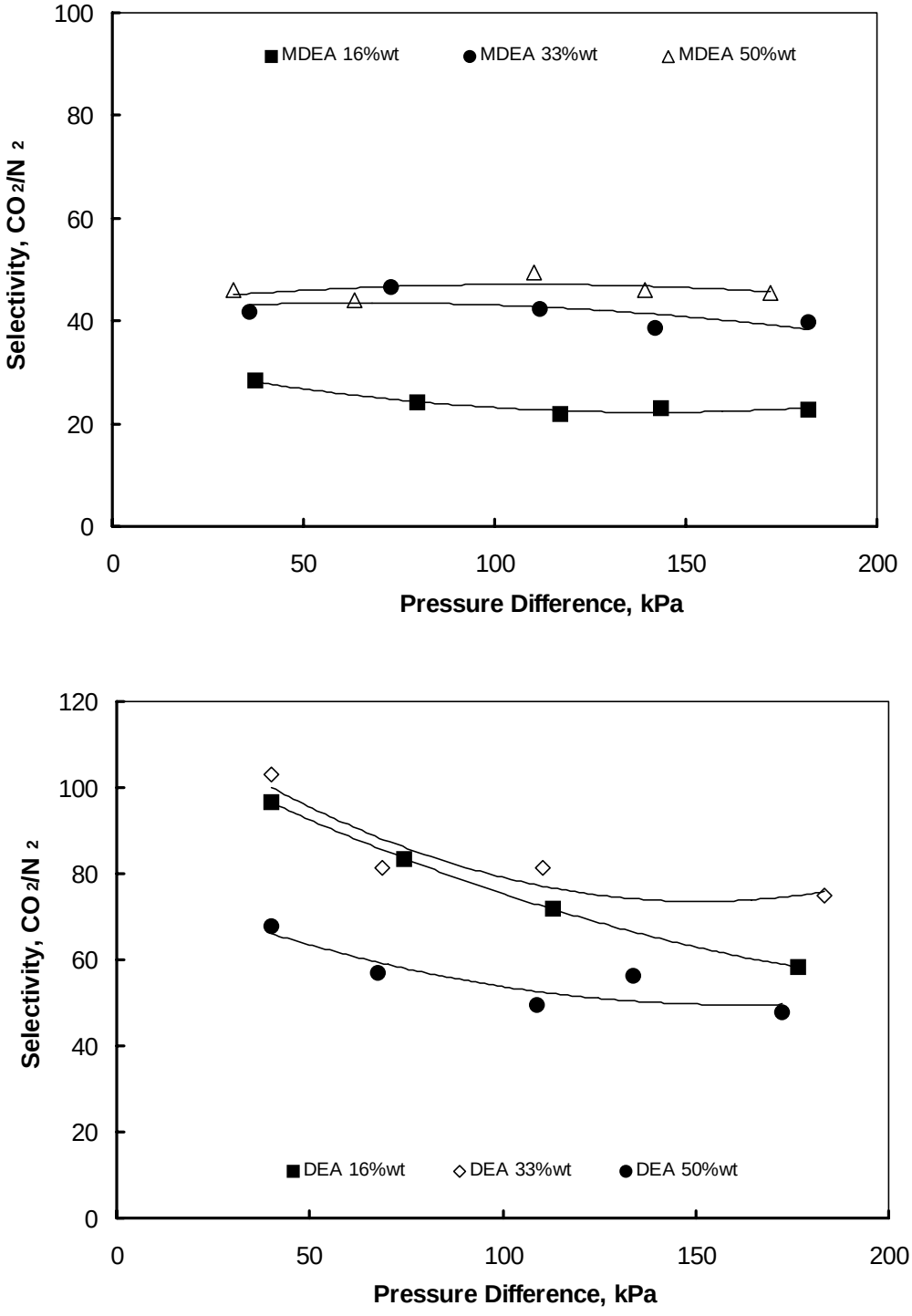

Figure 5.15 Selectivity of CO_2 over N_2 for the PVA-MDEA and PVA-DEA membranes as a function of feed pressure at different concentrations.

On the other hand, the CO_2 flux in the amine membranes increases with pressure differential and then approaches nearly constant value at higher feed pressure. For the non-reactive PVA membrane, the flux was approximately linearly proportional to the pressure differentials. Among the amine membranes tested, the CO_2 flux was found to increase with amine concentrations and decreases when the amine concentrations were approximately 50%wt. However, the N_2 flux increases almost linearly with pressure differentials similar to CO_2 in the PVA membrane. But with increasing amine concentration, the N_2 flux decreases.

The difference in CO_2 permeances among the amines studied may be attributed to kinetics of CO_2-amine system. Thus, it is useful to have a brief discussion about the chemistry of CO_2 – amine reactions. The widely accepted description of the reaction between CO_2 and amine as discussed in Chapter 3, is the Dankwerts zwitterion mechanism. In particular for primary and secondary amines the reactions are:

$$CO_2 + R_1R_2NH \underset{k_2}{\overset{k_1}{\rightleftharpoons}} R_1R_2NH^+CO_2^- \tag{5.2}$$

$$R_1R_2NH^+CO_2^- + R_1R_2NH \underset{k_4}{\overset{k_3}{\rightleftharpoons}} R_1R_2NCO_2^- + R_1R_2NH_2^+ \tag{5.3}$$

The overall reaction maybe expressed as follows:

$$CO_2 + 2R_1R_2NH \rightleftharpoons R_1R_2NCOO^- + R_1R_2NH_2^+ \tag{5.4}$$

$$K_{eq} = \frac{k_1k_3}{k_2k_4} \qquad k_r = \frac{k_1}{K_{eq}}$$

where K_{eq} and k_r are the equilibrium and reverse reaction rate constant respectively. As seen in Table 5.2, the equilibrium constant $\boldsymbol{K_{eq}}$ for MEA and AMP are large compared to DEA. This indicates that the reverse reaction rate constant $\boldsymbol{k_r}$ are low for MEA and AMP as shown in Table 5.2 because $\boldsymbol{K_{eq}}$ is inversely proportional to $\boldsymbol{k_r}$. This low reverse reaction rate constant makes desorption of CO_2 at the permeate side of the membrane slow. The lower $\boldsymbol{K_{eq}}$ of the reaction of CO_2 with DEA is favorable for the fast reverse reaction or the fast release of CO_2 in the permeate side which maybe the reason for the larger CO_2 permeances through the DEA membrane as compared to AMP and MEA membrane.

Table 5.2 Physicochemical properties of CO_2-amine system.

Amine	k_2 / k_3 [mol/cm^3]	k_1 [cm^3/mol.s]	K_{eq} [cm^3/mol]	$k_r = k_1/K_{eq}$ [1/s]
AMP	[a] 3.50×10^{-4}	[a] 8.10×10^5	[e] 2.28×10^6	0.355
DEA	[b] 1.18×10^{-3}	[b] 3.17×10^6	[b] 1.43×10^6	2.21
MEA	0	[c] 5.92×10^6	[f] 1.75×10^8	0.0338
MDEA	-	[d] 5.10×10^3	[d] 1.91×10^5	0.0267

a) Xu *et al*. (1996), b) Laddha and Dankwerts (1981), c) Hikita *et al*. (1977), d) Littel *et al*. (1990), e) Bosch *et al*. (1989), f) Teramoto *et al*.(1997). Temperature: 298K

MDEA being a tertiary amine has an extremely small value of $\boldsymbol{k_1}$, which is perhaps the reason for the lowest CO_2 permeance among the amines tested. MDEA does not react directly with CO_2 to form carbamate because this amine lacks the free proton (Blauwhoff *et al*., 1984). According to the reaction mechanism proposed by Donaldson and Nguyen (1980), the tertiary alkanolamines such as MDEA, act as bases, which catalyze the hydration of CO_2 that leads to the formation of bicarbonate. The overall reaction can be represented by:

$$CO_2 + R_3N + H_2O \longleftrightarrow R_3NH^+ + HCO_3^- \qquad (5.5)$$

MDEA is considered to be a sterically hindered amine due to the presence of 3-bulky alkyl groups attached to the amino group as seen in Figure 5.16. This may be the reason for the low tendency of MDEA to form stable carbamate in contrast to DEA and MEA. Carbamate stability has an important effect on the CO_2-amine stoichiometry. Referring to reaction (5.4), it shows that in the formation of stable carbamate, a half mole of CO_2 reacts per mole of amine. On the other hand, reaction (5.5) shows that one mole of CO_2 reacts per mole of amine. The rotation around the N-COO bond is somewhat less crowded and unrestricted in the carbamate of the unhindered amine (DEA, MEA), whereas rotation around H-CO_3^- bond in the carbamate of sterically hindered amine (MDEA) may only be possible if the bulky alkyl groups is to be compressed. We see how the bulkiness of R (alkyl group) has an important effect on the stability of the carbamate and consequently on the stoichiometry of the reaction with CO_2. By attaching a bulky

substituent to the amino group leads to a theoretical capacity of one mole of CO_2 reacting per mole of amine.

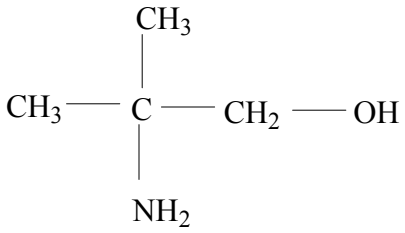

2-amino-2-methyl-1-propanol (AMP)

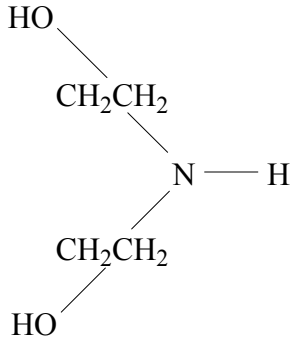

Diethanolamine (DEA)

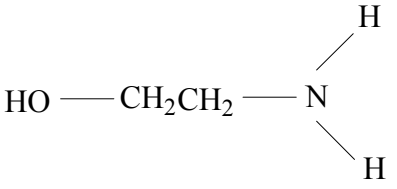

Monoethanolamine(MEA)

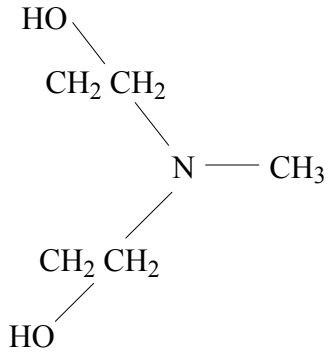

Methyldiethanolamine (MDEA)

Figure 5.16 Molecular structures of different alkanolamines.

During the reverse reaction, reaction (5.4) will be incomplete, owing to the stability of the carbamate formed by MEA or DEA, whereas reaction (5.5) will be complete. Thus, we may say that both the amount of CO_2 absorbed and the amount of CO_2 desorbed could be higher in the case of hindered amine like MDEA. Otherwise said, the capacity of MDEA is higher than that of MEA or DEA. This is probably the reason for moderately

low permeance of CO_2 in the MDEA membranes besides its extremely low forward reaction rate constant $\boldsymbol{k_1}$.

The nitrogen permeance for all the amine membranes are approximately constant because nitrogen permeates through the membranes by solution-diffusion mechanism. The slight reduction in the permeance of nitrogen with increasing pressure differential can be rationalized as follows. The physically dissolved nitrogen that permeates into the PVA-amine membranes has a little interaction with polymer segments and no chemical interaction with any of the amines. However, the application of larger pressure differential to a polymer membrane could slightly compress the polymer matrix leading to the reduction of the amount of free volume available for penetrate transport, thus, a decrease in permeance or permeability coefficient (Koros, 1990). Free volume is referred to as the fraction of total polymer volume that is not occupied by polymer molecules. The reduction of nitrogen permeance with an increase in the amine concentrations is likely due to the lowering of nitrogen solubility in the membrane matrix brought about by the presence of such ionic species as carbamates and protonated amines among others.

Based on these experimental results, it is decided to use DEA as a carrier to facilitate the transport of CO_2 across the PVA membrane.

5.4.4. Effect of DEA Concentrations

After choosing the effective carrier for CO_2, the next step is to determine the appropriate DEA concentration. Experiments were carried out with PVA and PVA-DEA membranes

with DEA concentrations from approximately 10-50wt%. The experimental results are presented in Fig. 5.16 and 5.17. All permeation measurements were performed at room temperature (296K). The CO_2 feed pressure was kept at 170 kPa (25 psia). The results for these experiments were in good agreement with the previous experiments (Fig.5.13). There are two major observations from these experiments. First, the CO_2 permeance was larger in the presence of DEA at any concentrations. Second, the permeance reaches a maximum value when the DEA content in the membrane was about 20-30wt%, and then decreases as DEA concentration increases. The increase in CO_2 permeance with increasing DEA concentration was simply due to the availability of more amine for CO_2 transport. However, as the amine concentration increases the permeance of CO_2 decreases since the ionic strength of the membrane increases with an increase in DEA concentration. These ionic species, formed by the reaction of DEA with CO_2 are likely to be carbamates and protonated amines. In other words, the CO_2 permeance did not increased appreciably at DEA concentrations greater than 20 – 30 wt% because there is trade-off between the favorable facilitation effect of high DEA concentration and the reduction in both diffusivity of the ionic species and solubility of CO_2 at high DEA concentrations. Another probable reason is that the sites or void spaces that should be used for the transport of free CO_2 were occupied by these ionic species. As a result, the transport due to solution-diffusion decreases. An explanation for these observations is proposed in next Chapter 7 with the aid of diffusion-reaction equations.

Next, the effects of CO_2 feed pressures, temperature and membrane thickness on CO_2 facilitated transports were investigated.

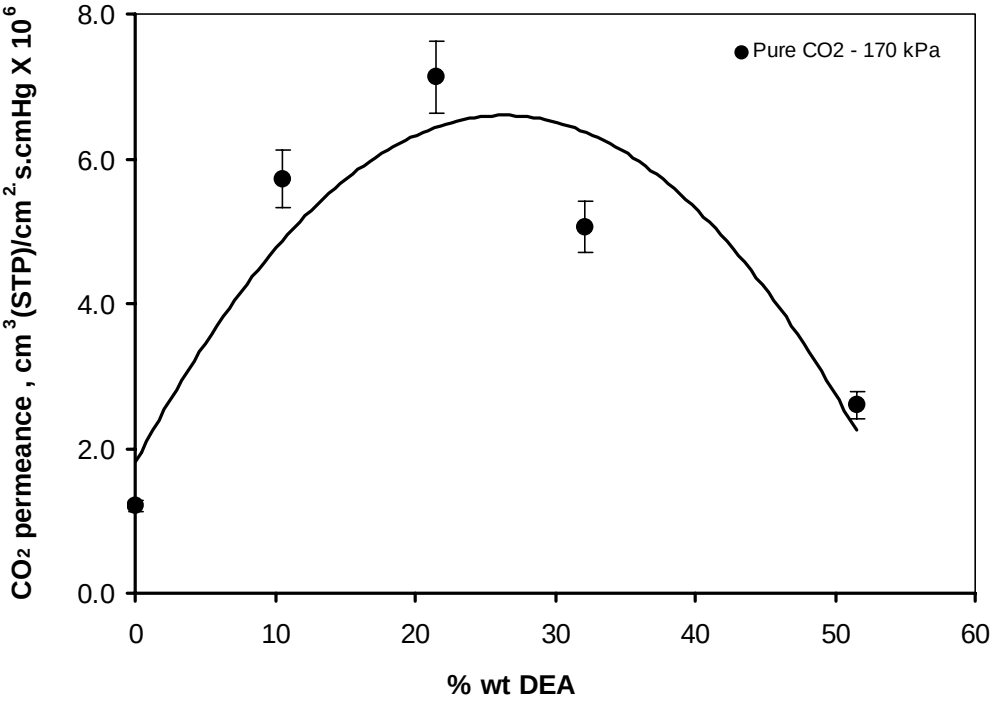

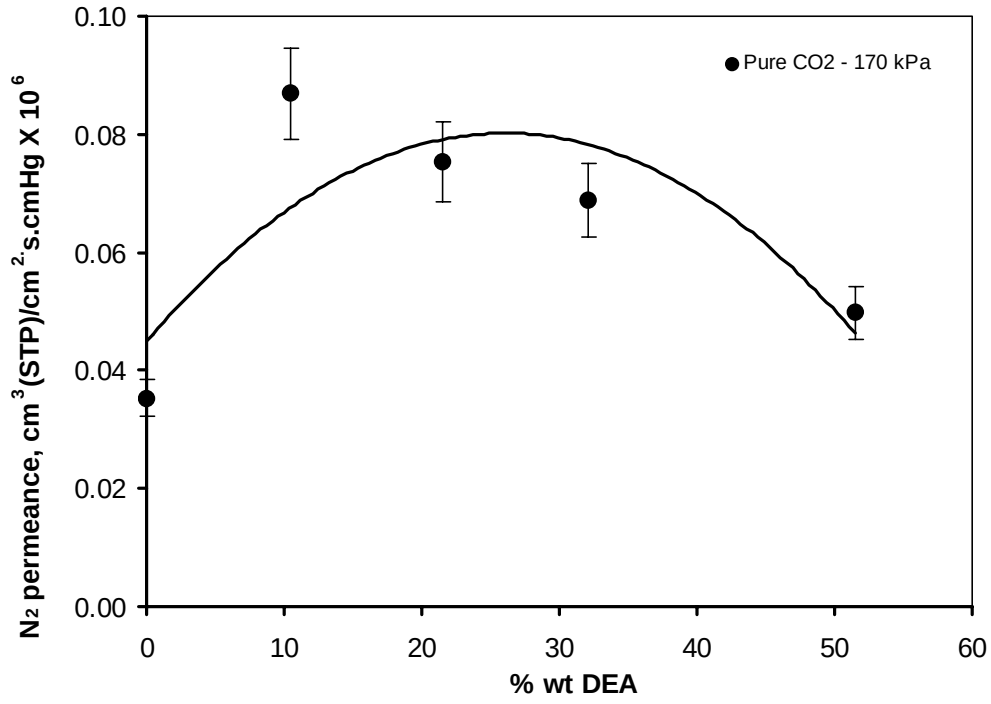

Figure 5.16 Permeances of CO_2 and N_2 for the PVA-DEA membranes as a function of DEA concentration at feed pressure of 170 kPa.

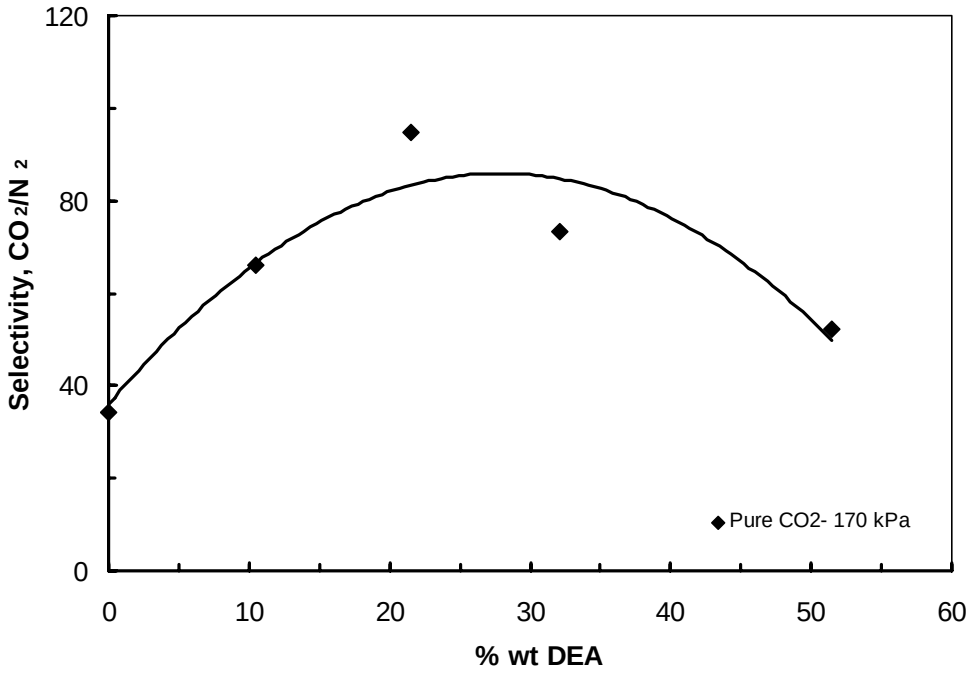

Figure 5.17 Selectivity of CO_2 over N_2 for the PVA-DEA membranes as a function of DEA concentration at feed pressure of 170 kPa.

5.4.5. Effect of CO_2 Feed Pressure

Figures 5.18 to 5.21 show CO_2 and N_2 flux and permeance as a function of feed pressure through PVA and PVA-DEA membranes. A total of 4-membranes were tested to demonstrate the membrane preparation reproducibility. The feed pressures were varied from approximately 112-508 kPa (16 to 74 psia) to determine the dependence of permeance on the applied trans-membrane pressure differentials.

The CO_2 permeance in the PVA-DEA membrane was greatly enhanced at low feed pressure. Such pressure dependence of CO_2 is consistent with CO_2 permeation by

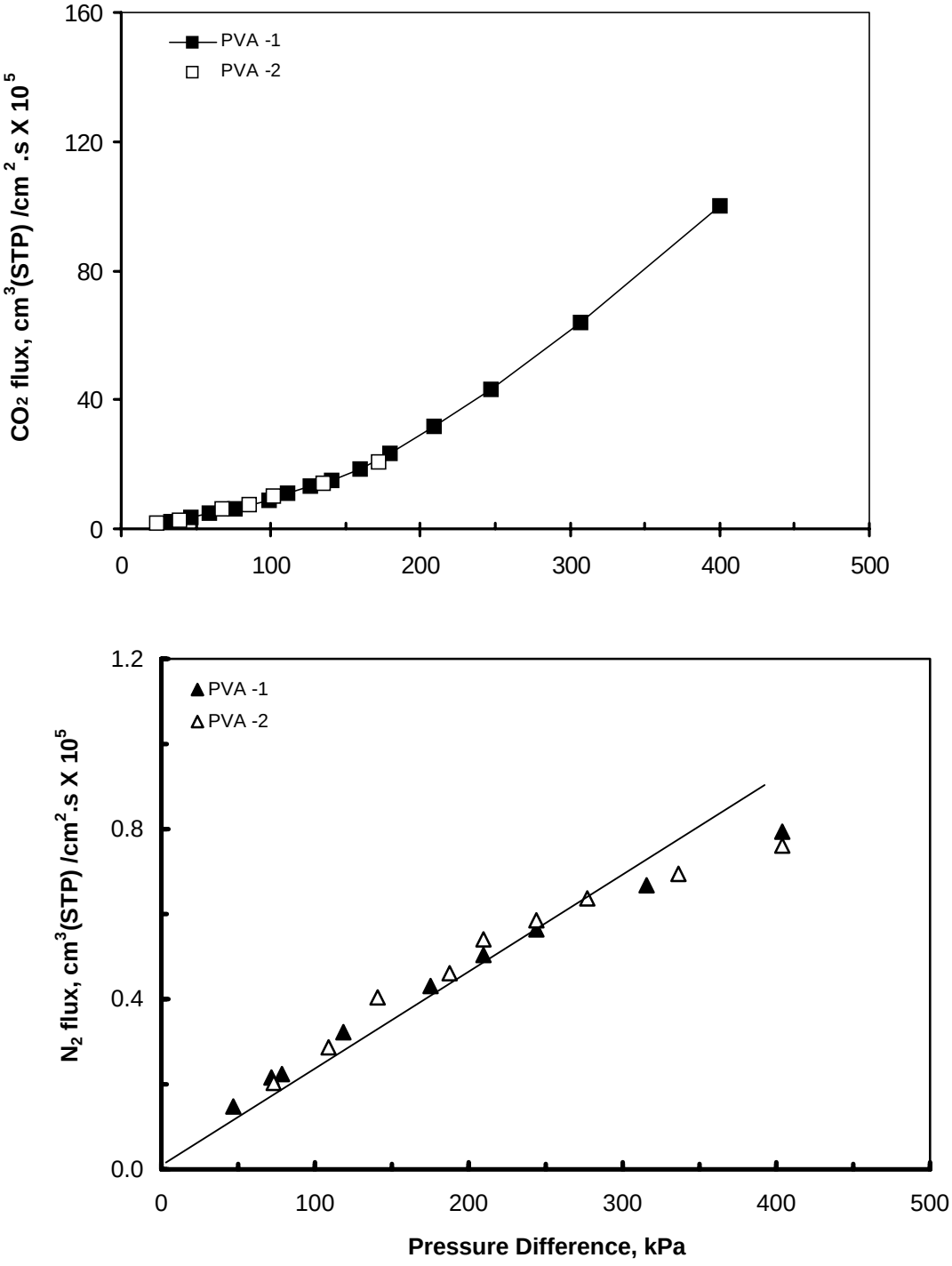

Figure 5.18 Fluxes of CO_2 and N_2 for the PVA membranes as a function of feed pressures.

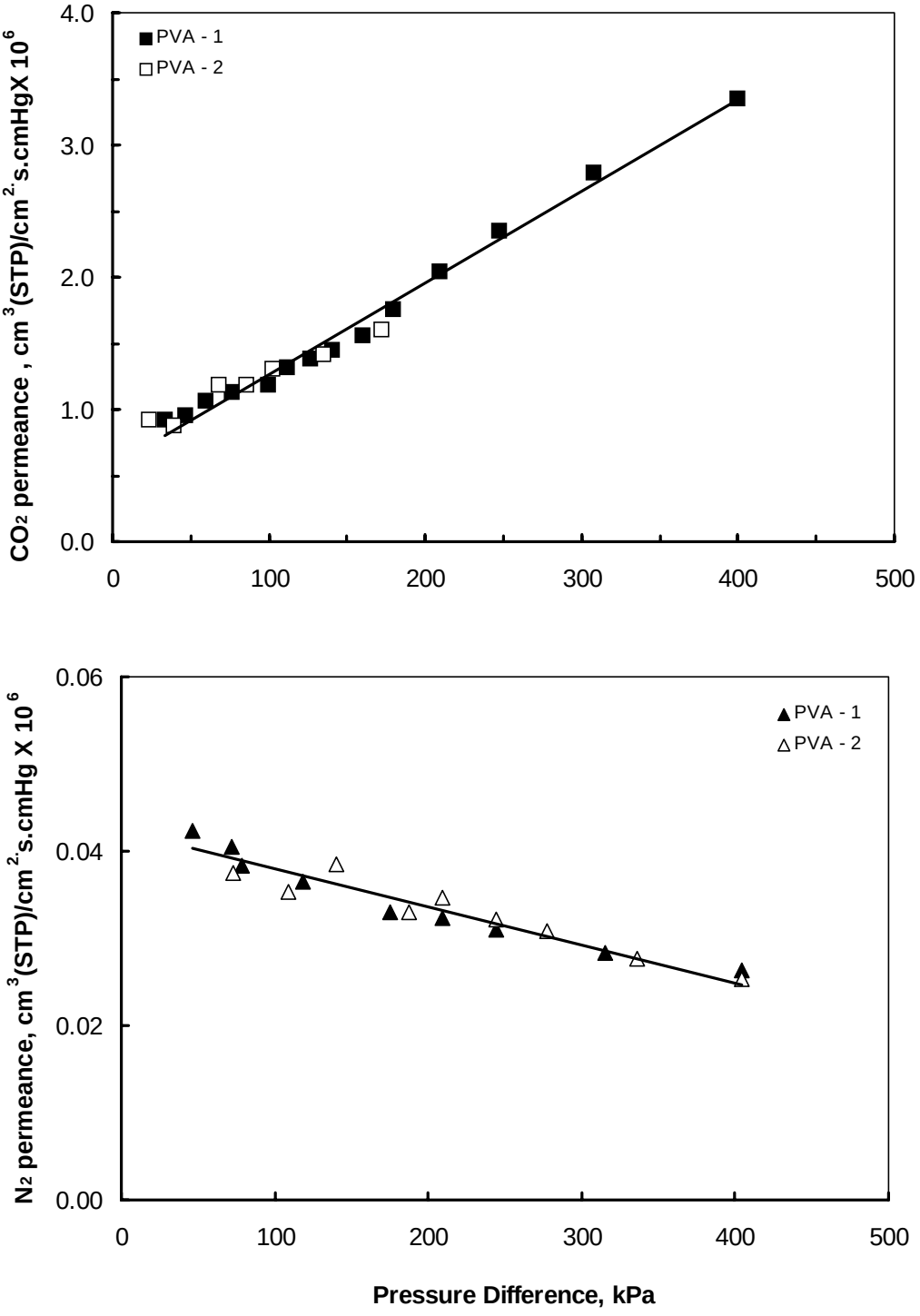

Figure 5.19 Permeance of CO_2 and N_2 for the PVA membranes as a function of feed pressures.

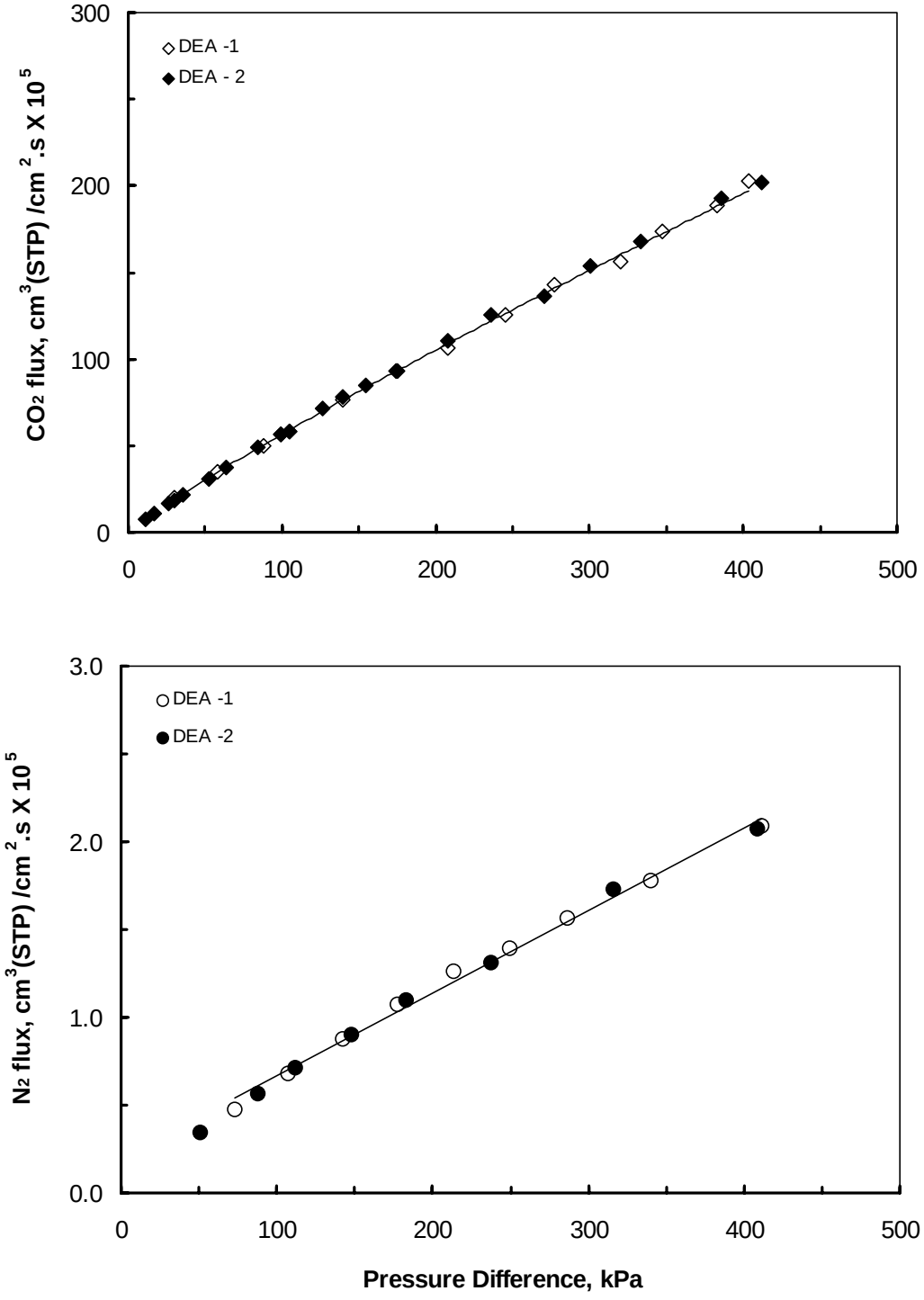

Figure 5.20 Fluxes of CO_2 and N_2 for the PVA-DEA membranes as a function of feed pressures. DEA concentration: 20wt%.

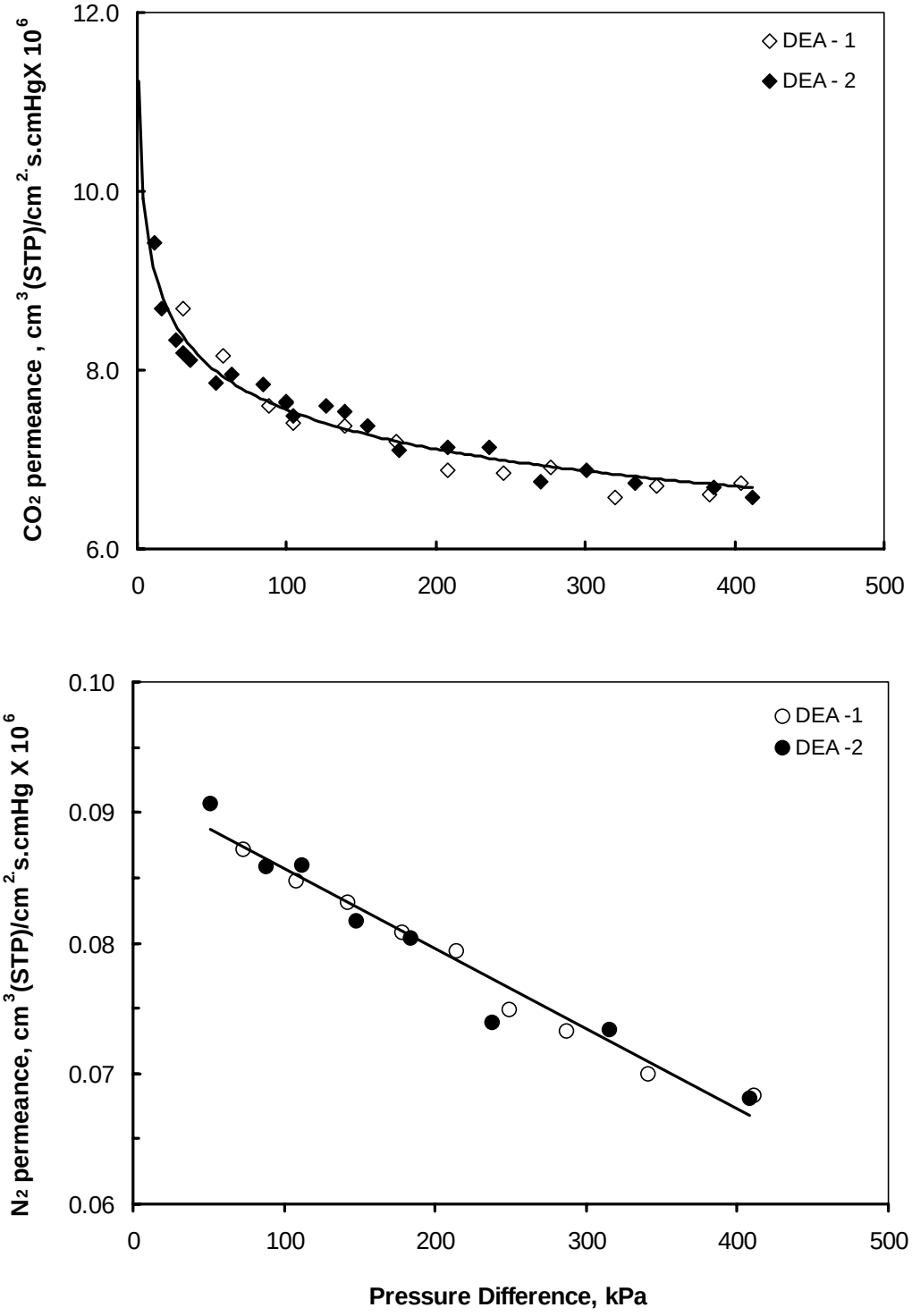

Figure 5.21 Permeances of CO_2 and N_2 for the PVA-DEA membranes as a function of feed pressures. DEA concentration: 20wt%.

facilitated transport mechanism particularly in the case where the facilitation at higher CO_2 feed pressure was limited by the saturation of the carrier. A discussion of this phenomenon is presented in Chapter 6 and 7.

Criteria that can be adopted for identifying facilitated transport are generally based on experimental observations and not on theoretical expectations (Cussler, 1997). One characteristic of the facilitative permeance, which was clearly illustrated in these experiments was the dramatic decreased in the CO_2 permeance as the feed pressure were increased. The CO_2 permeance continuously decreases as the feed pressure increases and may approach a constant value. This is the situation where almost all the DEA molecules available in the membrane have reacted with CO_2 or much of the amine is tied-up with the CO_2 molecules and therefore not available for further reaction. This phenomenon is referred to as carrier saturation. This behaviour of CO_2 permeance is a clear evidence of facilitated transport. N_2 permeance just like the previous experiments were almost constant with increasing feed pressure, a clear indication that this gas is permeating through the reactive membranes by solution-diffusion mechanism. The slight reduction in the N_2 permeance with increasing pressures as discussed previously was due to the compaction of the polymer matrix that resulted due to the decrease in the amount of free volume, thereby reducing the gas diffusion coefficient.

5.4.6 Effect of Operating Temperature on Permeation.

In some polymeric membranes, gas permeability tends to increase with increasing temperature. In PVA-DEA membranes, it is expected that the transport of N_2 will compete with the facilitated and unfacilitated transport of CO_2 at higher temperatures. To evaluate the influence of temperature on the membrane performance, experiments were carried out in a temperature controlled water bath. Temperature was adjusted to 303, 313, 323 and 333K. For each temperature, the feed pressure was also changed to 173, 208, 278 kPa (25, 30 and 40 psia). Steady state permeations were usually reached after five hours. The results are depicted in Fig. 5.22. As anticipated, CO_2 permeance increased with temperature. The temperature dependence of CO_2 and N_2 permeance through the PVA-DEA membranes appeared well fitted by Arrhenius law expression:

$$J = J_0 \, exp\left(- \frac{E_a}{RT} \right) \tag{5.6}$$

where J_0 is pre-exponential factor, E_a, the activation energy of permeation. *Log J* of the CO_2 and N_2 for the reactive membrane are plotted as a function of *1/T* and was provided in Fig.5.22. The activation energies of permeation for the gases as function of pressure differentials in the membrane are shown in Fig.5.23.

Fig.5.23 illustrates that E_a of CO_2 is larger than N_2. Generally, the more permeable gas has lower activation energy for permeation. An increase in temperature could supply more energy to increase the mobility of the penetrating gas and also increases the

segmental motion of the polymer chain leading to an increase in the penetrate diffusion coefficient. Hence, the activation energy for diffusion is generally positive. In other cases, if solubility were the dominating factor for permeation, elevation in temperature would result to a lower permeation rate, and negative activation energy (Stern, 1987). This situation is usually observed for condensable gases like hydrocarbons. Based on the solution-diffusion mechanism, the activation energy for permeation is the total of the activation energy of diffusion and the heat of solution (Eq.2.13).

Going back to the reactive membrane, for N_2, Fig. 5.23 suggests that diffusion process was the controlling factor for permeation within the range of pressures tested. The transport of CO_2 across the reactive membrane is governed by solution-diffusion-reaction mechanism. The large E_a for CO_2 relative to N_2 suggests that free CO_2 is less permeable. However, experimental data show that CO_2 have larger permeance compared to N_2. This can be explained as follows. The relative proportion of CO_2 that permeates in physically dissolved form and in chemically combined form is dependent on the kinetics of the CO_2-DEA reaction. CO_2-DEA is a fast reaction (Astarita, 1983), the total CO_2 permeance are mostly due to the contribution of chemically combined form of CO_2 rather than free CO_2. The reaction process is the controlling factor in the permeation through the reactive membrane.

With the increase in temperature, reaction rate increases. In addition, K_{eq} is also affected by an increase in temperature. Since reaction of DEA with CO_2 is exothermic, K_{eq}

decreases with increasing temperature. This temperature dependency is based on the following expression (Alberty, R.A., Silbey, R.J., 1992):

$$\frac{d\left(lnK_{eq}\right)}{dT} = \frac{\Delta Q_r}{RT^2} \tag{5.8}$$

where ΔQ_r is the heat of reaction.

However, the increase of forward reaction rate constant, $\boldsymbol{k_1}$ and diffusivity are more significant resulting to an increase in CO_2 permeances. Further discussions are provided in Chapter 6.

In practical separation of CO_2 from flue gases, a membrane must be operated at more than 323K (Matsuyama, H., *et al.*, 2001). Based on experimental results on the effect of temperature, it appears that the DEA membrane was stable at temperature ranges of 303 to 333K presumably due to humidification of the gas prior to entering the membrane unit, which may reduced the rate of drying of the membrane at elevated temperature.

It is evident that DEA membrane exhibits an excellent permeation characteristic towards CO_2. From the pure gas permeance data, the selectivity, which is the permeance ratio of CO_2 over N_2 are plotted as a function of pressure differentials at various operating temperature in Fig. 5.24. The selectivity of CO_2 over N_2 increases with operating temperature and decrease with increasing pressure differential.

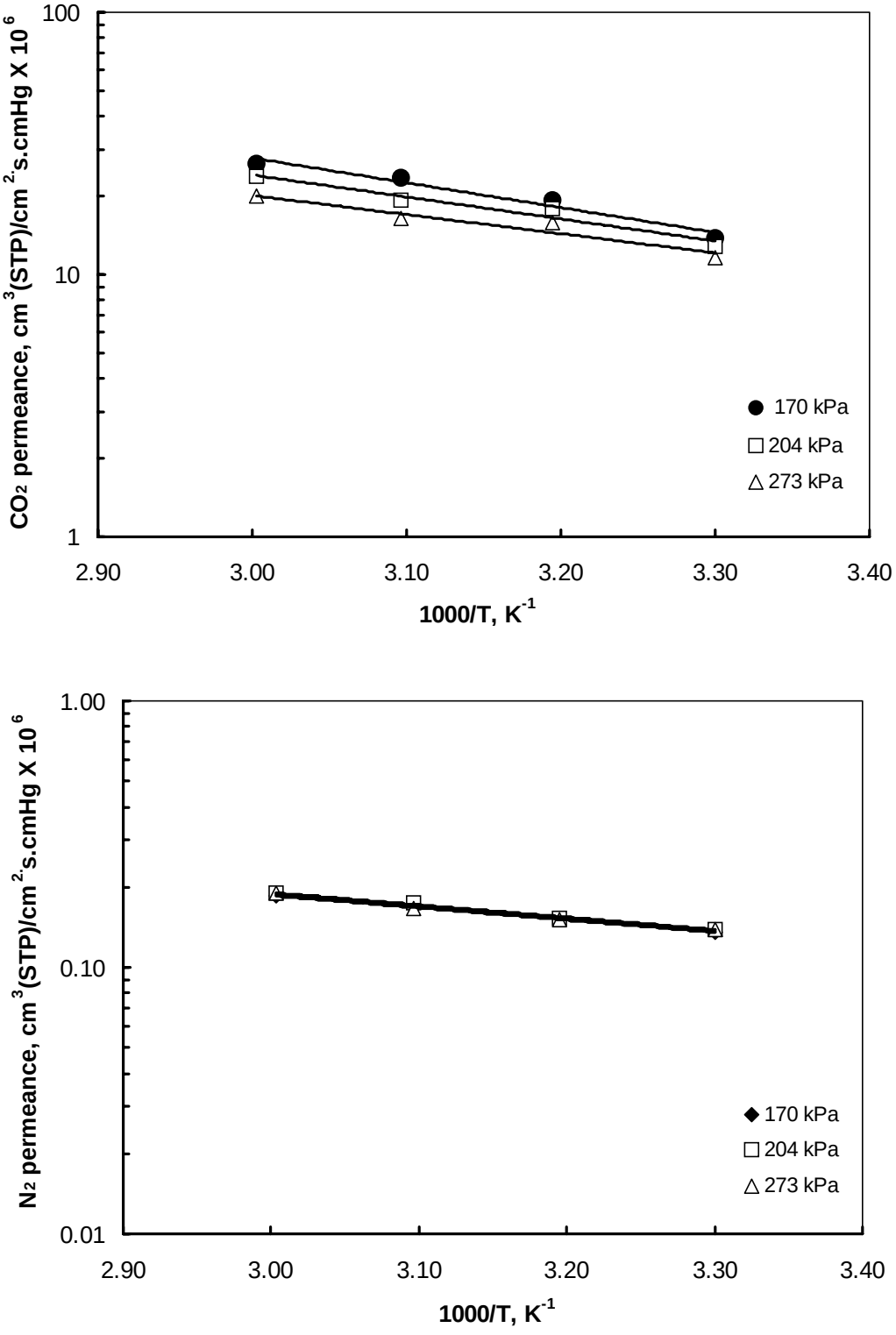

Figure 5.22 Permeance of CO_2 and N_2 for the PVA-DEA membranes as a function operating temperatures at various feed pressures. DEA concentration: 20wt%.

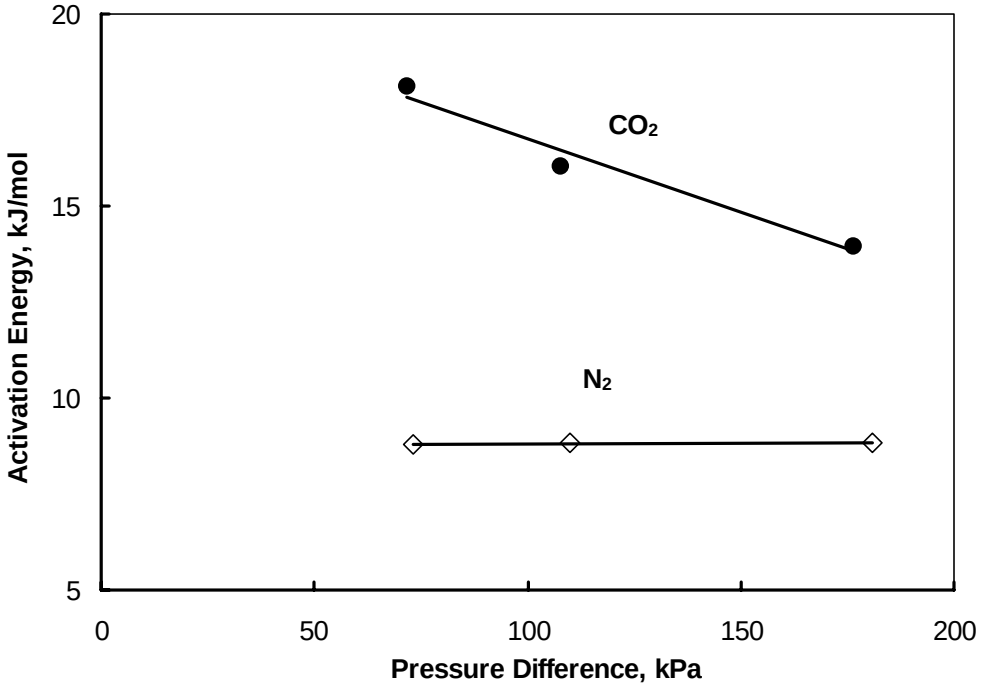

Figure 5.23 Activation energy of permeation through the PVA-DEA membranes as function of feed pressures. DEA concentration: 20wt%.

5.4.7 Effect of Membrane Thickness

Membrane thickness is likely to have an affect on CO_2 transport across the membrane. To investigate this concept, three membranes were prepared with effective thickness of about 16, 40 and 55 μm respectively. Variations in thickness were achieved by repeatedly casting the polymer solution into the substrate. The reported thickness for each case was the average of 10 measurements around the perimeter of the membrane using a digital thickness gauge (Mitutoyo). Fig. 5.25 to 5.27 show the results for these experiments. Both CO_2 and N_2 flux decreases with an increase in the membrane thickness because the diffusion rate in the membrane is inversely proportional to the membrane thickness. The

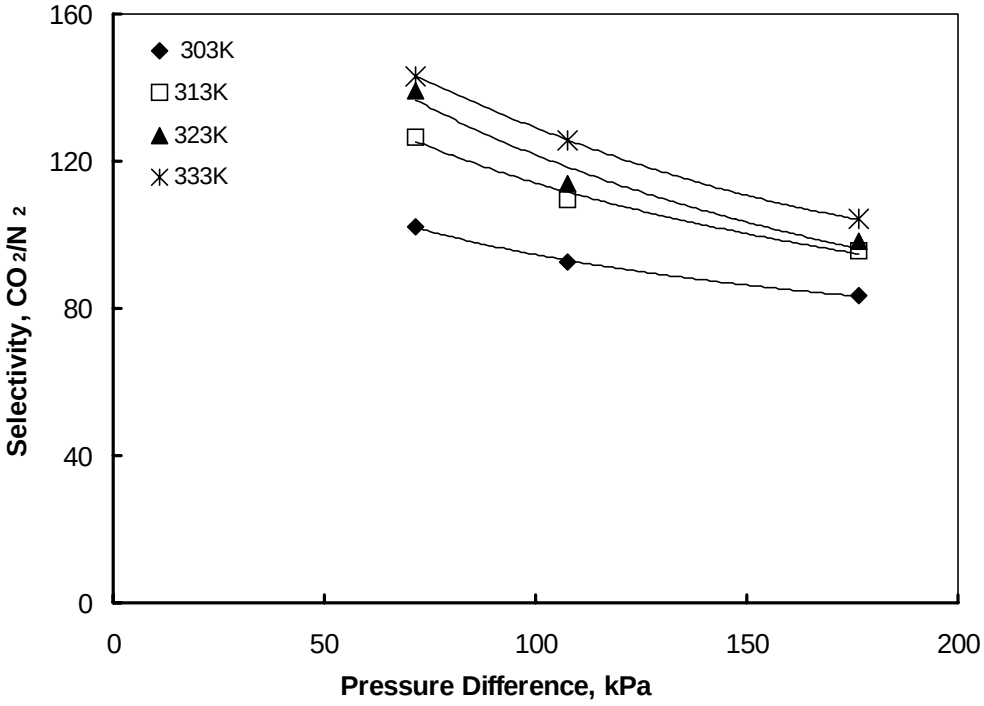

Figure 5.24 Selectivity of CO_2 over N_2 for the PVA-DEA membranes as a function of feed pressure at various operating temperatures. DEA concentration: 20wt%.

membrane thickness is likely to have an impact on the selectivity between CO_2 and N_2. For thicker membranes (*i.e.* 40 and 55 μm), the residence time of CO_2 was longer so that it consumes more DEA to react with. The effect was greater facilitation leading to an increase in selectivity. Theoretically, if the residence time is large, chemical equilibrium can be reached. This will provide higher facilitation and equilibrium can be achieved if the membrane thickness is sufficiently large. Fig. 5.27 shows the effect of membrane thickness on selectivity. The reaction rate and membrane thickness are somewhat interrelated in such a way as to achieved higher selectivity by increasing the membrane thickness leading to reduction of permeance.

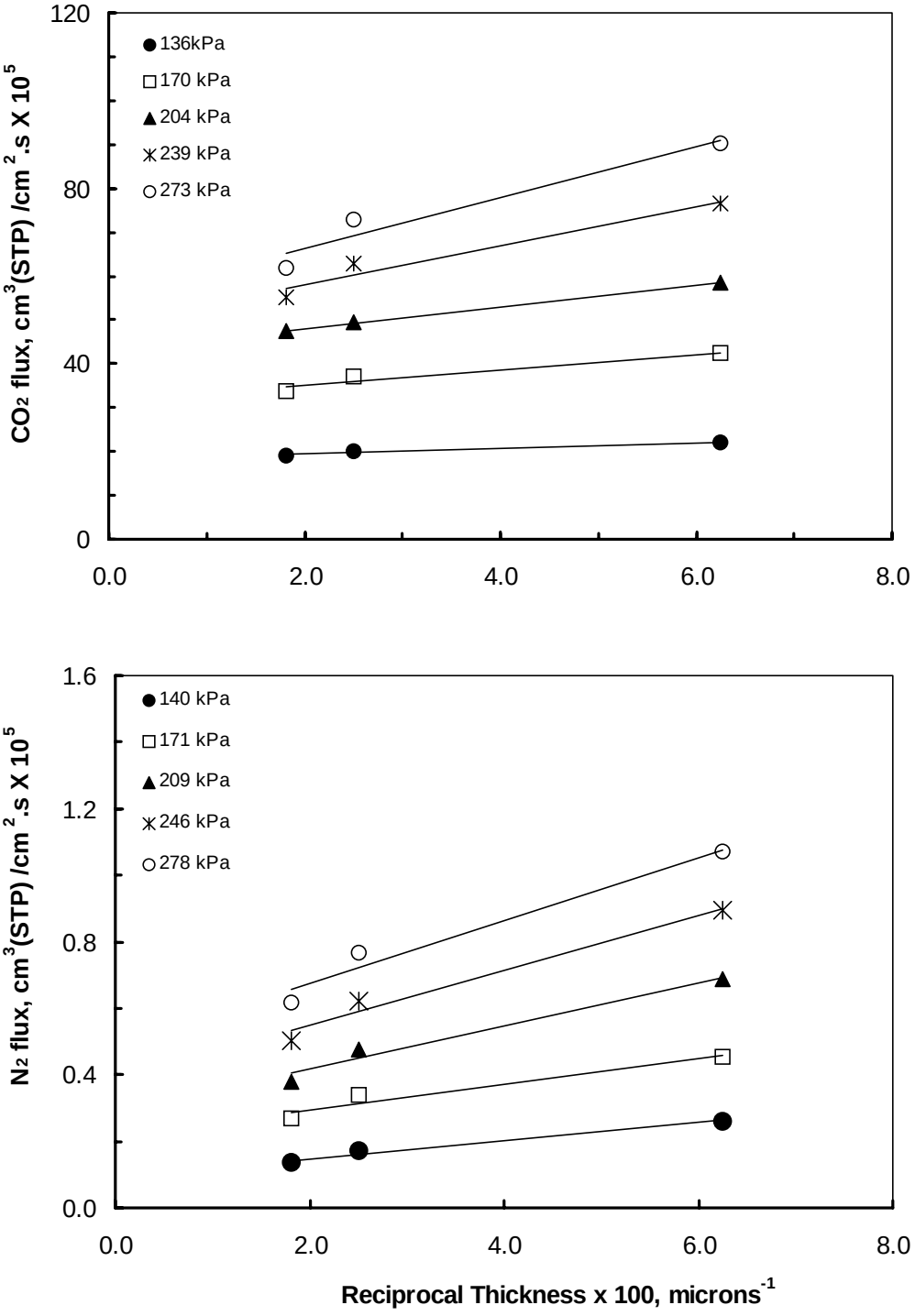

Figure 5.25 Fluxes of CO_2 and N_2 for the PVA-DEA membranes as a function membrane thickness at various feed pressures. DEA concentration: 20wt%.

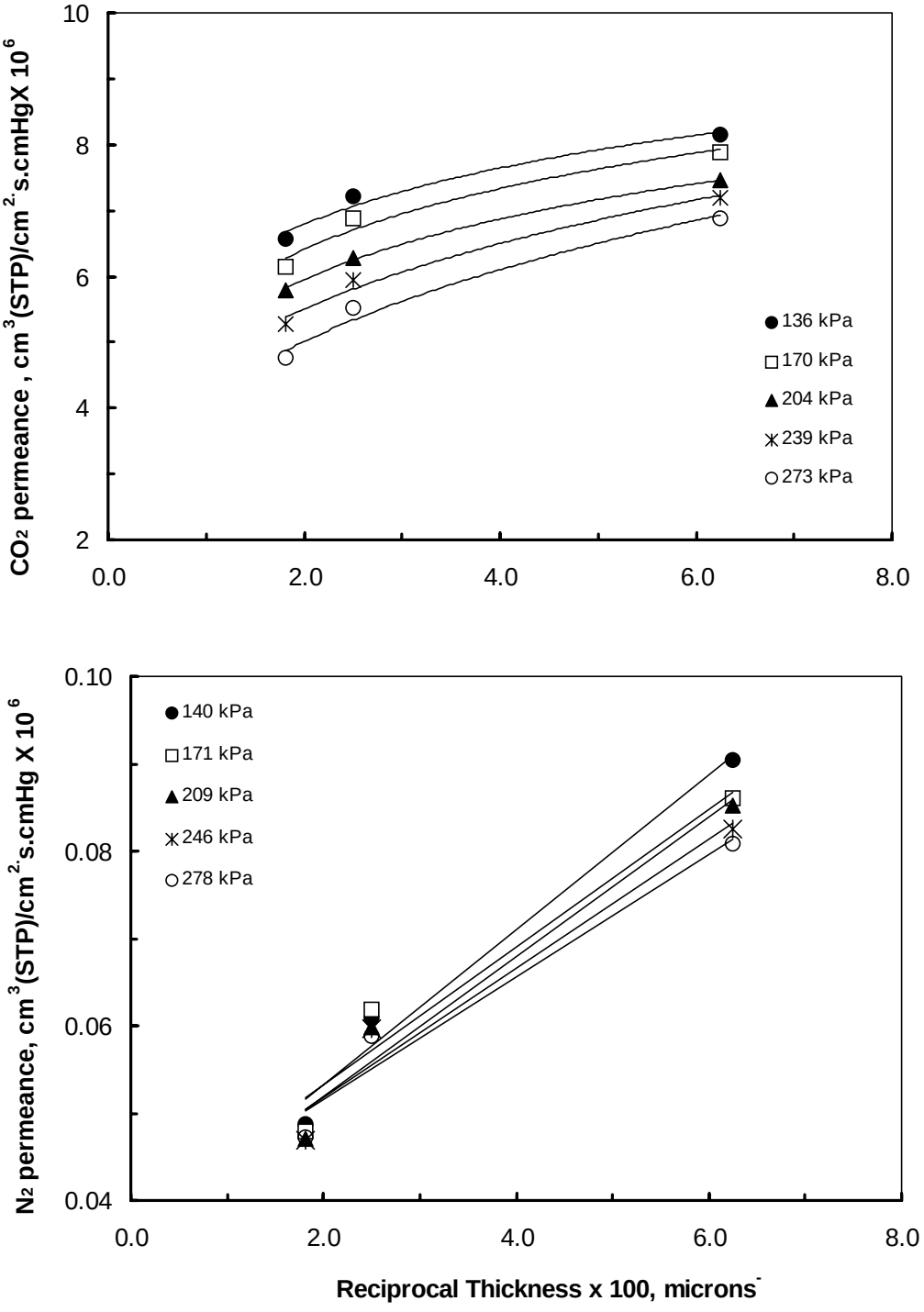

Figure 5.26 Permeance of CO_2 and N_2 for the PVA-DEA membranes as a function membrane thickness at various feed pressures. DEA concentration: 20wt%.

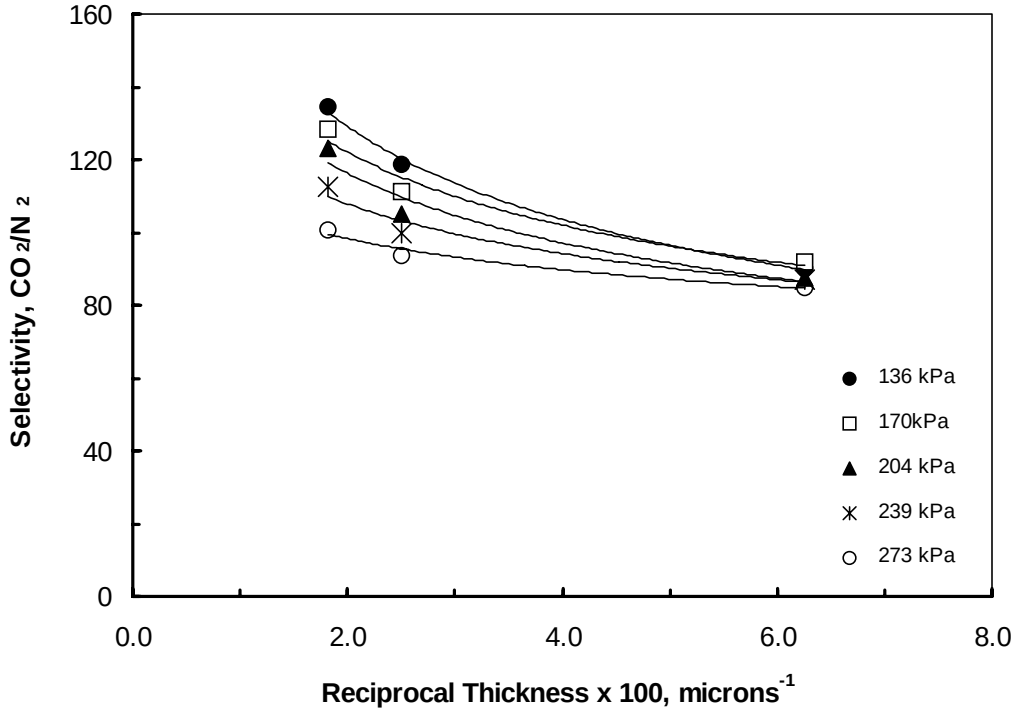

Figure 5.27 Selectivity of CO_2 over N_2 for the PVA-DEA membranes as a function of membrane thickness at various feed pressures. DEA concentration: 20wt%.

Likewise, the selectivity increases and the CO_2 permeance decreases with increasing membrane thickness. Thus, it is not simply a matter of decreasing the membrane thickness to improve the transport. There is a subtle compromise between shortening the diffusional path length and the additional carrier-mediated transport of the permeating species (Davis, A.D. and Sandall, O.C., 1993).

5.4.8 Long-term Membrane Tests

a) Effect of humidification

In evaluating the practicality of these facilitated transport membranes for CO_2 separation, one parameter of paramount importance is the membrane lifetime. Facilitated transport membranes have not yet been found to be suitable for industrial applications. The main problem that needs to be overcome in terms of commercial viability of such membranes is the stability. In this section, experiments were performed to study some factors that may contribute to the deterioration of the membrane performance. Pure gas permeation experiments were conducted in the presence and absence of humidification. As reference base line, PVA membrane (without amine) was also tested. The results are illustrated in Fig. 5.28.

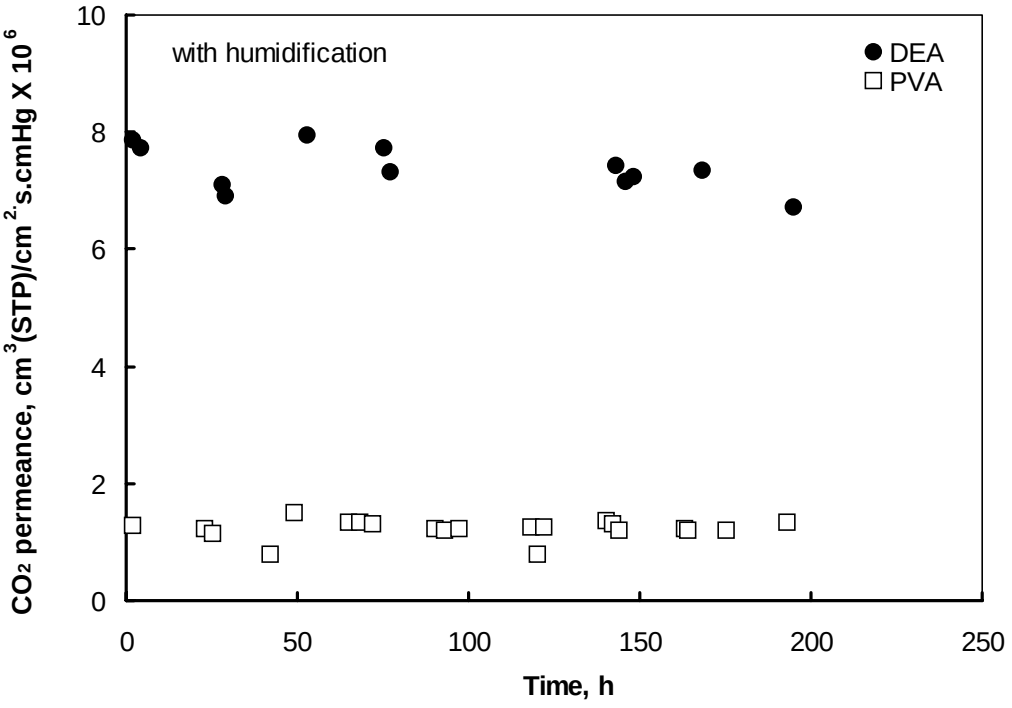

Figure 5.28 Permeances of CO_2 for the PVA-DEA and PVA membranes as a function of time at feed pressure of 169 kPa. DEA concentration: 20wt%. Temperature: 296K

With humidification, the membrane showed roughly constant permeance for more than 190 hours. There are two possible reasons for these observations. First, the stability was probably due to hydrophilicity of the PVA-DEA membrane. Secondly, the DEA retainment by entrapment within the PVA chains prevents from pushing out of the matrix when large pressure differential was applied. Fig. 5.29 shows that in the absence of humidification, the CO_2 permeance of PVA-DEA membrane started to decline after about 30 hours presumably because of membrane drying. Injecting 0.50 mL of deionized water

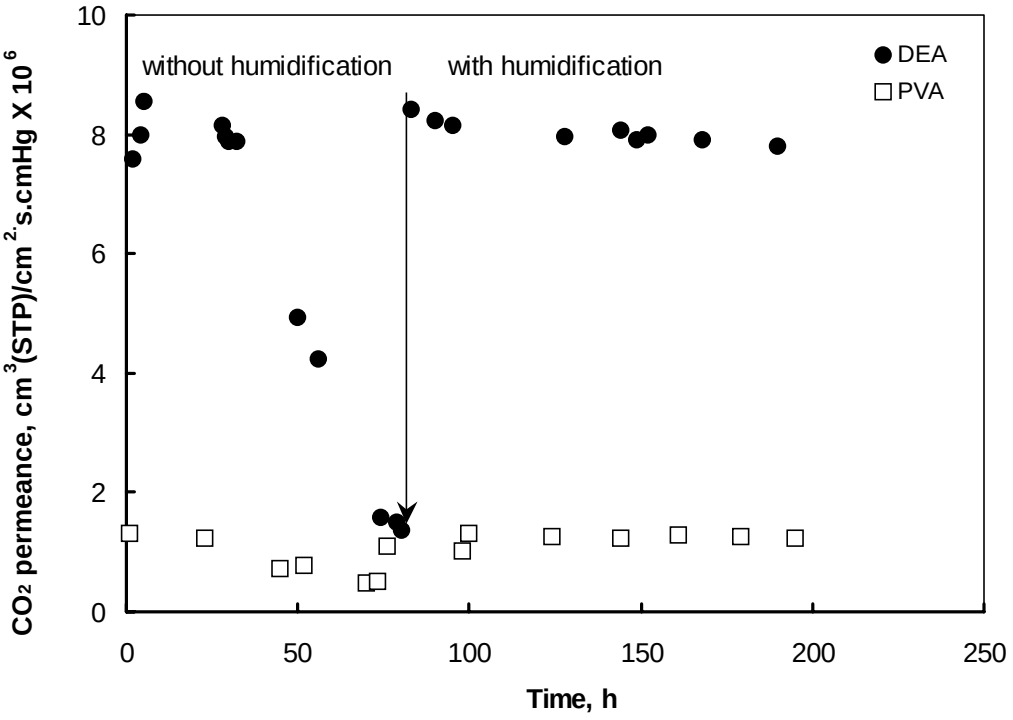

Figure 5.29 Permeances of CO_2 for the PVA-DEA and PVA membranes as a function of time at feed pressure of 169 kPa. DEA concentration: 20wt%. Temperature: 296K

into the permeation unit regenerated the membrane as shown in the Fig.5.29. Perhaps, one advantage of the presence of moisture in the membrane is that higher permeability was obtained because of the high mobility of the CO_2-DEA complex.

With PVA membrane, in the absence of humidification, the decline in CO_2 permeance occurs after about 24 hours as shown in Fig. 5.30. After 42 hours, 0.50 mL of deionized water was injected resulting to an increase in permeance. A much longer period of stability tests was conducted during gas mixture permeation, presented in Chapter 6.

5.5 Summary

Membrane materials suitable for CO_2 separation and membrane preparation procedures have been experimentally determined using pure gas permeation. The reactive membranes containing DEA achieved higher permeance and selectivity for CO_2 compared to AMP, MEA and MDEA. CO_2 permeance increase initially with increasing amine concentration but decreased with further increase in concentration. Likewise, CO_2 permeance is larger at lower CO_2 pressure differentials and almost reached constant values at larger CO_2 pressure differential where carrier saturation is observed. Nitrogen permeance appear to be almost independent of the applied pressure indicating that it permeates through the reactive membrane by solution-diffusion mechanism. The slight decreased in the nitrogen permeance at higher partial pressure differential maybe due to the compaction of the membrane matrix. Selectivity of more than 100 was observed in

the PVA-DEA membrane and was higher than PVA membrane. The PVA-DEA membrane also shows stability and dependency with temperature. It is also stable for more than 190 hours of continuous operation at 296K.

Chapter 6

Permeation of Gas Mixtures

In industrial applications, CO_2 needs to be separated from the gas mixtures. To evaluate the viability of the PVA-DEA membranes for realistic separation of CO_2 from flue gases, the performance of this reactive membrane for CO_2/N_2 mixture separation were investigated.

The permeance of CO_2/N_2 mixture was measured at different operating conditions. The effects of feed composition, feed pressures and operating temperatures on the permeances and selectivity were examined. Also, the possibility of the existence of mass transfer resistance in the boundary layer was studied as well as long-term stability of the membrane.

Furthermore, a methodology for the calculation of CO_2 permeance based on the diffusion-reaction transport equations were also presented.

6.2 Experimental Procedures

6.2.1 Permeation Measurement for CO_2/N_2 Mixture

The apparatus used for gas mixture permeation experiments is presented schematically in Figure 6.1. The flow rates of individual gas streams were controlled by electronic mass

flow meters/controllers (Model: UFC 1200A, Unit Instruments Inc.). The mass flow controllers were calibrated and the calibratioin curves were provided in the appendix D. The actual composition of the gas mixtures was determined by gas chromatograph (GC) (Model: 6890 N, Agilent Technologies). The gases passing through the mass flow controllers are mixed in a 1/8 inch diameter copper tubes before entering the permeation unit. For temperature study, the permeation unit was placed in a temperature controlled water bath. The pressure of the gas stream of each gas cylinders was adjusted with pressure regulators to 859 kPa (125 psia). The feed pressure was controlled by a needle valve located on the residue of the permeation unit. Typically, at the start of the experiments, the needle valve was closed in order for the feed pressure to build-up to the desired level. When the desired pressure was reached, the valve was slowly opened to maintain the feed pressure at the desired level. The feed stream consisting of CO_2 and N_2 passed through the gas bubbler (humidifier) before entering the permeation unit. The compositions of gas entering and exiting the permeation unit were determined using gas chromatograph equipped with a thermal conductivity detector (TCD). The GC analysis was checked for deviations from their corresponding calibration curves by introducing standard sample of CO_2/N_2 mixture obtained from Praxair. The GC was calibrated once in every week to ensure reliable data acquisitions.

The experiments were carried out at a room temperature of 296 ± 2K and environmental pressure of 101 ± 2 kPa. The volumetric flow rates of permeate was measured at each operating conditions by the used of bubble flow meter at room temperature and pressure. At steady state conditions, the permeance of a component in the mixture was calculated

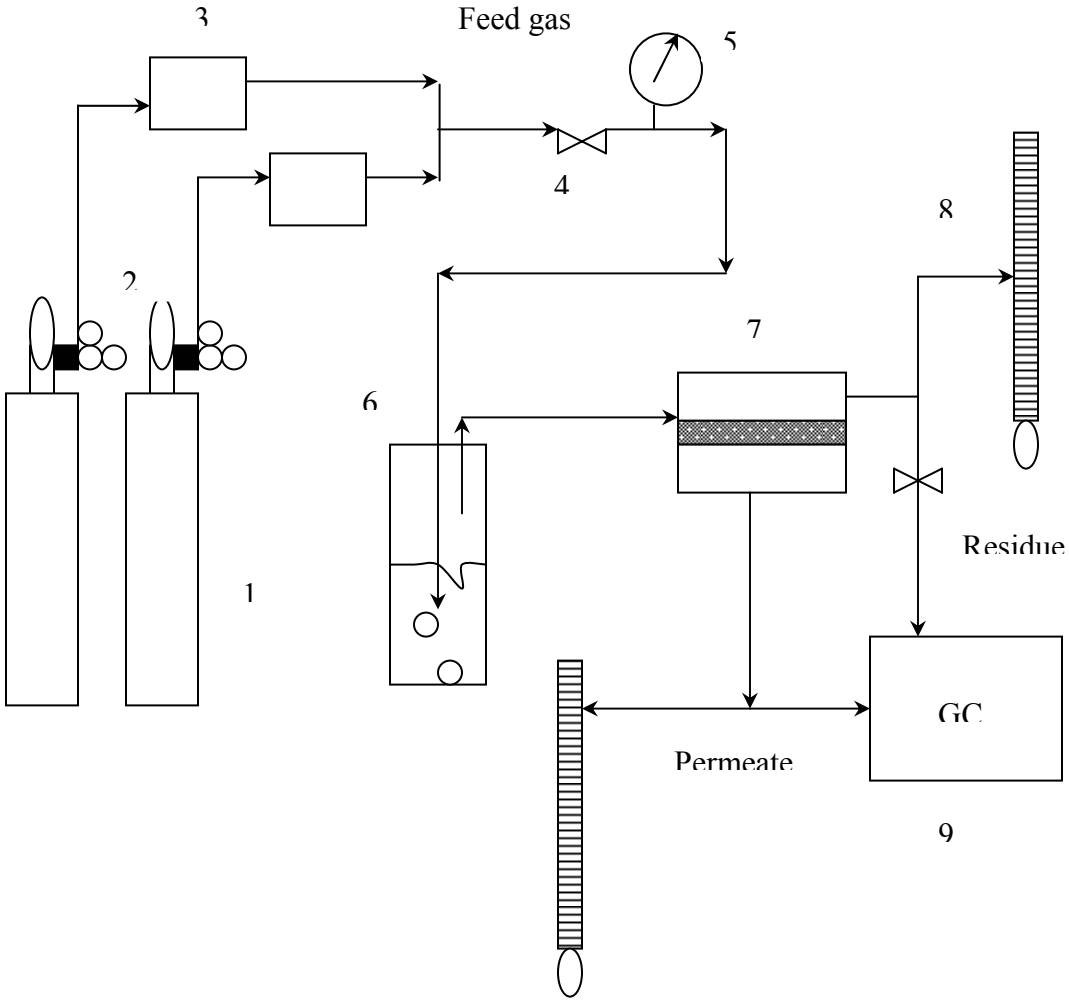

Figure 6.1 Schematic diagram for gas mixture permeation experiments. 1. Gas cylinders 2. Pressure regulators 3. Mass flow controllers 4.Valve 5. Pressure gauge 6. Gas bubbler 7. Permeation unit 8. Bubble flow meter 9. Gas chromatograph

according to the following:

$$J_i = \frac{Q(y_i)}{A(p^0 x_i - p^L y_i)} \cdot \frac{273.15}{T} \qquad (6.1)$$

where J_i (cm^3(STP). $cm^{-2}.s^{-1}.cmHg^{-1}$) is the permeance of component ***i*** in the mixture, **Q** (cm^3/mL) is the flow rate of the mixture permeating through the membrane and ***A*** (cm^2) is the effective membrane area. p^0 and p^L are the upstream and downstream pressure (cmHg). ***T*** (K) is the room temperature, x_i is the mole fraction of component ***i*** in the feed stream and y_i is the mole fraction of component ***i*** in permeate stream.

The selectivity was based on the permeance ratio of CO_2 and N_2. Sample calculations were provided in Appendix A.2.

Steady state permeation was assumed to be attained once the flow rate of the gas mixture and the permeate compositions were constant. Typically, it required approximately 4-5 hours for the system to reached steady state.

The facilitation factor, ***F***, is related to the flux according to the following:

$$N_i = \frac{FD_i H_i \Delta P}{L} \cdot \frac{273.15K}{T} \cdot \frac{22400cm^3}{mol} \qquad (6.2)$$

where $\boldsymbol{N}$ (cm^3(STP). $cm^{-2}.s^{-1}$)) is the flux of component ***i***, **D** ($cm^2.s^{-1}$) is diffusivity coefficient of component ***i***, $\boldsymbol{H}$ ($mol.cm^{-3}.cmHg^{-1}$) is Henry's constant of component ***i*** in the solution, ΔP (cmHg) is the pressure differential and $\boldsymbol{L}$ (cm) is the membrane thickness.

6.3 Results and Discussions

6.3.1 Effects of Feed Flow Rate

Permeation experiments were performed to determine whether an external mass transfer resistance existed due to boundary layers in the gas phase by varying feed flow rates. These experiments were carried out with a feed gas of fixed concentration (15.6% CO_2 and balance N_2). The effect of feed flow rates on the permeances of CO_2 through the PVA and DEA membranes is illustrated in Figure 6.2 to 6.5. As can be observed, the CO_2 permeances remains almost unaffected by the variation of the feed flow rates for both membranes. The results clearly show that the gas phase mass transfer resistance in the feed side of the membrane was negligible for the range of experimental conditions used in this study.

6.3.2 Effects of DEA Concentration

Results obtained using pure gas permeation suggests that reactive membranes with 20 – 30 wt% DEA exhibit very good CO_2 permeance and selectivity. To further evaluate the

results obtained in the Chapter 5, experiments were conducted to obtain the permeance of CO_2 and N_2 in the PVA-DEA membranes containing 0 – 50 wt% DEA. These experiments were carried out with a feed gas of fixed composition (15.6% CO_2 and 84.4% N_2). The feed pressure was varied from about 170, 239, 308, 377, 446 and 515 kPa (25, 35, 45, 55, 65 and 75 psia). Figures 6.6 and 6.7 show the effects of changing the carrier concentration on the performance of facilitated transport membrane. There are three significant observations arising from these results. First, the permeance of CO_2 is larger in the presence of DEA. Second, the permeance reaches a maximum value then decreases as the DEA concentration elevates. This is most likely due to the increased in CO_2-DEA complex concentration in the membrane matrix leading to the reduction of CO_2 solubility. The third observation is that the permeance is much larger at low CO_2 partial pressure differential. It should be noted that similar trends were observed during the pure gas permeation experiments. An explanation for these observations is proposed with the aid of the numerical solutions of diffusion-reaction equation in the Chapter 7.

On the other hand, the N_2 permeances at various DEA concentrations are somewhat staggered probably due to the presence of the CO_2-DEA complexes that were likely affecting the transport of N_2 by solution-diffusion mechanism. With increasing DEA concentration, the N_2 permeance wildly decreased probably because of the increasing amount of CO_2-DEA complexes accumulating in the membrane matrix making the membrane more crowded thereby reducing its solubility into the membrane. This behaviour of N_2 permeance was different from pure gas permeation. Further discussion is presented in section 6.3.3.

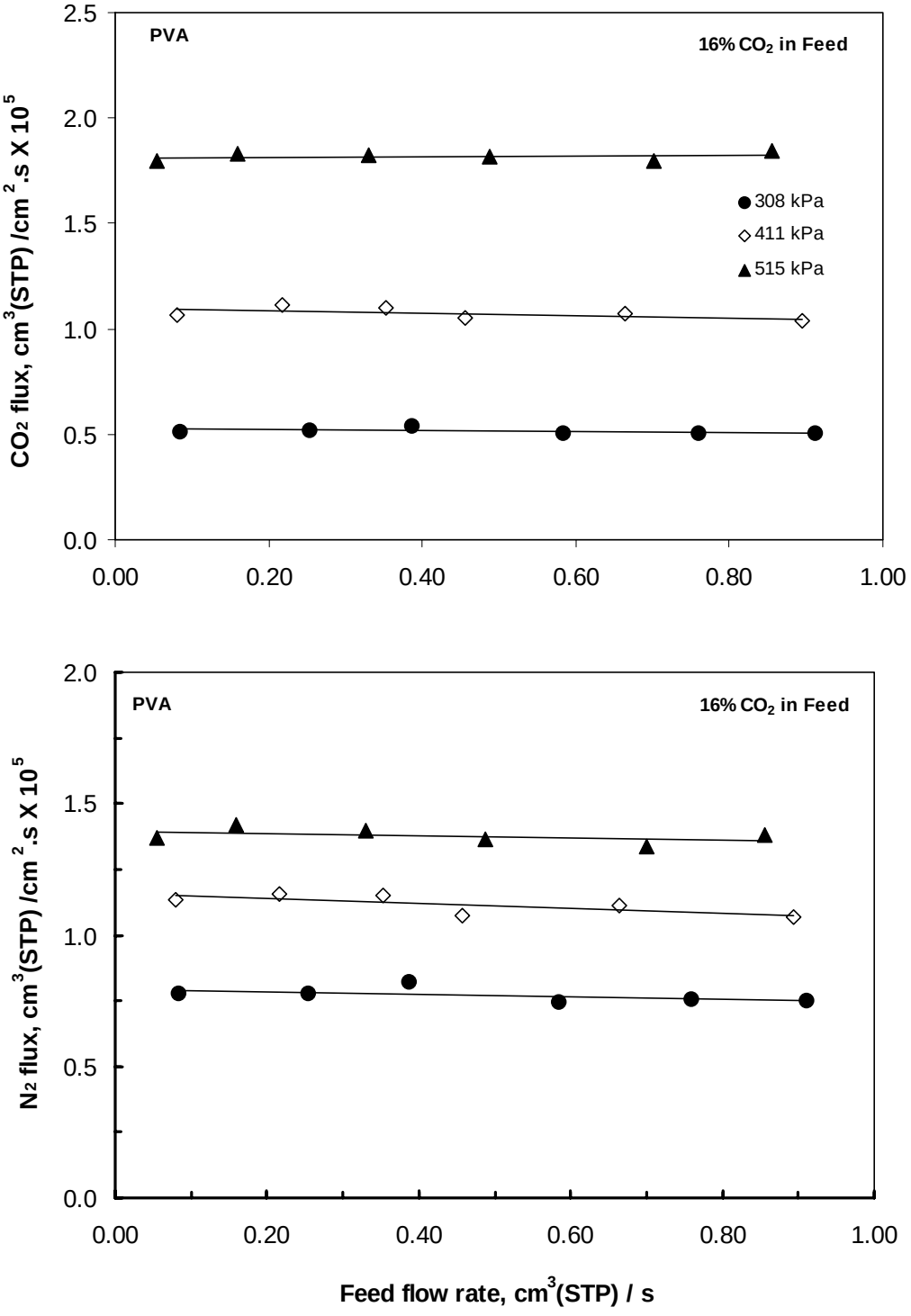

Figure 6.2 Fluxes of carbon dioxide and nitrogen in the CO_2/N_2 mixtures for the PVA membrane as a function of feed gas flow rates at variable feed pressures. Temperature: 296K

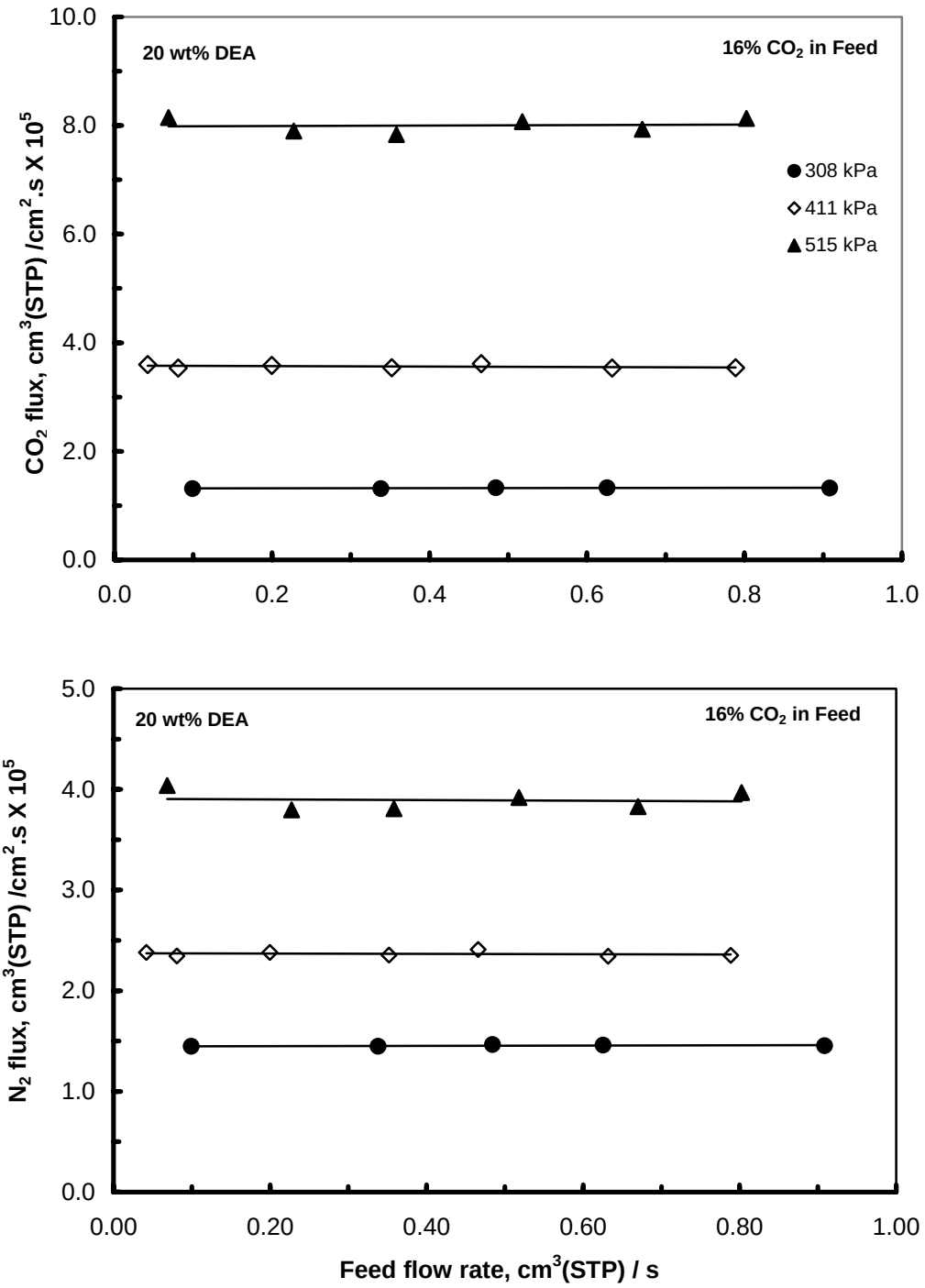

Figure 6.3 Fluxes of carbon dioxide and nitrogen in the CO_2/N_2 mixtures for the PVA-DEA membrane as a function of feed gas flow rates at variable feed pressures.

Temperature: 296K

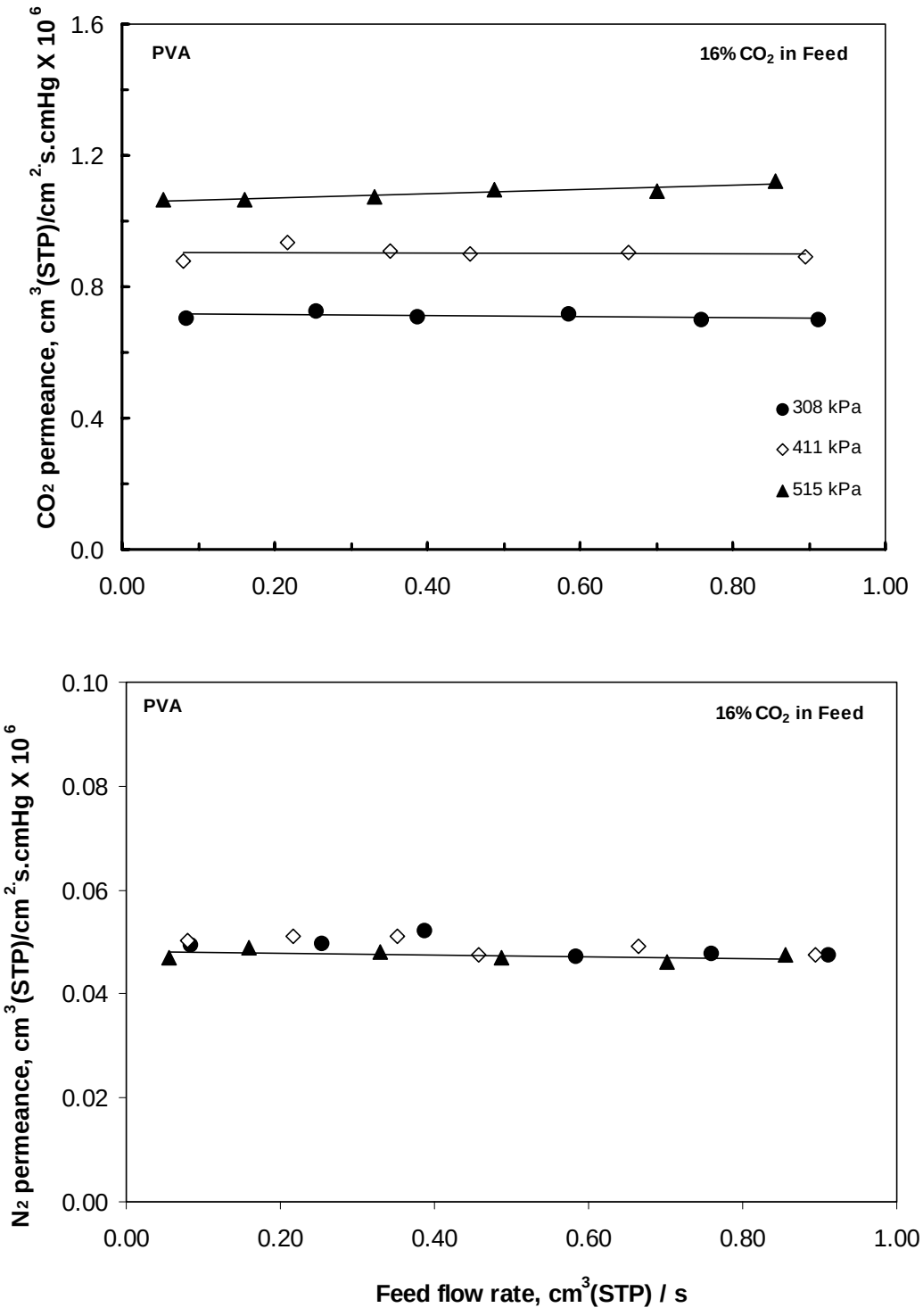

Figure 6.4 Permeance of carbon dioxide and nitrogen in the CO_2/N_2 mixtures for the PVA membrane as a function of feed gas flow rates at variable feed pressures.

Temperature: 296K

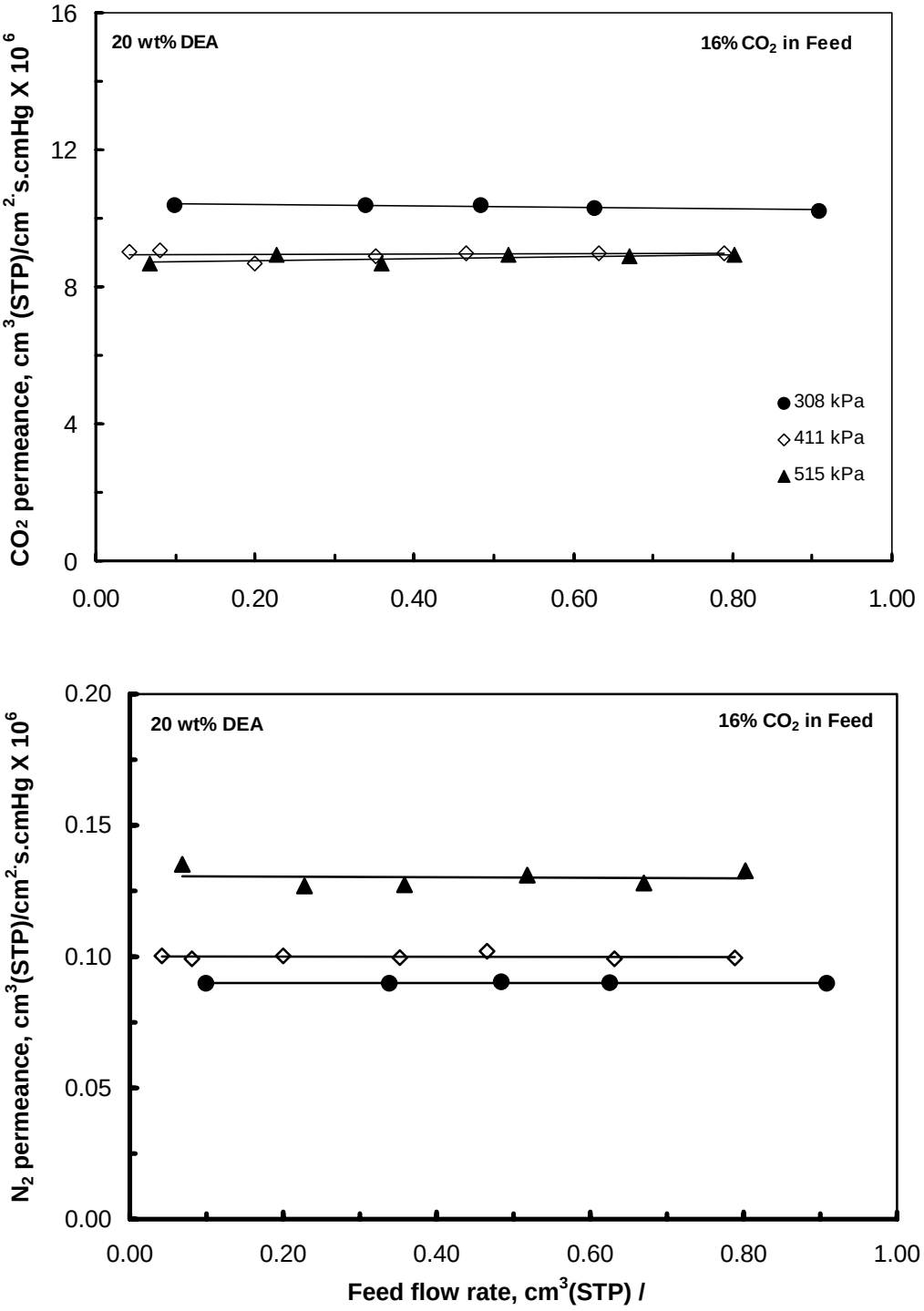

Figure 6.5 Permeance of carbon dioxide and nitrogen in the CO_2/N_2 mixtures for the PVA-DEA membrane as a function of feed gas flow rates at variable feed pressures. Temperature: 296K

Fig. 6.8 shows the variation of the CO_2/N_2 selectivity with CO_2 partial pressure differential and concentration of DEA in the membrane. The selectivity for the non-reactive PVA membrane is almost constant. For the PVA-DEA membrane, the selectivity increases with the DEA concentration. However, when the concentration is about 50wt% DEA, the selectivity was similar to the 30wt% probably because the facilitation due to the presence of DEA in the membrane was being reduced by the negative effects of high concentration of ions in the matrix. It can be observed that the reactive membrane containing 20wt% DEA provide the highest selectivity. The variation in selectivity suggests that the separation was more significant at lower pressure differential relative to the higher ones.

The CO_2 permeances calculated based on the numerical solution of diffusion-reaction equations (Eq4.37 and 4.38) are shown in Figure 6.9. The parameters used in the numerical calculations are given Table 6.1. It can be seen that the CO_2 permeance (Fig. 6.7 and 6.9) predicts almost similar trends for the experimental permeances as a function of CO_2 partial pressure differentials and DEA concentrations. A proposed explanation for these trends based on the numerical solution of the diffusion-reaction equation is presented Chapter 7.

6.3.3 Effect of Feed Concentration

Next, the feed CO_2 concentrations were varied in the range of approximately 5 to 50% CO_2. At each CO_2 feed concentration, the feed pressures were adjusted from about 170 to 514 kPa (25 to 75 psia). The results for these experiments are presented in Figures 6.10 to

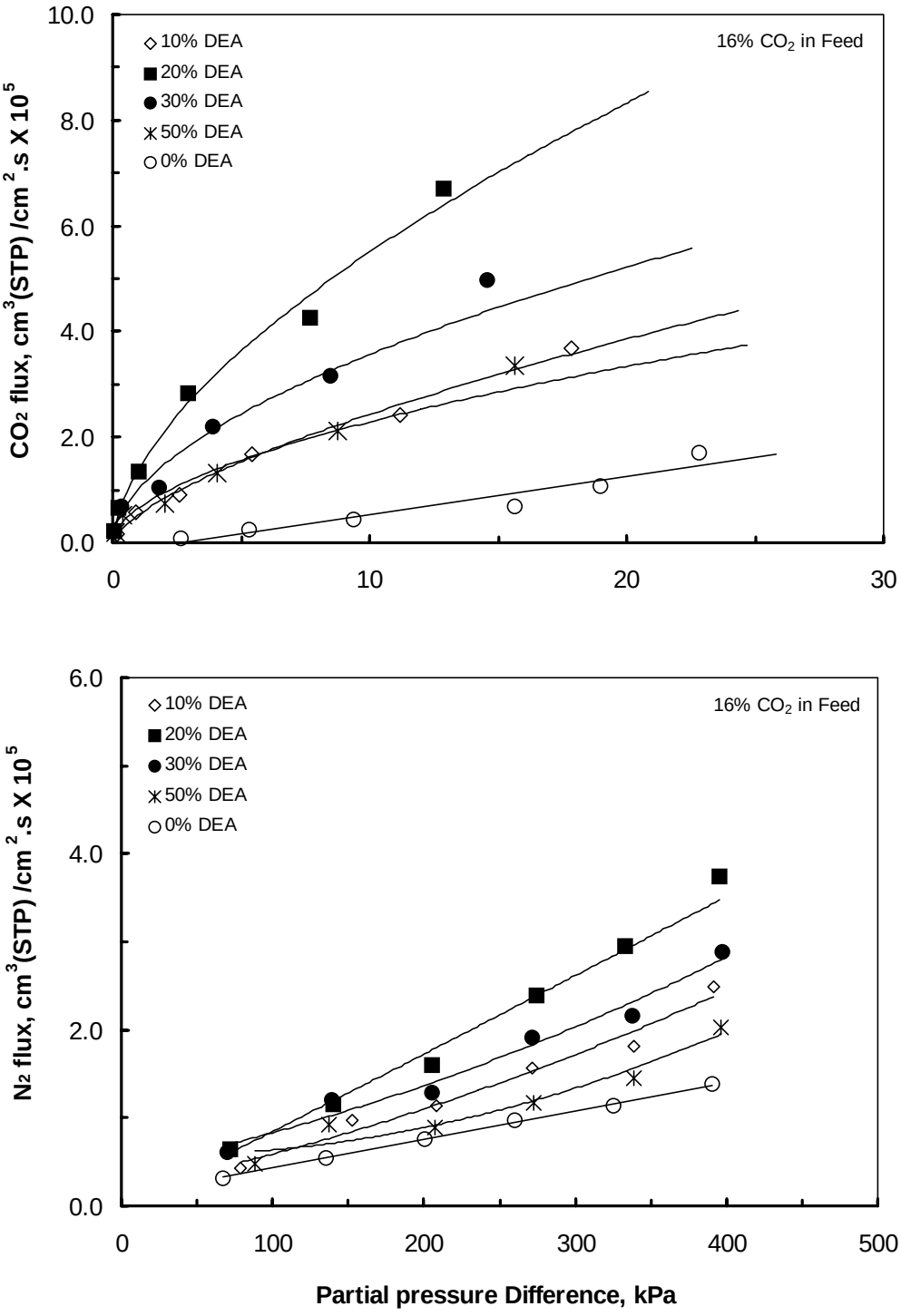

Figure 6.6 Fluxes of carbon dioxide and nitrogen in the CO_2/N_2 mixtures as a function of their partial pressure differences at different DEA concentrations. Temperature: 296K

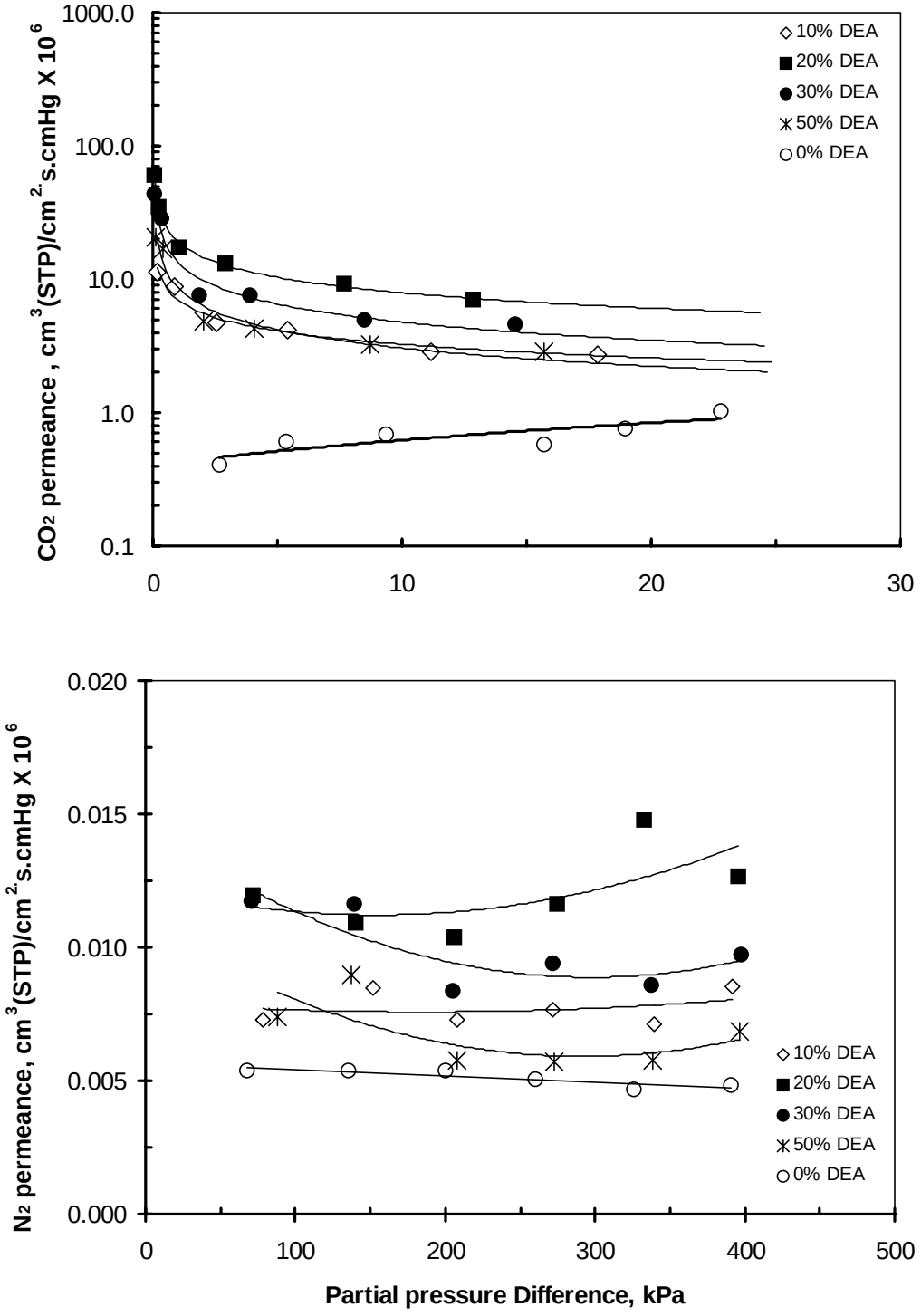

Figure 6.7 Permeances of carbon dioxide and nitrogen in the CO_2/N_2 mixtures as a function of their partial pressure differences at different DEA concentrations. Temperature: 296K

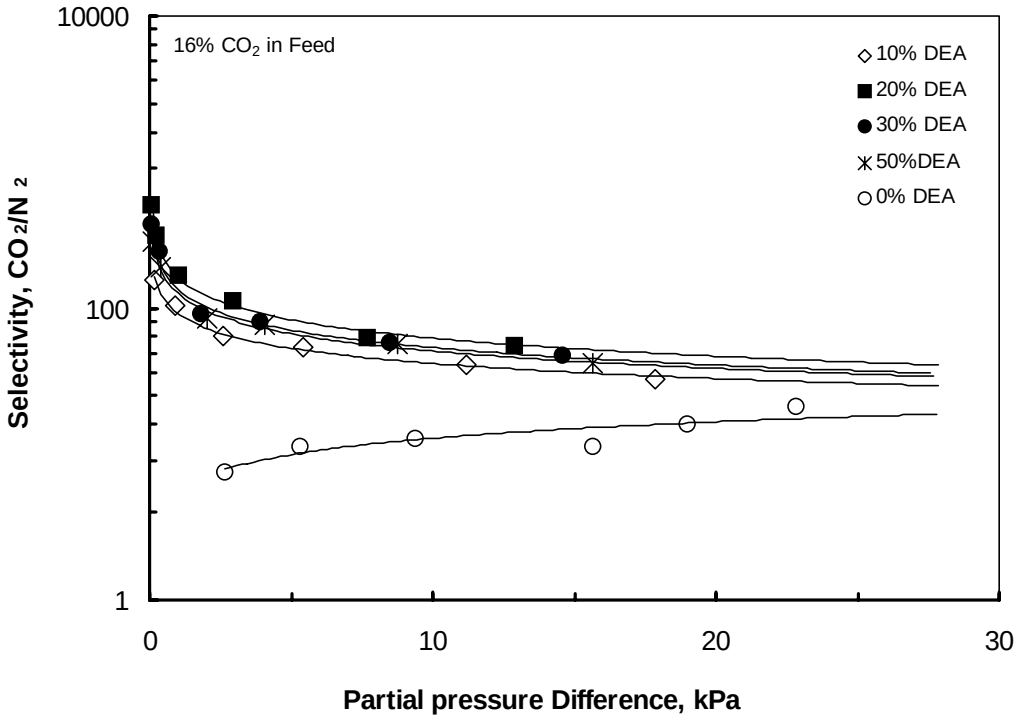

Figure 6.8 Selectivity of CO_2 over N_2 for the PVA-DEA membranes as a function of CO_2 partial pressure differences at various DEA concentrations. Temperature: 296K

Figure 6.16.

It is evident that the permeation fluxe increases with increasing CO_2 feed concentrations as well as increasing feed pressure for both PVA and PVA-DEA membranes. The PVA-DEA membranes demonstrate a higher permeation fluxes than the PVA membranes, which is a strong evidence of the effects of the presence of DEA in the PVA-DEA membranes. The data presented in theses figures also indicates that the permeate concentration of CO_2 is always larger than that in the feed and increases with increasing

feed pressures. Also, results suggest that the CO_2 were permeable for both PVA and PVA-DEA membranes.

The fluxes of CO_2 through the PVA were approximately linearly proportional to its partial pressure differentials, which is an evidence of Fickian diffusion. For the PVA-DEA membranes, the CO_2 flux were non- linear function of its partial pressure differential. The flux initially increases with partial pressure differential in the range of about 0.02 to 10 kPa and tend to increase almost linearly as the pressure differential increases. The non-linearity at low-pressure differential suggests the facilitated transport effect induced by the presence of DEA in the membranes. This observation is clearly illustrated in Fig. 6.13. Figures 6.14 and 6.15 also show that the permeation of pure CO_2 agreed within experimental errors to the gas mixture permeation for the PVA and PVA-DEA membranes respectively.

The CO_2 flux across the facilitated transport membranes (PVA-DEA membrane) is generally dependent on the concentration of CO_2 as well as the CO_2-DEA complex across the membrane. These CO_2-DEA complexes may be in the form of carbamates, protonated amines, bicarbonates or zwitterions. The higher the concentration of dissolved CO_2, the greater is the rate of formation of CO_2-DEA complex. Thereby, at higher feed concentration of CO_2, most of the DEA molecules in the membrane are fully utilized or tied-up with the CO_2 molecules, this in turn lowers the amount of DEA available for further CO_2 uptake. In other words, essentially all the available DEA molecules are complexed on the feed side and essentially none are complexed on the permeate side of

Table 6.1 Dimensionless parameters for CO_2 transport in PVA-DEA membrane.

T= 298K.

CO_2 Pressure Differential kPa	wt% DEA	m1	m2	m3	m4	Facilitation Factor	Permeance
0.19	10	4.78	0.09	63104	7258.01	37.65	27.91
0.89	10	4.78	0.42	63104	1535.14	27.81	20.62
2.58	10	4.78	1.21	63104	526.87	15.62	11.58
5.40	10	4.78	2.53	63104	252.00	5.69	4.22
11.17	10	4.78	5.24	63104	121.80	1.85	1.37
17.85	10	4.78	8.38	63104	76.24	1.23	0.91
0.25	20	2.36	0.11	169938	12137.53	80.41	43.13
1.04	20	2.36	0.47	169938	2943.12	59.76	32.06
2.91	20	2.36	1.32	169938	1049.85	31.21	16.74
7.67	20	2.36	3.47	169938	398.21	6.47	3.47
12.87	20	2.36	5.82	169938	237.40	2.54	1.36
0.07	30	1.56	0.03	366376	92426.24	158.13	53.58
0.32	30	1.56	0.13	366376	19050.75	134.32	45.51
1.83	30	1.56	0.74	366376	3329.41	86.32	29.25
3.88	30	1.56	1.57	366376	1570.46	43.74	14.82
8.47	30	1.56	3.44	366376	719.64	11.07	3.75
14.56	30	1.56	5.90	366376	418.90	3.76	1.27
0.12	50	0.91	0.05	3904336	315754.81	580.85	29.65
0.40	50	0.91	0.15	3904336	97022.64	511.20	26.10
2.02	50	0.91	0.77	3904336	19422.77	348.42	17.79
4.09	50	0.91	1.56	3904336	9597.93	202.72	10.35
8.75	50	0.91	3.34	3904336	4484.88	58.07	2.96
15.67	50	0.91	5.98	3904336	2503.86	16.40	0.84

Unit of permeance: cm^3 (STP)/cm^2.s.cmHg x 10^5

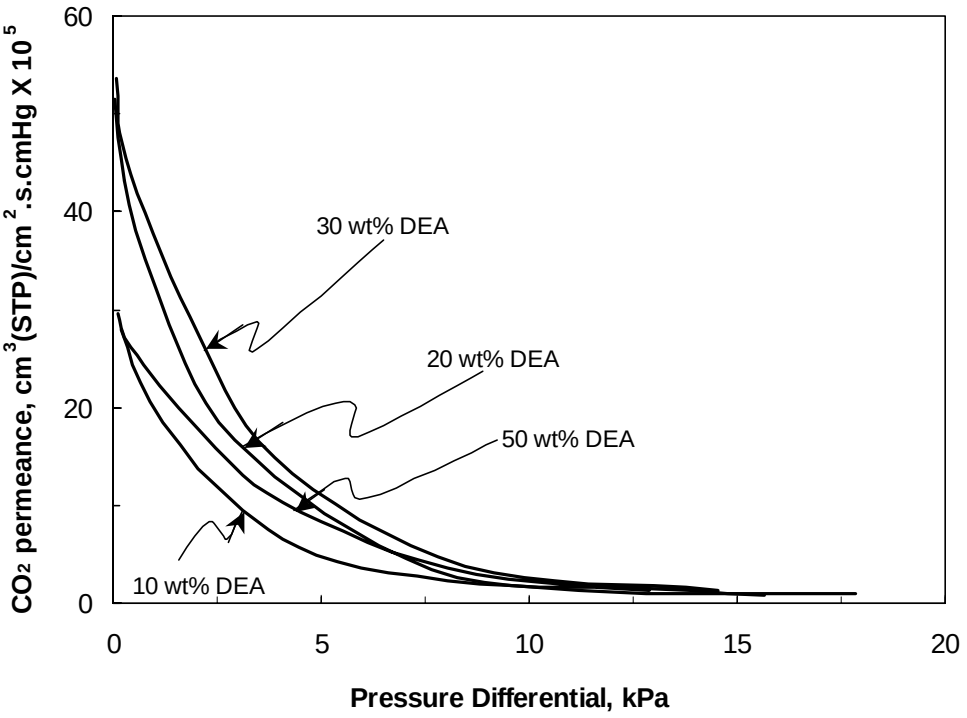

Figure 6.9 Calculated permeances of carbon dioxide based on the numerical solution as a function pressure differential at various DEA concentrations.

the membrane. Because of this condition, the facilitation effect due to the presence of the carrier markedly decreases leading to the reduction in the rate of flux variation with CO_2 partial pressure differentials. This phenomenon is referred to as carrier saturation.

Another important factor to be considered is the salting out effect. In the reaction of CO_2 and DEA as mentioned above, ionic species are formed, *i.e*. carbamates, protonated amines and zwitterions. In the presence of these ions, portion of the PVA molecular chain interacts with these ions in such a way that the PVA chains could surround these ions leading to the reduction of the physical solubility of the free CO_2 and

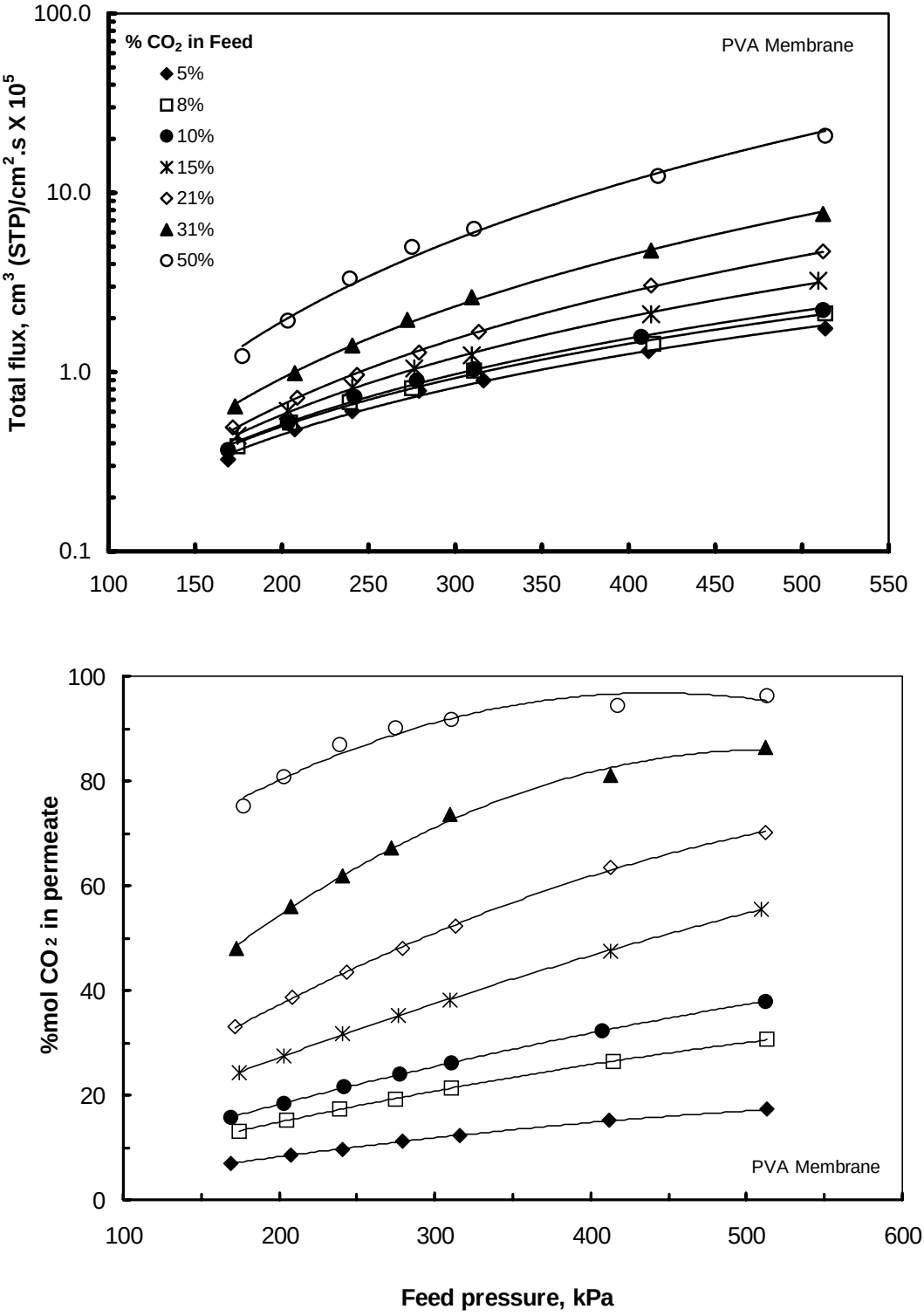

Figure 6.10. Total fluxes of CO_2/N_2 mixtures and the permeate concentration of CO_2 for the PVA membrane as a function of their partial pressure difference. Temperature: 296K

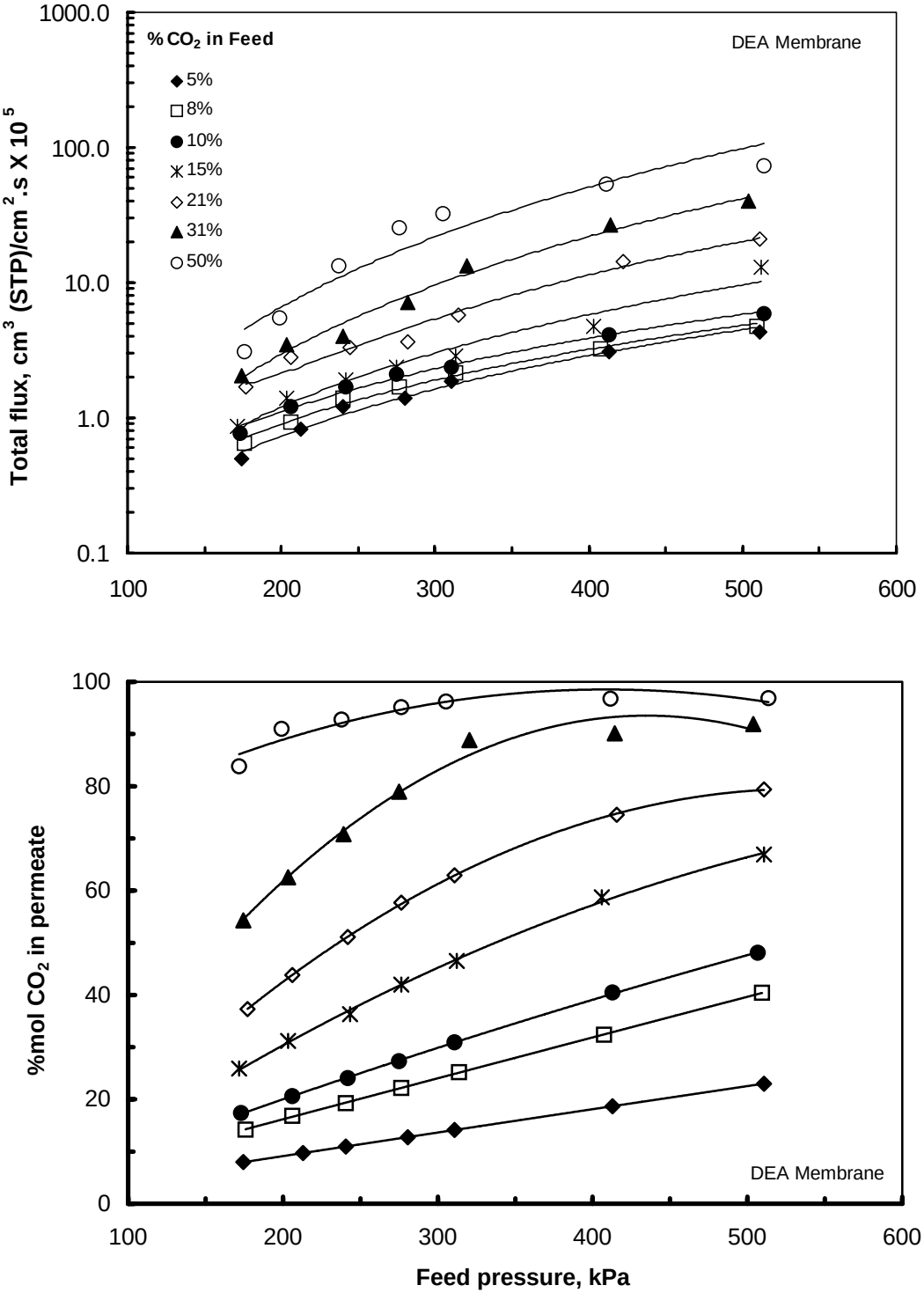

Figure 6.11 Total fluxes of CO_2/N_2 mixtures and the permeate concentration of CO_2 for the PVA-DEA membrane as a function of their partial pressure difference. Temperature: 296K

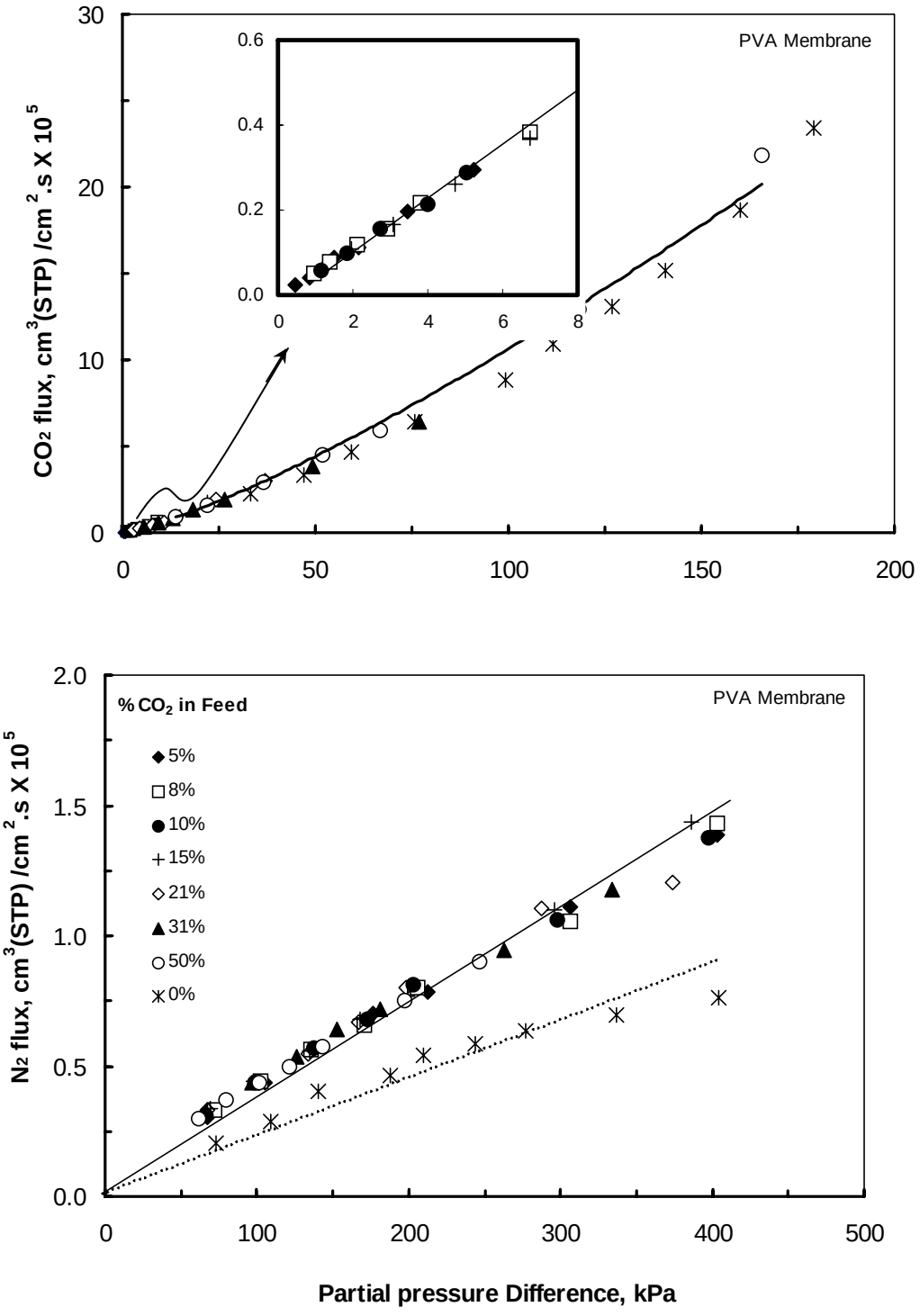

Figure 6.12 Fluxes of carbon dioxide and nitrogen in the CO_2/N_2 mixtures for the PVA membrane as a function of their partial pressure difference. Temperature: 296K

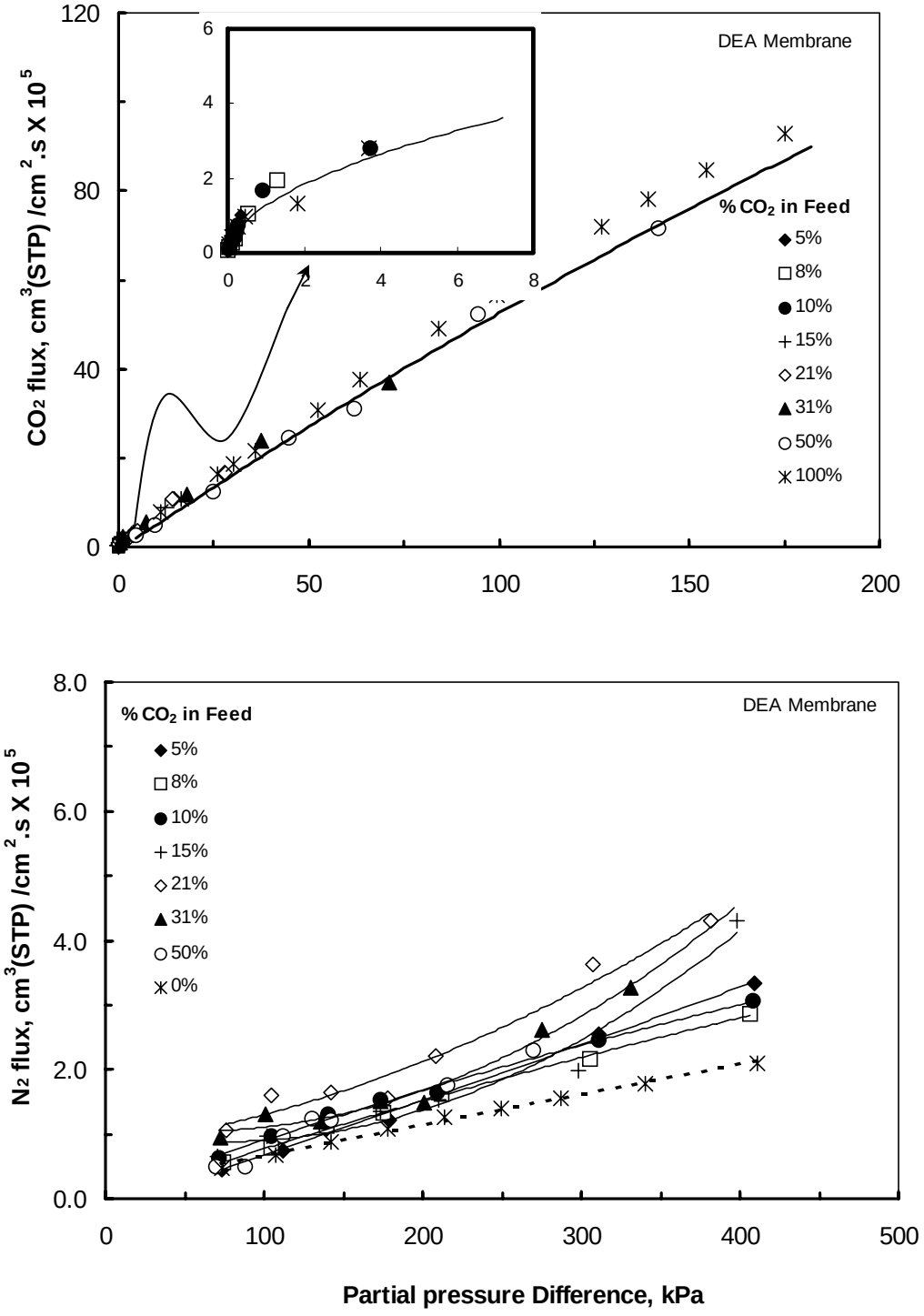

Figure 6.13 Fluxes of carbon dioxide and nitrogen in the CO_2/N_2 mixtures for the PVA-DEA membrane as a function of their partial pressure difference. Temperature: 296K

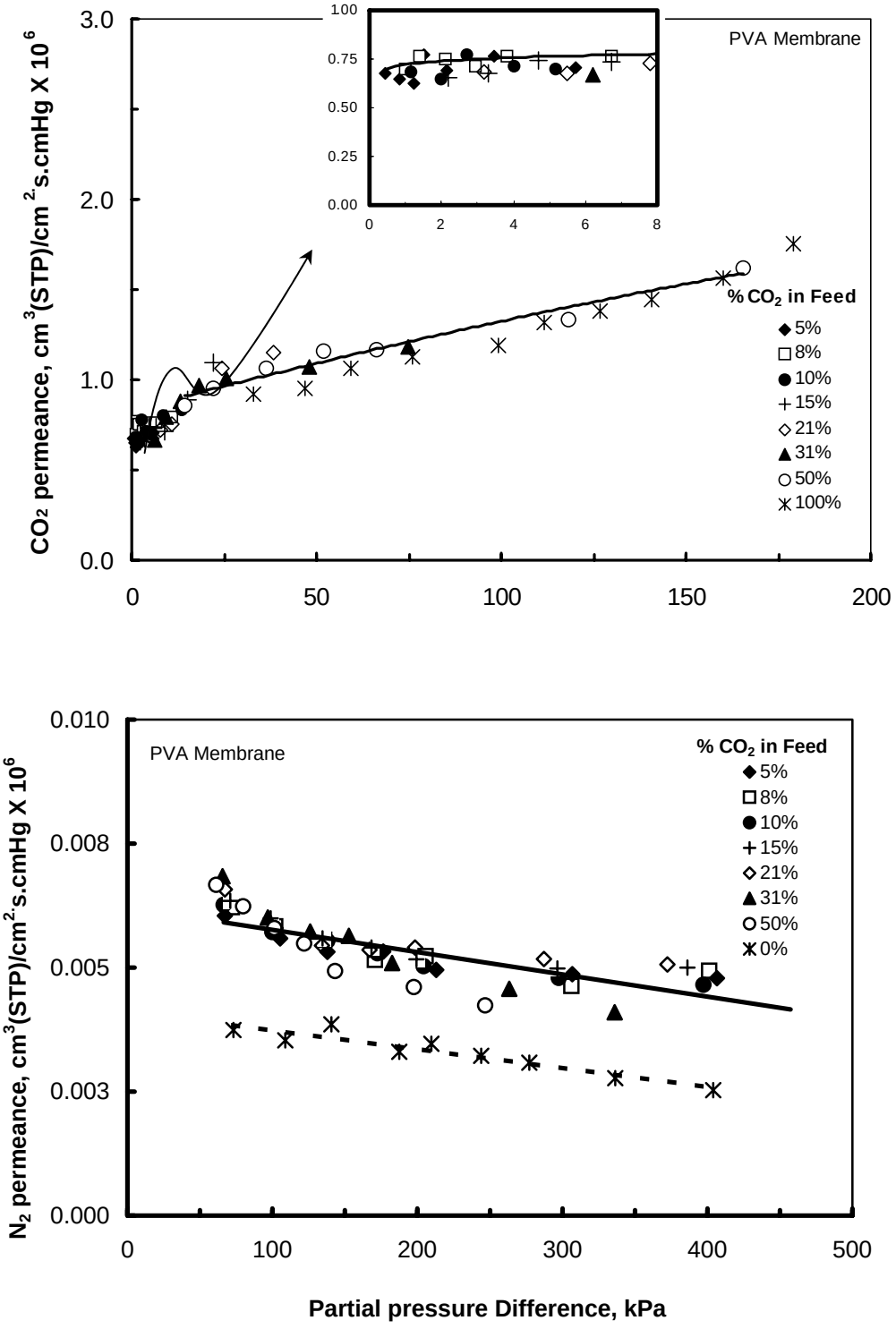

Figure 6.14 Permeance of carbon dioxide and nitrogen in the CO_2/N_2 mixtures for the PVA membrane as a function of their partial pressure difference. Temperature: 296K

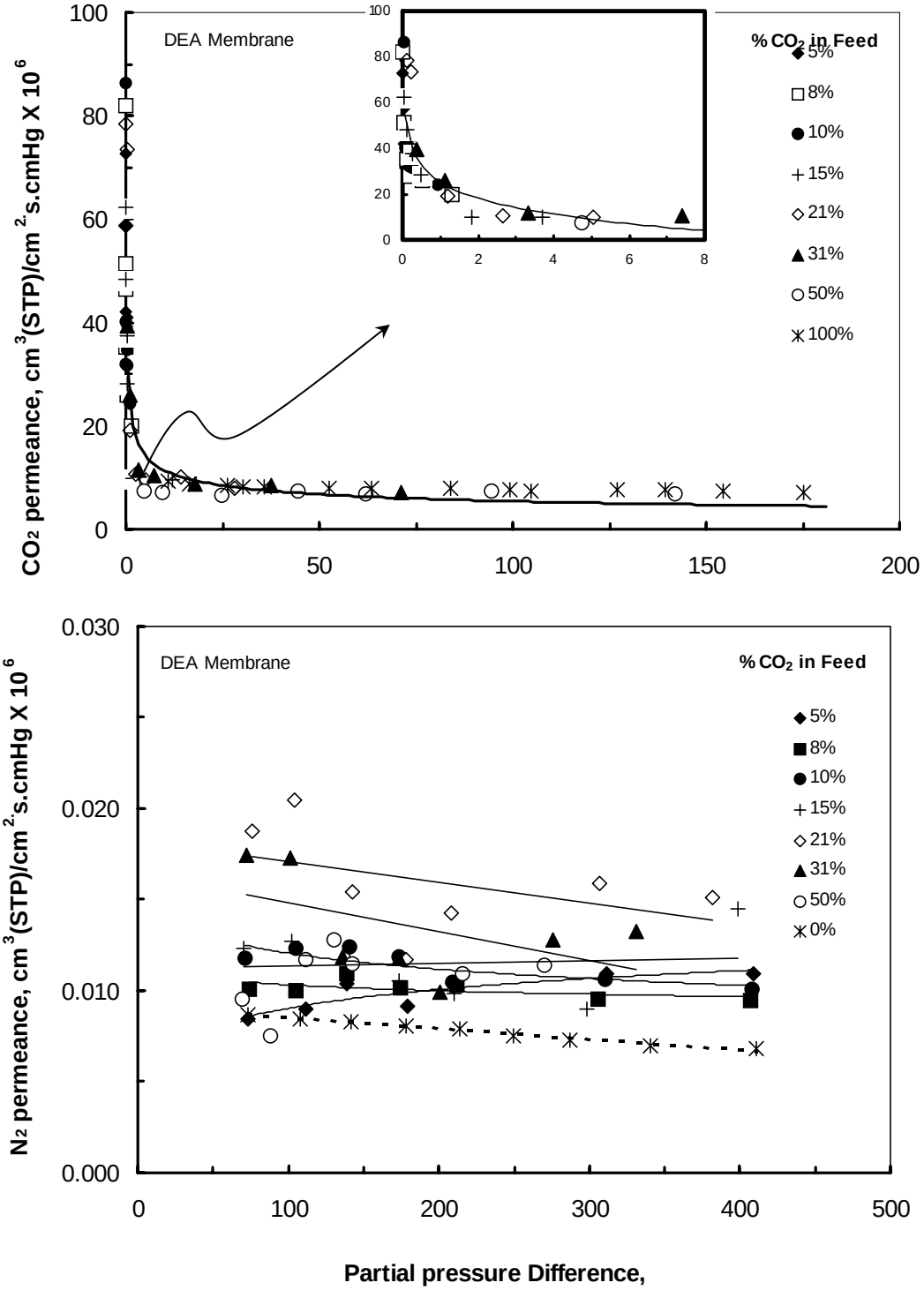

Figure 6.15 Permeance of carbon dioxide and nitrogen in the CO_2/N_2 mixtures for the PVA-DEA membrane as a function of their partial pressure difference. Temperature: 296K

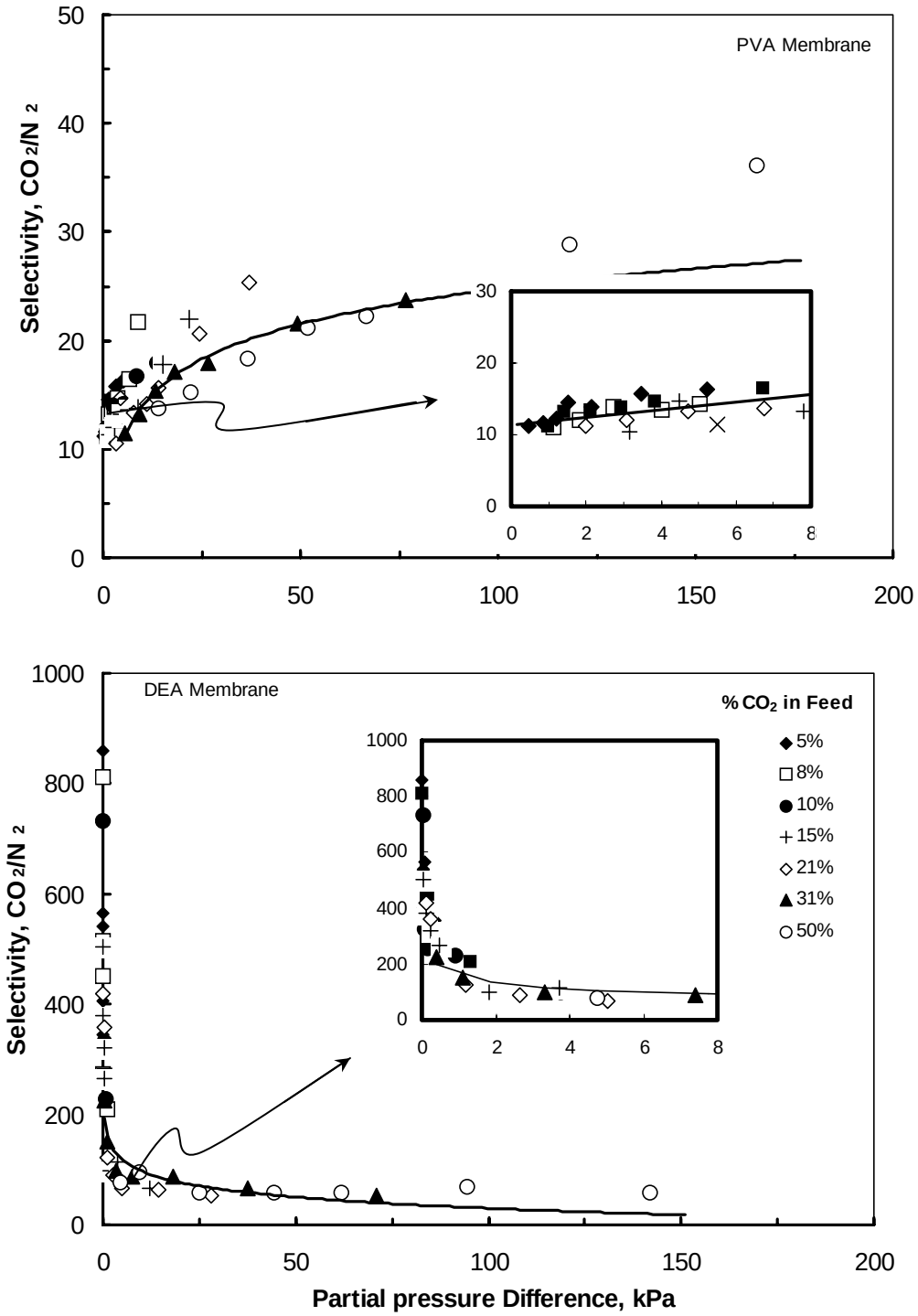

Figure 6.16 Selectivity of carbon dioxide over nitrogen in the CO_2/N_2 mixtures for the PVA and PVA-DEA membranes as a function of CO_2 partial pressure difference. Temperature: 296K

N_2 in the PVA matrix.

The N_2 flux for the PVA-DEA membranes show a different behaviour compared to the PVA membranes. The flux of N_2 through the PVA membranes increases with its pressure differential in approximately linear manner suggesting that N_2 is transporting by solution-diffusion mechanism. For the PVA-DEA membranes, the fluxes go up and downs, staggered and higher than that of the PVA membrane. This characteristic behaviour of N_2 permeance may be rationalized by the following. The higher flux of N_2 in the PVA-DEA membrane compared to the PVA membrane was probably due to the plasticising effect of the DEA and CO_2 in the PVA chains. PVA forms a rigid membrane when casted on a glass plate while in the presence of DEA it forms a soft membrane suggesting that interaction of DEA with PVA may disrupt the inter and intra-molecular hydrogen bonding, thereby swelling the polymer. The staggering of the N_2-data points in the PVA-DEA membrane was probably the effects of the carrier saturation or salting out or a combination of both as mentioned above. These results were reproducible for the sets of experiments carried out (see Fig. 6.13 and Appendix E).

The CO_2 permeance through the PVA membrane increases with its pressure differential and therefore pressure dependent (see Figures 6.14). These results may be due to the interaction of CO_2 with the PVA chain that appears to plasticize the membrane matrix resulting to an increase in flexibility of the PVA chain segments. CO_2 would then diffuse faster through the membrane. On the other hand, N_2 permeance decreases slightly with

Table 6.2. Dimensionless parameters for CO_2 transport for the PVA-DEA membrane.

T=296K

CO_2 Pressure Differential kPa	m1	m2	m3	m4	Facilitation Factor	Permeance Without Facilitation	Permeance With facilitation
0.05	2.36	0.02	169938	56388.6	96.12	0.54	49.93
0.26	2.36	0.12	169938	11662.47	79.39	0.54	42.59
0.63	2.36	0.28	169938	4883.94	68.27	0.54	36.62
1.27	2.36	0.57	169938	2402.58	55.87	0.54	29.97
1.69	2.36	0.77	169938	1804.09	48.65	0.54	26.09
2.22	2.36	1.00	169938	1375.74	40.73	0.54	21.85
5.33	2.36	2.41	169938	573.60	12.75	0.54	6.84
13.88	2.36	6.28	169938	220.11	2.26	0.54	1.21
31.58	2.36	14.28	169938	96.75	1.12	0.54	0.60
61.86	2.36	27.97	169938	49.38	1.02	0.54	0.54
89.45	2.36	40.45	169938	34.15	1.01	0.54	0.54
129.24	2.36	58.44	169938	23.64	1.00	0.54	0.54
142.21	2.36	64.31	169938	21.48	1.00	0.54	0.54
177.82	2.36	80.41	169938	17.18	1.00	0.54	0.54
210.92	2.36	95.37	169938	14.48	1.00	0.54	0.54
317.07	2.36	143.37	169938	9.63	1.00	0.54	0.54
357.97	2.36	161.87	169938	8.53	1.00	0.54	0.54
405.17	2.36	183.21	169938	7.54	1.00	0.54	0.54

Unit of permeance: cm^3 (STP)/cm^2.s.cmHg x 10^5

DEA: 20wt%

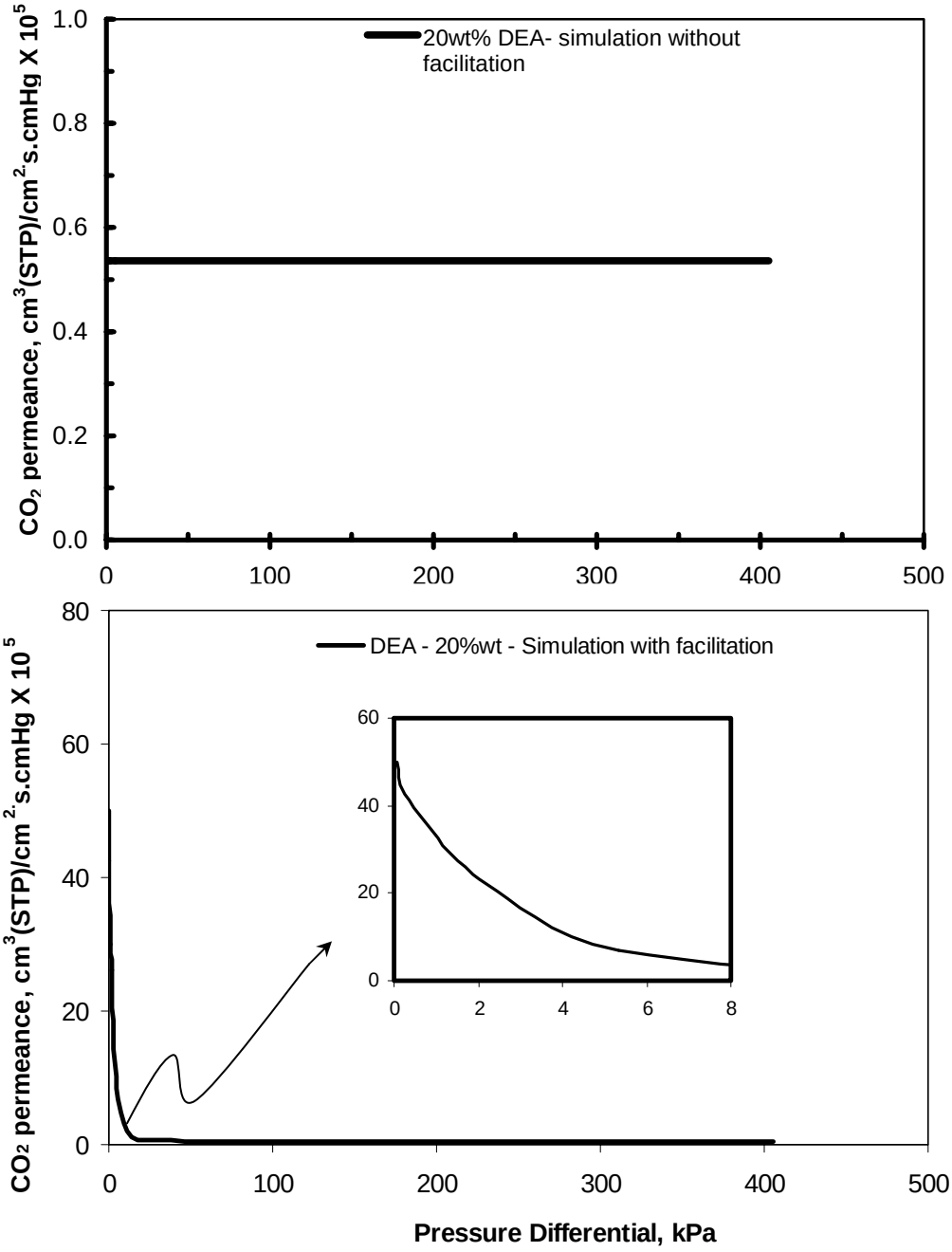

Figure 6.17 Calculated fluxes and permeance of carbon dioxide as a function of their partial pressure difference in the absence (above) and presence of facilitation (below). Temperature: 296K

increasing partial pressure differential which may be caused by the compression of the membrane and would slightly reduced the N_2 diffusion across the membrane. These observations were in agreement with the previous results from pure gas permeation.

For the PVA-DEA membranes, the variation of CO_2 permeance with concentration and feed pressure are shown in Figures 6.15. At a lower partial pressure differential, the pemeance of CO_2 was enhanced, but as the partial pressure differential reaches above 60 kPa, the permeances is similar to that of the PVA membranes. The reduction of the permeance with high CO_2 partial pressure differential is probably the negative effect of carrier saturation or salting out effect. Hence, at larger CO_2 partial pressure differential, the reactive membrane no longer serve as a facilitating medium, so that the permeance and selectivity are simply governed by the effects of increasing concentration of CO_2-DEA complexes.

Figures 6.16 shows the variation of CO_2/N_2 selectivity as a function of partial pressure differential. For the non-reactive PVA membrane the selectivity increases slightly with an increase in the feed CO_2 concentration as well as feed pressure. This is most likely due to the plasticizing effect of CO_2 into the PVA matrix, making the polymer chains more mobile resulting to an increased in the diffusion rate. As the feed concentration of CO_2 is increased, the possibility to plasticize the membrane matrix increases resulting to an increased in selectivity. This phenomenon was also observed during pure gas permeation experiments in the Chapter 5.

For the PVA-DEA membrane, the selectivity decreases substantially with increasing partial pressure differential or driving force. The trends in the selectivity suggest that the separation was more significant at lower partial pressure differential than at the higher ones. At lower partial pressure differential, it can be inferred that the gas mixture reaches a greater degree of chemical separation whereas at higher partial pressure differentials, physical separation occurs as it becomes less sensitive to the applied driving force.

In an effort to verify the results of the experimental data that were observed so far, a series of experiments were also carried out by fixing the total feed pressures to about 308, 311 and 515 kPa (45, 60and 75 psia). At each feed pressure, the CO_2 feed concentration were varied from approximately 5 to 100% CO_2. The results for these experiments are presented in Appendix E. From these figures, it can be concluded that satisfactory agreement exists between these and the previous results.

Fig.6.17 shows the CO_2 permeance as a function of its pressure differential based on the numerical solution of the transport equations. The dimensionless parameters and facilitation factors is listed in Table 6.2. Insert shows the effect at low-pressure differential. Without chemical facilitation, the CO_2 permeance was independent of driving force or pressure differential. However, with chemical facilitation the trends were almost similar to the observed experimental trends. Further discussions is presented in Chapter 7.

6.3.4 Effect of Operating Temperatures

Figures 6.18 to 6.20 represents the results on the effect of temperature on the membrane performance. The temperature was varied from 303 to 333K. The feed concentration of CO_2 is 15.6% and the rest N_2. The feed pressure was varied from about 308, 377, 446 and 515 kPa (45, 55, 65 and 75 psia).

It is evident that the CO_2 and N_2 permeance increase with increasing temperature for both PVA-DEA and PVA membranes. For the PVA membranes, the CO_2 and N_2 permeance increases with increasing temperatures and are not largely affected by the feed pressure. A closer look at the experimental results plotted in Fig 6.18 appears to suggests that the CO_2 concentration in the feed was not sufficient enough to plasticized the membrane matrix in contrast to pure gas permeation where the CO_2 permeance increases slightly with feed pressure. On the other hand, the increased in permeance with temperature suggest that CO_2 is permeating by the virtue of its diffusivity and less on its solubility through PVA membrane. It further implies that an increase in its diffusivity with increasing temperatures can overcome the reduction in solubility resulting to a higher selectivity with increasing temperature. The same observations were obtained during pure gas permeation experiments.

The activation energy of permeation, $\boldsymbol{E_a}$, was calculated based on the experimental data. The activation energies for CO_2 and N_2 for the PVA and PVA-DEA membranes as a function of feed pressure are shown in Fig. 6.21. The figures show that an elevation of

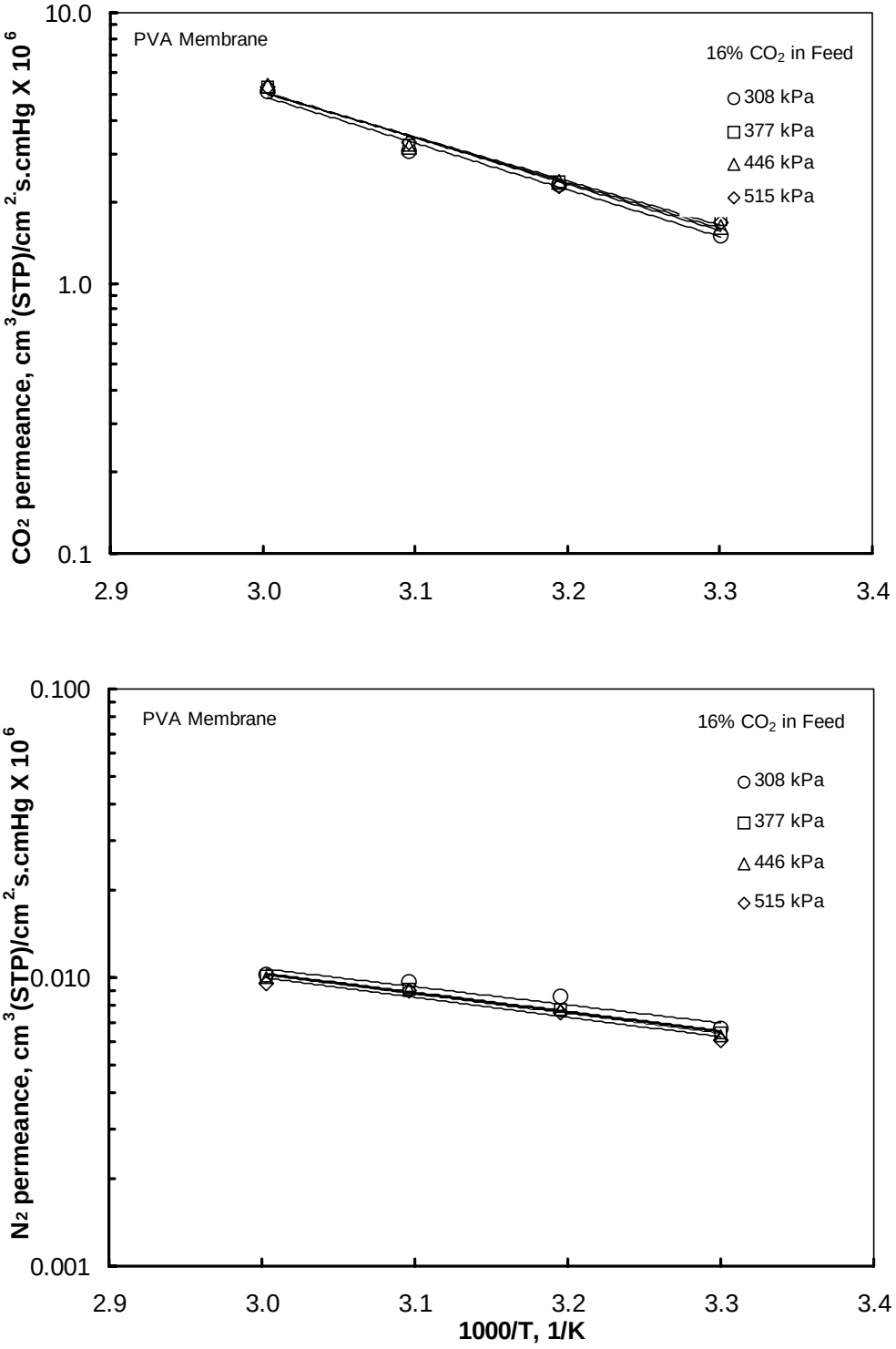

Figure 6.18. Permeance of carbon dioxide and nitrogen in the CO_2/N_2 mixtures with 16% CO_2 in feed for PVA membrane as a function of 1/T at variable feed pressures.

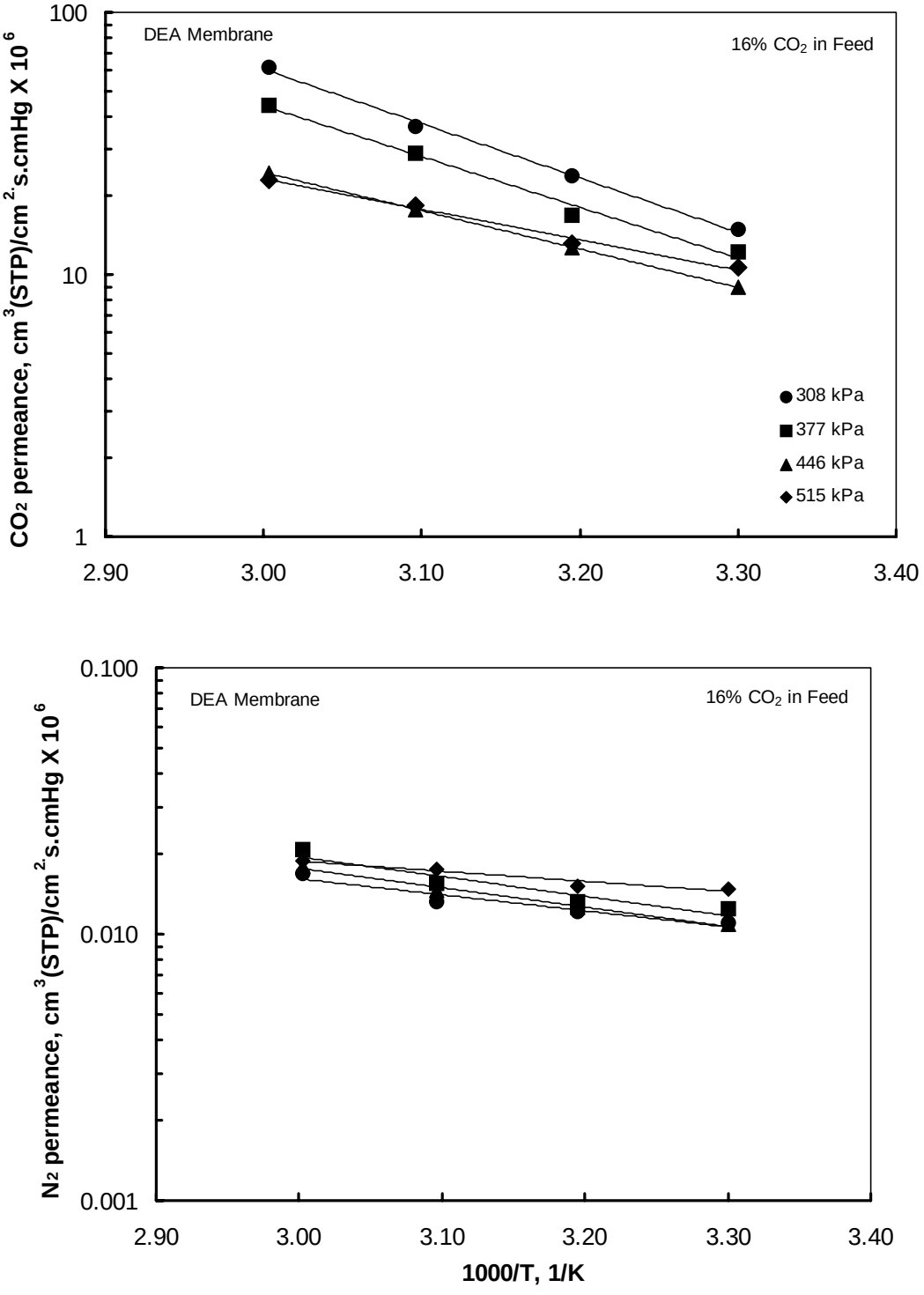

Figure 6.19 Permeance of carbon dioxide and nitrogen in the CO_2/N_2 mixtures with 16% CO_2 in feed for PVA-DEA membrane as a function of 1/T at variable feed pressures.

temperature increases the permeance of CO_2 and N_2 in the mixtures. The $\boldsymbol{E_a}$ for CO_2 and N_2 in the PVA membrane were less dependent on feed pressure, which could be due to the lower solubility of CO_2 in the membrane matrix. Also, the figure clearly shows that the feed concentration of CO_2 has less effect on the $\boldsymbol{E_a}$ values of N_2.

Fig. 6.20 shows the selectivity of CO_2 over N_2 based on temperature and feed pressure. The selectivity evidently increases with temperature but almost unchanged with feed pressure. The pressure effect on selectivity was similar to the results from the pure gas permeation experiments. The selectivity increased to about 37 at 323K and 414 kPa (60 psig)

For the PVA-DEA membranes, the $\boldsymbol{E_a}$ of CO_2 decreases with increasing feed concentration. The CO_2 has a higher value of $\boldsymbol{E_a}$ than N_2 and the permeance of CO_2 increase faster than the permeance of N_2 with increasing temperature. Hence, the selectivity of CO_2 over N_2 increases with increasing temperature as shown in Fig. 6.20.

The reaction of CO_2 with DEA is highly exothermic, it follows that the equilibrium constant decreases with increasing operating temperatures based on Eq. (5.8). A higher value of equilibrium constant means a fast absorption rate in feed stream compared to the stripping rate in the permeate stream of the membrane while a smaller value of equilibrium constant corresponds to slow absorption rate and a fast stripping (reverse reaction) rate. However, the combined effect of increased in diffusivity and forward

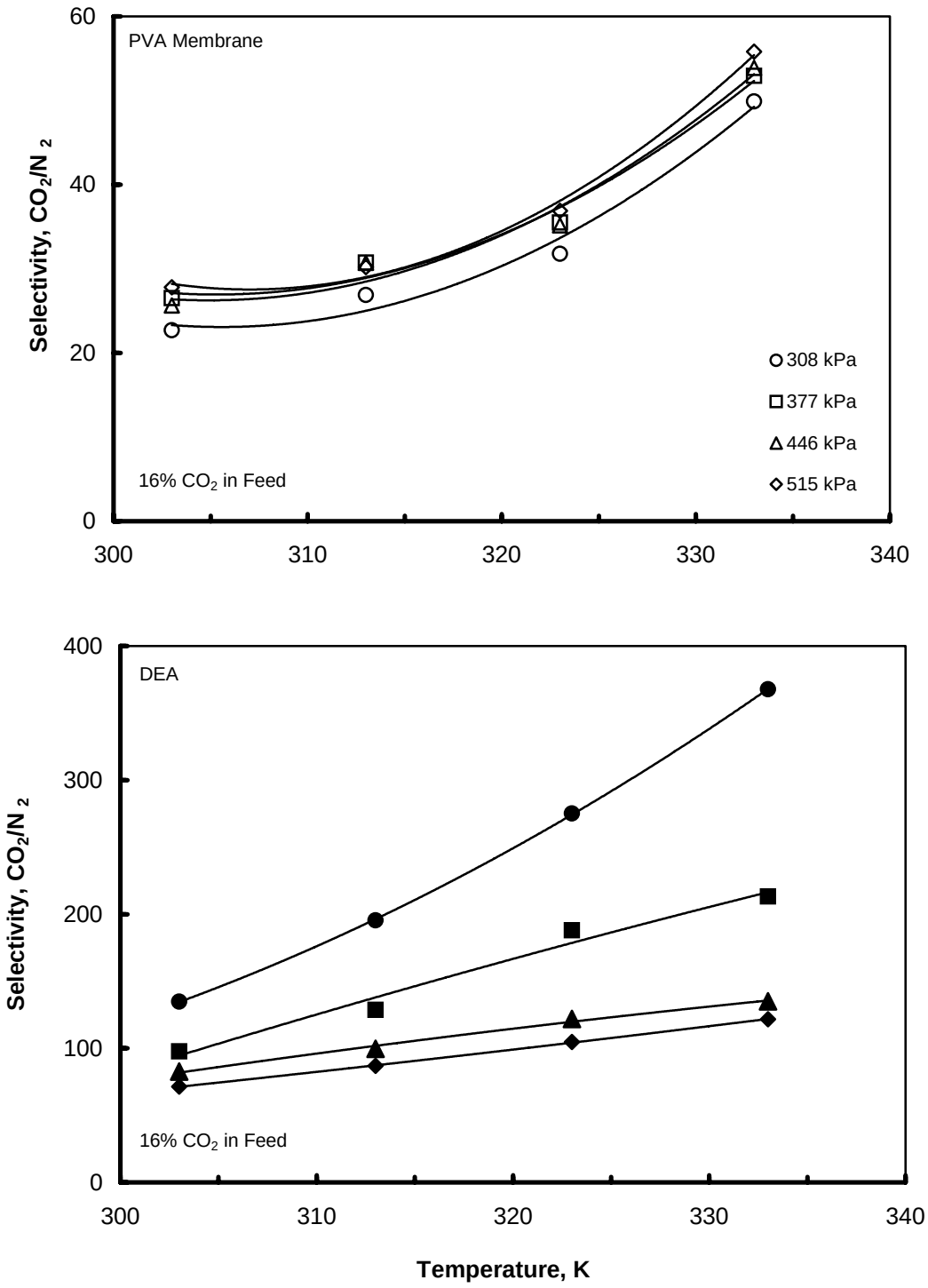

Figure 6.20 Selectivity of carbon dioxide over nitrogen in the CO_2/N_2 mixtures with 16% CO_2 in feed for PVA and PVA-DEA membrane as a function of temperature at variable feed pressures.

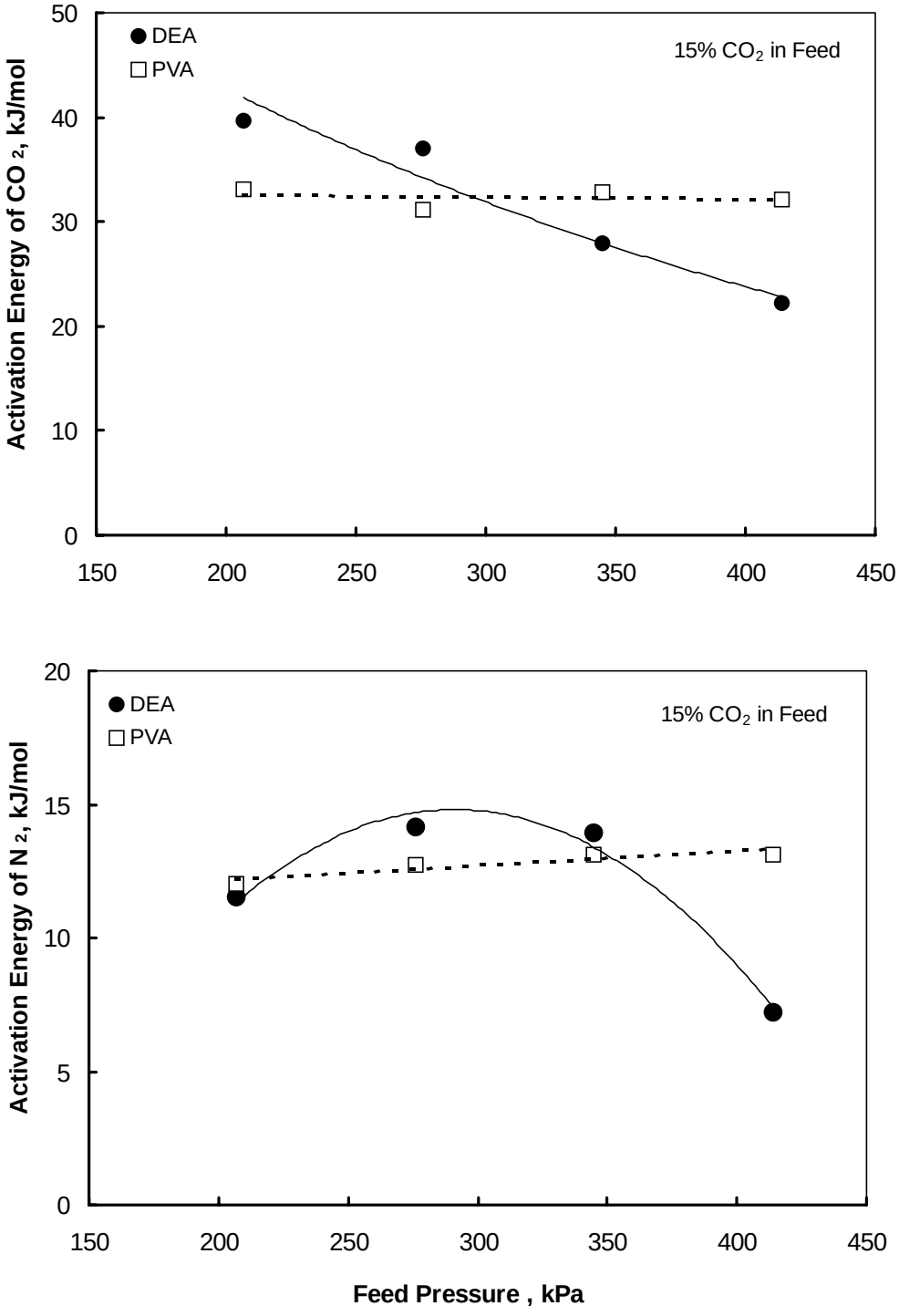

Figure 6.21 Activation energies for carbon dioxide and nitrogen in the CO_2/N_2 mixtures for the PVA and PVA-DEA membrane as a function of feed pressures.

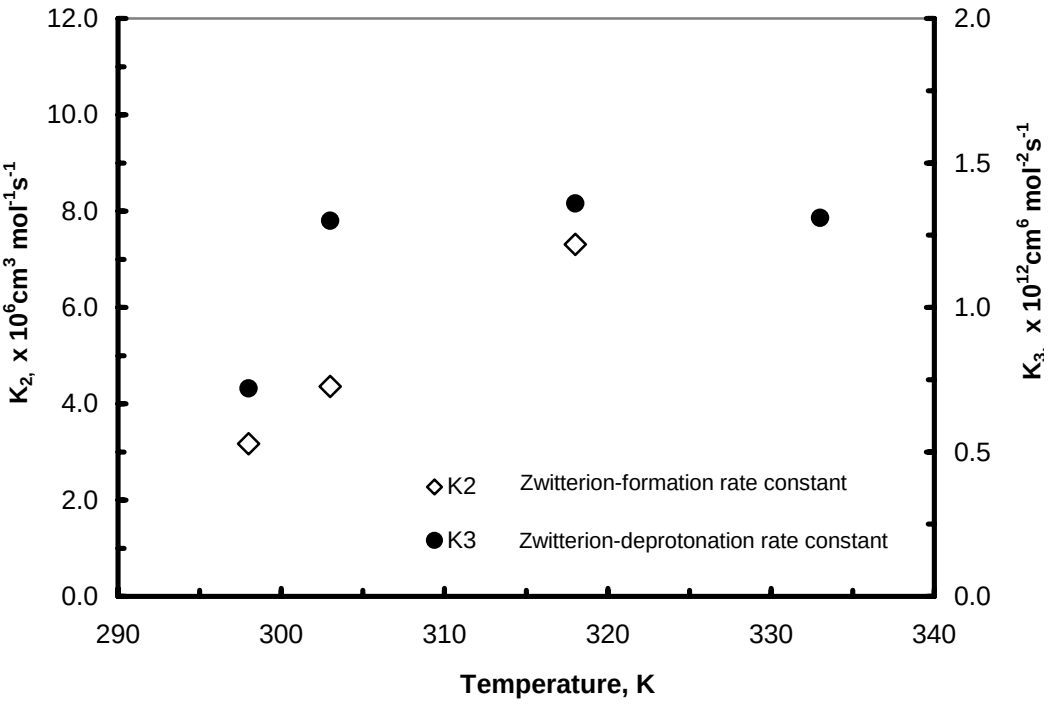

Figure 6.22 Zwitterion rate constants for the CO_2 – DEA reaction as a function of temperatures (adapted from Littel *et. al*. 1992).

reaction rate constants with increase in temperatures are favourable enough for higher CO_2 permeances and higher selectivity at higher temperature.

Furthermore, the temperature may also influenced the zwitterion formation and deprotonation rates (Littel, *et al*., 1992). Going back to the zwitterions reaction mechanism reintroduced by Dankwerts (1979):

$$CO_2 + R_1R_2NH \underset{k_2}{\overset{k_1}{\rightleftharpoons}} R_1R_2NH^+CO_2^- \qquad (6.3)$$

$$R_1R_2NH^+CO_2^- + R_1R_2NH \underset{k_4}{\overset{k_3}{\rightleftharpoons}} R_1R_2NCO_2^- + R_1R_2NH_2^+ \qquad (6.4)$$

Eq. (6.3) and (6.4) are the zwitterion formation and deprotonation reactions respectively. This group studied the effects of temperature on the kinetics of the reactions of CO_2 with DEA and various amines. Their experimental results are presented in Fig.6.22 (for DEA). Zwitterion-formation rate constant (K_1) show a definite temperature dependence while zwitterion-deprotonation constant (K_3) are approximately insensitive to temperature changes at 303, 318 and 333K. They concluded that temperature could influenced the overall reaction rate for primary and secondary amines based on the following: a significant temperature dependence is observed when the zwitterion-formation is the rate determining step, whereas a slight temperature dependence happens when the zwitterion-deprotonation is the rate determining reaction. They further concluded that depending on the relative values of the zwitterion formation and deprotonation rates, an amine can shift from the first to the second order with increasing temperature leading to a decreasing temperature dependence of the overall reaction rate.

6.3.5 Stability of Membrane

As mentioned previously, membrane lifetime is one crucial factor that needs to be examined. In this stability study, the feed gas concentration was fixed at 15.6% CO_2 (balance N_2) and feed pressure was maintained at approximately 308 kPa (45 psia). Two sets of PVA-DEA membranes were tested.

Figures 6.23 and 6.24 show the stability tests of the PVA-DEA membrane. No significant reduction in the CO_2 permeance and selectivity were observed during the continuous

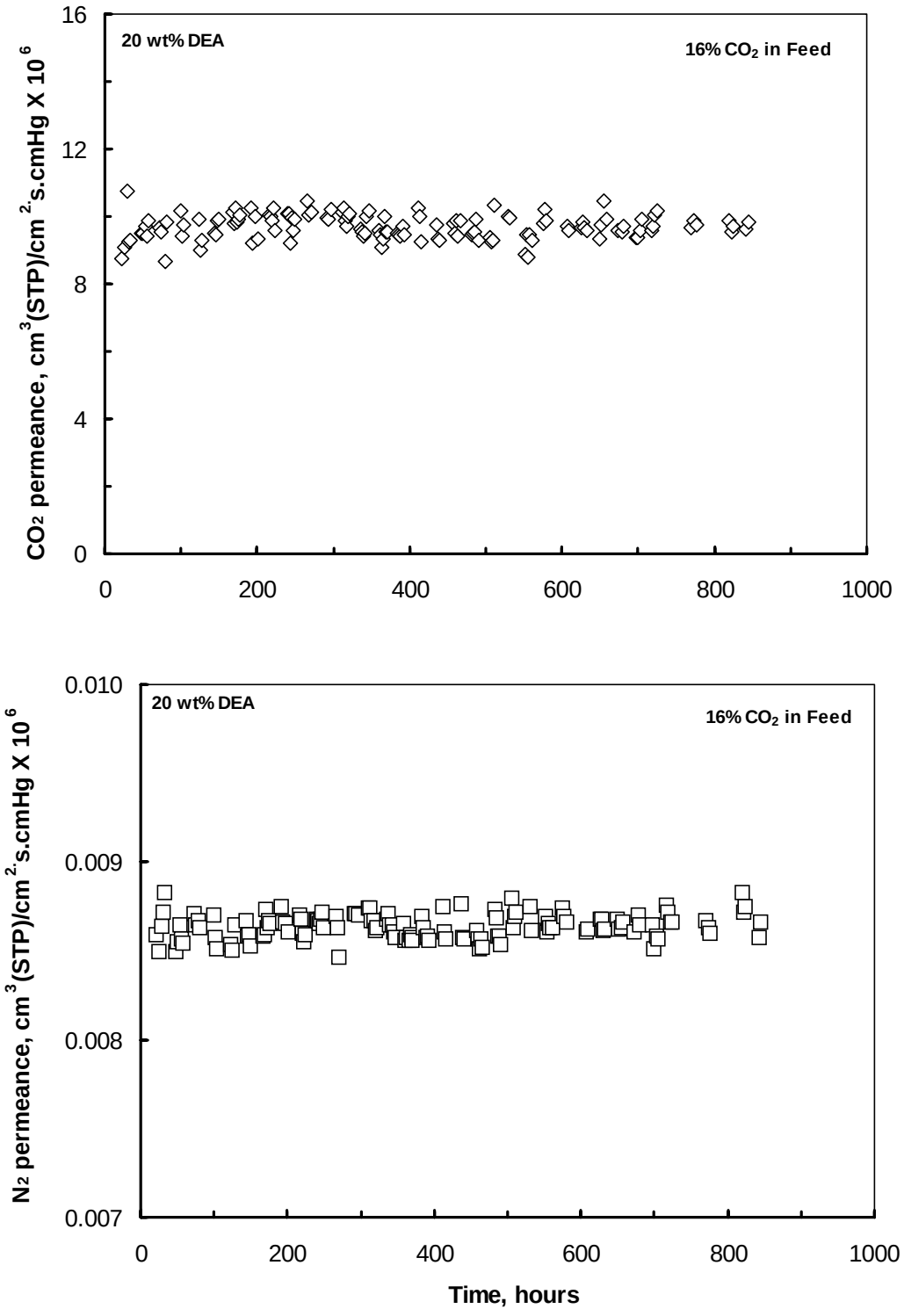

Figure 6.23 Permeance of carbon dioxide and nitrogen in the CO_2/N_2 mixtures through the PVA-DEA membrane at a feed pressure of 308 kPa as a function of time. Temperature: 296K

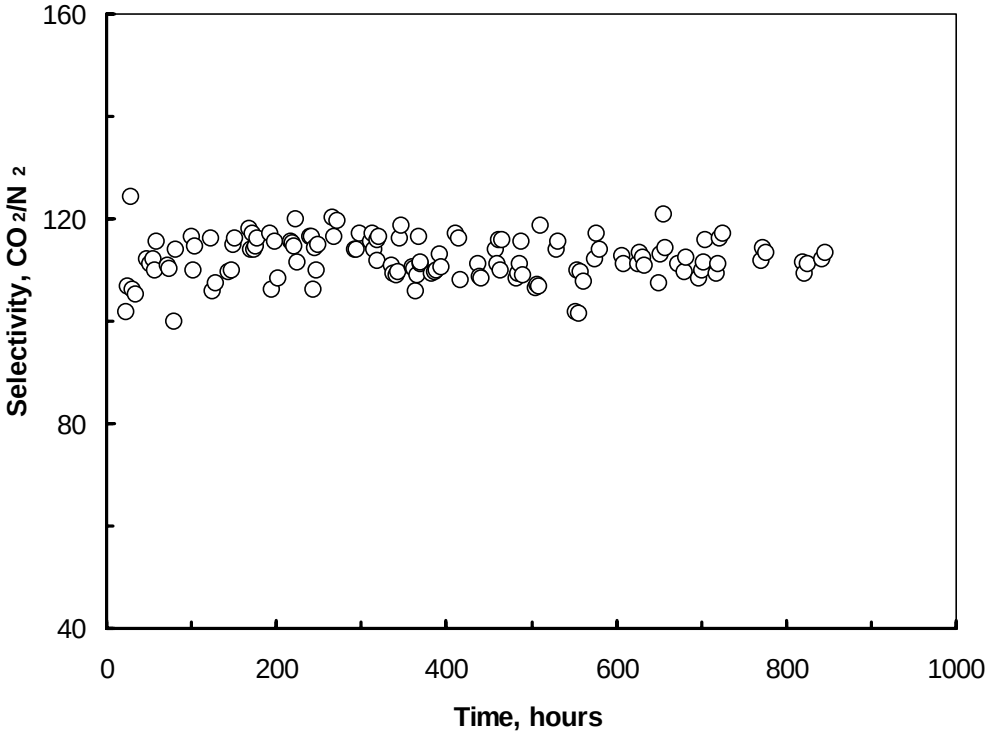

Figure 6.24. Selectivity of carbon dioxide over nitrogen in the CO_2/N_2 mixtures at a feed pressure of 308 kPa (16% CO_2) as a function of time. Temperature: 296K

membrane operation for more than 800 hours. This was because drying-up of the membrane and carrier being push-out of the matrix by large pressure differential could be avoided by the humidification of the gas stream and the entrapment of the carrier into the PVA matrix.

In a separate experiment, humidification was discontinued after about 450 hours of continuous operation as shown in Fig. 6.25. This resulted in the significant depression of CO_2 permeance. However, just like the previous results, the permeance returned to its original values after 0.5 mL of deionized water was injected to the permeation unit. These

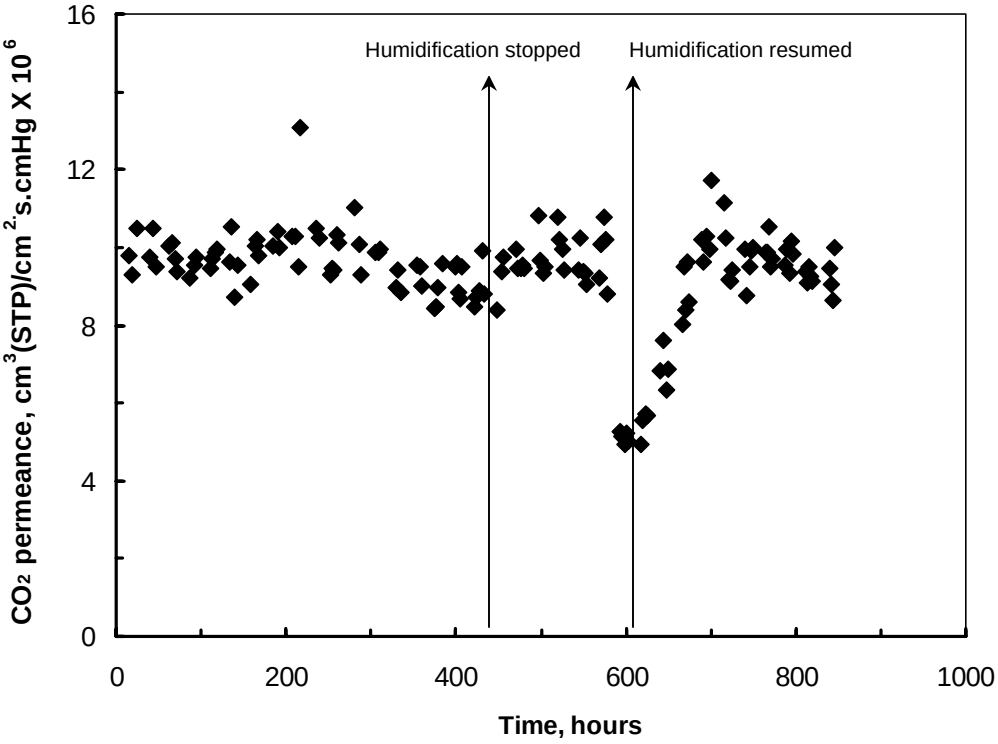

Figure 6.25 Effect of humidification on the CO_2 permeance through the PVA-DEA membrane as a function of time. The feed pressure is 308 kPa containing 16% CO_2. Temperature 296K

results clearly indicate that the reactive membrane could be regenerated and that the humidification of the gas prior to entering the permeation unit contributed substantially to the stability and effectiveness of the reactive membrane.

6.4 Summary

The PVA-DEA membrane demonstrates higher permeance for CO_2 relative to the PVA membrane in agreement with pure gas permeation experiments. The CO_2 permeance increased with increasing concentration of DEA but tend to decrease with further increased in concentration. Facilitation is more significant at lower CO_2 partial pressure differential across the membrane. However, at higher partial pressure differential, the reactive membrane may no longer serve as a facilitating medium, and the permeance values and selectivity are simply due to the solubility and diffusivity of the CO_2 and N_2 in the membrane matrix.

It was shown experimentally that the presence of DEA affects the transport properties in the membrane matrix. The selectivity of CO_2 over N_2 changes proportionally to DEA concentration resulting to greater facilitation at lower CO_2 partial pressure differentials whereas physical separation occurs at larger pressure differential. Selectivity of up to 500 was obtained.

The combined effect of increase in diffusivity and forward reaction rate constants with increase in temperature were favourable enough for higher CO_2 permeance and yielded higher selectivity at higher temperature.

The membrane shows long-term stability over a period of more than 800 hours. Also, humidification of the feed gas stream plays a vital role in the membrane stability. The

PVA-DEA membrane can also be regenerated by introducing water into the membrane unit.

CO_2 flux and permeance calculated based on the diffusion-reaction transport equations was also presented. The trends that were observed experimentally are in good agreement with the calculated results. It can be concluded that enhancement due to the presence of DEA was more at lower-pressure differential across the membrane whereas, at higher-pressure differential, saturation of the carrier was observed. Further discussion is presented in the Chapter 7.

Chapter 7

Conclusions, Contributions to Research and Recommendations

7.1 Overall Conclusions and Contributions to Research

Based on the results of this research, the following were recapped here:

1. In this research, a hydrophilic polymer, polysulfone was experimentally selected as the substrate for poly(vinyl) alcohol-amine mixture. The effects of rate constants and chemical equilibrium constants of the reaction of CO_2 with amines on the facilitated transport of CO_2 through the reactive membranes were studied using various amines (MEA, AMP, DEA, and MDEA). Among the amines tested, diethanolamine shows an excellent improvement in the permeance and selectivity of the membrane for CO_2 over N_2. The experimental results indicate that the presence of DEA in the PVA membrane attained higher permeance and better separation of CO_2 than the PVA membrane alone.

2. Experimental observations suggest that the addition of reactive carrier changes the transport properties in the membrane matrix. The CO_2 permeance increased with increasing DEA concentration but the changes was not proportional. The selectivity of CO_2 over N_2 changes proportionally to DEA concentration that results to greater facilitation at lower CO_2 partial pressure differential and the

physical separation occurs at higher-pressure differential where the effect of solution-diffusion mechanism is more pronounced. Significant facilitation were observed at concentration of 20-30wt% DEA.

3. CO_2 permeance as high as 8.63 x 10^{-5} cm^3 (STP)/cm^2.s.cmHg and selectivity of exceeding 500 were measured in the case of lower CO_2 partial pressure differential. At higher CO_2 partial pressure differential, the selectivity goes down to about 60. It can be concluded that PVA-DEA membrane would be appropriate for low-pressure power plant flue gases particularly as a secondary procedure in a set-up where the first process is the bulk removal of CO_2.

4. Analytical descriptions of the mass transport equations were performed. The zwitterions mechanism originally proposed by Caplow(1969) was applied to interpret the kinetics of CO_2-DEA reaction. Numerical integration of the governing equations was performed using MATLAB (Mathworks). A proposed explanation of the phenomenon observed experimentally were carried out with the aid of the profiles generated based on the numerical solution.

5. The PVA-DEA membrane shows a good long-term stability over a period of more than 800 hours. Likewise, it also exhibits thermal stability. The hydrophilic character of the PVA-DEA blend membrane and the retention of DEA by interaction with the PVA chain is probably the reason for such stability especially at elevated trans-membrane pressure differential.

6. This is one of the reactive membrane, which does not operate under a sweep-gas mode and can able to withstand trans-membrane pressure differentials of up to approximately 500 kPa. Because of the lack of stability under pressurized condition, most of the reactive membrane reported in the literature operates at a maximum pressure of about 102 kPa.

7. Lastly, it can be concluded that the reactive membrane is technically feasible for CO_2 separation from flue gases. Information based on the experimental observations that are important for optimizing the parameters (*e.g*. pressure differentials, composition and temperature) has been experimentally established thereby allowing the sensible design of a reactive membrane system.

7.2 Recommendations for Future Work

1. The incorporation of carrier, DEA, in the PVA solution shows to be an excellent material in preparing reactive membrane for the separation of CO_2 from N_2. The utilization of amines blends to maximize the good properties of amines, which brings about a significant enhancement in the absorption may permit better permeation rates and selectivity. AMP has similar loading capacity as MDEA but exhibits larger reaction rate constant for its reaction with CO_2. Mixture of primary or secondary amines with AMP incorporated into the PVA solution could be an attractive carrier for CO_2. Preliminary results are presented in the Appendix G.

2. The diffusion-reaction mass transport equations require kinetic parameters so that it can effectively simulate the transport of CO_2. There is a need to experimentally determine the kinetic properties of CO_2-DEA system.

3. For practical utilization of the reactive membrane developed in this study, it would be appropriate to:
    a) use hollow fibers as the substrate
    b) demonstrate the membrane stability to about 1-year
    c) expose the reactive membrane to a real-life streams containing various contaminants.

References

Alberty, R.A., Silbey, R.J., Physical Chemistry, 1st Ed, John Wiley and Sons, 159, 1992.

Al-Marzouqi, M.H., Hogendoorn, K.J.A., Versteeg, G.F., Analytical Solution for Facilitated Transport Across a Membrane, *Chem. Eng. Sci*. (2002), *57*, 4817-4829.

Astarita, G.; Savage, D.W.; Bisio, A., *Gas Treating with Chemical Solvents*, John Wiley and Sons, New York, 207, 1983.

Babcock, W.C., Baker, R.W., LaChapell, E.D., Smith, K.L. Coupled Transport Membranes II: The Mechanism of Uranium Transport with a Tertiary Amine, *J. Membr. Sci*.(1980), *7*, 71-87.

Barrer, R. M. and Chio, H.T., Solution and Diffusion of Gases and Vapours in Silicone Rubber Membranes, *J. Polym. Sci*. (1965), Part C, *10*, 111-138.

Basaran, O.A., Burban, P.M., Auvil, S.R., Facilitated Transport with Unequal Carrier and Complex Diffusivities, *Ind. Eng. Chem. Res*. (1989), *28*, 108-119.

Blanc, C, Demarais, G., The Reaction Rate of CO_2 with Diethanolamine, *Int. Chem. Eng.* (1984), 24, 43-52.

Blauwhoff, P.M.M., Versteeg, G.F., van Swaaij, W.P.M., A Study of the Reaction Between CO_2 and Alkanolamines in Aqueous Solutions, *Chem. Eng. Sci.* (1984), *39,* 207-225.

Bloch, R., Finkelstein, A., Kedem, O., Vofsi, D., Metal-Ion Separations by Dialysis through Solvent Membranes, *Ind. Eng. Chem. Proc. Des. Dev*. (1967), *6*, 231-237.

Bloch, R., Kedem, O., Vofsi, D., Ion Specific Polymer Membrane**,** *Nature* (1963), *199*, 802-803.

Bosch, H., Versteeg, G.F., van Swaaij, W.P.M., Gas-Liquid Transfer with Parallel Reversible Reactions III. Absorption of CO_2 into Solutions of Blends of Amines, *Chem, Eng. Sci.* (1989), *44*, 2745-2750.

Bosch, H., Versteeg, G.F., van Swaaij, W.P.M., Kinetics of the Reaction of CO_2 with Sterically Hindered Amine 2-amino-2-methylpropanol at 298K, *Chem, Eng. Sci.* (1990), *45*, 1167-1173.

Carvalho, L.B.; Araujo, A.M.; Almeda, A.M.P., Azevedo, W.M.,The Use of Polyvinyl Alcohol Glutaraldehyde Antigen Coated Discs for Laser Induced Fluorescence Detection of Plague, *Sensors and Actuators B* (1996), *36*, 427-430.

Choi, H.W. Kim, D.B., Choi, D.K., Ahn, B.S., Kim, H., Lee, C.H., Sung, J.Y., Highly Selective Facilitated Transport Membranes for Isoprene/n-pentane Separation, *J. Membr Sci*. (2006), *276.*

Coldrey, P.W., Harris, I.J., Kinetics of the Liquid Phase Reaction Between Carbon Dioxide and Diethanolamine, *Can. J. Chem. Eng.* (1976), *54*, 566.

Cussler, E.L., Membranes which Pump, *AIChE J*.(1971), *17*, 1300-1303**.**

Cussler, E.L., *Diffusion- Mass Transfer in Fluid System*, 2nd Ed. Cambridge University Press, New York, 460-465, 1997.

Dankwerts, P.V., The Reaction of CO_2 with Ethanolamines, *Chem, Eng. Sci.* (1979), *34,* 443-445.

Davis, R.A., Sandall, O.C., CO_2/CH4 Separation by Facilitated Transport in Amine-Polyethylene Glycol Mixtures, *AIChE J.* (1993), *39*, 1135-1145.

Donaldson, T.L., Nguyen, Y.N., Carbon Dioxide Kinetics and Transport in Aqueous Amine Membranes, *Ind. Eng. Chem. Fundam*. (1980), *19*, 260-266.

Donaldson, T.L., Quinn, J.A., Carbon Dioxide Transport through Enzymatically Active Synthetic Membranes**,** *Chem. Eng. Sci.* (1975), *1*, 103-115.

Enns, T., Facilitation by Carbonic Anhydrase of Carbon Dioxide, *Science* (1967), *155*, 44-47.

Figoli, A., Sager, W.F.C., Mulder, M.H.V., Facilitated Oxygen Transport in Liquid Membranes: Review and New Concepts, *J. Membr. Sci*. (2001), *181*, 97-110.

Finch, C.A., *Polyvinyl Alcohol*, John Wiley & Sons Ltd., 1, 1992.

Folkner, C.A., Noble, R.D., Transient Response of Facilitated Transport Membranes**,** *J. Membr. Sci*. (1983), *12*, 289-301.

Glasscock, D.A., Critchfield, J.E., Rochelle, R.T., CO_2 Absorption/Desorption in Mixtures of Methyldiethanolamine with Monoethanolamine or Diethanolamine, *Chem. Eng. Sci*. (1991), *46*, 2829-2845.

Goddard, J.D., Schultz, S.S., Bassest, R.J., On Membrane Diffusion with Near-equilibrium Reaction, *Chem. Eng. Sci*.(1970), *25*, 665-683.

Guha, A.K., Majumdar, S., Sirkar, K.K., Facilitated Transport of CO_2 through an Immobilized Liquid Membrane of Aqueous Diethanolamine, *Ind. Eng. Chem. Res*. (1990), *29*, 2093-2100.

Halmann, M.M., Steinberg, M., *Greenhouse Gas Carbon Dioxide Mitigation*, Lewis Publishers, New York, 1, 1999.

Hess, S., Staudt-Bickel, C. Lichtenthaler, R.N., Propene/propane Separation with Copolyimide Membranes Containing Silver Ions, *J. Membr. Sci*. (2006), *275*, 52-60.

Hikita, H., Asai, S., Ishikawa, H., Honda, M., The Kinetics of Reactions of Carbon Dioxide with MEA, DEA and TEA by Rapid Mixing Method, *Chem. Eng. J*. (1977), *13*, 7-12.

Hirayama, Y., Kase, Y., Nozomu T., Sumiyama, Y., Yoshihiro, Y., Haraya, K., Permeation Properties to CO_2 and N_2 of Poly(ethylene oxide)-Containing and Crosslinked Polymer Films, *J. Membr. Sci.* (1999), *160*, 87-99.

Hodge, R.M, Bastow, I.J.; Edward, G.H.; Simon, G.P., Free Volume and the Mechanism of Plasticization in Water-Swollen Poly(vinyl alcohol), *Macromolecules* (1996), *29*, 8137-8143.

Hughes, R.D., Steigelman, E.F., Mahoney, J.A., In: Proceedings of the Paper Presented at the 1981 *AIChE* Spring National Meeting, Houston, TX, April 1981.

Jain, R., Schultz, J.S., A Numerical Technique for Solving Carrier-mediated Transport Problems, *J. Membr. Sci.* (1982), 11, 79-106.

Kemena, L.L., Noble, R.D., Kemp, N.J., Optimal Regimes of Facilitated Transport, *J. Membr. Sci*. (1983), *15*, 259-274.

King, C.J., Chapter 15 in *Handbook of Separation Processes*, R. Rousseau, (Ed.), Wiley, New York, 1988.

Kohl, A.L., Nielsen, R.B., *Gas Purification* 5th Ed., Gulf Publishing Co., Houston, TX, 49 1997.

Koros, W.J., Fleming, G.K., Membrane-based Gas Separation, *J. Membr. Sci*. (1993), *83*, 1-80.

Koros, W.J., Hellums, M.W. in *Encyclopedia of Polymer Science and Technology*; Korschwitz, J.I.(Ed.), Wiley, New York, 1990, 714-802.

Kovvali, A.S., Sirkar, K.K., Carbon Dioxide Separation with Novel Solvents as Liquid Membranes, *Ind. Eng. Chem. Res*. (2002), *41*, 2287-2295.

Kulkarni, S.S., Funk, E. W., Li, N. N., Riley, R. L., Membrane Separation Processes for Acid Gases, *AIChE Symp. Ser*., (1983), 229, 172.

Kutchai, H.A.,Jacquez, J.A., Mather, F.J., Nonequilibrium-Facilitated Oxygen Transport in Hemoglobin Solution, *Biophys. J*.(1970), *10*, 38-53.

Laddha, S.S, Dankwerts, P.V., Reaction of CO_2 with Ethanolamines: Kinetics from Gas Absorption, *Chem Eng. Sci.* (1981), *36*, 479-482.

Li, N.N., Emulsion Membranes, U.S. Patent 340794 (1968).

Littel, R.J., Versteeg, G.F., van Swaaij, W.P.M., Kinetics of CO_2 with Primary and Secondary Amines in Aqueous Solutions, Influence of Temperature on Zwitterion Formation and Deprotonation Rates, *Chem, Eng. Sci.* (1992), *47,* 2037-2045.

Martien, F.L., In Encyclopedia of Polymer Science and Engineering, Wiley, New York, 1986, *17*, 167.

Matson, S.L., Herrink, C.S., Ward, W.J., Progress on Selective Removal of H_2S from Gasified Coal Using an Immobilized Liquid Membrane, *Ind. Eng. Chem. Proc. Des. Dev*.(1977), *16*, 370-378.

Matsuyama, H., Teramoto, M., Matsui, K., Kitamura, Y. *J.* Preparation of Poly(acrylic acid)/Poly(vinyl alcohol) Membrane for the Facilitated Transport of CO_2, *J. Appl. Polym. Sci*. (2001), *81*, 936-942.

Matsuyama, H., Teramoto, M., Sakakura, H., Selective Permeation of CO_2 through Poly{2-(N,N-dimethyl) aminoethyl methacrylate} Membrane Prepared by Plasma-graft Polymerization Technique, *J. Membr. Sci*. (1996), *114*, 193-200.

Mathworks Inc. (MATLAB 7.1).

Meldon, J.H., Stroeve, P., Gregoire, C., Facilitated Transport of Carbon Dioxide: A Review,*Chem. Eng. Commun*. (1982), *16*, 263-300.

Merkel, T.C., Bondar, V.I., Freeman, B.D., Pinnau, I. Gas Sorption, Diffusion and Permeation in Poly(dimethylsiloxane), *J. Polym. Sci.* Part B. Polymer Physics (2000), *38*, 415-434.

Miyauchi, T., Liquid-Liquid Extraction Process of Metals, U.S. Patent 4051230 (1970).

Moody, G.J., Thomas, J.D.R., *Ion-selective Electrode Methodology*, A.K. Covington (Ed), CRC Press, Florida, 1979.

Morales, M.A., Perez-Cisneros, E.S., Ochoa, J.A., Approximate meyhod for the Solution of Facilitated Transport Problems in Liquid Membranes, *Ind. Eng. Chem. Res*. (2002), *41*, 4626-4631.

Mulder, M.H.V., *Basic Principles of Membrane Technology*, Kluwer Academic Publisher, Dordrecht, Netherlands, 222-223, 1996.

Newman, J.S., *Electrochemical Systems*, Prentice Hall, N.J., 1991.

Oda, S.; Tanaka, J.I.; Ohta, H., Interface Bioreactor Packed with Synthetic Polymer Pad: Application to Hydrolysis of neat 2-ethylhexyl acetate, *J. Ferment. Bioeng*. (1998), *86*, 84-89.

Olander, D.R., Simultaneous Mass transfer and Equilibrium Chemical Reaction. *AIChE J*. (1960), *6,* 233-239.

Osterhout, W.J.V., *Proc. Nat. Acad. Sci*. (1935), *21*, 125.

Park, Y., Lee, K. J., Preparation of Water-Swollen Hydrogel Membranes for Gas Separation, *J. Appl. Polym. Sci*. (2001), *80*, 1785- 1791.

Poling, B.E., Prausnitz, J.M., O'Connel, J.P., *The Properties of Gases and Liquids*, 5th Ed., McGraw-Hill, New York, 11.21-11.22, 2000.

Porter, M.C., *Handbook of Industrial Membrane Technology*, Noyes Data Publications, New Jersey, 513-515, 1990.

Sada, E., Kumazawa, H., Butt, M.A., Solubility and Diffusivity of Gases in Aqueous Solutions of Amines, *J. Chem. Eng. Data* (1978), *23*, 161-163.

Schultz, S.S, Goddard, J.D., Suchedo, S.R., Facilitated Transport via Carrier-mediated Diffusion in Membranes: Part I. Mechanistic Aspects, Experimental Systems and Characteristic Regimes, *AIChE J*. (1974), *20*, 417-445.

Smith, D.R., Quinn. J.A., The Prediction of Facilitation Factors for Reaction Augmented Membrane Transport, *AIChE J.* (1979), *25*, 197-199.

Snijder, E.D., Versteeg, G.F., van Swaaij, W.P.M., Diffusion Coefficients of Several Aqueous Alkanolamine Solutions, *J. Chem. Eng. Data* (1993), *38*, 475-480.

Solner, K., Shean, G.M., Liquid Ion-Exchange Membranes of Extreme Selectivity and High Permeability for Anions, *J. Am. Chem. Soc*. (1964), *86*, 1901-1902.

Steigelman, E.F., Hughes, R.D., Process for Separation of Unsaturated Hydrocarbons, US Patent 3,758,603 (1973).

Stern, S.J., Polymers for Gas Separation: The Next Decade, *J. Membr. Sci*. (1994), *94*, 1-65.

Stern, S.J., Shah, V.M., Hardy, B.J., Structure-Permeability Relationships in Silicone Polymers, *J. Polym. Sci*, Part B (1987), *25*, 1263-1298.

Tamimi, A., Rinker, E.B., Sandal, O.C., Diffusivity of nitrous Oxide in Aqueous Solutions of N-methyldiethanolamine and Diethanolamine from 293 to 368K, *J. Chem. Eng. Data* (1994), *39*, 396-398.

Teramoto, M., Approximate Solution of Facilitation Factors in Facilitated Transport, *Ind. Eng. Chem. Res*. (1995), *34*, 1267-1272.

Teramoto, M., Huang, Q., Watari, T., Tokunaga, Y., Nakatani, R., Maeda, T., Matsuyama, H., Facilitated Transport of CO2 through Supported Liquid membranes of Various Amine Solutions- Effects of Rate and Equilibrium Reaction Between CO_2 and Amine, *J. Chem Eng. Japan* (1997), *30*, 328-335.

Terramoto, M., Ohnishi, N., Takeuchi, N., Kitada, S., Matsuyama, H., Matsumiya, N., Mano, H., Separation and Enrichment of Carbon Dioxide by Capillary Membrane with permeation of Carrier Solution, *Sep. Pur. Tech*. (2003), *30*, 215-227.

Versteeg, G.F. van Swaaij, W.P.M., On the Kinetics Between CO_2 and Alkanolamines both in Aqueous and Non-aqueous Solutions, *Chem, Eng. Sci.* (1988), *43*, 573-585.

Versteeg, G.F., Kuipers, J.A.M., van Beckum, F.P.H., van Swaaij, W.P.M., Mass Transfer with Complex Reversible Reactions-1. Parallel Reversible Chemical Reactions, *Chem, Eng. Sci.* (1990), *45*, 183-197.

Versteeg, G.F., Oyevaar, M.H., The Reaction of CO_2 and Diethanolamine at 298K, *Chem, Eng. Sci.* (1989), *44*, 1264-1268.

Versteeg, G.F., van Swaaij, W.P.M., Solubility and Diffusivity of Acid Gases (CO_2, N_2O) in Aqueous Alkanolamine Solutions, *J. Chem. Eng. Data* (1988), *33*, 29-34.

Ward, W. J., Robb, J.C., Carbon Dioxide-Oxygen Separations: Facilitated Transport of Carbon Dioxide Across a Liquid Film, *Science*, (1967), *156*, 1481-1484.

Ward, W. J., Analytical and Experimental Studies of Facilitated Transport, *AIChE J*. (1970), *16*, 405-410.

Ward, W.J., Robb, W.L., Carbon Dioxide-Oxygen Separation: Facilitated Transport of CO_2 Across a Liquid Film, Science (1967), *156*, 1481.

Way, J. D., Noble R. D., Facilitated Transport in *Membrane Handbook*. W.S.W. Ho and K.K. Sirkar (Eds), Van Nostrand Reinhold, N.Y., 40, 1992.

Wijmans, J.G., Baker, R.W., The Solution-Diffusion Model, *J. Membr. Sci*. (1995), *107*, 1-21.

Xu, S., Wang, Y.M., Otto, F.D., Mather, A.E., Kinetics of the Reaction of Carbon Dioxide with 2-amino-2-methyl-1-propanol Solutions, *Chem. Eng. Sci*. (1996), *51*, 841-850.

Notation

A	effective membrane area, cm^2
C	concentration, mol/cm^3
$\overline{C}$	dimensionless concentration
D	diffusion coefficient, cm^2/s
E	activation energy, kJ/mol
F	facilitation factor
H	Henry's constant, $mol/cm^3.cmHg$
J	permeance, $cm^3(STP)/cm^2.s.cmHg$
K	equilibrium constant, cm^3/mol
K_2, K_3	zwitterions formation and deprotonation rate constants
k_1, k_2, k_3, k_4	reaction rate constants, $cm^3/mol.s$ or $1/s$
k_f	forward reaction rate constant, $cm^3/mol.s$
k_r	reverse reaction rate constant, $1/s$
L	membrane thickness, microns
m_1	dimensionless reaction arte constant
m_2	dimensionless reaction equilibrium constant
m_3	dimensionless Damkohler number
m_4	mobility ratio
M_i	molecular weight of species i, gram/mol
N	flux, $cm^3(STP)/cm^2.s$
P	permeability coefficient, $cm^3(STP).cm/cm^2.s.cmHg$

p	partial pressure on the feed stream, cmHg
Q	heat of reaction, J/mol
r_i	reaction rate of species *i*
$\bar{r}$	dimensionless reaction expression
$\boldsymbol{R}$	functional group on the amine
R	gas constant, J/mol.K
S	heat of solution, kJ/mol
T	temperature, K
t	time, s
V_i	molar volume of species *i*, cm^3/mol
x_i	mol fraction of component *i* in the feed stream
y_i	mol fraction of component *i* in the permeate stream
z	coordinate in the direction of transport
$\bar{z}$	dimensionless length
Z	ionic valence
Z^*	zwitterions intermediate

Greek symbol

α	separation factor
μ_j	mobility of the ion *j*, m^2.mol./J.s
Π	Faraday's constant, *C*.mol^{-1}
ϕ	electrical potential ,volts

δ	permittivity for water, C^2./J.m
λ	Debye length, microns
ω	dimensionless association factor
η	viscosity, centipoise

Subscripts

A	CO_2
B	DEA
C	carbamates, $R_2NCO_2^-$
d	diffusion
D	protonated amines, $R_2NH_2^+$
eq	equilibrium condition
j	ionic species
p	permeation
T	total amine concentration

Superscripts

0	at the feed stream, z = 0
a	water as solvent
L	at the permeate stream, z = L
T	total flux

Abbreviations

AMP	2-amino-2-methylpropanol
CO_2	carbon dioxide
CO_3^{2-}	carbonate ion
DEA	diethanolamine
FTM	facilitated transport membrane
H_2S	hydrogen sulfide
HCO_3^-	bicarbonate ion
ILM	immobilized liquid membrane
MDEA	N-methyldiethanolamine
NO	nitrogen monoxide
N_2O	dinitrogen oxide
OH^-	hydroxyl ion
PSF	polysulfone
PVA	poly(vinyl alcohol)
PVC	poly(vinyl chloride)
PVDF	poly(vinylidene flouride)
R_1R_2NH	secondary amine
$R_1R_2NH_2^+$	protonated amine
$R_1R_2NCO_2^-$	alkyl carbamate
$R_1R_2NH^+CO_2^-$	zwitterion intermediate

Appendix A - Sample Calculations

A.1 Experimental Errors

Membrane: DEA membrane

Operating temperature: 296K

Feed pressure: 30 psig (308 kPa absolute)

Feed concentration of CO_2: 16%mol

Permeate pressure: 101 kPa

The permeances of CO_2 is provided below:

Gas	Permeances, $cm^3(STP)/cm^2.s.cmHg \times 10^5$				
CO_2	0.91	1.07	0.92	0.93	0.95

The average measurement is:

$$\overline{A} = \frac{0.91 + 1.07 + 0.92 + 0.93 + 0.95}{5} = 0.96$$

The standard deviation is:

$$SD = \sqrt{\frac{(0.91-0.96)^2 + (1.07-0.96)^2 + (0.92-0.96)^2 + (0.93-0.96)^2 + (0.95-096)^2}{(5-1)}}$$

$$= 0.06$$

Frequently, we report the standard deviation of *n*- measurements as the estimated uncertainty. For five measurements, we would report a permeance of 0.91 ± 0.06 cm^3(STP)/cm^2.s.cmHg x 10^5.

A.2 Sample Calculations for Pure Gas Permeation

Gas Permeance

The permeance of pure gasses were calculated from the following data:

Membrane: DEA membrane (reactive membrane)

Gas: Carbon dioxide

Operating temperature: 296K

Feed pressure: 25.2 psig (275 kPa absolute)

Membrane area: 13.85 cm^2

Downstream pressure: 76 cm Hg (101.4 kPa absolute)

Permeate flow rate: 0.01408 ml/s

The permeate flow rate can be corrected to standard temperature and pressure (STP):

From the ideal gas laws: $\frac{p_1 V_1}{T_1} = \frac{p_2 V_2}{T_2}$,

$$V_2 = V_{STP} = V_1 \left(\frac{p_1}{p_2} \right) \left(\frac{T_2}{T_1} \right), \text{ since } p_1 = p_2 = 76 \text{ cmHg}$$

$$V_{STP} = V_{296\,K} \times \frac{T_{273K}}{T_{296\,K}}$$

The CO_2 flux ($\boldsymbol{N}$) is then calculated as:

$$N = \frac{V_{STP}}{Membrane\ area}$$

$$N = \frac{(0.01408\ cm^3)\ (273K)}{(s)\ (13.85\ cm^2)}$$

$$= 9.31 \times 10^{-4}\, cm^3 (STP) / cm^2 \cdot s$$

The permeance (***J***) for CO_2 can be calculated as follows:

$$J = \frac{N}{\Delta P}$$

$$J = \frac{9.31 \times 10^{-4}\, cm^3 (STP) / cm^2 \cdot s}{130\ cmHg}$$

$$= 7.16 \times 10^{-6}\, cm^3 (STP) / cm^2 \cdot s \cdot cmHg$$

For the nitrogen, the calculated permeance at the same conditions is 8.09 x 10^{-6} cm^3(STP)/cm^2.s.cmHg.

Selectivity

The pure gas selectivity of carbon dioxide over nitrogen can be calculated as the ratio of carbon dioxide permeance to nitrogen permeance.

$$Selectivity = \frac{J_{CO_2}}{J_{N_2}}$$

A.3 Temperature Dependency on Permeance

As mentioned in Chapter 5 (section 5.3.7), the temperature dependence of permeance can be expressed by Arrhenius law expression:

$$J = J_O \, exp\left(\frac{-E_a}{RT}\right) \qquad \text{(A3.1)}$$

where Jo is the pre-exponential factor and Ea is the activation energy of permeation.

Equation (A3.1) can be rewritten as:

$$ln(J) = \frac{-E_a}{R} \cdot \frac{1}{T} + ln(J_O) \qquad \text{(A3.2)}$$

Using the permeation of carbon dioxide through the DEA membrane at an absolute feed pressure of 172 kPa:

Temperature, ^{0}C	1000/T, K^{-1}	Permeance $cm^3(STP)/cm^2.s.cm\ Hg \times 10^5$
30	3.30	1.16
40	3.19	1.58
50	3.10	1.64
60	3.00	1.99

The exponential regression of the plot of ***ln (J)*** against ***1000/T*** result to:

$E_a/R = 1.6804 \times 10^3$

$E_a = (1.6804 \times 10^3)(R)$

$= (1.6804 \times 10^3)(8.314)$

$= 13970.85\ J/mol$

$= 13.97\ kJ/mol$

A.4 Sample Calculations for Gas Mixture Permeation

Gas Permeance

The permeances of gas mixtures were obtained from the calculation detailed below:

Membrane: DEA membrane (reactive membrane)

Gas Mixture: Carbon dioxide/Nitrogen

Operating temperature: 296K

Total feed pressure: 31.8 psig (321 kPa absolute)

Feed concentration of carbon dioxide: 15.6164 mol%

Permeate concentration of carbon dioxide: 47.5856 mol%

Permeate pressure: 101.3 kPa

Permeate flow rate: 4.04×10^{-4} cm^3/s

The partial flux of CO_2 ($\boldsymbol{N_{CO2}}$) in the permeate is:

$$N_{CO_2} = \frac{273K}{T} \times \frac{V}{t} \times \frac{1}{A} \times y_{CO_2}$$

$$= \frac{273K}{296K} \times 4.04 \times 10^{-4} \frac{mL}{s} \times \frac{1}{13.85\ cm^2} \times 0.475856$$

$$= 1.28 \times 10^{-5}\, cm^3 (STP) / cm^2 .s$$

The partial flux of N_2 ($\boldsymbol{N_{N2}}$) in the permeate is:

$$N_{N_2} = \frac{273K}{296K} \times 4.04 \times 10^{-4} \frac{mL}{s} \times \frac{1}{13.85} \times (1 - 0.475856)$$

$$= 1.41 \times 10^{-5}\, cm^3 (STP) / cm^2 .s$$

The permeance of CO_2 ($\boldsymbol{J_{CO2}}$) can be calculated as the partial flux of CO2 normalized to its partial pressure difference:

$$J_i = \frac{N_i}{\Delta P_i} = \frac{N_i}{(p_2 x_i - p_1 y_i)}$$

$$J_{CO_2} = \frac{1.28 \times 10^{-5}\, cm^3 (STP) / cm^2 \cdot s}{[(31.8 + 14.7)(0.156164) - (14.7)(0.475856)]\, psia} \times \frac{14.7\ psia}{76\ cmHg}$$

$$= 9.29 \times 10^{-6}\, cm^3 (STP) / cm^2 \cdot s \cdot cmHg$$

The permeance of nitrogen ($\boldsymbol{J_{N2}}$) in the mixture is:

$$J_{N_2} = \frac{1.41 \times 10^{-5}\, cm^3 (STP) / cm^2 \cdot s}{[(31.8 + 14.7)(0.843836) - (14.7)(0.524144)]\, psia} \times \frac{14.7\ psia}{76\ cmHg}$$

$$= 8.65 \times 10^{-8}\, cm^3 (STP) / cm^2 \cdot s \cdot cmHg$$

Selectivity

The selectivity for carbon dioxide over nitrogen in the mixture can be calculated as the ratio of carbon dioxide permeance to nitrogen permeance.

$$Selectivity = \frac{J_{CO_2}}{J_{N_2}}$$

$$= \frac{9.29 \times 10^{-6}}{8.65 \times 10^{-8}}$$

$$= 107$$

Appendix B - Gas Chromatograph (GC) Analysis

GC Analysis Method for CO_2/N_2 Gas Mixtures

GC Instrument: Agilent 6890 N, Agilent Tecnologies.

GC Settings:

1. Oven

   Temperature: 35^0C (5 min) to 220^0C (3 min) at 20^0C/min

2. Column

   Type: Packed column (Carboxen-1000, a spherical carbon molecular sieves)

   Length: 4.5 meter

   Diameter: 1/8 inch (2.1 mm ID)

   Carrier gas: Helium at 30 ml/min

3. Detector

   Type: Thermal conductivity detector (TCD)

   Filament temperature: 265^0C

   Make-up gas (helium): 3 ml/min

   Reference gas (helium): 20 ml/min

Sample of GC plot for CO_2/N_2 analysis is shown as follows:

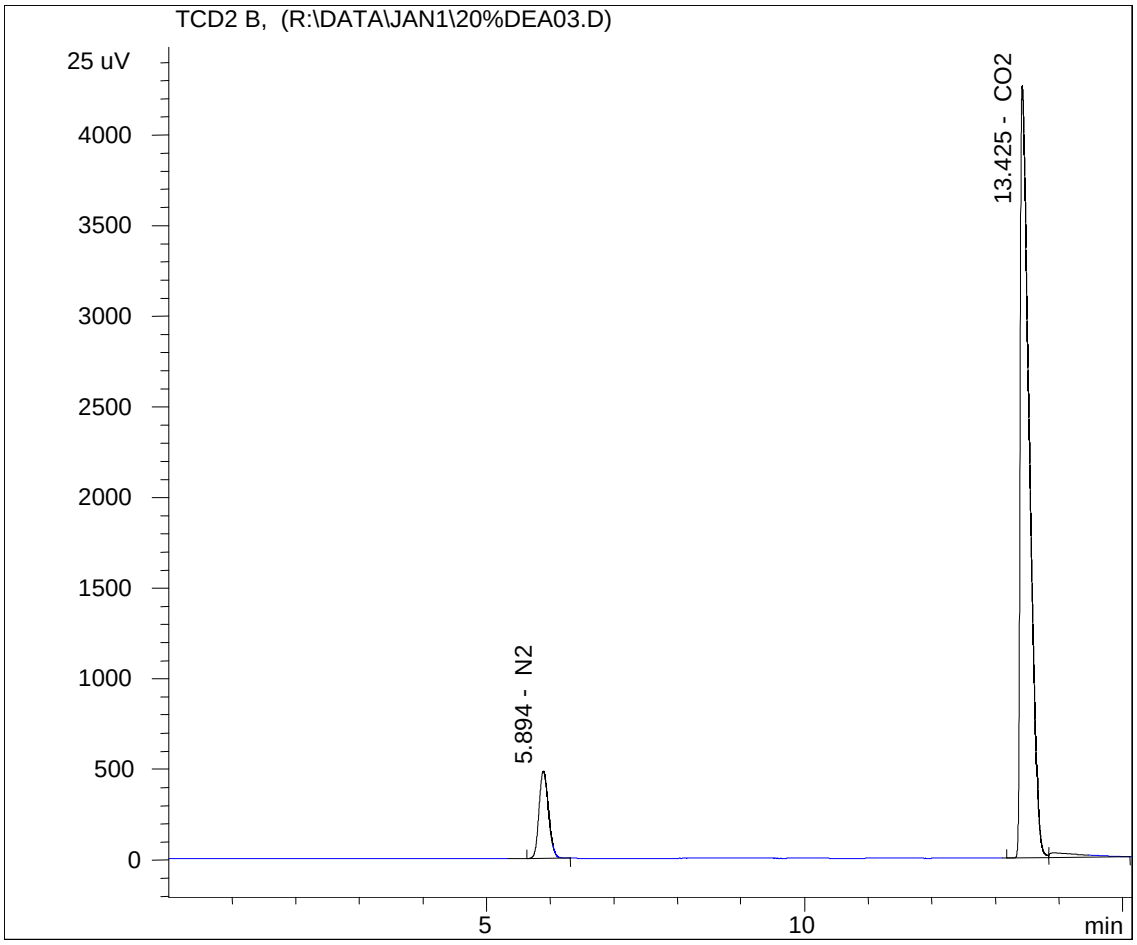

Appendix C - Derivations of the Dimensionless Parameters

The governing rate equations and boundary conditions are cast into dimensionless forms using the membrane thickness L as the characteristic length while the feed CO_2 concentration C_A^0 and total amine concentration C_T as the characteristic concentration. The dimensionless concentrations and length are defined as follow:

$$\overline{C}_A = \frac{C_A}{C_A^0} \tag{C.1}$$

$$\overline{C}_B = \frac{C_B}{C_T} \tag{C.2}$$

$$\overline{z} = \frac{z}{L} \tag{C.3}$$

The non-dimensional governing equations are:

$$\overline{r}_A = \frac{d^2\overline{C}_A}{d\overline{z}^2} \tag{C.4}$$

$$\overline{r}_B = \frac{d^2\overline{C}_B}{d\overline{z}^2} \tag{C.5}$$

where $\overline{r}_A$ and $\overline{r}_B$ is the dimensionless reaction rate expression for CO_2 and amine, respectively, Eq. (C.4) can be written in the form:

$$\overline{r}_A = \frac{d^2\overline{C}_A}{d\overline{z}^2} = \left(\frac{d}{d\overline{z}}\right)\left(\frac{d\overline{C}_A}{d\overline{z}}\right) = \left(\frac{d}{d\overline{z}}\right)\left(\frac{d\overline{C}_A}{dz}.\frac{dz}{d\overline{z}}\right) \tag{C.6}$$

from Eq. (C.1) and (C.3), $\frac{dz}{d\bar{z}} = L, \quad d\overline{C}_A = \frac{dC_A}{C_A^0}$, substituting these to Eq. (C.6) gives

$$\bar{r}_A = \frac{d}{d\bar{z}}\left(\frac{L}{C_A^0}\right)\left(\frac{dC_A}{dz}\right) \tag{C.7}$$

$$\bar{r}_A = \frac{L}{C_A^0}\left(\frac{d}{dz}\right)\left(\frac{dz}{d\bar{z}}\right)\left(\frac{dC_A}{dz}\right) = \left(\frac{L^2}{C_A^0}\right)\left(\frac{d^2C_A}{dz^2}\right) = \frac{L^2}{C_A^0}\left(\frac{r_A}{D_A}\right) \tag{C.8}$$

$$\text{but } r_A = \frac{C_A C_B - \frac{(C_T - C_B)^2}{4KC_B}}{\frac{k_2}{k_1 k_3 C_B} + \frac{1}{k_1}} \tag{C.9}$$

$$\bar{r}_A = \frac{L^2}{D_A C_A^0}\left\{\frac{C_A C_B - \frac{(C_T - C_B)^2}{4KC_B}}{\frac{k_2}{k_1 k_3 C_B} + \frac{1}{k_1}}\right\} = \frac{L^2}{D_A C_A^0}\left\{\frac{\frac{4KC_A C_B^2 - (C_T - C_B)^2}{4KC_B}}{\frac{k_3 C_B + k_2}{k_1 k_3 C_B}}\right\} \tag{C.10}$$

from Eq. (C.2), $C_T = \frac{C_B}{\overline{C}_B}$, thus;

$$\bar{r}_A = \frac{L^2}{D_A C_A^0}\left\{\frac{4KC_A C_B^2 - \left(\frac{C_B}{\overline{C}_B} - C_B\right)^2}{\frac{4K}{\frac{k_3 C_B + k_2}{k_1 k_3}}}\right\} = \frac{L^2}{D_A C_A^0}\left\{\frac{4KC_A C_B^2 - \frac{(C_B - C_B\overline{C}_B)^2}{\overline{C}_B^2}\left[\frac{1}{4K}\right]}{\frac{k_3 C_B + k_2}{k_1 k_3}}\right\} \tag{C.11}$$

$$\bar{r}_A = \frac{L^2}{D_A C_A^0}\left\{\frac{\frac{4KC_A C_B^2 \overline{C}_B^2 - C_B^2(1-\overline{C}_B)^2}{4K\overline{C}_B^2}}{\frac{k_3 C_B + k_2}{k_1 k_3}}\right\} = \frac{L^2}{D_A C_A^0}\left\{\frac{\frac{C_B^2\left[4KC_A\overline{C}_B^2 - (1-\overline{C}_B)^2\right]}{4K\overline{C}_B^2}}{\frac{k_3 C_B + k_2}{k_1 k_3}}\right\} \tag{C.12}$$

Substituting $C_A = \overline{C}_A C_A^0$ and $C_B = \overline{C}_B C_T$ in Eq.(C.12) gives:

$$\bar{r}_A = \frac{L^2}{D_A C_A^0}\left\{\frac{\dfrac{\overline{C}_B^2 C_T^2\left[4KC_A^0\overline{C}_A\overline{C}_B^2 - \left(1-\overline{C}_B\right)^2\right]}{4K\overline{C}_B^2}}{\dfrac{k_3\overline{C}_B C_T + k_2}{k_1 k_3}}\right\} = \frac{L^2}{D_A C_A^0}\left\{\frac{\dfrac{C_T^2\left[4KC_A^0\overline{C}_A\overline{C}_B^2 - \left(1-\overline{C}_B\right)^2\right]}{4K}}{\dfrac{k_3 C_T\left[\overline{C}_B + \left(\dfrac{k_2}{k_3 C_T}\right)\right]}{k_1 k_3}}\right\} \quad \text{(C.13)}$$

If we let $m_1 = \dfrac{k_2}{k_3 C_T}$ and $m_2 = KC_A^0$, a dimensionless reaction rate and equilibrium constant respectively,

$$\bar{r}_A = \frac{L^2}{D_A C_A^0}\left\{\frac{\dfrac{C_T\left[4KC_A^0\overline{C}_A\overline{C}_B^2 - \left(1-\overline{C}_B\right)^2\right]}{4K}\left(\dfrac{C_A^0}{C_A^0}\right)}{\dfrac{\overline{C}_B + m_1}{k_1}}\right\} = \frac{L^2}{D_A C_A^0}\left\{\frac{\dfrac{C_T C_A^0\left[4KC_A^0\overline{C}_A\overline{C}_B^2 - \left(1-\overline{C}_B\right)^2\right]}{4KC_A^0}}{\dfrac{\overline{C}_B + m_1}{k_1}}\right\} \quad \text{(C.14)}$$

$$\bar{r}_A = \frac{L^2}{D_A C_A^0}\left\{\frac{\dfrac{C_T C_A^0\left[4m_2\overline{C}_A\overline{C}_B^2 - \left(1-\overline{C}_B\right)^2\right]}{4m_2}}{\dfrac{\overline{C}_B + m_1}{k_1}}\right\} = \frac{L^2}{D_A C_A^0}\left\{\frac{k_1 C_T C_A^0\left[4m_2\overline{C}_A\overline{C}_B^2 - \left(1-\overline{C}_B\right)^2\right]}{4m_2\left(\overline{C}_B + m_1\right)}\right\} \quad \text{(C.15)}$$

$$\bar{r}_A = \frac{k_1 C_T L^2}{D_A}\left\{\frac{4m_2\overline{C}_A\overline{C}_B^2 - \left(1-\overline{C}_B\right)^2}{4m_2\left(\overline{C}_B + m_1\right)}\right\} \quad \text{(C.16)}$$

Furthermore, $m_3 = \frac{k_1 C_T L^2}{D_A}$, a dimensionless number which resembles Damkohler number,

$$\bar{r}_A = m_3 \left\{ \frac{4m_2 \bar{C}_A \bar{C}_B^2 - \left(1 - \bar{C}_B\right)^2}{4m_2\left(\bar{C}_B + m_1\right)} \right\} = \frac{m_3}{m_2} \left\{ \frac{m_2 \bar{C}_A \bar{C}_B^2 - \frac{1}{4}\left(1 - \bar{C}_B\right)^2}{\bar{C}_B + m_1} \right\} \qquad \text{(C.17)}$$

For $\bar{r}_B$,

$$\bar{r}_B = \frac{d^2 \bar{C}_B}{d\bar{z}^2}, \qquad r_B = D_B \frac{d^2 C_B}{dz^2} \qquad \text{(C.18)}$$

$$\bar{r}_B = \frac{L^2}{C_T}\left(\frac{d^2 C_B}{dz^2}\right) = \frac{L^2}{C_T}\left(\frac{r_B}{D_B}\right) \quad \text{but } r_B = 2r_A \qquad \text{(C.19)}$$

$$\bar{r}_B = \frac{L^2}{C_T}\left(\frac{2r_A}{D_B}\right), \qquad r_A = \frac{\bar{r}_A D_A C_A^0}{L^2} \qquad \text{(C.20)}$$

$$\bar{r}_B = \frac{L^2}{C_T}\left[\frac{2\left(\frac{\bar{r}_A D_A C_A^0}{L^2}\right)}{D_B}\right] = \frac{2\bar{r}_A D_A C_A^0}{D_B C_T} \qquad \text{(C.21)}$$

If we let $m_4 = \frac{D_B C_T}{D_A C_A^0}$, another dimensionless parameter, eq. (C.21) becomes:

$$\bar{r}_B = \frac{2}{m_4}\bar{r}_A \qquad \text{(C.22)}$$

The dimensionless group of parameters that were derived here are:

a) $m_1 = \frac{k_2}{k_3 C_T}$, dimensionless reaction rate constant

b) $m_2 = KC_A^0$, dimensionless reaction equilibrium constant

c) $m_3 = \frac{k_1 C_T L^2}{D_A}$, resembles a Damkohler number that measures diffusion time to reaction time.

d) $m_4 = \frac{D_B C_T}{D_A C_A^0}$, mobility ratio

Appendix D - Calibration of Mass Flow Controllers

Mass flow controllers: Model UFC 1200A, Unit Instruments Inc.

Calibration is performed with the used of an electronic flow meter.

Inlet pressure: 110 psig (860 kPa absolute)

Outlet pressure: 110 kPa absolute

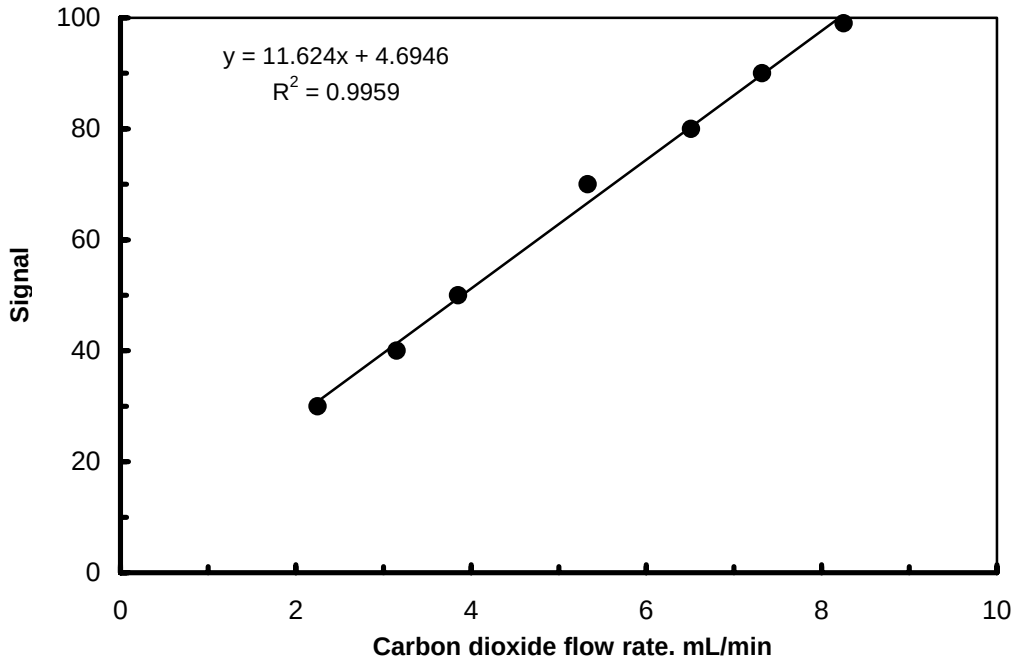

Figure D.1 Calibration plot for carbon dioxide.

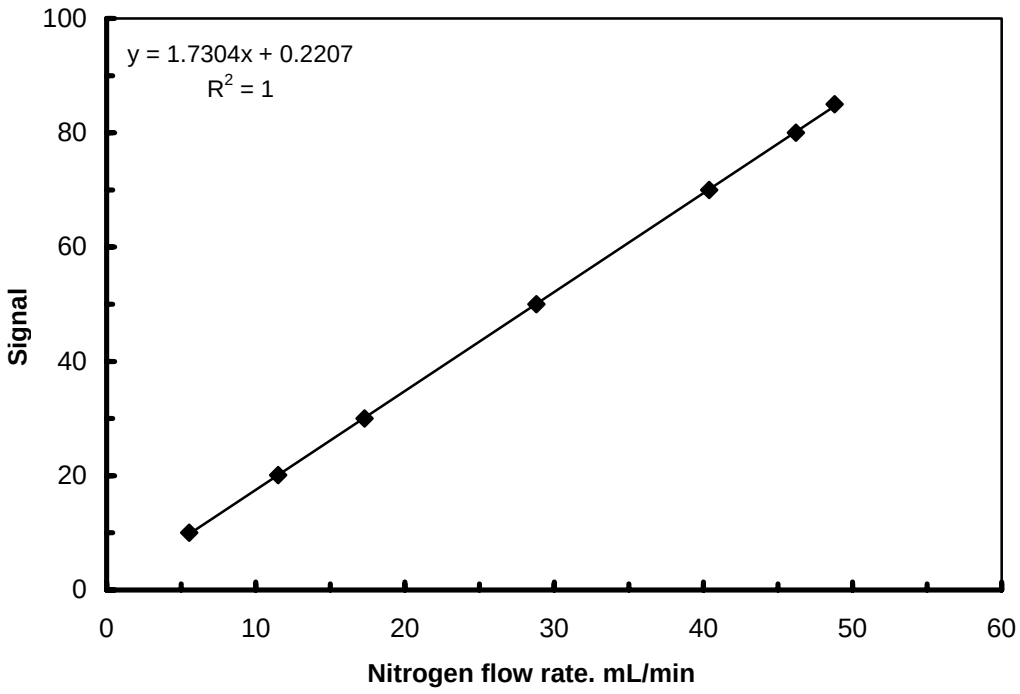

Figure D.2 Calibration plot for nitrogen.

Appendix E – Permeation for Gas Mixture

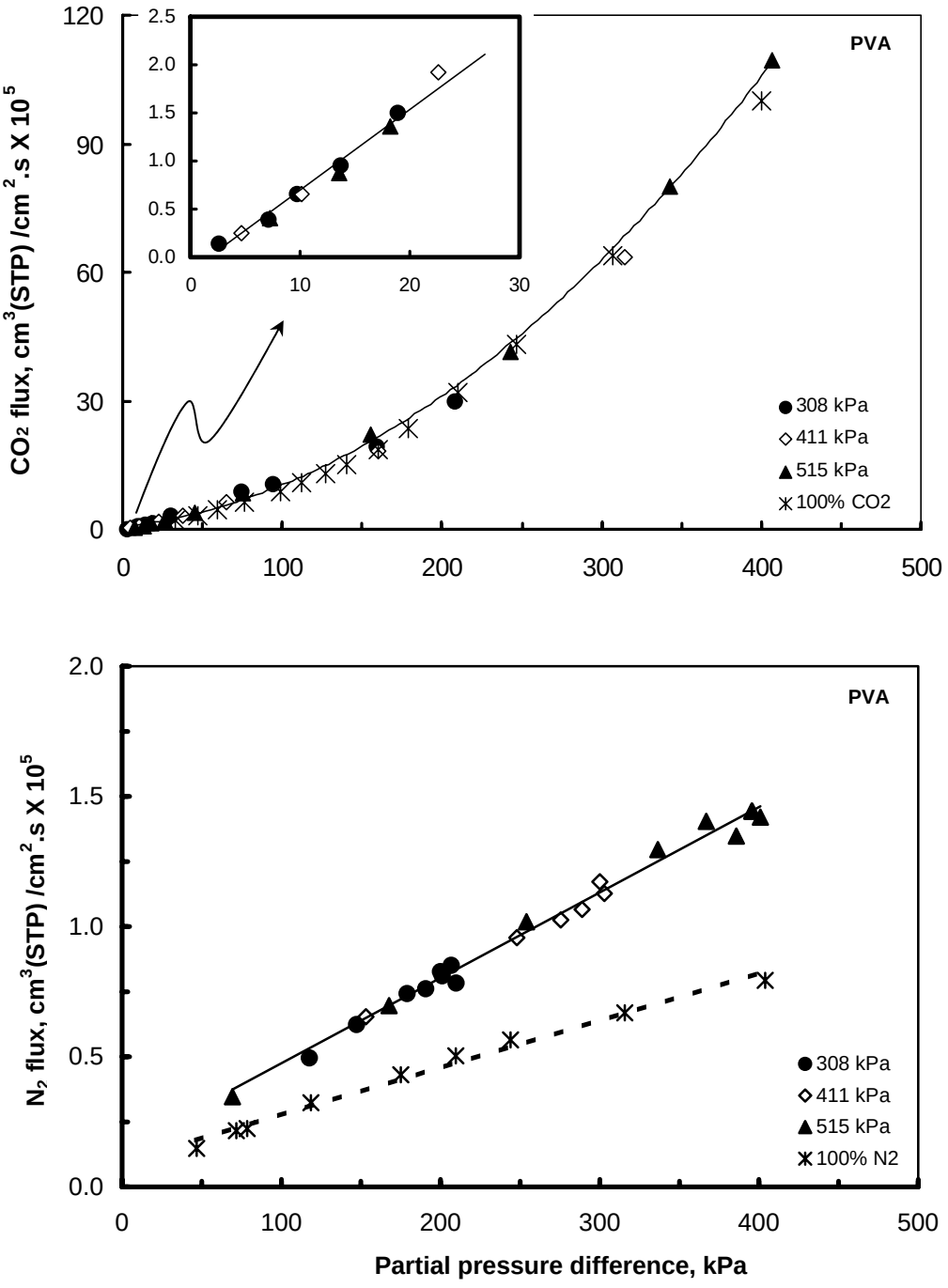

Figure E.1 Fluxes of carbon dioxide and nitrogen in the CO_2/N_2 mixture (5 to 100% CO_2) for the PVA membrane as a function of their partial pressure differences. Temperature: 296K

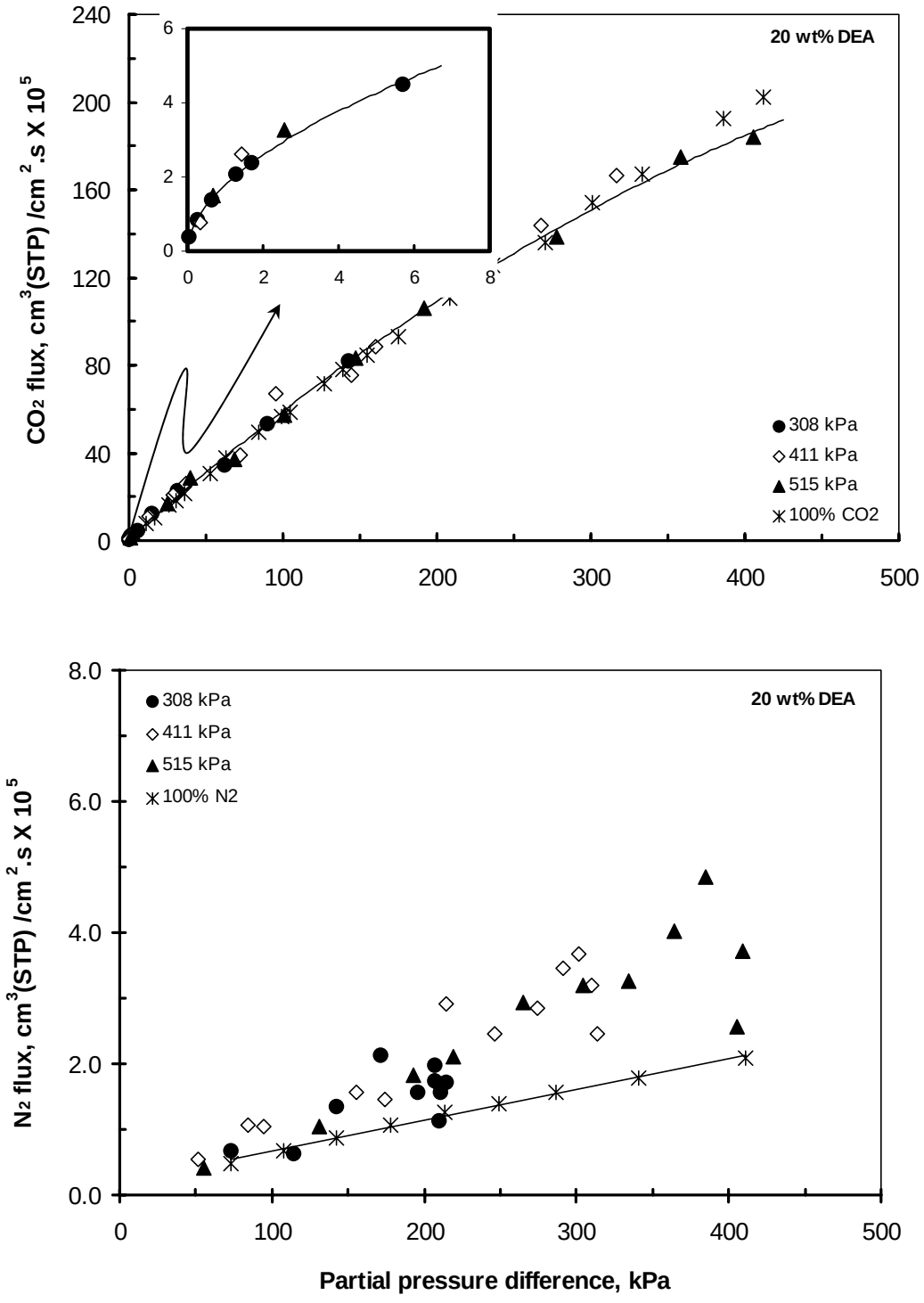

Figure E.2 Fluxes of carbon dioxide and nitrogen in the CO_2/N_2 mixture (5 to 100% CO_2) for the DEA membrane as a function of their partial pressure differences. Temperature: 296K

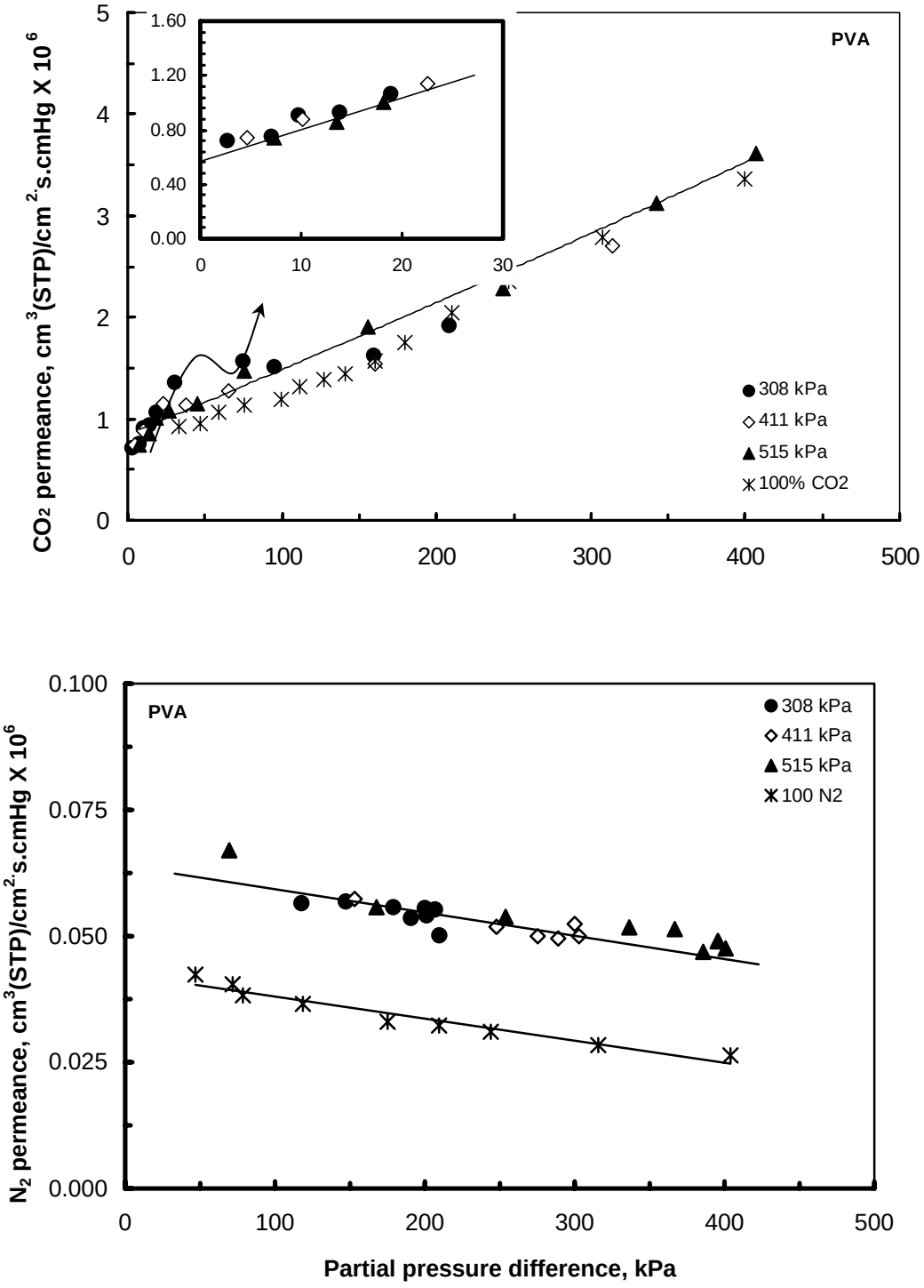

Figure E.3 Permeance of carbon dioxide and nitrogen in the CO_2/N_2 mixture (5 to 100% CO_2) for the PVA membrane as a function of their partial pressure differences.

Temperature: 296K

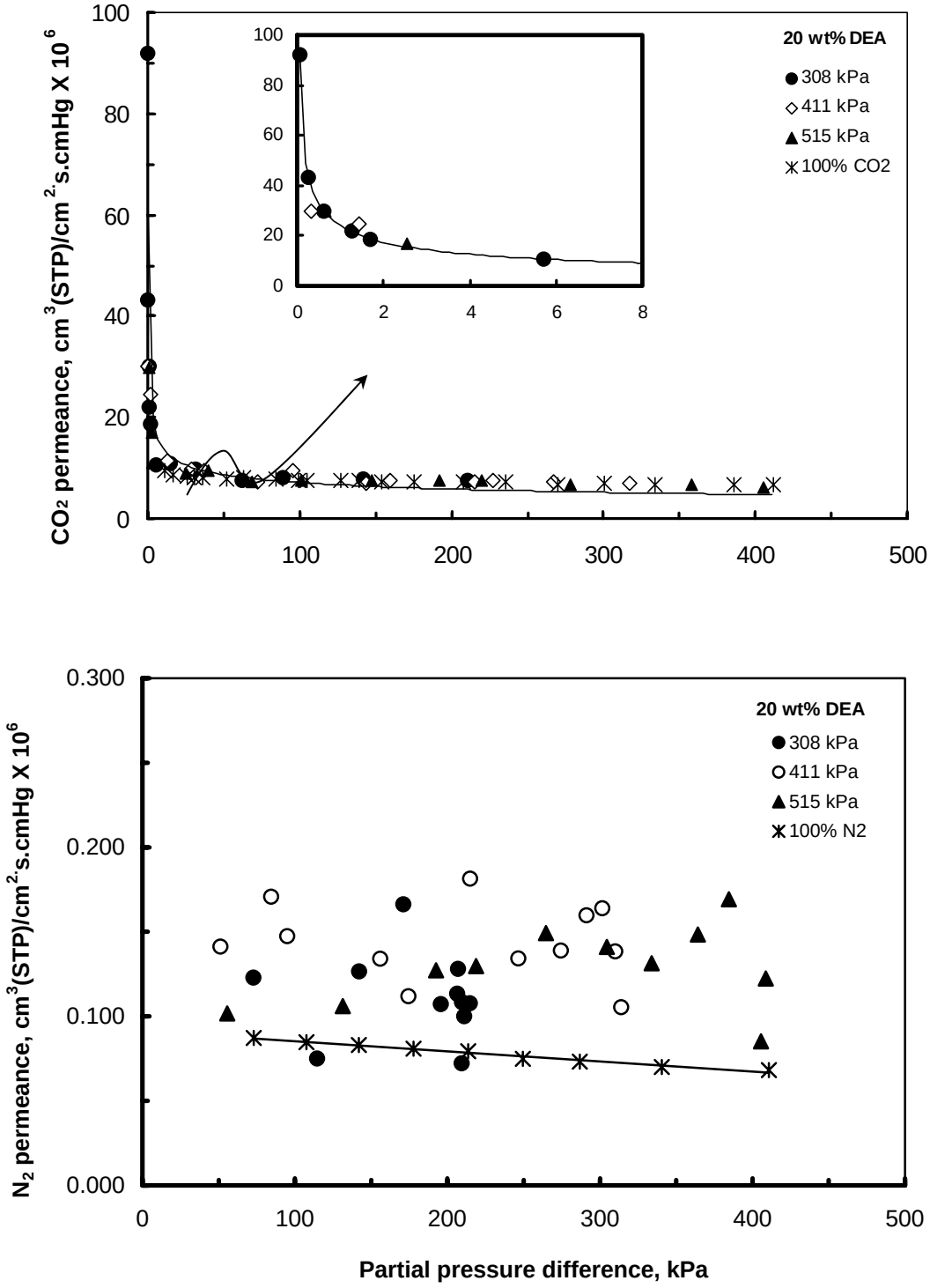

Figure E.4 Permeance of carbon dioxide and nitrogen in the CO_2/N_2 mixture (5 to 100% CO_2) for the DEA membrane as a function of their partial pressure differences.

Temperature: 296K

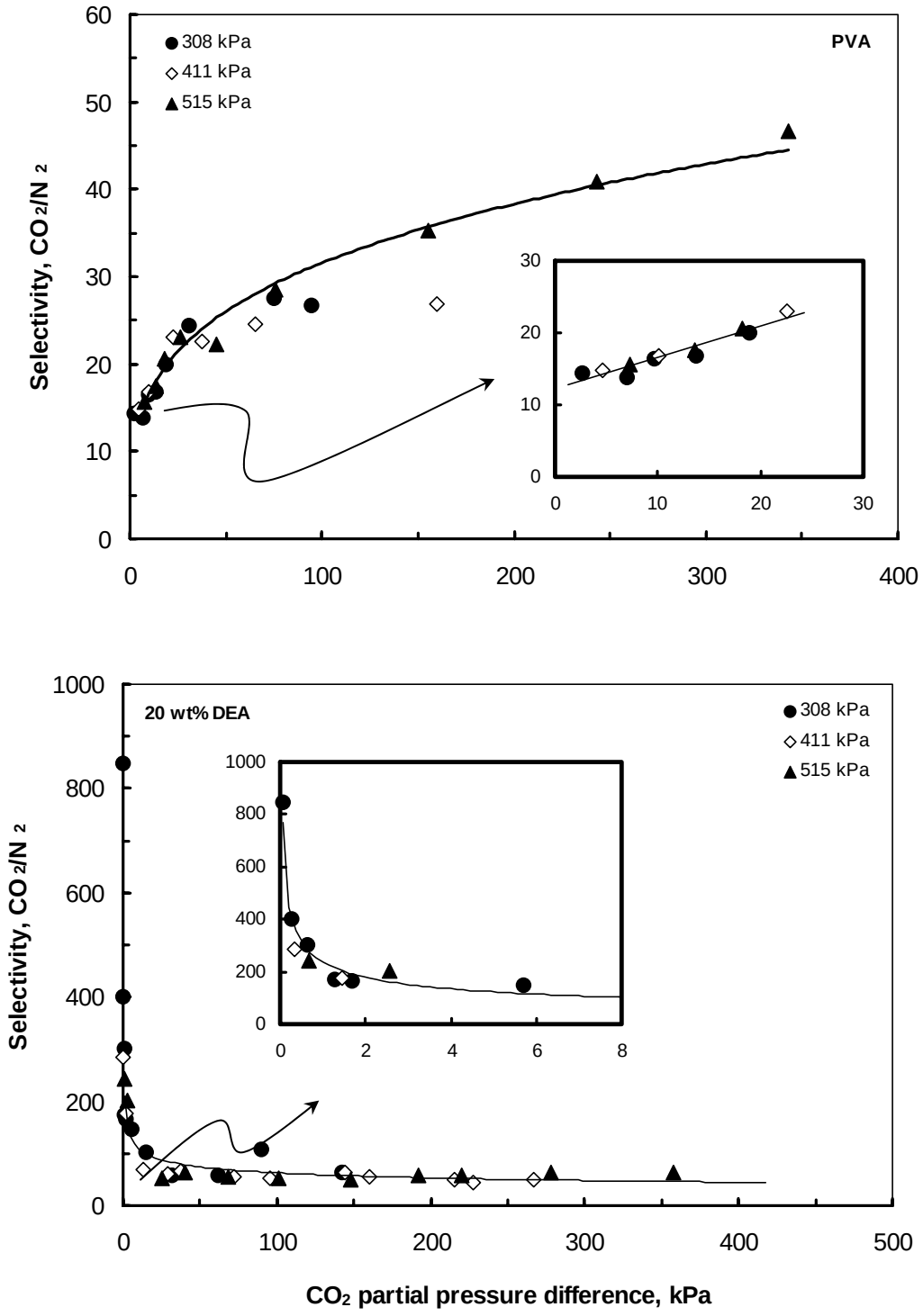

Figure E.5 Selectivity of CO_2 over N_2 in the CO_2/N_2 mixture for the PVA and DEA membranes as a function of their CO_2 partial pressure differences. Temperature: 296K

Appendix F- Computer Program

```
function mod12


global m1 m2 m3 m4


mxgrid = 401;
neqns  = 4;
ninit  = 401;
xinit  = zeros(ninit,1);
DATA = load('mod12.dat');
m1 = DATA(1);
m2 = DATA(2);
m3 = DATA(3);
m4 = DATA(4);
dx=1/(mxgrid-1);
nh=(mxgrid+1)/2;


%---------------------------------


for jj=1:nh


     xinit(jj)          = 4 * ((jj-1)*dx)^3;
     xinit(mxgrid+1-jj) = 1 - xinit(jj);
end
```

```
solinit = bvpinit(xinit',[1 0 0 0]);
sol = bvp4c( @odefun, @bcfun, solinit );
x = [0 : 0.001 : 1];
y = deval( sol, x );
odesy   = y';
odesx   = x';
figure(1)
plot(x, y(1,:),'k-')
hold on
plot(x, y(3,:),'k:')
xlabel('z')
ylabel('CA')
ra = m3/m2*(m2*y(1,:).*y(3,:).^2-1/4.*(1-y(3,:)).^2)./(y(3,:)+m1);
ra = ra';
figure(2)
plot(x, ra,'k-')
xlabel('z')
ylabel('Reaction rate of CO2')

save('output','odesy','odesx','ra');


%_____________________________________________________________________
function dydx = fcneqn(neqns,x,y)
global m1 m2 m3 m4
dydx(1)=y(2);
dydx(2)=m3/m2*[(m2*y(1)*y(3)^2-1/4*(1-y(3))^2)/(y(3)+m1)];
dydx(3)=y(4);
dydx(4)=2*m3/m4*m2*[(m2*y(1)*y(3)^2-1/4*(1-y(3))^2)/(y(3)+m1)];
```

```
dydx = dydx';
%_____________________________________________________________________
function dydx = odefun(x,y)
neqns = 4;
dydx = fcneqn(neqns,x,y);

%_____________________________________________________________________

function f = fcnbc(neqns,yleft,yright)
f(1)=yleft(1)-1.0;
f(2)=yleft(4);
f(3)=yright(1);
f(4)=yright(4);
f = f';
%_____________________________________________________________________

function res = bcfun(ya,yb)
neqns = 4;
res = fcnbc(neqns,ya,yb);
```

Appendix G – Gas Permeation Using PVA-Mixed Amines Membranes

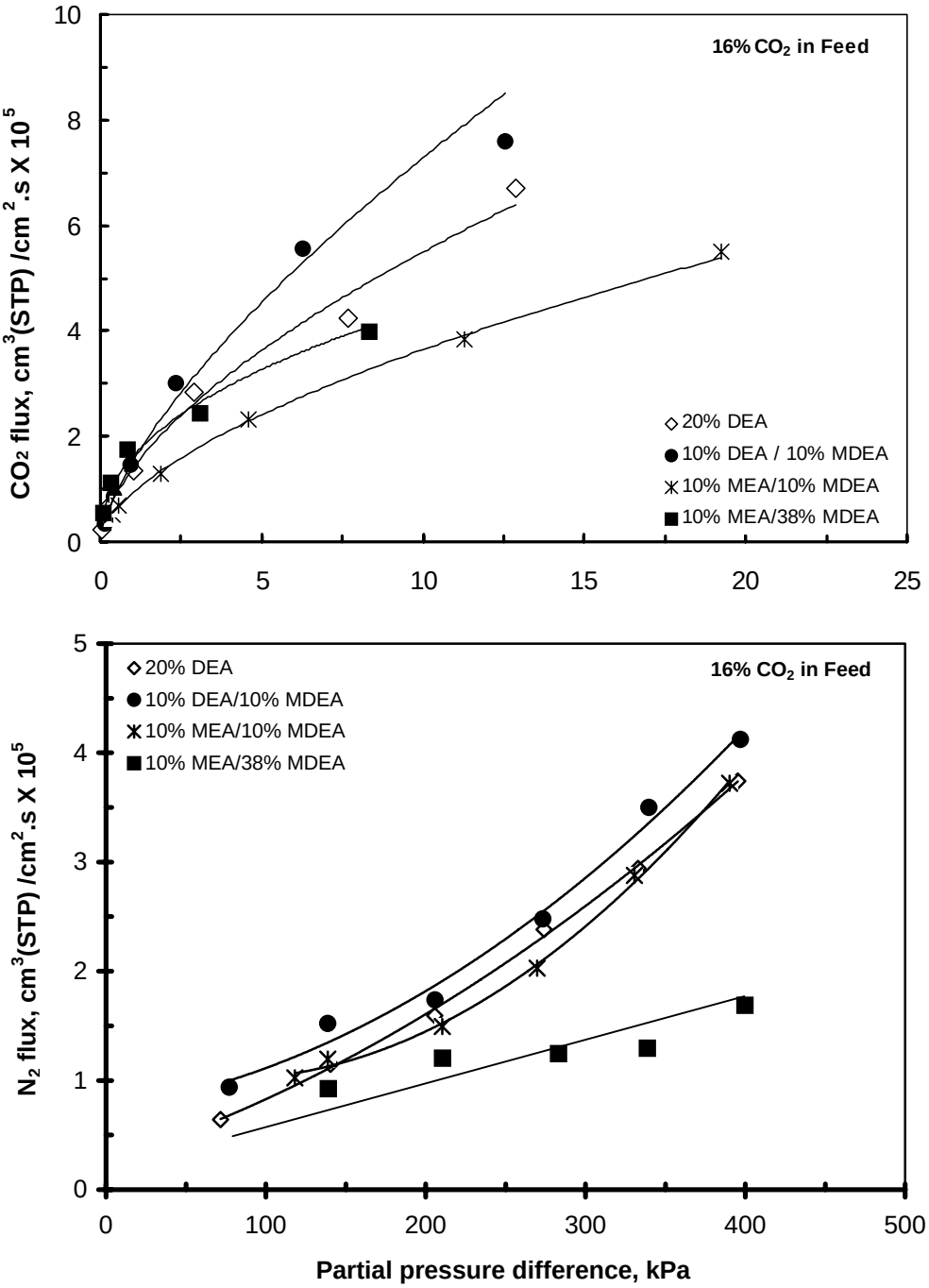

Figure G.1 Fluxes of carbon dioxide and nitrogen in the CO_2/N_2 mixture for the mixed-amine membranes as a function of their partial pressure differences.Temperature: 296K.

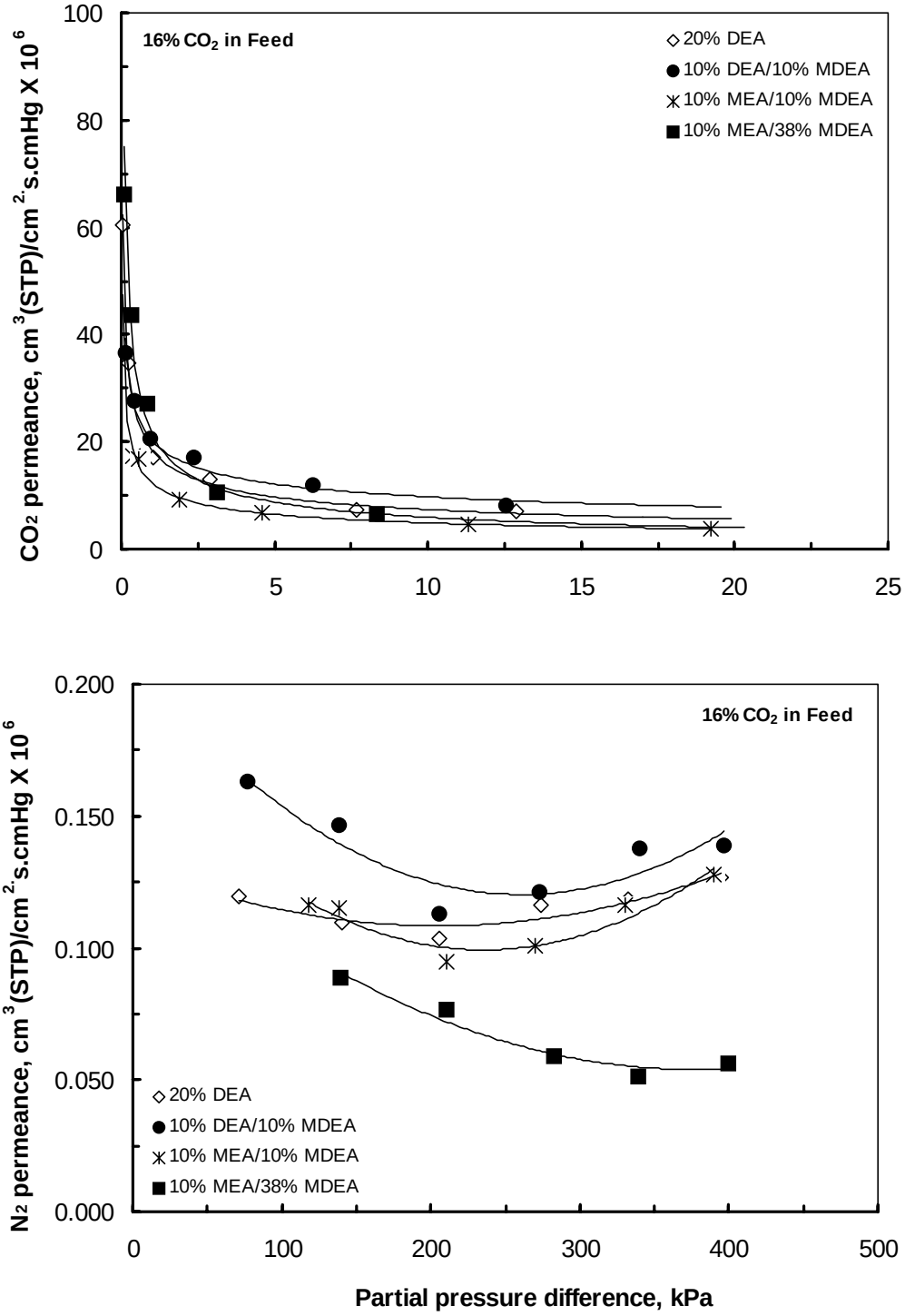

Figure G.2 Permeance of carbon dioxide and nitrogen in the CO_2/N_2 mixture for the mixed-amine membranes as a function of their partial pressure differences.

Temperature: 296K.

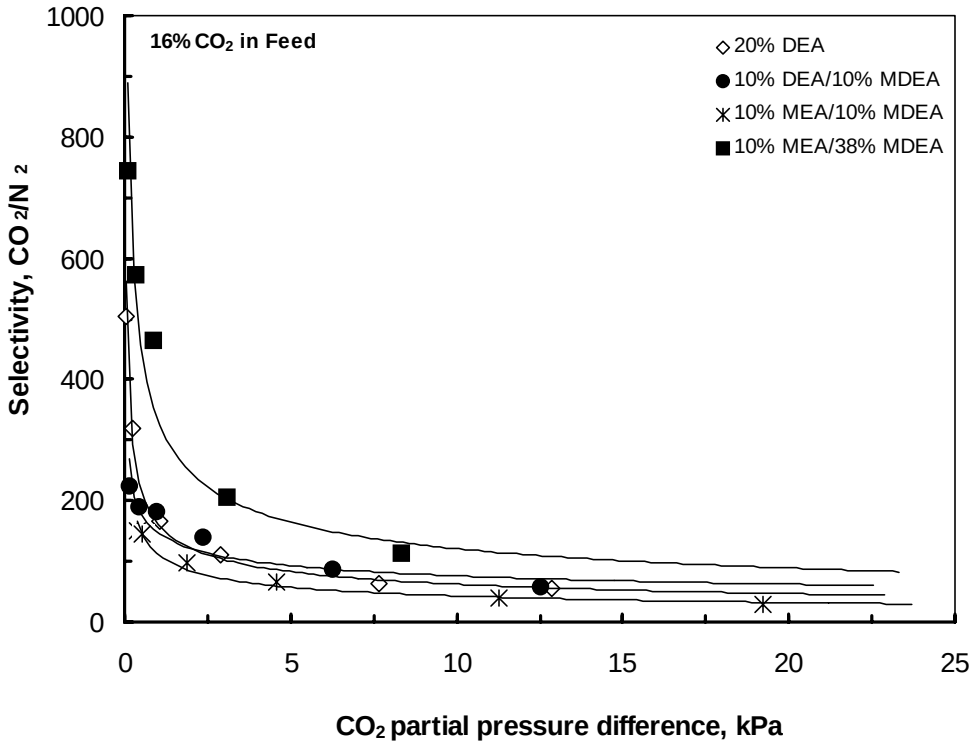

Figure G.2 Selectivity of CO_2 over N_2 in the CO_2/N_2 mixture for the mixed-amine membranes as a function of CO_2 partial pressure differences. Temperature: 296K

Appendix H - Experimental Data

H.1 Pure Gas Permeation

Note:

1. The unit of CO_2 and N_2 flux in the experimental data is expressed in $cm^3(STP)/cm^2.s. \times 10^5$
2. The unit of CO_2 and N_2 permeance is $cm^3(STP)/cm^2.s.cmHg \times 10^6$.

Table H.1 Swelling Effect of Water in the PVA and DEA Membrane, Temperature: 296K.

Membrane	wt% water	Feed pressure psig	Gas	Flux	Permeance	Selectivity JCO2/JN2
PVA	0.00	15.80	CO2	0.00	0.00	
PVA	20.35	15.60	CO2	10.51	0.13	37
PVA	40.18	15.50	CO2	10.71	0.13	35
PVA	50.31	15.60	CO2	11.38	0.14	36
PVA	70.25	15.20	CO2	34.73	0.44	1
PVA	80.11	15.40	CO2	36.71	0.46	1
PVA	0.00	16.00	N2	0.00	0.00	
PVA	20.35	15.80	N2	0.29	0.36	
PVA	40.18	15.60	N2	0.30	0.38	
PVA	50.31	15.60	N2	0.32	0.40	
PVA	70.25	15.40	N2	25.23	3.19	
PVA	80.11	15.40	N2	25.01	3.16	

(continuation)

Membrane	wt% water	Feed pressure psig	Gas	Flux	Permeance	Selectivity JCO2/JN2
DEA	0.00	15.40	CO2	0.00	0.00	
DEA	20.12	15.40	CO2	48.67	0.62	75
DEA	40.18	15.40	CO2	58.70	0.74	86
DEA	50.22	15.20	CO2	59.25	0.76	86
DEA	70.11	15.60	CO2	129.08	1.61	5
DEA	80.25	15.80	CO2	133.42	1.64	5
DEA	0.00	15.60	N2	0.01	0.01	
DEA	20.12	15.40	N2	0.65	0.82	
DEA	40.18	15.80	N2	0.70	0.86	
DEA	50.22	15.20	N2	0.69	0.88	
DEA	70.11	15.00	N2	26.82	3.48	
DEA	80.25	15.40	N2	27.23	3.44	

Table H.2 Gas Permeation through PVA-AMP Blend Membrane.
Temperature: 296K

Membrane	wt% amine	Feed pressure psig	Gas	Flux	Permeance	Selectivity JCO2/JN2
AMP	16	7.60	CO2	15.05	0.39	45
AMP	16	11.80	CO2	18.52	0.31	37
AMP	16	14.60	CO2	22.09	0.29	37
AMP	16	20.60	CO2	30.89	0.29	36
AMP	16	25.40	CO2	33.77	0.26	33
AMP	16	8.00	N2	0.35	0.85	
AMP	16	12.20	N2	0.52	0.83	
AMP	16	14.80	N2	0.61	0.81	
AMP	16	20.20	N2	0.85	0.82	
AMP	16	25.60	N2	1.03	0.78	
AMP	33	7.80	CO2	17.76	0.44	62
AMP	33	9.00	CO2	19.28	0.42	58
AMP	33	14.40	CO2	26.79	0.36	54
AMP	33	18.20	CO2	31.62	0.34	51
AMP	33	27.00	CO2	41.34	0.30	47
AMP	33	8.60	N2	0.32	0.72	
AMP	33	10.20	N2	0.38	0.72	
AMP	33	15.00	N2	0.52	0.68	
AMP	33	18.20	N2	0.62	0.66	
AMP	33	27.20	N2	0.89	0.63	
AMP	50	8.00	CO2	9.79	0.24	
AMP	50	10.60	CO2	10.98	0.20	43
AMP	50	15.60	CO2	15.29	0.19	38

(continuation)						
AMP	50	20.80	CO2	15.87	0.15	36
AMP	50	26.80	CO2	17.53	0.13	29
AMP	50	8.20	N2	0.23	0.55	27
AMP	50	10.60	N2	0.29	0.53	
AMP	50	15.40	N2	0.42	0.53	
AMP	50	20.6	N2	0.54	0.51	
AMP	50	26.8	N2	0.65	0.48	

Table H.3Gas Permeation through PVA-MEA Blend Membrane.

Temperature: 296K

Membrane	wt% amine	Feed pressure psig	Gas	Flux	Permeance	Selectivity JCO2/JN2
MEA	16	5.8	CO2	7.67	0.26	38
MEA	16	11.4	CO2	12.17	0.21	35
MEA	16	16.2	CO2	15.35	0.18	29
MEA	16	20.6	CO2	15.68	0.15	26
MEA	16	24.8	CO2	18.65	0.15	25
MEA	16	6.2	N2	0.21	0.67	
MEA	16	11.8	N2	0.37	0.60	
MEA	16	16.8	N2	0.54	0.63	
MEA	16	21	N2	0.62	0.57	
MEA	16	25.4	N2	0.76	0.58	
MEA	33	5.8	CO2	11.77	0.40	70
MEA	33	9.8	CO2	18.72	0.37	66
MEA	33	15.2	CO2	23.35	0.30	62
MEA	33	20.2	CO2	31.15	0.30	59
MEA	33	25.2	CO2	33.20	0.26	54
MEA	33	6.8	N2	0.20	0.56	
MEA	33	10.6	N2	0.31	0.57	
MEA	33	16.2	N2	0.40	0.48	
MEA	33	20.8	N2	0.54	0.51	
MEA	33	24.2	N2	0.59	0.48	
MEA	50	5.6	CO2	8.17	0.28	57
MEA	50	11.4	CO2	13.96	0.24	52
MEA	50	15.6	CO2	16.26	0.20	48
MEA	50	20.2	CO2	18.65	0.18	44
MEA	50	25.4	CO2	22.20	0.17	45
MEA	50	5.2	N2	0.13	0.50	
MEA	50	11	N2	0.26	0.45	
MEA	50	17.2	N2	0.37	0.42	
MEA	50	20.8	N2	0.44	0.41	
MEA	50	26.4	N2	0.52	0.38	

Table H.4 Gas Permeation through PVA-MDEA Blend Membrane.

Temperature: 296K

Membrane	wt% amine	Feed pressure psig	Gas	Flux	Permeance	Selectivity JCO2/JN2
MDEA	16	5.4	CO2	5.51	0.20	28
MDEA	16	11.6	CO2	8.94	0.15	24
MDEA	16	17	CO2	12.44	0.14	22
MDEA	16	20.80	CO2	15.19	0.14	23
MDEA	16	26.40	CO2	17.56	0.13	23
MDEA	16	8.00	N2	0.29	0.70	
MDEA	16	11.60	N2	0.37	0.62	
MDEA	16	16.80	N2	0.56	0.65	
MDEA	16	22.00	N2	0.69	0.61	
MDEA	16	24.80	N2	0.72	0.57	
MDEA	33	5.20	CO2	6.46	0.24	41.66
MDEA	33	10.60	CO2	12.31	0.23	46.69
MDEA	33	16.20	CO2	17.19	0.21	42.37
MDEA	33	20.60	CO2	20.43	0.19	38.71
MDEA	33	26.40	CO2	24.28	0.18	39.65
MDEA	33	9.00	N2	0.27	0.58	
MDEA	33	12.80	N2	0.32	0.48	
MDEA	33	16.80	N2	0.42	0.49	
MDEA	33	21.20	N2	0.54	0.50	
MDEA	33	26.80	N2	0.62	0.45	
MDEA	50	4.60	CO2	5.68	0.24	46
MDEA	50	9.20	CO2	8.80	0.19	44
MDEA	50	16.00	CO2	14.75	0.18	49
MDEA	50	20.20	CO2	16.60	0.16	46
MDEA	50	25.00	CO2	19.51	0.15	46
MDEA	50	5.40	N2	0.14	0.52	
MDEA	50	9.60	N2	0.21	0.42	
MDEA	50	16.40	N2	0.31	0.36	
MDEA	50	20.80	N2	0.37	0.35	
MDEA	50	25.80	N2	0.44	0.33	

Table H.5 Gas Permeation through PVA-DEA Blend Membrane, Temperature: 296K

Membrane	wt% amine	Feed pressure psig	Gas	Flux	Permeance	Selectivity JCO2/JN2
DEA	16	5.80	CO2	25.66	0.86	97
DEA	16	10.80	CO2	38.76	0.70	83
DEA	16	16.40	CO2	49.94	0.59	72
DEA	16	25.60	CO2	62.87	0.48	58
DEA	16	6.00	N2	0.27	0.89	
DEA	16	11.60	N2	0.50	0.84	
DEA	16	16.20	N2	0.69	0.83	
DEA	16	25.40	N2	1.07	0.82	
DEA	33	5.80	CO2	20.84	0.70	103
DEA	33	10.00	CO2	27.22	0.53	82
DEA	33	16.00	CO2	42.14	0.51	81
DEA	33	26.60	CO2	62.66	0.46	75
DEA	33	5.80	N2	0.20	0.68	
DEA	33	10.40	N2	0.35	0.65	
DEA	33	16.20	N2	0.52	0.63	
DEA	33	25.60	N2	0.80	0.61	
DEA	50	5.80	CO2	12.01	0.40	68
DEA	50	9.80	CO2	15.02	0.30	57
DEA	50	15.80	CO2	21.51	0.27	49
DEA	50	19.40	CO2	25.47	0.26	56
DEA	50	25.00	CO2	29.90	0.23	48
DEA	50	6.20	N2	0.19	0.59	
DEA	50	10.00	N2	0.27	0.52	
DEA	50	15.00	N2	0.41	0.54	
DEA	50	20.20	N2	0.47	0.45	
DEA	50	25.20	N2	0.63	0.49	

Table H.6 Effect of DEA Concentrations.Temperature: 296K

Membrane	wt% amine	Feed pressure psig	Gas	Flux	Permeance J	Selectivity JCO2/JN2
DEA	0.00	10.20	CO2	6.31	0.12	34
DEA	10.5	10.80	CO2	31.78	0.57	66
DEA	21.5	10.20	CO2	37.37	0.71	95
DEA	32.12	10.60	CO2	27.50	0.51	73
DEA	51.5	10.20	CO2	13.63	0.26	52
DEA	0.00	10.40	N2	0.19	0.35	
DEA	10.5	10.20	N2	0.46	0.87	
DEA	21.5	10.80	N2	0.42	0.75	
DEA	32.12	10.20	N2	0.36	0.69	
DEA	51.5	10.80	N2	0.28	0.50	

Table H.7 Effect of CO_2 Feed Pressure on PVA Membrane Performance.
Temperature: 296K.

(First Batch)

Membrane	Feed pressure psig	Gas	Flux	Permeance J
PVA	4.80	CO2	2.28	0.09
PVA	6.80	CO2	3.33	0.10
PVA	8.60	CO2	4.71	0.11
PVA	11.00	CO2	6.38	0.11
PVA	14.40	CO2	8.81	0.12
PVA	16.20	CO2	10.94	0.13
PVA	18.40	CO2	13.05	0.14
PVA	20.40	CO2	15.15	0.14
PVA	23.20	CO2	18.65	0.16
PVA	26.00	CO2	23.44	0.18
PVA	30.40	CO2	31.95	0.20
PVA	35.80	CO2	43.32	0.24
PVA	44.60	CO2	63.83	0.28
PVA	58.00	CO2	99.91	0.34
PVA	10.6	N2	0.20	0.37
PVA	15.8	N2	0.29	0.35
PVA	20.4	N2	0.40	0.39
PVA	27.2	N2	0.46	0.33
PVA	30.4	N2	0.54	0.35
PVA	35.4	N2	0.59	0.32
PVA	40.2	N2	0.64	0.31
PVA	48.8	N2	0.69	0.28
PVA	58.6	N2	0.76	0.25

(Second Batch)

Membrane	Feed pressure psig	Gas	Flux	Permeance J
PVA	3.40	CO2	1.62	0.09
PVA	5.60	CO2	2.53	0.09
PVA	9.80	CO2	5.96	0.12
PVA	12.40	CO2	7.54	0.12
PVA	14.80	CO2	9.94	0.13
PVA	19.60	CO2	14.23	0.14
PVA	25.00	CO2	20.57	0.16
PVA	6.8	N2	0.15	0.42
PVA	10.4	N2	0.22	0.40
PVA	11.4	N2	0.22	0.38
PVA	17.2	N2	0.32	0.37
PVA	25.4	N2	0.43	0.33
PVA	30.4	N2	0.50	0.32
PVA	35.4	N2	0.56	0.31
PVA	45.8	N2	0.67	0.28
PVA	58.6	N2	0.79	0.26

Table H.8 Effect of CO_2 Feed Pressure on DEA Membrane Performance.
Temperature: 296K

(First Batch)

Membrane	wt% amine	Feed pressure psig	Gas	Flux	Permeance J
DEA	20	1.60	CO2	7.74	0.94
DEA	20	2.40	CO2	10.72	0.87
DEA	20	3.80	CO2	16.27	0.83
DEA	20	4.40	CO2	18.52	0.82
DEA	20	5.20	CO2	21.66	0.81
DEA	20	7.60	CO2	30.64	0.79
DEA	20	9.20	CO2	37.57	0.80
DEA	20	12.20	CO2	49.15	0.78
DEA	20	14.40	CO2	56.49	0.76
DEA	20	15.20	CO2	58.41	0.75
DEA	20	18.40	CO2	71.87	0.76
DEA	20	20.20	CO2	78.20	0.75
DEA	20	22.40	CO2	84.76	0.74
DEA	20	25.40	CO2	92.74	0.71
DEA	20	30.20	CO2	110.73	0.71
DEA	20	34.20	CO2	125.45	0.71
DEA	20	39.20	CO2	135.93	0.68
DEA	20	43.60	CO2	154.12	0.69
DEA	20	48.40	CO2	167.48	0.67
DEA	20	56.00	CO2	192.48	0.67
DEA	20	59.80	CO2	201.99	0.66
DEA	20	10.60	N2	0.47	0.87
DEA	20	15.60	N2	0.68	0.85
DEA	20	20.60	N2	0.88	0.83
DEA	20	25.80	N2	1.07	0.81
DEA	20	31.00	N2	1.26	0.79
DEA	20	36.20	N2	1.39	0.75
DEA	20	41.60	N2	1.56	0.73
DEA	20	49.40	N2	1.78	0.70
DEA	20	59.60	N2	2.09	0.68

Table H.9 Effect of CO_2 Feed Pressure on DEA Membrane Performance.

Temperature: 296K.

(Second Batch)

Membrane	wt% amine	Feed pressure psig	Gas	Flux	Permeance J
DEA	20	4.40	CO2	19.65	0.87
DEA	20	8.40	CO2	35.19	0.82
DEA	20	12.80	CO2	49.94	0.76
DEA	20	14.40	CO2	56.55	0.76
DEA	20	15.20	CO2	57.88	0.74
DEA	20	20.20	CO2	76.46	0.74
DEA	20	25.20	CO2	93.13	0.72
DEA	20	30.20	CO2	106.74	0.69
DEA	20	35.60	CO2	125.28	0.69
DEA	20	40.20	CO2	142.60	0.69
DEA	20	46.40	CO2	156.53	0.66
DEA	20	50.40	CO2	173.50	0.67
DEA	20	55.60	CO2	188.78	0.66
DEA	20	58.60	CO2	202.54	0.67
DEA	20	7.4	N2	0.34	0.91
DEA	20	12.8	N2	0.56	0.86
DEA	20	16.2	N2	0.72	0.86
DEA	20	21.4	N2	0.90	0.82
DEA	20	26.6	N2	1.10	0.80
DEA	20	34.5	N2	1.31	0.74
DEA	20	45.8	N2	1.73	0.73
DEA	20	59.2	N2	2.07	0.68

Table H.10 Effect of Operating Temperature on Permeation through the DEA Membrane.

(20wt% DEA Membrane)

Temperature 0C	Feed pressure psig	Gas	Permeance	Selectivity JCO2/JN2
30	10.4	CO2	1.381	102
40	10.4	CO2	1.922	126
50	10.4	CO2	2.339	139
60	10.4	CO2	2.646	143
30	15.6	CO2	1.286	93
40	15.6	CO2	1.794	110
50	15.6	CO2	1.911	114
60	15.6	CO2	2.378	126
30	25	CO2	1.156	83
40	25	CO2	1.578	96
50	25	CO2	1.637	98
60	25	CO2	1.985	104
30	10	N2	1.35	
40	10	N2	1.52	
50	10	N2	1.68	
60	10	N2	1.85	
30	16	N2	1.39	
40	16	N2	1.535	
50	16	N2	1.75	
60	16	N2	1.89	
30	26.2	N2	1.385	
40	26.2	N2	1.51	
50	26.2	N2	1.666	
60	26.2	N2	1.905	

Table H.11 Effect of Membrane Thickness on the Performance of the DEA Membrane.

Temperature: 296K

(20wt% DEA Membrane)

Membrane Thickness, microns	Feed pressure psig	Gas	Flux	Permeance	Selectivity JCO2/JN2
161	5.2	CO2	21.93	0.82	90
161	10.4	CO2	42.38	0.79	92
161	15.2	CO2	58.56	0.75	87
161	20.6	CO2	76.52	0.72	87
161	25.4	CO2	90.24	0.69	85
185	5.4	CO2	20.14	0.72	119
185	10.4	CO2	37.02	0.69	111
185	15.2	CO2	49.39	0.63	105
185	20.4	CO2	62.81	0.60	100
185	25.6	CO2	73.02	0.55	94
200	5.6	CO2	18.99	0.66	134
200	10.6	CO2	33.68	0.61	128
200	15.8	CO2	47.33	0.58	123
200	20.2	CO2	55.10	0.53	113
200	25.2	CO2	61.95	0.48	101
161	5.60	N2	0.26	0.91	
161	10.20	N2	0.45	0.86	
161	15.60	N2	0.69	0.85	
161	21.00	N2	0.90	0.83	
161	25.60	N2	1.07	0.81	
185	5.4	N2	0.17	0.61	
185	10.6	N2	0.34	0.62	
185	15.4	N2	0.48	0.60	
185	20.2	N2	0.62	0.60	
185	25.2	N2	0.77	0.59	
200	5.4	N2	0.14	0.49	
200	10.8	N2	0.27	0.48	
200	15.6	N2	0.38	0.47	
200	20.8	N2	0.50	0.47	
200	25.4	N2	0.62	0.47	

Table H.12 Stability Test for the DEA and PVA Membrane

Temperature: 296K

Time, h	Membrane	Humidification	CO2 permeance
2	DEA	with humid	0.79
4	DEA	with humid	0.77
28	DEA	with humid	0.71
29	DEA	with humid	0.69
53	DEA	with humid	0.79
75	DEA	with humid	0.77
77	DEA	with humid	0.73
143	DEA	with humid	0.74
146	DEA	with humid	0.72
148	DEA	with humid	0.72
168	DEA	with humid	0.73
195	DEA	with humid	0.67
2	PVA	with humid	0.13
23	PVA	with humid	0.12
25	PVA	with humid	0.11
42	PVA	with humid	0.08
49	PVA	with humid	0.15
65	PVA	with humid	0.13
68	PVA	with humid	0.13
72	PVA	with humid	0.13
90	PVA	with humid	0.12
93	PVA	with humid	0.12
97	PVA	with humid	0.12
118	PVA	with humid	0.12
120	PVA	with humid	0.08
122	PVA	with humid	0.13
140	PVA	with humid	0.14
142	PVA	with humid	0.13
144	PVA	with humid	0.12
163	PVA	with humid	0.12
164	PVA	with humid	0.12
175	PVA	with humid	0.12
193	PVA	with humid	0.13

Table H.13 Effect of Humidification on the Performance of the DEA and PVA Membrane. Temperature: 296K

Time, h	Membrane	Humidification	CO2 permeance
2	DEA	without humid	0.76
4	DEA	without humid	0.80
5	DEA	without humid	0.86
28	DEA	without humid	0.82
29	DEA	without humid	0.80
30	DEA	without humid	0.79
32	DEA	without humid	0.79
50	DEA	without humid	0.49
56	DEA	without humid	0.42
74	DEA	without humid	0.16
79	DEA	without humid	0.15
80	DEA	without humid	0.14
83	DEA	with humid	0.84
90	DEA	with humid	0.82
95	DEA	with humid	0.82
128	DEA	with humid	0.80
144	DEA	with humid	0.81
149	DEA	with humid	0.79
152	DEA	with humid	0.80
168	DEA	with humid	0.79
190	DEA	with humid	0.78
1	PVA	without humid	0.13
23	PVA	without humid	0.12
45	PVA	with humid	0.07
52	PVA	with humid	0.08
70	PVA	with humid	0.05
73	PVA	with humid	0.05
76	PVA	with humid	0.11
98	PVA	with humid	0.10
100	PVA	with humid	0.13
124	PVA	with humid	0.13
144	PVA	with humid	0.12
161	PVA	with humid	0.13
179	PVA	with humid	0.13
195	PVA	with humid	0.12

H.2 Gas Mixture Permeation

Table H.14 Effect of Feed Flow Rate on the Performance of the DEA Membrane.

Temperature: 236K.

20wt% DEA

Feed pressure	mol frac CO2	mol frac CO2	mol frac N2	Flux	Permeance	Flux	Permeance	Flow rate
psig	in feed	in permeate	in permeate	CO2	CO2	N2	N2	cm3(STP)/s
31.60	0.1565	0.4762	0.5238	1.32	1.04	1.45	0.90	0.10
31.60	0.1565	0.4760	0.5240	1.31	1.04	1.45	0.90	0.34
31.80	0.1558	0.4759	0.5241	1.33	1.04	1.46	0.90	0.48
31.80	0.1561	0.4767	0.5233	1.33	1.03	1.46	0.90	0.63
31.80	0.1560	0.4764	0.5236	1.32	1.02	1.46	0.90	0.91
47.00	0.1560	0.6019	0.3981	3.60	0.90	2.38	1.00	0.04
46.80	0.1561	0.6012	0.3988	3.54	0.90	2.35	0.99	0.08
47.00	0.1561	0.6007	0.3993	3.58	0.87	2.38	1.00	0.20
46.80	0.1561	0.6004	0.3996	3.54	0.89	2.35	1.00	0.35
46.80	0.1561	0.5999	0.4001	3.61	0.90	2.41	1.02	0.47
46.80	0.1561	0.6011	0.3989	3.53	0.90	2.34	0.99	0.63
46.80	0.1561	0.6007	0.3993	3.54	0.90	2.35	1.00	0.79
60.00	0.1560	0.6686	0.3314	8.15	0.87	4.04	1.35	0.07
60.00	0.1560	0.6754	0.3246	7.90	0.89	3.80	1.27	0.23
60.00	0.1560	0.6729	0.3271	7.83	0.87	3.81	1.27	0.36
60.00	0.1560	0.6731	0.3269	8.07	0.89	3.92	1.31	0.52
60.00	0.1560	0.6743	0.3257	7.93	0.89	3.83	1.28	0.67
60.00	0.1560	0.6720	0.3280	8.13	0.89	3.97	1.33	0.80

Table H.15 Effect of Feed Flow Rate on the Performance of the PVA Membrane.

Temperature: 296K.

PVA

Feed pressure	mol frac CO2	mol frac CO2	mol frac N2	Flux	Permeance	Flux	Permeance	Flow rate
psig	in feed	in permeate	in permeate	CO2	CO2	N2	N2	cm3(STP)/s
32.00	0.1560	0.3989	0.6011	0.51	0.07	0.78	0.49	0.08
32.00	0.1560	0.4006	0.5994	0.52	0.07	0.78	0.50	0.25
32.00	0.1560	0.3955	0.6045	0.54	0.07	0.82	0.52	0.39
32.00	0.1560	0.4030	0.5970	0.50	0.07	0.74	0.47	0.58
32.20	0.1560	0.4019	0.5981	0.51	0.07	0.76	0.48	0.76
32.20	0.1560	0.4020	0.5980	0.51	0.07	0.75	0.48	0.91
46.20	0.1560	0.4853	0.5147	1.07	0.09	1.13	0.50	0.08
46.40	0.1560	0.4905	0.5095	1.12	0.09	1.16	0.51	0.22
46.40	0.1560	0.4882	0.5118	1.10	0.09	1.15	0.51	0.35
46.40	0.1560	0.4939	0.5061	1.05	0.09	1.08	0.47	0.46
46.40	0.1560	0.4913	0.5087	1.07	0.09	1.11	0.49	0.66
46.20	0.1560	0.4923	0.5077	1.04	0.09	1.07	0.47	0.89
59.80	0.1560	0.5675	0.4325	1.79	0.11	1.37	0.47	0.05
59.80	0.1560	0.5631	0.4369	1.83	0.11	1.42	0.49	0.16
59.80	0.1560	0.5658	0.4342	1.82	0.11	1.40	0.48	0.33
59.80	0.1560	0.5710	0.4290	1.81	0.11	1.36	0.47	0.49
59.80	0.1560	0.5726	0.4274	1.79	0.11	1.34	0.46	0.70
59.80	0.1560	0.5722	0.4278	1.85	0.11	1.38	0.48	0.86

Table H.16 Effect of DEA Concentration on the Performance of the DEA Membrane.

Temperature: 296K

Feed pressure psig	wt% DEA	mol frac CO2 in feed	mol frac CO2 in permeate	mol frac N2 in permeate	Flux CO2	Permeance CO2	Flux N2	Permeance N2	Selectivity JCO2/JN2
10.20	0	0.1512	0.2299	0.7701	0.09	0.05	0.31	0.62	8
20.40	0	0.1512	0.3085	0.6915	0.24	0.06	0.54	0.54	11
30.40	0	0.1515	0.3724	0.6276	0.45	0.06	0.76	0.51	13
40.00	0	0.1510	0.4073	0.5927	0.67	0.06	0.98	0.50	11
50.00	0	0.1530	0.4862	0.5139	1.07	0.08	1.13	0.46	16
60.00	0	0.1531	0.5530	0.4470	1.70	0.10	1.38	0.47	21
11.40	10	0.1531	0.2700	0.7300	0.16	1.13	0.43	0.73	155
22.20	10	0.1531	0.3756	0.6244	0.58	0.88	0.96	0.85	103
30.60	10	0.1531	0.4462	0.5538	0.92	0.47	1.14	0.73	65
40.20	10	0.1530	0.5182	0.4818	1.68	0.42	1.56	0.77	54
50.80	10	0.1531	0.5718	0.4282	2.41	0.29	1.81	0.71	41
59.40	10	0.1531	0.5956	0.4044	3.67	0.27	2.49	0.85	32
10.40	20	0.1510	0.2574	0.7426	0.22	6.04	0.64	1.20	504
20.40	20	0.1532	0.3632	0.6368	0.65	3.48	1.15	1.09	318
30.00	20	0.1531	0.4553	0.5447	1.33	1.72	1.59	1.04	166
40.20	20	0.1531	0.5430	0.4570	2.83	1.30	2.38	1.16	112
49.40	20	0.1529	0.5911	0.4089	4.25	0.74	2.94	1.18	63
59.20	20	0.1530	0.6422	0.3578	6.71	0.70	3.74	1.27	55
10.20	30	0.1531	0.2587	0.7413	0.22	4.36	0.62	1.17	372
20.20	30	0.1532	0.3606	0.6394	0.68	2.84	1.21	1.16	245
30.00	30	0.1530	0.4472	0.5528	1.04	0.76	1.29	0.84	91
40.00	30	0.1535	0.5329	0.4671	2.18	0.75	1.91	0.94	80
50.20	30	0.1531	0.5923	0.4077	3.15	0.50	2.17	0.86	58
59.80	30	0.1532	0.6325	0.3675	4.97	0.46	2.89	0.97	47
12.80	50	0.1530	0.2850	0.7150	0.19	2.08	0.49	0.74	283
20.00	50	0.1531	0.3574	0.6426	0.51	1.70	0.92	0.90	189
30.40	50	0.1533	0.4503	0.5497	0.74	0.49	0.90	0.58	84
40.20	50	0.1531	0.5315	0.4685	1.32	0.43	1.16	0.57	76
50.40	50	0.1531	0.5918	0.4082	2.11	0.32	1.46	0.58	56
59.80	50	0.1532	0.6216	0.3784	3.34	0.28	2.03	0.69	42

Table H.17 Effects of Feed Concentration on the Permeation through the PVA Membrane. Temperature: 296K

PVA

Feed pressure	mol frac CO2	mol frac CO2	mol frac N2	Flux	Permeance	Flux	Permeance	Selectivity
psig	in feed	in permeate	in permeate	CO2	CO2	N2	N2	JCO2/JN2
9.80	0.0446	0.0699	0.9301	0.02	0.07	0.30	0.60	11
15.40	0.0461	0.0860	0.9140	0.04	0.06	0.44	0.56	12
20.00	0.0459	0.0966	0.9034	0.06	0.07	0.56	0.55	12
25.80	0.0458	0.1113	0.8887	0.09	0.08	0.70	0.53	15
31.20	0.0463	0.1235	0.8765	0.11	0.07	0.79	0.50	14
45.00	0.0457	0.1512	0.8488	0.20	0.08	1.11	0.49	16
59.20	0.0451	0.1750	0.8250	0.29	0.08	1.39	0.46	16
10.60	0.0821	0.1317	0.8683	0.05	0.07	0.33	0.62	11
15.00	0.0821	0.1522	0.8478	0.08	0.08	0.44	0.58	13
20.00	0.0819	0.1726	0.8274	0.12	0.08	0.56	0.56	13
25.20	0.0816	0.1925	0.8075	0.16	0.07	0.66	0.52	14
30.40	0.0819	0.2135	0.7865	0.22	0.08	0.80	0.52	15
45.40	0.0811	0.2653	0.7347	0.38	0.08	1.06	0.46	16
59.80	0.0816	0.3254	0.6746	0.69	0.10	1.43	0.48	22
9.80	0.1015	0.1580	0.8420	0.06	0.07	0.31	0.63	11
14.60	0.1014	0.1838	0.8162	0.10	0.07	0.44	0.59	12
20.40	0.1016	0.2157	0.7843	0.16	0.08	0.57	0.55	14
25.60	0.1016	0.2390	0.7610	0.21	0.07	0.68	0.53	14
30.20	0.1016	0.2606	0.7394	0.29	0.08	0.81	0.54	14
44.40	0.1013	0.3235	0.6765	0.51	0.08	1.06	0.48	17
59.60	0.1015	0.3795	0.6205	0.84	0.08	1.38	0.47	18
10.40	0.1532	0.2421	0.7579	0.11	0.07	0.34	0.65	11
14.60	0.1533	0.2749	0.7251	0.17	0.07	0.44	0.61	12
20.20	0.1534	0.3175	0.6825	0.26	0.07	0.56	0.56	13
25.40	0.1536	0.3526	0.6474	0.37	0.07	0.68	0.54	14
30.20	0.1536	0.3812	0.6188	0.47	0.07	0.77	0.52	14
45.20	0.1533	0.4757	0.5243	1.00	0.09	1.10	0.50	18
59.20	0.1534	0.5547	0.4453	1.79	0.11	1.44	0.50	22
10.20	0.2133	0.3301	0.6699	0.16	0.07	0.33	0.66	10
15.40	0.2134	0.3928	0.6072	0.28	0.08	0.44	0.58	15
20.6	0.2135	0.4359	0.5641	0.42	0.07	0.54	0.54	13
25.8	0.2138	0.4811	0.5189	0.62	0.08	0.67	0.54	14
30.8	0.2135	0.5236	0.4764	0.88	0.08	0.80	0.54	16
45.2	0.2148	0.6356	0.3644	1.93	0.11	1.11	0.52	21
59.6	0.2139	0.7154	0.2846	3.03	0.11	1.21	0.43	25

(Continuation - Effects of Feed Concentration through PVA Membrane)

PVA

Feed pressure	mol frac CO2	mol frac CO2	mol frac N2	Flux	Permeance	Flux	Permeance	Selectivity
psig	in feed	in permeate	in permeate	CO2	CO2	N2	N2	JCO2/JN2
10.4	0.3176	0.4881	0.5119	0.31	0.08	0.32	0.66	12
15.4	0.3177	0.5591	0.4410	0.55	0.08	0.43	0.60	13
20.2	0.3151	0.6177	0.3823	0.87	0.09	0.54	0.57	15
24.8	0.3172	0.6720	0.3280	1.31	0.10	0.64	0.56	17
30.2	0.3235	0.7250	0.2750	1.89	0.10	0.72	0.53	18
45.2	0.3157	0.8012	0.1988	3.81	0.10	0.95	0.48	22
59.6	0.3172	0.8451	0.1549	6.43	0.11	1.18	0.47	24
11.00	0.5119	0.7570	0.2430	0.93	0.09	0.30	0.65	14
14.80	0.5119	0.8087	0.1913	1.57	0.09	0.37	0.62	15
20.00	0.5208	0.8685	0.1315	2.89	0.11	0.44	0.58	18
25.20	0.5201	0.9002	0.0998	4.49	0.12	0.50	0.55	21
30.40	0.5118	0.9123	0.0878	5.96	0.12	0.57	0.54	22
45.80	0.5129	0.9453	0.0547	12.96	0.15	0.75	0.51	29
59.80	0.5120	0.9605	0.0395	21.83	0.18	0.90	0.49	36

Table H.18 Effects of Feed Concentration on the Permeation through the DEA Membrane. Temperature: 296K.

20wt% DEA

Feed pressure	mol frac CO2	mol frac CO2	mol frac N2	Flux	Permeance	Flux	Permeance	Selectivity
psig	in feed	in permeate	in permeate	CO2	CO2	N2	N2	JCO2/JN2
10.60	0.0463	0.0797	0.9204	0.04	7.28	0.46	0.85	860
16.20	0.0463	0.0972	0.9028	0.08	4.86	0.75	0.90	542
20.20	0.0463	0.1096	0.8904	0.13	4.22	1.08	1.04	405
26.00	0.0463	0.1275	0.8725	0.18	3.16	1.22	0.91	346
30.40	0.0463	0.1415	0.8585	0.27	5.88	1.62	1.04	566
45.20	0.0463	0.1869	0.8131	0.58	4.11	2.54	1.09	375
59.40	0.0463	0.2301	0.7699	1.00	3.92	3.34	1.09	358
10.80	0.0819	0.1419	0.8581	0.09	8.19	0.56	1.01	811
15.20	0.0819	0.1683	0.8317	0.16	5.12	0.78	1.00	513
20.20	0.0819	0.1927	0.8073	0.27	3.51	1.13	1.09	321
25.40	0.0819	0.2216	0.7784	0.38	2.78	1.33	1.02	273
30.80	0.0829	0.2519	0.7481	0.55	4.65	1.63	1.03	452
44.40	0.0829	0.3239	0.6761	1.04	2.58	2.17	0.95	272
59.20	0.0816	0.4041	0.5959	1.94	1.99	2.86	0.94	210

(Continuation - Effects of Feed Concentration through DEA Membrane)

20wt% DEA

Feed pressure	mol frac CO2	mol frac CO2	mol frac N2	Flux	Permeance	Flux	Permeance	Selectivity
psig	in feed	in permeate	in permeate	CO2	CO2	N2	N2	JCO2/JN2
10.40	0.1019	0.1738	0.8263	0.13	8.63	0.63	1.18	732
15.20	0.1016	0.2059	0.7941	0.25	4.01	0.96	1.23	326
20.40	0.1016	0.2409	0.7591	0.41	3.21	1.30	1.24	259
25.20	0.1015	0.2731	0.7269	0.58	3.18	1.53	1.18	268
30.40	0.1017	0.3092	0.6908	0.73	3.47	1.64	1.05	330
45.20	0.1016	0.4048	0.5952	1.68	2.44	2.46	1.06	229
59.80	0.1017	0.4785	0.5215	2.80	1.01	3.06	1.00	100
10.20	0.1532	0.2590	0.7410	0.23	6.24	0.65	1.24	504
14.80	0.1560	0.3119	0.6881	0.44	4.84	0.97	1.27	380
20.40	0.1532	0.3634	0.6366	0.69	3.74	1.21	1.16	322
25.20	0.1564	0.4197	0.5803	0.99	2.81	1.36	1.06	267
30.80	0.1561	0.4651	0.5349	1.34	0.98	1.54	0.98	99
43.80	0.1560	0.5842	0.4158	2.80	1.01	1.99	0.90	113
59.60	0.1562	0.6690	0.3310	8.68	0.95	4.29	1.45	66
11.00	0.2138	0.3728	0.6272	0.63	7.85	1.06	1.88	419
15.20	0.2165	0.4380	0.5620	1.24	7.35	1.59	2.05	359
20.80	0.2165	0.5108	0.4892	1.71	1.90	1.64	1.54	123
26.20	0.2169	0.5772	0.4228	2.11	1.07	1.55	1.17	91
31.00	0.2155	0.6202	0.3798	3.61	0.96	2.21	1.42	67
46.60	0.2124	0.7452	0.2548	10.63	1.00	3.63	1.59	63
59.40	0.2124	0.7939	0.2061	16.55	0.79	4.30	1.51	52
10.60	0.3177	0.5430	0.4570	1.12	3.95	0.94	1.74	226
14.80	0.3172	0.6255	0.3745	2.17	2.60	1.30	1.73	150
20.20	0.3101	0.7033	0.2967	2.85	1.15	1.20	1.19	97
26.20	0.3101	0.7896	0.2104	5.71	1.03	1.52	1.18	88
31.80	0.3372	0.8885	0.1115	11.87	0.88	1.49	0.99	89
45.40	0.3112	0.9015	0.0985	23.96	0.86	2.62	1.28	67
58.40	0.3259	0.9190	0.0810	37.11	0.70	3.27	1.32	53
10.80	0.5101	0.8381	0.1619	2.57	0.73	0.50	0.96	76
14.20	0.5101	0.9100	0.0900	4.99	0.71	0.49	0.75	95
19.80	0.5001	0.9274	0.0726	12.43	0.67	0.97	1.17	57
25.40	0.5101	0.9515	0.0485	24.46	0.74	1.25	1.28	57
29.60	0.5219	0.9624	0.0376	31.14	0.68	1.22	1.15	59
45.00	0.4677	0.9674	0.0326	52.21	0.74	1.76	1.10	68
59.80	0.4677	0.9689	0.0311	71.72	0.68	2.30	1.14	59

Table H.19 Effects of Operating Temperature on the Performance of the PVA and DEA Membrane.

PVA

Feed pressure	mol frac CO2	Temp	mol frac CO2	mol frac N2	Flux	Permeance	Flux	Permeance	Selectivity
psig	in feed	oC	in permeate	in permeate	CO2	CO2	N2	N2	JCO2/JN2
29.20	0.156044	30	0.4076	0.5924	0.68	0.15	0.99	0.66	23
30.60	0.155917	40	0.4248	0.5752	1.03	0.23	1.39	0.86	27
30.40	0.156015	50	0.4306	0.5694	1.21	0.31	1.60	0.96	32
31.00	0.156244	60	0.4515	0.5485	1.49	0.51	1.81	1.03	50
42.00	0.156058	30	0.4986	0.5014	1.36	0.17	1.37	0.64	27
41.60	0.156189	40	0.5067	0.4933	1.73	0.24	1.68	0.77	31
42.60	0.155871	50	0.5213	0.4787	2.30	0.32	2.11	0.91	35
43.00	0.155899	60	0.5468	0.4532	2.96	0.53	2.45	1.01	53
50.20	0.155788	30	0.5389	0.4611	1.85	0.16	1.58	0.63	26
50.00	0.155933	40	0.5541	0.4459	2.50	0.24	2.01	0.77	31
50.00	0.155891	50	0.5650	0.4350	3.20	0.32	2.47	0.91	35
50.00	0.155911	60	0.5957	0.4043	4.12	0.54	2.80	0.99	54
59.40	0.155847	30	0.5882	0.4118	2.56	0.17	1.79	0.60	28
59.00	0.155901	40	0.5953	0.4047	3.38	0.23	2.30	0.75	30
59.00	0.155922	50	0.6151	0.3849	4.56	0.33	2.85	0.90	37
59.00	0.155983	60	0.6518	0.3482	5.90	0.53	3.15	0.96	56

20wt% DEA

Feed pressure	mol frac CO2	Temp	mol frac CO2	mol frac N2	Flux	Permeance	Flux	Permeance	Selectivity
psig	in feed	oC	in permeate	in permeate	CO2	CO2	N2	N2	JCO2/JN2
30.00	0.1562	30	0.4619	0.5381	1.48	1.48	1.72	1.10	135
30.10	0.1558	40	0.4657	0.5343	1.72	2.36	1.97	1.21	195
31.60	0.1559	50	0.4837	0.5163	2.20	3.66	2.35	1.33	275
31.60	0.1559	60	0.4856	0.5144	2.90	6.20	3.07	1.69	368
39.00	0.1559	30	0.5382	0.4618	2.94	1.21	2.52	1.24	98
39.00	0.1561	40	0.5455	0.4545	3.31	1.69	2.76	1.32	129
39.00	0.1560	50	0.5527	0.4473	4.15	2.91	3.36	1.55	188
42.00	0.1561	60	0.5835	0.4165	7.02	4.44	5.01	2.08	213
48.60	0.1559	30	0.6099	0.3901	4.26	0.90	2.73	1.09	83
49.00	0.1561	40	0.6224	0.3776	5.45	1.26	3.31	1.26	100
49.00	0.1560	50	0.6301	0.3699	6.72	1.78	3.94	1.46	122
50.40	0.1560	60	0.6453	0.3547	9.44	2.44	5.19	1.81	135
59.80	0.1561	30	0.6757	0.3243	9.45	1.06	4.54	1.49	71
59.20	0.1561	40	0.6859	0.3141	10.39	1.32	4.76	1.52	87
59.40	0.1561	50	0.6990	0.3010	13.18	1.83	5.68	1.74	105
59.20	0.1559	60	0.7057	0.2943	15.22	2.30	6.35	1.89	122

Table H.20 Stability Tests for DEA Membrane. Temperature: 296K

20wt% DEA

Feed press psig	Humid	Time, hour	mol frac CO2 in feed	mol frac CO2 in permeate	mol frac N2 in permeate	Flux CO2	Permeance CO2	Flux N2	Permeance N2	Selectivity JCO2/JN2
31.80	with humid	22	0.1561	0.4746	0.5254	1.26	0.87	1.39	0.86	102
31.80	with humid	25	0.1561	0.4756	0.5244	1.25	0.91	1.38	0.85	107
31.80	with humid	29	0.1561	0.4778	0.5222	1.28	1.07	1.40	0.86	124
31.80	with humid	31	0.1562	0.4756	0.5244	1.28	0.92	1.41	0.87	106
31.80	with humid	33	0.1560	0.4751	0.5249	1.29	0.93	1.43	0.88	105
32.00	with humid	48	0.1560	0.4779	0.5221	1.27	0.95	1.38	0.85	112
31.80	with humid	50	0.1562	0.4764	0.5236	1.26	0.95	1.39	0.86	111
31.80	with humid	54	0.1559	0.4759	0.5241	1.27	0.97	1.40	0.86	112
31.80	with humid	56	0.1559	0.4755	0.5245	1.26	0.94	1.39	0.86	110
31.80	with humid	58	0.1561	0.4769	0.5231	1.26	0.99	1.38	0.85	116
31.60	with humid	72	0.1561	0.4743	0.5257	1.26	0.97	1.40	0.87	111
31.60	with humid	74	0.1560	0.4739	0.5261	1.25	0.95	1.39	0.86	110
31.60	with humid	79	0.1561	0.4725	0.5275	1.25	0.87	1.39	0.87	100
31.60	with humid	81	0.1561	0.4748	0.5252	1.26	0.98	1.39	0.86	114
31.80	with humid	99	0.1561	0.4769	0.5232	1.29	1.01	1.41	0.87	117
31.80	with humid	102	0.1561	0.4762	0.5238	1.26	0.94	1.39	0.86	110
31.80	with humid	104	0.1560	0.4764	0.5236	1.25	0.98	1.38	0.85	115
31.80	with humid	123	0.1561	0.4768	0.5232	1.26	0.99	1.38	0.85	116
31.80	with humid	125	0.1561	0.4754	0.5246	1.25	0.90	1.38	0.85	106
31.80	with humid	128	0.1562	0.4759	0.5241	1.27	0.93	1.40	0.87	107
31.60	with humid	144	0.1561	0.4740	0.5260	1.26	0.95	1.40	0.87	110
31.60	with humid	146	0.1559	0.4735	0.5265	1.24	0.95	1.38	0.86	110
31.60	with humid	148	0.1559	0.4744	0.5256	1.25	0.99	1.38	0.86	115
31.60	with humid	150	0.1560	0.4747	0.5253	1.24	0.99	1.37	0.85	116
31.60	with humid	167	0.1559	0.4747	0.5253	1.25	1.01	1.38	0.86	118
31.60	with humid	169	0.1559	0.4743	0.5257	1.25	0.98	1.38	0.86	114
31.60	with humid	171	0.1560	0.4747	0.5253	1.27	1.02	1.41	0.87	117
31.60	with humid	173	0.1561	0.4748	0.5252	1.26	0.99	1.39	0.86	114
31.60	with humid	175	0.1561	0.4747	0.5253	1.26	0.99	1.40	0.87	115
31.60	with humid	177	0.1562	0.4752	0.5248	1.26	1.01	1.39	0.87	116
31.60	with humid	192	0.1560	0.4748	0.5252	1.27	1.03	1.41	0.88	117
31.60	with humid	194	0.1560	0.4734	0.5266	1.25	0.92	1.39	0.87	106
31.60	with humid	197	0.1560	0.4748	0.5252	1.26	1.00	1.39	0.87	115
31.60	with humid	202	0.1560	0.4736	0.5264	1.25	0.93	1.39	0.86	109
31.60	with humid	216	0.1560	0.4745	0.5255	1.27	1.01	1.40	0.87	116
31.60	with humid	218	0.1559	0.4743	0.5257	1.26	1.00	1.40	0.87	115
31.60	with humid	220	0.1560	0.4746	0.5254	1.25	0.99	1.38	0.86	115

(Continuation- Stability Test)

20wt% DEA

Feed press psig	Humid	Time, hour	mol frac CO2 in feed	mol frac CO2 in permeate	mol frac N2 in permeate	Flux CO2	Permeance CO2	Flux N2	Permeance N2	Selectivity JCO2/JN2
31.60	with humid	222	0.1568	0.4776	0.5224	1.26	1.02	1.38	0.85	120
31.60	with humid	224	0.1562	0.4746	0.5254	1.25	0.96	1.38	0.86	112
31.60	with humid	239	0.1561	0.4749	0.5251	1.26	1.01	1.40	0.87	116
31.60	with humid	241	0.1559	0.4745	0.5255	1.26	1.01	1.40	0.87	116
31.60	with humid	243	0.1561	0.4735	0.5265	1.25	0.92	1.39	0.87	106
31.60	with humid	245	0.1561	0.4749	0.5251	1.26	0.99	1.40	0.87	115
31.60	with humid	247	0.1561	0.4741	0.5259	1.26	0.96	1.40	0.87	110
31.60	with humid	249	0.1561	0.4748	0.5252	1.26	0.99	1.39	0.86	115
31.60	with humid	266	0.1559	0.4749	0.5251	1.27	1.05	1.40	0.87	120
31.60	with humid	268	0.1560	0.4747	0.5253	1.26	1.01	1.39	0.86	117
31.60	with humid	271	0.1559	0.4748	0.5252	1.23	1.01	1.36	0.85	120
31.60	with humid	292	0.1559	0.4743	0.5257	1.26	0.99	1.40	0.87	114
31.60	with humid	294	0.1560	0.4744	0.5256	1.27	0.99	1.40	0.87	114
31.60	with humid	297	0.1559	0.4746	0.5254	1.27	1.02	1.40	0.87	117
31.60	with humid	311	0.1560	0.4746	0.5254	1.27	1.01	1.41	0.87	116
31.60	with humid	313	0.1559	0.4744	0.5256	1.27	1.02	1.41	0.87	117
31.60	with humid	315	0.1560	0.4746	0.5254	1.26	0.99	1.40	0.87	114
31.60	with humid	318	0.1562	0.4746	0.5254	1.26	0.97	1.40	0.87	112
31.60	with humid	319	0.1560	0.4747	0.5254	1.25	1.00	1.39	0.86	116
31.60	with humid	321	0.1560	0.4748	0.5252	1.26	1.01	1.39	0.86	117
31.60	with humid	336	0.1561	0.4743	0.5257	1.26	0.96	1.40	0.87	111
31.60	with humid	338	0.1561	0.4739	0.5261	1.26	0.95	1.40	0.87	109
31.60	with humid	340	0.1561	0.4740	0.5260	1.25	0.94	1.39	0.86	109
31.60	with humid	342	0.1560	0.4739	0.5261	1.25	0.95	1.39	0.86	110
31.60	with humid	344	0.1561	0.4749	0.5251	1.25	1.00	1.39	0.86	116
31.60	with humid	346	0.1560	0.4750	0.5251	1.25	1.02	1.38	0.86	119
31.80	with humid	359	0.1560	0.4758	0.5242	1.27	0.96	1.40	0.87	111
31.80	with humid	361	0.1560	0.4758	0.5242	1.26	0.95	1.39	0.86	110
31.80	with humid	363	0.1560	0.4751	0.5249	1.26	0.91	1.39	0.86	106
31.80	with humid	365	0.1561	0.4758	0.5242	1.26	0.93	1.39	0.86	109
31.80	with humid	367	0.1560	0.4768	0.5232	1.27	1.00	1.39	0.86	117
31.80	with humid	369	0.1560	0.4760	0.5240	1.26	0.95	1.39	0.86	111
31.80	with humid	370	0.1561	0.4762	0.5238	1.26	0.96	1.39	0.86	112
31.80	with humid	383	0.1560	0.4758	0.5242	1.28	0.95	1.41	0.87	109
31.80	with humid	386	0.1560	0.4758	0.5242	1.27	0.95	1.40	0.86	110
31.80	with humid	388	0.1561	0.4759	0.5241	1.26	0.94	1.39	0.86	110

(Continuation- Stability Test)

20wt% DEA

Feed press	Humid	Time,	mol frac	mol frac CO2	mol frac N2	Flux	Permeance	Flux	Permeance	Selectivity
psig		hour	CO2 in feed	in permeate	in permeate	CO2	CO2	N2	N2	JCO2/JN2
31.80	with humid	391	0.1561	0.4765	0.5235	1.27	0.97	1.39	0.86	113
31.80	with humid	393	0.1561	0.4762	0.5238	1.26	0.95	1.39	0.86	111
31.80	with humid	411	0.1560	0.4768	0.5232	1.29	1.03	1.42	0.88	117
31.80	with humid	414	0.1560	0.4767	0.5233	1.27	1.00	1.39	0.86	116
31.80	with humid	416	0.1560	0.4756	0.5244	1.26	0.93	1.39	0.86	108
31.80	with humid	436	0.1560	0.4761	0.5239	1.29	0.97	1.42	0.88	111
31.80	with humid	438	0.1561	0.4759	0.5241	1.26	0.93	1.39	0.86	109
31.80	with humid	440	0.1560	0.4756	0.5244	1.26	0.93	1.39	0.86	108
32.00	with humid	458	0.1560	0.4781	0.5219	1.29	0.98	1.40	0.86	114
32.00	with humid	460	0.1560	0.4777	0.5223	1.28	0.95	1.40	0.86	111
32.00	with humid	462	0.1561	0.4788	0.5212	1.28	0.99	1.39	0.85	116
32.00	with humid	464	0.1562	0.4782	0.5218	1.28	0.94	1.40	0.86	110
32.00	with humid	466	0.1561	0.4787	0.5213	1.28	0.99	1.39	0.85	116
32.00	with humid	482	0.1562	0.4779	0.5221	1.30	0.95	1.42	0.87	108
32.00	with humid	484	0.1560	0.4777	0.5223	1.29	0.95	1.42	0.87	109
32.00	with humid	486	0.1560	0.4778	0.5222	1.28	0.96	1.40	0.86	111
32.00	with humid	488	0.1560	0.4784	0.5216	1.28	0.99	1.40	0.86	115
32.00	with humid	490	0.1566	0.4792	0.5208	1.28	0.93	1.39	0.85	109
31.80	with humid	505	0.1560	0.4754	0.5246	1.29	0.94	1.42	0.88	107
31.80	with humid	507	0.1562	0.4758	0.5242	1.27	0.93	1.40	0.86	107
31.80	with humid	509	0.1561	0.4756	0.5244	1.28	0.93	1.41	0.87	107
31.60	with humid	511	0.1560	0.4751	0.5249	1.27	1.03	1.40	0.87	119
31.60	with humid	530	0.1562	0.4749	0.5251	1.27	1.00	1.41	0.88	114
31.60	with humid	532	0.1561	0.4748	0.5252	1.25	1.00	1.39	0.86	116
31.80	with humid	552	0.1560	0.4744	0.5256	1.27	0.89	1.41	0.87	102
31.80	with humid	554	0.1560	0.4757	0.5243	1.27	0.95	1.39	0.86	110
31.80	with humid	556	0.1562	0.4748	0.5252	1.27	0.88	1.40	0.87	101
31.80	with humid	558	0.1561	0.4760	0.5240	1.27	0.95	1.40	0.86	110
31.80	with humid	561	0.1562	0.4759	0.5241	1.27	0.93	1.40	0.86	108
31.60	with humid	575	0.1561	0.4744	0.5256	1.27	0.98	1.41	0.87	112

(Continuation- Stability Test)

20wt% DEA

Feed press psig	Humid	Time, hour	mol frac CO2 in feed	mol frac CO2 in permeate	mol frac N2 in permeate	Flux CO2	Permeance CO2	Flux N2	Permeance N2	Selectivity JCO2/JN2
31.60	with humid	577	0.1559	0.4745	0.5255	1.26	1.02	1.40	0.87	117
31.60	with humid	580	0.1559	0.4741	0.5259	1.26	0.99	1.40	0.87	114
31.80	with humid	607	0.1559	0.4759	0.5241	1.27	0.97	1.39	0.86	113
31.80	with humid	609	0.1559	0.4756	0.5244	1.27	0.96	1.40	0.86	111
31.80	with humid	626	0.1559	0.4757	0.5243	1.28	0.97	1.41	0.87	111
31.80	with humid	628	0.1559	0.4760	0.5240	1.28	0.98	1.41	0.87	113
31.80	with humid	630	0.1562	0.4766	0.5234	1.27	0.97	1.40	0.86	112
31.80	with humid	633	0.1560	0.4759	0.5241	1.27	0.96	1.40	0.86	111
31.80	with humid	649	0.1561	0.4756	0.5244	1.27	0.93	1.41	0.87	108
31.80	with humid	652	0.1560	0.4761	0.5239	1.27	0.97	1.40	0.86	113
31.80	with humid	655	0.1559	0.4769	0.5231	1.28	1.04	1.40	0.86	121
31.80	with humid	658	0.1560	0.4765	0.5235	1.28	0.99	1.40	0.87	114
31.80	with humid	673	0.1561	0.4762	0.5238	1.27	0.96	1.39	0.86	111
31.80	with humid	679	0.1560	0.4758	0.5242	1.28	0.96	1.41	0.87	110
31.80	with humid	681	0.1561	0.4763	0.5237	1.27	0.97	1.40	0.86	112
31.80	with humid	697	0.1561	0.4758	0.5242	1.27	0.94	1.40	0.86	108
31.80	with humid	700	0.1560	0.4758	0.5242	1.25	0.94	1.38	0.85	110
31.80	with humid	703	0.1559	0.4758	0.5242	1.26	0.96	1.39	0.86	112
31.80	with humid	705	0.1560	0.4765	0.5235	1.26	0.99	1.39	0.86	116
31.80	with humid	717	0.1560	0.4757	0.5243	1.29	0.96	1.42	0.88	109
31.80	with humid	719	0.1560	0.4761	0.5239	1.28	0.97	1.41	0.87	111
31.80	with humid	722	0.1560	0.4765	0.5235	1.28	1.01	1.40	0.87	116
31.80	with humid	725	0.1559	0.4765	0.5235	1.28	1.01	1.40	0.87	117
31.80	with humid	770	0.1559	0.4757	0.5243	1.27	0.97	1.40	0.87	112
31.80	with humid	773	0.1559	0.4760	0.5241	1.27	0.99	1.40	0.86	114
31.80	with humid	776	0.1560	0.4762	0.5238	1.27	0.98	1.39	0.86	113
31.60	with humid	819	0.1560	0.4741	0.5259	1.28	0.99	1.42	0.88	112
31.60	with humid	822	0.1561	0.4740	0.5260	1.26	0.95	1.40	0.87	109
31.80	with humid	824	0.1560	0.4759	0.5241	1.29	0.97	1.42	0.87	111
31.80	with humid	842	0.1561	0.4762	0.5238	1.26	0.96	1.39	0.86	112
31.80	with humid	845	0.1561	0.4764	0.5236	1.28	0.98	1.40	0.87	114

Table H.21 Effect of Feed Concentration on the permeation of CO_2 and N_2 through the PVA Membrane. Temperature: 296K.

PVA

Feed pressure	mol frac CO2	mol frac CO2	mol frac N2	Flux	Permeance	Flux	Permeance	Selectivity
psig	in feed	in permeate	in permeate	CO2	CO2	N2	N2	JCO2/JN2
30.80	0.0574	0.1518	0.8482	0.37	9.19	0.78	0.50	14
30.20	0.1302	0.3280	0.6720	0.40	0.08	0.81	0.54	14
31.40	0.1693	0.4354	0.5646	0.66	0.09	0.85	0.55	16
31.00	0.2159	0.5356	0.4644	0.95	0.09	0.83	0.56	17
30.40	0.2770	0.6636	0.3364	1.50	0.11	0.76	0.54	20
30.40	0.3613	0.8066	0.1934	3.10	0.14	0.74	0.56	24
32.20	0.5236	0.9331	0.0669	8.70	0.16	0.62	0.57	28
30.80	0.6103	0.9555	0.0445	10.63	0.15	0.50	0.57	27
29.40	0.8540	0.9884	0.0116	19.29	0.16	0.23	0.71	23
30.20	1.0000	1.0000	0.0000	29.85	0.19	0.00	0.00	-----
44.60	0.0574	0.1850	0.8150	0.26	0.07	1.13	0.50	15
45.00	0.1135	0.3611	0.6389	0.66	0.09	1.17	0.52	17
45.20	0.2124	0.6430	0.3570	1.92	0.11	1.07	0.50	23
45.40	0.2753	0.7551	0.2449	3.16	0.11	1.02	0.50	23
45.40	0.3687	0.8656	0.1344	6.16	0.13	0.96	0.52	25
47.80	0.4582	0.9314	0.0686	10.92	0.14	0.80	0.48	30
45.40	0.6221	0.9656	0.0344	18.35	0.15	0.65	0.57	27
45.60	1.0000	1.0000	0.0000	63.37	0.27	0.00	0.00	------
59.20	0.0584	0.2217	0.7783	0.40	0.07	1.42	0.48	16
59.40	0.1011	0.3756	0.6244	0.87	0.09	1.44	0.49	18
60.00	0.1310	0.4862	0.5138	1.37	0.10	1.44	0.49	21
59.80	0.1721	0.6121	0.3879	2.13	0.11	1.35	0.47	23
59.80	0.2330	0.7334	0.2666	3.86	0.11	1.40	0.51	22
59.80	0.3183	0.8654	0.1346	8.33	0.15	1.30	0.52	29
59.40	0.4941	0.9558	0.0442	22.02	0.19	1.02	0.54	35
59.60	0.6693	0.9834	0.0166	41.32	0.23	0.70	0.56	41
59.80	0.8640	0.9957	0.0043	79.87	0.31	0.35	0.67	47
59.00	1.0000	1.0000	0.0000	109.47	0.36	0.00	0.00	--------

Table H.22 Effect of Feed Concentration on the permeation of CO_2 and N_2 through the DEA Membrane at Feed Pressure of 207kPa (30 psig). Temperature: 296K.

20wt% DEA

Feed pressure	mol frac CO2	mol frac CO2	mol frac N2	Flux	Permeance	Flux	Permeance	Selectivity
psig	in feed	in permeate	in permeate	CO2	CO2	N2	N2	JCO2/JN2
30.40	0.0588	0.1799	0.8201	0.37	9.19	1.69	1.08	848
31.20	0.1061	0.3286	0.6714	0.84	4.32	1.72	1.08	401
30.20	0.1451	0.4707	0.5293	1.40	3.00	1.57	1.00	300
30.20	0.1727	0.5150	0.4850	2.10	2.21	1.97	1.28	173
30.20	0.1940	0.5759	0.4241	2.37	1.88	1.74	1.13	166
31.20	0.2131	0.6435	0.3565	3.41	2.06	1.89	1.19	173
31.20	0.2744	0.8004	0.1996	4.51	1.06	1.13	0.72	147
30.60	0.3372	0.8885	0.1115	12.46	1.09	1.56	1.07	102
29.40	0.4092	0.9159	0.0841	23.07	0.98	2.12	1.66	59
29.60	0.5219	0.9624	0.0376	34.32	0.74	1.34	1.27	59
29.60	0.6209	0.9882	0.0118	53.54	0.80	0.64	0.75	107
30.20	0.7414	0.9891	0.0109	92.68	0.96	1.02	1.74	55
31.20	0.7672	0.9920	0.0080	82.20	0.78	0.67	1.23	63
31.40	0.8773	0.9961	0.0039	112.14	0.85	0.44	1.51	56
30.60	1.0000	1.0000	0.0000	118.93	0.76	0.00	0.00	-----

Table H.23 Effect of Feed Concentration on the permeation of CO_2 and N_2 through the DEA Membrane at Feed Pressure of 310kPa and 414 kPa (45 and 60 psig). Temperature: 296K.

20wt% DEA

Feed pressure	mol frac CO2	mol frac CO2	mol frac N2	Flux	Permeance	Flux	Permeance	Selectivity
psig	in feed	in permeate	in permeate	CO2	CO2	N2	N2	JCO2/JN2
45.60	0.0585	0.2367	0.7633	0.76	3.00	2.47	1.05	284
45.20	0.1142	0.4510	0.5490	2.63	2.45	3.20	1.38	177
45.60	0.2124	0.7452	0.2548	10.77	1.13	3.68	1.64	69
46.40	0.2744	0.8571	0.1429	20.78	0.97	3.47	1.60	61
45.20	0.3112	0.9015	0.0985	25.99	0.94	2.84	1.39	68
46.20	0.3985	0.9407	0.0593	39.09	0.73	2.47	1.34	54
45.00	0.4677	0.9584	0.0416	66.88	0.94	2.90	1.81	52
46.20	0.5799	0.9810	0.0190	75.13	0.70	1.45	1.12	63
45.80	0.6220	0.9827	0.0173	88.46	0.74	1.56	1.34	55
45.00	0.7672	0.9912	0.0088	117.03	0.73	1.04	1.47	49
45.20	0.7933	0.9915	0.0085	125.59	0.74	1.07	1.71	43
46.20	0.8773	0.9963	0.0037	143.66	0.72	0.54	1.41	51
46.00	1.0000	1.0000	0.0000	166.35	0.70	0.00	0.00	----
59.40	0.0579	0.2851	0.7149	1.49	2.98	3.73	1.22	244
59.20	0.1162	0.5588	0.4412	3.26	1.71	2.57	0.85	201
59.40	0.2024	0.7739	0.2261	16.59	0.89	4.85	1.69	53
58.60	0.2544	0.8755	0.1245	28.32	0.95	4.03	1.48	64
58.40	0.3209	0.9190	0.0810	37.11	0.73	3.27	1.31	55
58.80	0.3885	0.9469	0.0531	57.09	0.76	3.20	1.41	54
59.80	0.4781	0.9659	0.0341	83.39	0.76	2.94	1.49	51
59.60	0.5689	0.9805	0.0195	106.15	0.74	2.11	1.30	57
59.80	0.6220	0.9853	0.0147	122.59	0.75	1.82	1.27	59
59.40	0.7414	0.9926	0.0074	138.73	0.67	1.04	1.06	63
60.00	0.8915	0.9976	0.0024	175.07	0.66	0.42	1.02	64
59.20	0.9943	1.0000	0.0000	183.89	0.61	0.00	0.00	-------

Table H.24 Effect of Humidification on the Stability of the DEA Membrane

20wt% DEA

Feed press psig	Humid	Time, hour	mol frac CO2 in feed	mol frac CO2 in permeate	mol frac N2 in permeate	Flux CO2	Permeance CO2	Flux N2	Permeance N2	Selectivity JCO2/JN2
31.6	with humid	15	0.1558	0.4740	0.5260	1.23	0.98	1.36	0.85	116
31.4	with humid	19	0.1558	0.4711	0.5289	1.23	0.93	1.38	0.86	108
32.2	with humid	24	0.1557	0.4808	0.5192	1.26	1.05	1.36	0.83	126
31.4	with humid	40	0.1558	0.4717	0.5283	1.24	0.97	1.39	0.87	112
31.4	with humid	44	0.1556	0.4722	0.5278	1.24	1.05	1.39	0.87	121
31.4	with humid	48	0.1559	0.4717	0.5283	1.24	0.95	1.39	0.87	110
31.4	with humid	62	0.1560	0.4727	0.5273	1.26	1.00	1.40	0.88	114
31.4	with humid	66	0.1562	0.4734	0.5266	1.25	1.01	1.39	0.87	116
31.6	with humid	69	0.1562	0.4749	0.5251	1.25	0.97	1.39	0.86	113
31.6	with humid	72	0.1562	0.4742	0.5258	1.25	0.94	1.39	0.86	109
31.6	with humid	87	0.1563	0.4732	0.5268	1.31	0.92	1.46	0.91	101
31.8	with humid	92	0.1561	0.4761	0.5239	1.26	0.95	1.39	0.86	111
31.8	with humid	95	0.1562	0.4769	0.5231	1.26	0.97	1.38	0.85	114
31.8	with humid	111	0.1562	0.4765	0.5235	1.26	0.95	1.38	0.85	111
31.8	with humid	113	0.1562	0.4768	0.5232	1.26	0.97	1.38	0.85	114
31.6	with humid	116	0.1561	0.4747	0.5253	1.25	0.99	1.38	0.86	115
31.6	with humid	119	0.1559	0.4745	0.5255	1.25	1.00	1.38	0.86	116
31.8	with humid	133	0.1559	0.4759	0.5241	1.25	0.96	1.38	0.85	113
31.8	with humid	136	0.1538	0.4711	0.5289	1.22	1.05	1.37	0.84	125
31.8	with humid	140	0.1560	0.4743	0.5257	1.25	0.87	1.39	0.86	101
31.8	with humid	143	0.1558	0.4755	0.5245	1.25	0.96	1.38	0.85	112
31.6	with humid	159	0.1559	0.4728	0.5272	1.25	0.91	1.39	0.87	105
31.6	with humid	163	0.1559	0.4745	0.5255	1.26	1.00	1.39	0.86	116
31.4	with humid	165	0.1559	0.4726	0.5274	1.25	1.02	1.40	0.87	117
31.4	with humid	167	0.1557	0.4714	0.5286	1.25	0.98	1.40	0.87	112
31.4	with humid	185	0.1559	0.4726	0.5274	1.25	1.00	1.39	0.87	116
31.6	with humid	190	0.1558	0.4748	0.5252	1.26	1.04	1.39	0.86	120
31.4	with humid	192	0.1559	0.4724	0.5276	1.25	1.00	1.40	0.87	115
31.8	with humid	208	0.1560	0.4772	0.5228	1.26	1.03	1.38	0.85	120
31.6	with humid	211	0.1559	0.4748	0.5252	1.26	1.03	1.39	0.86	119
31.4	with humid	214	0.1561	0.4720	0.5280	1.25	0.95	1.40	0.87	109
31.8	with humid	216	0.1559	0.4804	0.5196	1.27	1.31	1.37	0.85	155
31.4	with humid	236	0.1560	0.4733	0.5267	1.25	1.05	1.39	0.87	120
31.4	with humid	239	0.1559	0.4726	0.5274	1.25	1.02	1.40	0.87	117
31.8	with humid	252	0.1557	0.4746	0.5254	1.25	0.93	1.39	0.86	108
31.6	with humid	254	0.1558	0.4732	0.5268	1.25	0.94	1.39	0.86	109
31.6	with humid	256	0.1558	0.4731	0.5269	1.25	0.94	1.39	0.87	109
31.6	with humid	260	0.1558	0.4746	0.5254	1.25	1.03	1.39	0.86	120
31.6	with humid	262	0.1558	0.4743	0.5257	1.25	1.01	1.39	0.86	117
31.8	with humid	281	0.1559	0.4780	0.5220	1.26	1.10	1.38	0.85	129

(Continuation- Effect of Humidification)

20wt% DEA

Feed press psig	Humid	Time, hour	mol frac CO2 in feed	mol frac CO2 in permeate	mol frac N2 in permeate	Flux CO2	Permeance CO2	Flux N2	Permeance N2	Selectivity JCO2/JN2
31.6	with humid	286	0.1558	0.4744	0.5256	1.25	1.01	1.39	0.86	117
31.6	with humid	289	0.1559	0.4719	0.5281	1.34	0.93	1.49	0.93	100
31.6	with humid	305	0.1558	0.4739	0.5261	1.25	0.99	1.39	0.86	114
31.8	with humid	309	0.1557	0.4758	0.5242	1.25	0.99	1.38	0.85	116
31.8	with humid	311	0.1562	0.4773	0.5227	1.26	1.00	1.38	0.85	117
31.8	with humid	330	0.1561	0.4754	0.5246	1.24	0.90	1.37	0.84	107
32	with humid	332	0.1560	0.4776	0.5224	1.27	0.94	1.39	0.85	110
31.8	with humid	336	0.1559	0.4744	0.5256	1.25	0.88	1.38	0.85	103
31.8	with humid	354	0.1559	0.4758	0.5242	1.25	0.95	1.38	0.85	112
31.8	with humid	358	0.1560	0.4760	0.5240	1.26	0.95	1.38	0.85	111
31.8	with humid	360	0.1562	0.4755	0.5245	1.26	0.90	1.39	0.86	105
31.6	with humid	374	0.1563	0.4729	0.5271	1.24	0.84	1.38	0.86	99
31.6	with humid	376	0.1561	0.4722	0.5278	1.25	0.85	1.39	0.87	98
31.6	with humid	379	0.1561	0.4732	0.5268	1.24	0.90	1.38	0.86	105
31.6	with humid	384	0.1561	0.4744	0.5256	1.26	0.96	1.39	0.86	111
31.4	with humid	399	0.1558	0.4713	0.5287	1.24	0.95	1.39	0.87	110
31.6	with humid	401	0.1558	0.4734	0.5266	1.25	0.96	1.39	0.86	111
31.6	with humid	403	0.1558	0.4721	0.5279	1.24	0.88	1.39	0.86	102
31.6	with humid	405	0.1562	0.4728	0.5272	1.26	0.87	1.40	0.87	100
31.6	with humid	407	0.1561	0.4742	0.5258	1.25	0.95	1.38	0.86	111
31.6	with humid	421	0.1561	0.4709	0.5291	1.33	0.85	1.49	0.93	91
31.6	with humid	423	0.1561	0.4725	0.5275	1.25	0.87	1.40	0.87	101
31.6	with humid	427	0.1561	0.4730	0.5270	1.26	0.89	1.40	0.87	102
31.6	with humid	431	0.1559	0.4742	0.5258	1.26	0.99	1.40	0.87	114
31.6	with humid	433	0.1560	0.4726	0.5274	1.25	0.88	1.40	0.87	102
31.6	with humid	448	0.1562	0.4723	0.5277	1.24	0.84	1.39	0.86	97
31.8	without	453	0.1561	0.4760	0.5240	1.25	0.94	1.38	0.85	110
31.8	without	455	0.1558	0.4758	0.5242	1.26	0.97	1.39	0.86	114
31.4	without	471	0.1557	0.4719	0.5281	1.23	1.00	1.38	0.86	115
31.4	without	473	0.1559	0.4716	0.5284	1.23	0.95	1.38	0.86	110
31.4	without	476	0.1559	0.4716	0.5284	1.24	0.94	1.39	0.87	109
31.4	without	478	0.1559	0.4717	0.5283	1.23	0.96	1.38	0.86	111
31.4	without	481	0.1559	0.4715	0.5285	1.24	0.95	1.38	0.87	109
31.4	without	497	0.1560	0.4741	0.5259	1.23	1.08	1.36	0.85	127
31.4	without	499	0.1558	0.4717	0.5283	1.24	0.97	1.39	0.87	111
31.4	without	502	0.1559	0.4715	0.5285	1.23	0.93	1.38	0.86	108
31.4	without	504	0.1560	0.4721	0.5279	1.23	0.95	1.37	0.86	111

(Continuation- Effect of Humidification)

20wt%
DEA

Feed press	Humid	Time,	mol frac	mol frac CO2	mol frac N2	Flux	Permeance	Flux	Permeance	Selectivity
psig		hour	CO2 in feed	in permeate	in permeate	CO2	CO2	N2	N2	JCO2/JN2
31.4	without	520	0.1559	0.4737	0.5263	1.24	1.08	1.38	0.86	125
31.4	without	522	0.1563	0.4739	0.5261	1.25	1.02	1.39	0.87	118
31.4	without	526	0.1559	0.4722	0.5278	1.26	1.00	1.41	0.88	113
31.6	without	528	0.1559	0.4737	0.5263	1.24	0.94	1.38	0.86	110
31.6	without	545	0.1559	0.4734	0.5266	1.25	0.94	1.39	0.87	109
31.6	without	547	0.1559	0.4748	0.5252	1.25	1.02	1.39	0.86	119
31.6	without	549	0.1559	0.4735	0.5265	1.25	0.94	1.39	0.87	108
31.6	without	551	0.1559	0.4732	0.5268	1.25	0.93	1.39	0.87	108
31.6	without	553	0.1559	0.4728	0.5272	1.25	0.91	1.39	0.87	105
31.6	without	568	0.1559	0.4730	0.5270	1.26	0.92	1.41	0.87	105
31.6	without	570	0.1560	0.4750	0.5250	1.24	1.01	1.37	0.85	118
31.6	without	574	0.1562	0.4764	0.5236	1.25	1.08	1.38	0.85	126
31.6	without	576	0.1560	0.4759	0.5241	1.19	1.02	1.31	0.82	125
31.8	without	578	0.1561	0.4761	0.5239	1.18	0.88	1.29	0.80	110
31.8	without	593	0.1560	0.4774	0.5226	0.64	0.53	0.70	0.43	122
31.8	without	595	0.1562	0.4774	0.5226	0.64	0.51	0.70	0.43	118
31.8	without	598	0.1563	0.4774	0.5226	0.63	0.49	0.69	0.43	116
32	without	600	0.1561	0.4799	0.5201	0.63	0.52	0.69	0.42	124
32	without	602	0.1561	0.4793	0.5207	0.63	0.50	0.68	0.42	121
31.8	without	618	0.1561	0.4783	0.5217	0.57	0.49	0.63	0.39	128
31.8	without	620	0.1561	0.4781	0.5219	0.65	0.55	0.71	0.44	126
31.8	without	623	0.1560	0.4778	0.5222	0.67	0.57	0.73	0.45	126
31.8	without	625	0.1560	0.4777	0.5223	0.68	0.57	0.74	0.46	125
32	with humid	641	0.1561	0.4773	0.5227	0.97	0.68	1.06	0.65	105
32	with humid	645	0.1561	0.4785	0.5215	0.99	0.76	1.08	0.66	115
32	with humid	648	0.1562	0.4755	0.5245	0.98	0.63	1.08	0.67	95
32	with humid	650	0.1560	0.4768	0.5233	0.98	0.69	1.08	0.66	104
31.4	with humid	666	0.1562	0.4706	0.5294	1.15	0.80	1.30	0.81	99
31.4	with humid	668	0.1558	0.4715	0.5285	1.22	0.95	1.37	0.86	111
32	with humid	670	0.1560	0.4756	0.5244	1.26	0.84	1.39	0.85	99
32	with humid	672	0.1558	0.4776	0.5224	1.26	0.96	1.38	0.84	114
32	with humid	674	0.1560	0.4759	0.5241	1.27	0.86	1.40	0.86	100

(Continuation- Effect of Humidification)

20wt% DEA

Feed press	Humid	Time,	mol frac	mol frac CO2	mol frac N2	Flux	Permeance	Flux	Permeance	Selectivity
psig		hour	CO2 in feed	in permeate	in permeate	CO2	CO2	N2	N2	JCO2/JN2
31.6	with humid	690	0.1558	0.4745	0.5255	1.25	1.02	1.38	0.86	119
31.6	with humid	692	0.1560	0.4737	0.5263	1.27	0.96	1.42	0.88	110
31.6	with humid	694	0.1560	0.4750	0.5250	1.27	1.03	1.41	0.87	118
31.6	with humid	698	0.1560	0.4754	0.5246	1.20	1.00	1.32	0.82	121
31.8	with humid	700	0.1559	0.4789	0.5211	1.25	1.17	1.36	0.84	140
31.6	with humid	716	0.1558	0.4757	0.5243	1.26	1.12	1.39	0.86	129
31.6	with humid	718	0.1559	0.4748	0.5252	1.25	1.02	1.38	0.86	119
31.6	with humid	721	0.1560	0.4732	0.5268	1.25	0.92	1.39	0.87	106
31.6	with humid	723	0.1559	0.4731	0.5269	1.24	0.91	1.38	0.86	107
31.6	with humid	725	0.1559	0.4735	0.5265	1.23	0.94	1.37	0.85	110
31.6	with humid	740	0.1558	0.4738	0.5262	1.27	1.00	1.42	0.88	113
31.6	with humid	742	0.1559	0.4720	0.5280	1.25	0.87	1.40	0.87	101
31.6	with humid	745	0.1559	0.4736	0.5264	1.25	0.95	1.39	0.87	110
31.6	with humid	747	0.1560	0.4746	0.5254	1.25	0.99	1.38	0.86	116
31.6	with humid	749	0.1558	0.4742	0.5258	1.25	1.00	1.38	0.86	116
31.8	with humid	764	0.1559	0.4761	0.5239	1.26	0.99	1.39	0.86	115
31.8	with humid	766	0.1557	0.4757	0.5243	1.25	0.99	1.38	0.85	116
31.8	with humid	768	0.1563	0.4786	0.5214	1.26	1.05	1.37	0.84	125
31.8	with humid	770	0.1559	0.4757	0.5243	1.25	0.95	1.38	0.85	112
31.8	with humid	772	0.1559	0.4762	0.5238	1.24	0.97	1.37	0.84	115
31.6	with humid	788	0.1559	0.4737	0.5263	1.25	0.95	1.39	0.86	111
31.6	with humid	790	0.1559	0.4743	0.5257	1.26	1.00	1.39	0.86	115
31.6	with humid	793	0.1560	0.4737	0.5263	1.25	0.94	1.38	0.86	109
31.6	with humid	795	0.1559	0.4748	0.5252	1.24	1.02	1.37	0.85	119
31.6	with humid	797	0.1560	0.4743	0.5257	1.26	0.98	1.39	0.86	114
31.6	with humid	811	0.1560	0.4737	0.5263	1.24	0.94	1.38	0.86	109
31.6	with humid	813	0.1560	0.4732	0.5268	1.23	0.91	1.37	0.85	106
31.6	with humid	815	0.1561	0.4739	0.5261	1.26	0.95	1.40	0.87	109
31.6	with humid	817	0.1560	0.4734	0.5266	1.25	0.93	1.39	0.87	107
31.6	with humid	819	0.1560	0.4731	0.5269	1.25	0.91	1.39	0.87	105
31.8	with humid	839	0.1561	0.4760	0.5240	1.26	0.95	1.39	0.86	111
31.6	with humid	841	0.1561	0.4734	0.5266	1.25	0.90	1.39	0.87	104
31.6	with humid	843	0.1560	0.4725	0.5275	1.24	0.86	1.38	0.86	101
31.6	with humid	845	0.1561	0.4750	0.5250	1.26	1.00	1.39	0.86	116